Metabolic regulation of innate and adaptive immune responses of neonates

Sean Righardt Holm

Submitted to Swansea University in fulfilment of the requirements of the Degree of Doctor of Philosophy

2023

DECLARATION

This work has not previously been accepted in substance for any degree and is not being concurrently submitted in candidature for any degree.

Signed ..... (candidate)

Date 28/10/2024

STATEMENT 1

This thesis is the result of my own investigations, except where otherwise stated. Where correction services have been used, the extent and nature of the correction is clearly marked in a footnote(s).

Other sources are acknowledged by footnotes giving explicit references. A bibliography is appended.

Signed ..... (candidate)

Date 28/10/2024

Abstract

Immunometabolism is a burgeoning field of study providing novel insights into the mechanisms governing immune cell phenotype and function. However, most of this research has been conducted in adults resulting in a paucity of research concerning the metabolic features and requirements in early life including of human neonatal immune cells. This is despite the documented differences between adult and neonatal immune cell function. This thesis aims to address this by investigating the following questions: are the metabolic characteristics and requirements of neonatal immune cells different from adults and if so, do these unique characteristics and requirements explain the differences in immune cell phenotype and function seen in neonates? To explore these questions, immune cells, primarily naïve CD4+ T cells and neutrophils, were isolated from the peripheral blood of healthy adult donors and umbilical cord blood from term elective caesarean sections and experimentally interrogated ex vivo and in vitro. Functional assays, including bioenergetic flux, functional assays and phenotyping by flow cytometry were all used to provide insight into the metabolic and functional phenotype of adult and neonatal immune cells. For the first time, this thesis shows a distinctly enhanced glycolytic program on anti-CD3/28 activation in neonatal naïve CD4+ T cells accompanied by increased amino acid stabilised mTOR signalling highlighting an important role for metabolites in governing naïve CD4+ T cell activation. Furthermore, this thesis finds that failure to produce neutrophil extracellular traps by neonatal neutrophils is likely a result of reduced aerobic glycolytic capacity generating insufficient ATP to support this function. Together, these findings reveal the unique immunometabolic landscape of the neonate and begin to elucidate the mechanisms underpinning functional differences with adults, making a strong case for further investigation of neonatal immunometabolism, not only to provide novel therapeutic targets but also as a natural model of adult immune dysfunction.

Acknowledgements

I would like to express the enormous amount of gratitude I have for Professor Cathy Thornton who has tirelessly guided me through this PhD and has been instrumental in its completion. I would also like to extend my heartfelt thanks to Dr Nick Jones for his support and advice throughout the past four years as well as the wider research group and colleagues at Swansea university. Thanks should also go to all of the volunteers who donated blood; the nurses, doctors and phlebotomists who collected samples and made this research possible.

I am sincerely grateful for the love and support of my partner, family and friends who have helped me through the trials and tribulations over the course of this PhD. This work would not have been possible without your patient and caring support.

In loving memory of William Yates

Table of Contents

Table of Figure

Table of abbreviations

2-aminobicyclo-(2,2,1) heptanecarboxylic acid	**BCH**
2-Doxyglucose	2DG
Adenosine monophosphate	AMP
Adenosine triphosphate	ATP
Alpha ketoglutarate	αKG
Antigen presenting cell	APC
Antimycin A	AA
ATP citrate lyase	ACYL
Glucose-6-phosphate dehydrogenase	G6PDH
Carnitine palmitoyl transferase	CPT1
Cell trace violet	CTV
Central memory T cell	Tcm
Chemokine receptor	CCR
Cluster of differentiation	CD
Damage associated molecular pattern	DAMP
Dendritic cell	DC
dihydroxyacetone phosphate	DHAP
Effector memory RA+ T cell	Temra
Effector memory T cell	Tem
Electron transport chain	ETC
Extracellular acidification rate	ECAR
Extracellular oxidation rate	OCR
Fatty acid oxidation	FAO
flavin adenine dinucleotide	FAD
Fluorescent activated cell sorting	FACS
Fluorescence minus one	FMO
Forkhead box P3	FOXP3

fructose 6-phosphate	F6P
Glucose	Glu
Glucose Transporter	GLUT
Glucose-6-phosphate	G6P
Glyceraldehyde 3-phosphate dehydrogenase	GAPDH
Glycogen phosphorylase inhibitor	GPi
Hexokinase	HK
histone acetyl transferase	HAT
Human plasma like media	HPLM
Innate lymphoid cell	ILC
Interferon-γ	IFNg
Interleukin	IL
Lactate dehydrogenase	LDH
Lactate dehydrogenase inhibitor	LDHi
Magnetic activated cell sorting	MACS
Mammalian target of rapamycin	mTOR
Mononuclear cell	MNC
Myeloid derived suppressor cell	MDSC
Naive CD4+	nCD4+
Naive T cell	Tn
Natural killer	NK
Neutrophil extracellular trap	NET
Nicotinamide adenine dinucleotide	NAD
Nicotinamide mononucleotide	NMN
Nuclear factor of activated T cells	NFAT
Oligomycin	oligo
Optic atrophy type 1	OPA1
Oxidation-reduction	redox

Oxidative phosphorylation	OXPHOS
Pathogen associated molecular pattern	PAMP
Pattern recognition receptor	PRR
Pentose phosphate pathway	PPP
Peripheral blood mononuclear cells	PBMC
Peroxisome proliferator-activated receptor gamma coactivator 1-alpha	PGC-1α
Phorbol 12-myristate 13-acetate	PMA
Phosphate buffered saline	PBS
Phosphatidylinositol 3 kinase	PI3K
Phosphoenolpyruvate	PEP
Phosphofructokinase-1	PFK-1
Principal component analysis	PCA
Protein Kinase B	AKT
Pyruvate dehydrogenase	PDH
Pyruvate dehydrogenase kinase	PDK
Pyruvate kinase M2	PKM2
Ras homolog enriched in brain	RHEB
Reactive oxygen species	ROS
Recombinase-activating gene	RAG
Regulatory T cell	Treg
Ribosomal protein S6	S6
Ribosomal protein S6 kinase	S6K
Rotenone	rot
Sarcoendoplasmic reticulum calcium ATPase	SERCA
Signal activator and activator of transcription	STAT
sterol regulatory element binding proteins	SREBP
Store operate calcium entry	SOCE
Succinate dehydrogenase	SDH

T cell receptor	TCR
T-helper	Th
Toll like Receptor	TLR
Transforming growth factor b	TGF-b
Tricarboxylic acid	TCA
Tuberous sclerosis complex	TSC
Tumour necrosis factor	TNF
Extracellular flux	XF

Chapter One

Introduction

1 Introduction

Birth represents a relatively dramatic transition from an environment with a low microbial burden to one abundant in commensal and potentially pathogenic challenges that the neonatal immune system must be able to respond to. Immune responses in preterm and term neonates differ from those of adults, generally being characterised as diminished, tolerant or type II skewed; although we must be mindful that these are highly evolved, stage of life appropriate responses (Holm et al., 2021). Efforts to clarify the phenotypes and mechanisms prevalent at this time are ongoing so that we can better understand the significance of differences at this stage of development for immediate and long term health. The need to understand how the neonatal immune response differs to that of adults is driven by the mortality and morbidity associated with infection and sepsis in newborns and infants and the need for protective vaccine responses that can mitigate these. Recent decades have also seen growing appreciation that neonatal immune phenotypes, shaped predominantly by environmental factors during pregnancy, are linked to the later development of non-communicable immunoinflammatory diseases (Herberth et al., 2012; Campbell et al., 2015; Grieger et al., 2016). Finally, while the therapeutic capacity of umbilical cord blood is already being harnessed through transplantation, there is growing appreciation of the wider regenerative capacity of neonatal immune cells, for example in the regeneration of heart tissue (Sattler and Rosenthal, 2016). Given this diversity there is a real need to elucidate the mechanisms that uniquely programme neonatal immune cell phenotype.

The development and maturation of lymphoid progenitors during fetal and early post-natal life is influenced by a multitude of factors including cytokine profiles, transcription factors, expression of surface proteins, prostaglandins produced by the placenta and altered levels of metabolites, such as adenosine, in neonatal plasma (Saito, 2000; Levy et al., 2006; Kan et al., 2018). It has been long recognised that maternal and neonatal nutrition have lasting effects on immune development, contributing to the development of allergic disease, metabolic syndrome and chronic inflammatory conditions (Palmer, 2011). Energy demands in early life are extremely high with little to no energy, especially fatty acids and proteins, reserves. The

metabolic and energetic demands required for growth in early life severely limit nutrient availability for highly energetically demanding immune responses (Shew and Jaksic, 1999). Disease tolerance, wherein the goal is to limit disease immunopathology versus the pathogen per se, is suggested as an evolved method of host defence in early life to limit harm to the host in the face of these reduced energy reserves (Shew and Jaksic, 1999; Butte, 2005; Brook et al., 2017; Harbeson et al., 2018a; Harbeson et al., 2018b).

Immunometabolism is a relatively recently emerged field of research that seeks to elaborate on the crucial role metabolic pathways have in shaping immune cell fate and function. The activation and function of most immune cells is dependent on metabolic reprogramming to a state of aerobic glycolysis to enable effector function. In this setting, the primary fuel is glucose which is metabolised through the central metabolism pathways of glycolysis to pyruvate or lactate to generate ATP and other biosynthetic precursors. Additionally, the Krebs cycle, primarily supplied by pyruvate or glutaminolysis, fuels ATP production through mitochondrial oxidative phosphorylation. The differential utilisation of fuels, including in competition with other cells in the tissue microenvironment, can impact on cell fate and function (Geltink et al., 2018). This thesis suggests that immunometabolism provides a framework for understanding phenotypic and functional differences in the neonatal and adult immune response. While data supporting this are emerging these studies are still very much in their early days and there are many unanswered questions. This thesis will explore and discuss the differences between neonate and adult immune responses, how metabolism may influence these changes and the further work that is required.

1.1 A brief overview of the immune system

The immune system is a complex association of biological processes that protects the organism from disease whilst maintaining homeostasis and tissue integrity (Sattler, 2017). This multilayered system is comprised of barriers, innate immunity and the adaptive immune system, with all layers interacting and communicating in a tightly regulated manner. Barriers form the first line of defence preventing pathogens from

entering the body through both physical and chemical means such as mucous membranes and lysozymes (Dupont et al., 2014). Additionally, barriers are under constant surveillance by tissue resident immune cells and can release alarmins to attract other immune cells, particularly innate immune cells, to the site of offence. Innate immunity is the second layer of defence, with its ancient evolutionary origins stretching back as far as simple invertebrate organisms and its key function of phagocytosis reaching back to some of the first multicellular amoebas (Buchmann, 2014). This branch of the immune system is armed with powerful receptors capable of recognising pathogen associated molecular patterns (PAMP)s, empowering a rudimentary form of non-self recognition. Equipped with these receptors cells of the innate immune system are able to recognise foreign entities and engage immune functions such as degranulation and phagocytosis to kill and clear the threat. Furthermore, these cells also respond to damage associated molecular patterns (DAMP)s, supporting tissue repair and homeostasis. Evolution of the adaptive immune system created a diverse and adaptable third layer of immunity. The appearance of recombinase-activating gene (RAG) in the immunoglobulin superfamily exon of jawed vertebrates enabled the creation of an expansive, diverse and adaptable repertoire of antigen receptors (Cooper and Alder, 2006; Flajnik and Kasahara, 2010). This, along with distinguishing of self and non-self, through major histocompatibility complexes, creates a sophisticated system of defence and surveillance, capable of responding to the continual development of novel threats in the perpetual evolutionary arms race (Radwan et al., 2020). In this system, specialised professional antigen presenting cells (APC)s bridge the gap between the innate and adaptive immune systems, collecting and processing antigen from the environment to display on surface MHCs and selectively activate T cells with complementary T cell receptors (TCR)s which go on to clear pathogenic cells in response. Humoral immunity is also induced in an antigen specific manner as T cells induce the differentiation of plasma B cells which secrete large amounts of antibodies, activating phagocytes and the classical complement pathway. Together these complex, multilayered and integrated systems of surveillance and defence maintain tissue homeostasis and protect the organism from a range of internal and external threats.

1.2 Immunometabolism

1.2.1 Glycolysis and gluconeogenesis

From the Greek *glykis* for sweet and *lysis* for splitting, glycolysis describes the degradation of glucose, through a series of enzyme catalysed reactions, to yield two molecules of pyruvate, two molecules of NADH and a net production of two ATP molecules (Figure 1.1). Glycolysis also serves as an entry point into other metabolic pathways such as the tricarboxylic acid (TCA) cycle, also known as the Krebs cycle, and the pentose phosphate pathway. In addition to its role in energy production, glycolysis is an anabolic pathway providing precursors for various catabolic processes.

1.2.1.1 Glycolysis

Firstly, glucose enters the cell via glucose transporters (GLUTs), integral membrane proteins encoded by solute carrier family 2 (SLC2) genes. GLUTs bind glucose inducing a conformational change thus transporting the glucose or other carbohydrates molecule across the plasma membrane. There are 13 isoforms of GLUTs which differ in substrate specificity, transport kinetics and tissue expression (Roberts and Miyamoto, 2015). For example, immune cells, including T cells, neutrophils and monocytes primarily express GLUT1 which has been shown to support production of proinflammatory cytokines and other effector functions (Macintyre et al., 2014).

Glycolysis is a two-phase operation, starting with an energy consuming preparatory phase and ending with an energy producing payoff phase. In the first phase hexokinase isoforms catalyse the conversion of glucose in the cytosol to glucose-6-phosphate, consuming one molecule of ATP in the process. This first step regulates the entry of glucose into the glycolysis pathway and prevents the glucose molecule from exiting the cell. There are four hexokinase (HK) isozymes expressed in a tissue dependent manner. Hexokinase-IV is specifically expressed in the liver and is a 50 kDa protein with only one catalytic domain unlike other hexokinase isozymes. HK-II is unique in containing two catalytically functional sites and is upregulated in many cells with enhanced aerobic glycolysis (Roberts and Miyamoto, 2015). Glucose-6-

phosphate conversion to fructose 6-phosphate (F6P), via phosphohexose isomerase (GPI), precedes the second ATP consuming reaction generating fructose 1,6-bisphosphate, catalysed by phosphofructokinase-1 (PFK-1). This step is mostly irreversible under normal cellular conditions and marks the first committed step in glycolysis. Alternatively, F6P is converted to fructose 2,6-bisphosphate which is a potent allosteric activator of PFK-1, even in the presence of ATP, essentially uncoupling glycolysis from bioenergetics. Dysregulated allosteric control of PFK-1 is associated with T cell exhaustion in rheumatoid arthritis (Yang et al., 2013b). Aldolase then cleaves fructose 1,6-bisphosphate generating glyceraldehyde 3-phosphate and dihydroxyacetone phosphate. Only glyceraldehyde 3-phosphate is used directly in the second phase of glycolysis, therefore, dihydroxyacetone phosphate is converted to glyceraldehyde 3-phosphate, by triose phosphate isomerase, completing the first phase of glycolysis.

The first reaction of the second, energy producing phase is a two-stage process involving the oxidation of the aldehyde group of glyceraldehyde 3-phosphate to a carboxylic acid by NAD+ and the subsequent joining of an orthophosphate to form 1,3-bisphosphoglycerate, a step catalysed by glyceraldehyde 3-phosphate dehydrogenase. Substrate level phosphorylation of the energy rich molecule, 1,3-bisphosphoglycerate, yields ATP. Phosphoglycerate mutase catalyses the formation of 2-phosphoglycerate which is then converted to phosphoenolpyruvate (PEP) in a dehydration reaction by enolase. Both the enzyme and the product of this reaction regulate T cell function with enolase translocation to the nucleus inhibiting suppressor function of T regs and PEP promoting nuclear translocation of activated T cells (NFAT) (De Rosa et al., 2015; Ho et al., 2015). Phosphoenolpyruvate has a very high phosphoryl transfer potential enabling the transfer of the phosphoryl group to generate ATP and a pyruvate in another substrate level phosphorylation reaction catalysed by pyruvate kinase. Tuning of this rate limiting step is highly important and can be achieved through various mechanisms including expression of different isoforms and control of quaternary structure. The increased catalytic rate of tetrameric pyruvate kinase M2 (PKM2) favours energy production from glycolysis whilst dimeric or monomeric forms provides synthetic precursors for anabolic

processes by slowing the conversion of PEP to pyruvate. Limiting metabolite exit from glycolysis, through allosterically favouring the dimeric form of PKM2, is key to metabolic reprogramming of both T cells and macrophages and supports cell division and pro-inflammatory cytokine production (Palsson-McDermott et al., 2015; Angiari et al., 2020). Whilst, in neutrophils the activity of PKM2 is implicated in the ability to produce NETs (Awasthi et al., 2019).

Ultimately glycolysis consumes two molecules of ATP in the preparatory phase but generates four molecules of ATP during the payoff phase via substrate level phosphorylation resulting in a net gain of two ATP.

Additionally, glycolysis consumes two molecules of NAD+, per molecule of glucose, in the reaction catalysed by glyceraldehyde phosphate dehydrogenase (GAPDH). Maintaining sufficient levels of cellular NAD+ is crucial for cellular function and rapid glycolysis. Pyruvate can be reduced to lactate by the enzyme lactate dehydrogenase (LDH), regenerating NAD+ from NADH. This effect of reducing pyruvate to lactate in the presence of oxygen was first described by Otto Warburg in cancer cells and termed aerobic glycolysis (Heiden et al., 2009). Since its initial discovery in cancer cells aerobic glycolysis has been described as a key metabolic pathway induced in immune cells upon an activating stimulus. Whilst the pathway is highly inefficient, producing only two molecules of ATP per molecule of glucose, it is extremely rapid allowing for production of ATP at rate unmatched by the more efficient process of oxidative phosphorylation (Lunt and Vander Heiden, 2011; Desousa et al., 2023). However, a potentially more important role for glycolysis in actively dividing cells is to provide biosynthetic precursors for growth, proliferation and effector functions. For example, 3-phosphoglycerate is required for proline synthesis, a key precursor for purine nucleotide biosynthesis. This pathway is essential for the function of effector T cells which rely almost entirely on de novo biosynthesis of nucleotides to meet the demands of rapid cell division (Ma et al., 2019). Furthermore, glycolysis supplies both the pentose phosphate pathway and TCA cycle which have anabolic roles in actively dividing cells (Zhu and Thompson, 2019).

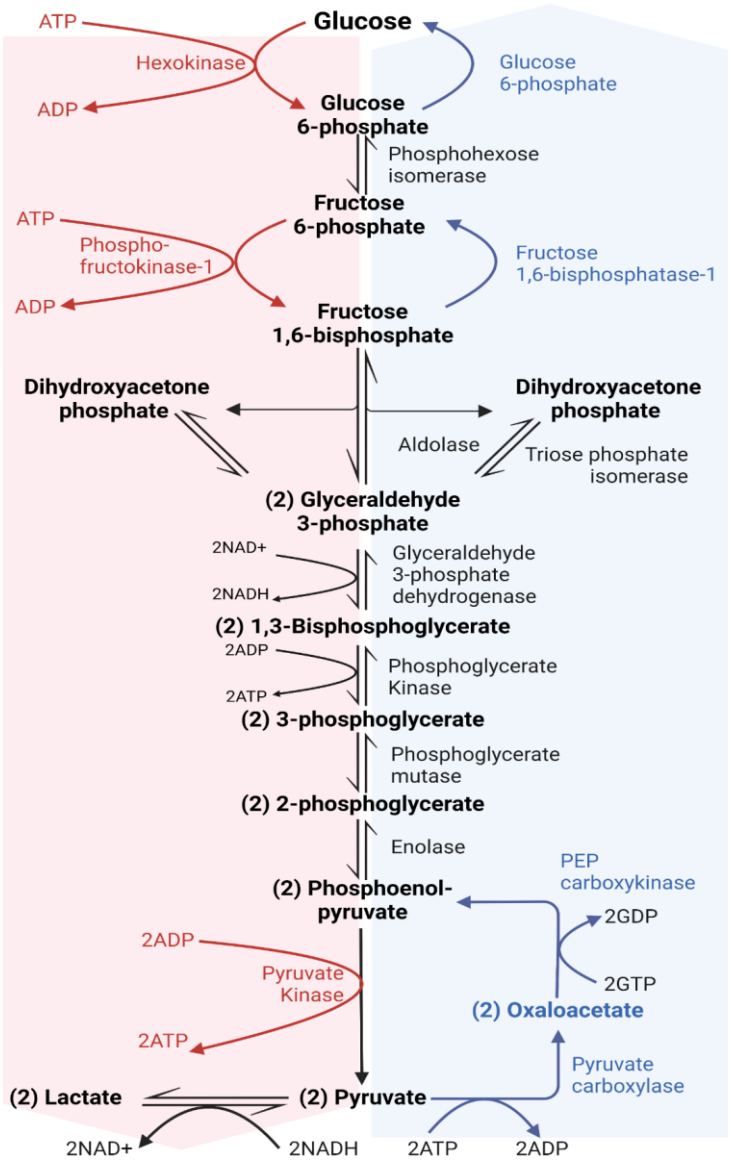

Figure 1.1 Glycolysis and gluconeogenesis

Glucose is metabolised through a series of mostly reversible reactions to pyruvate and lactate to produce ATP and NADH (shown in red). The reverse series of reactions

converts pyruvate to glucose through the formation of oxaloacetate (shown in blue) at the expense of 2ATP and 2GTP. Figure made using Biorender.com

1.2.1.2 Gluconeogenesis

Pyruvate can also be converted to glucose in a process called gluconeogenesis, however, this is not an exact reverse of glycolysis as the steps of glycolysis catalysed by hexokinase, phosphofructokinase and pyruvate kinase are essentially irreversible (Figure1.1). To generate phosphoenolpyruvate from pyruvate, mitochondrial pyruvate first must be converted to oxaloacetate through the action of pyruvate carboxylase at the expense of one ATP. Next, the malate-aspartate shuttle transports oxaloacetate from the mitochondria to the cytosol. In this shuttle system oxaloacetate is converted to aspartate, in a reaction catalysed by aspartate amino transferase which uses glutamate as an amine donor. Aspartate is transported from the mitochondria to the cytosol via the glutamate aspartate transporter, importing glutamate in return. Aspartate in the cytosol is converted back to oxaloacetate, by donating its amine group to alpha-ketoglutarate (α-KG) generating glutamate. Phosphoenolpyruvate carboxykinase converts cytosolic oxaloacetate to phosphoenolpyruvate consuming a molecule of GTP. From PEP, glycolysis is performed in reverse until fructose 1,6 bisphosphate where fructose 1,6-bisphosphatase catalyses its conversion to fructose 6-phosphate. Again, glycolysis is run in reverse generating glucose 6-phosphate which can be converted to free glucose via glucose 6-phosphatase.

Another fate of glucose 6-phosphate is to be transformed into glycogen, a branched polysaccharide storage molecule for glucose, via a process called glycogenesis. Here, the conversion of G6P to glucose 1-phosphate is catalysed by phosphoglucomutase which reacts with the nucleotide uridine diphosphate (UDP) to form UDP-glucose. This sugar nucleotide donates the glucose residue to the non-reducing end of glycogen in the rate limiting reaction catalysed by glycogen synthase. On activation neutrophils use gluconeogenesis to convert pyruvate to glycogen enabling them to survive and function in tissues with limited nutrients and oxygen supply (Sadiku et al., 2021). Stores of glycogen can be metabolised rapidly to glucose for glycolysis by the

actions of glycogen phosphorylase, which cleaves glycogen chains to give, glucose 1-phosphate which in turn is converted to G6P by phosphoglucomutase.

1.2.1.3 Alternative entry and exit points for glycolysis.

Glycolytic/glucogenic intermediates can also be supplemented by other monosaccharides and some amino acids and in some cases have been shown to have immunomodulatory effects. D-Fructose, a commonly found monosaccharide in the human diet, can enter glycolysis through two pathways. Fructose is converted to the glycolytic intermediate fructose 6-phosphate by hexokinase at the expense of ATP. In the liver, fructokinase converts fructose to fructose 1-phosphate consuming a molecule of ATP. Fructose 1-phosphate is then cleaved, by fructose 1-phosphate aldolase, to give dihydroxyacetone phosphate (DHAP) and glyceraldehyde and triose kinase converts glyceraldehyde to GAP at the expense of ATP. Fructose utilisation, in human monocytes, induces a strongly pro-inflammatory response upon lipopolysaccharides (LPS) stimulation (Jones et al., 2021). Galactose, a component of lactose in milk, enters glycolysis at G6P. Galactokinase consumes ATP, converting galactose to galactose 1-phosphate (G1P) which in turn is converted to G1P, by UDP-glucose:galactose 1-phosphate uridyltransferase, utilising UDP-glucose as a cofactor. Phosphoglucomutase converts G1P to G6P whilst the second product, UDP-galactose, is recycled to UDP-glucose via UDP-glucose 4-epimerase. The carbon skeletons of glucogenic amino acids, importantly glutamine and alanine, can enter glucogenic intermediates directly at pyruvate or via acetyl-CoA and the TCA cycle in the mitochondria. Furthermore, glycolysis is a central metabolic pathway that integrates several catabolic and anabolic processes. Whilst sugars and amino acids entering glycolysis can be catabolised to produce ATP for cellular processes, these molecules can also form the fundamental building blocks of larger molecules such as proteins, nucleotides and lipids. Carbons from glucose can be used for de novo lipid synthesis via the pentose phosphate pathway (PPP), glycerol or acetyl-CoA as well as for de novo nucleotide biosynthesis (Figure 1.2) which are required for cell growth and proliferation.

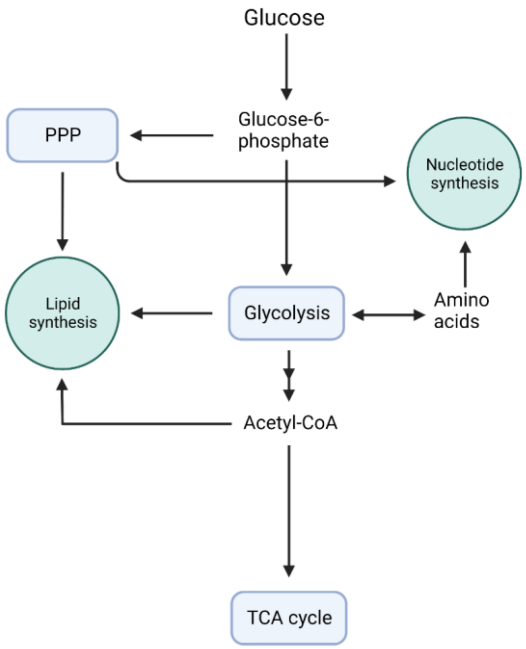

Figure 1.2 Glycolysis provides anabolic precursors.

Glycolysis is a central metabolic pathway that integrates anabolic and catabolic processes. Carbon from glucose and amino acids can be metabolised to acetyl-CoA and enter the TCA cycle producing ATP required for cellular processes. Alternatively, these metabolites can be used in anabolic processes for de novo synthesis of lipids and nucleotides. Figure made using BioRender.com

1.2.2 The pentose phosphate pathway

G6P derived from the first steps of glycolysis can enter into the PPP in a reaction catalysed by glucose-6-phosphate dehydrogenase (G6PDH), in the rate limiting step, producing 6-phosphogluconate (6PG) and NADPH. In a subsequent reaction 6-phosphogluconate dehydrogenase (6PGD) oxidases 6PG to generate 5-ribulose phosphate and a second molecule of NADPH. This oxidative phase of the PPP is followed by a non-oxidative phase generating pentose sugars for nucleotide synthesis (Figure 1.3).

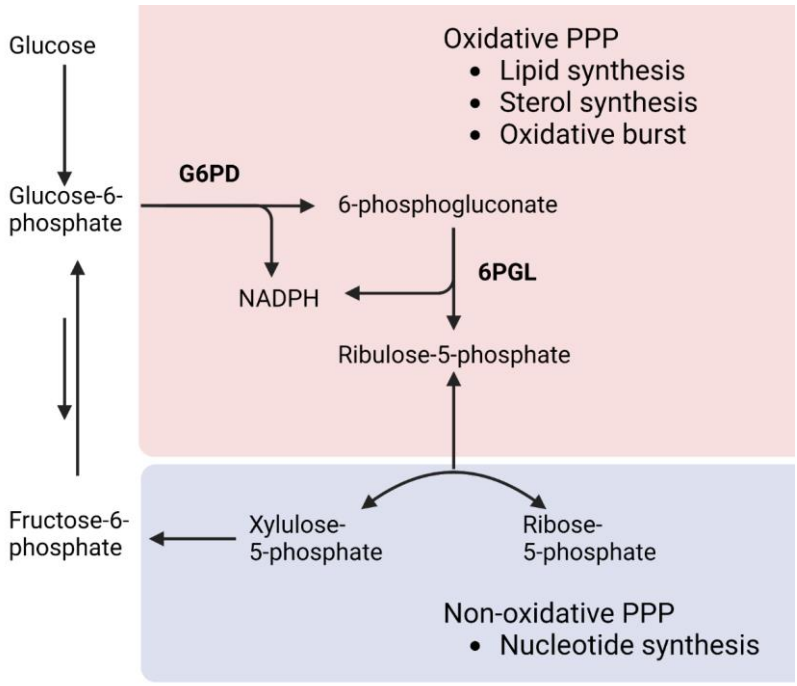

Figure 1.3 The pentose phosphate pathway

The Pentose phosphate pathway is a shunt off glycolysis starting at glucose-6-phosphate. The first stage is an oxidative process generating ribulose-5-phosphate and supports anabolic processes as well as the oxidative burst in innate immune cells. The non-oxidative phase can cycle back into glycolysis at fructose-6-phosphate or support nucleotide biosynthesis. Figure made using Biorender.com.

NADPH generated from the oxidative phase is used for fatty acid and cholesterol biosynthesis, supporting proliferating cells. The NADPH-dependent glutathione reductase (GR) utilises NADPH generated from the PPP to protect the cell from oxidative stress. Conversely, M1 macrophages require NADPH for generation of ROS by NADPH oxidase and for NO production (Pearce and Pearce, 2013). In neutrophils the PPP shifts to a cyclical pathway favouring just the oxidative portion and recycling PPP products through reversed GPI flux (Figure 1.3). This alternate PPP generates up to six molecules of NADPH for every molecule of glucose. Such rapid production of

large amounts of NADPH fuels the oxidative burst of neutrophils which consumes NADPH and oxygen ultimately inducing lytic NETosis (Britt et al., 2022).

1.2.3 The link reaction

Pyruvate, generated by glycolysis, can enter the TCA cycle fuelling oxidative phosphorylation and the highly efficient generation of ATP. Here, the pyruvate dehydrogenase (PDH) enzyme complex, comprised of three subunits E1, E2 and E3, catalyse the non-reversible oxidation of pyruvate to acetyl-CoA, carbon dioxide and NADH. In this reaction five coenzymes (thiamine pyrophosphate, flavin adenine dinucleotide (FAD), NAD, coenzyme A and lipoate) are required for the decarboxylation of pyruvate, the subsequent conversion to an acetyl group and the joining of the acetyl group to give acetyl-CoA.

The first step, catalysed by pyruvate dehydrogenase (E1), decarboxylates pyruvate and is the rate limiting step, thus, it can act as a molecular switch controlling entry of cytosolic pyruvate into TCA cycle as acetyl-CoA. In murine T cells, it has been demonstrated that inactivation of PDH by pyruvate dehydrogenase kinase (PDK) induces a rapid switch to aerobic glycolysis (Menk et al., 2018).

Alongside its role fuelling the TCA cycle, acetyl-CoA is also an important donor of the acetyl group for histone acetyl transferase (HAT) enzymes. Acetyl-CoA, generated from central carbon metabolism plays a crucial role in regulating the open chromatin landscape controlling cell fate and function (Martinez-Reyes and Chandel, 2020).

1.2.4 The tricarboxylic acid cycle

Acetyl-CoA from the link reaction, donates its acetyl group to oxaloacetate to form citrate at the start of the TCA cycle. In a series of following reactions citrate is oxidised back to oxaloacetate so that one full cycle produces one $FADH_2$ and three NADH supplying the electron transport chain (ETC) by yielding electrons and protons (Figure1.4).

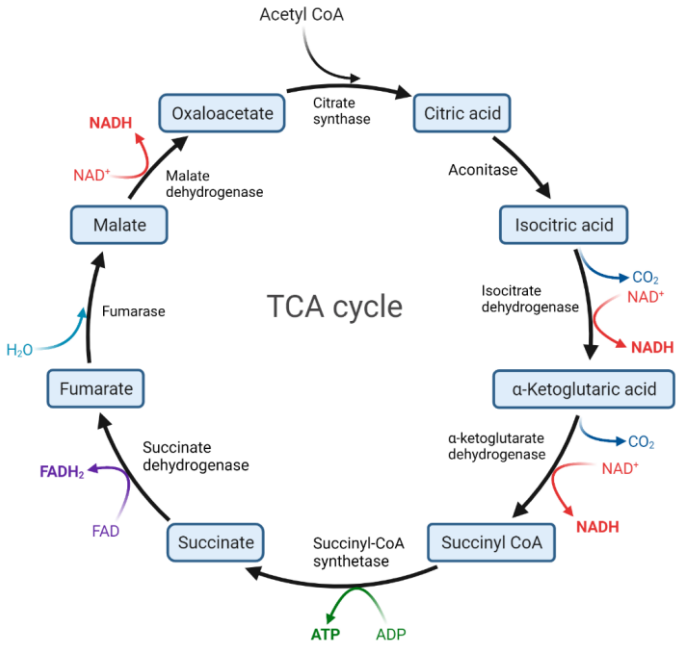

Figure 1.4 The TCA cycle

The tricarboxylic acid cycle (TCA cycle), also known as the Krebs cycle or citric acid cycle, is a series of chemical reactions that occur in the mitochondria of cells. The cycle consists of eight steps catalysed by eight different enzymes. The cycle is initiated when acetyl CoA reacts with oxaloacetate to form citrate and releases coenzyme A (CoA-SH). In a succession of following reactions, citrate is rearranged to form isocitrate by aconitase; isocitrate is decarboxylated and then undergoes oxidation to form alpha-ketoglutarate in a reaction catalysed by isocitrate dehydrogenase; alpha-ketoglutarate dehydrogenase catalyses the loss of another a molecule of carbon dioxide and oxidation to form succinyl CoA which is enzymatically converted to succinate by succinyl-CoA synthetase; succinate dehydrogenase oxidises succinate to fumarate which is then hydrated, by fumarase to produce malate; finally, to end the cycle, malate dehydrogenase oxidises malate to oxaloacetate. Each cycle results in the

regeneration of oxaloacetate and the formation of two molecules of carbon dioxide, 3 molecules of NADH, a molecule of $FADH_2$ and a molecule of ATP. β-fatty acid oxidation fuels the TCA cycle. Figure made using Biorender.com.

1.2.4.1 β-oxidation of fatty acids fuels the TCA cycle

Fatty acids are an important fuel source that can be easily stored and mobilised to meet demands. Fatty acid oxidation (FAO) is highly efficient, generating more energy per gram than any other fuel source. Fatty acid transporters, such as CD36, facilitate the uptake of fatty acids like palmitate into the cell. Fatty acids are then activated on the surface of mitochondria by linking to coenzyme A and carnitine palmitoyltransferase (CPT1) shuttles them into the mitochondria matrix for oxidation. The sequential removal of two carbons completely oxidises the fatty acid generating $FADH_2$, NADH and acetyl-CoA for oxidative phosphorylation and the TCA cycle respectively.

Acetyl-CoA provided by FAO is required for cell growth and proliferation in various immune cell types (Figure 1.5). However, utilisation of this pathway often differs depending on the cells' stage of function and differentiation. FAO is dependent on mitochondrial fusion and morphology governed by optic atrophy type 1 (OPA1). Effector T cells exhibit fissed mitochondria with loose cristae and do not rely on FAO. On the other hand, mitochondria are fused with tight cristate in FAO reliant memory T cells (Buck et al., 2016).

Commented [SH1]: Term for non fused mitochondria

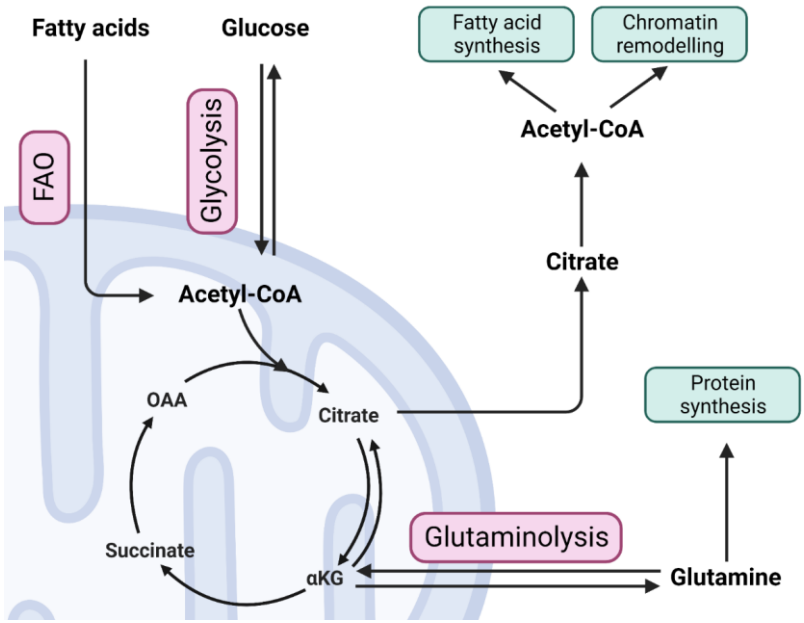

Figure 1.5 The Amphibolic TCA cycle

The TCA cycle is a central pathway in cell metabolism that converges the metabolism of the three main energy sources, (sugars, fats and amino acids), with both sugars and fats entering the TCA cycle via acetyl CoA whilst glutamine, the second most abundant metabolite, enters via α-KG. TCA components can also be used at to generate many of the essential building blocks of the cell fuelling growth and proliferation. Additionally, the TCA cycle is fundamentally tied to cellular phenotype through metabolite mediated control of the chromatin landscape. Figure made using Biorender.com.

1.2.4.2 The amphibolic TCA cycle

Whilst the TCA cycle is central to ATP production it also serves a more extensive role in cell growth, proliferation and function. For most quiescent immune cells, such as naïve T cells, the TCA cycle is primarily utilised to generate ATP for cell homeostasis. However, in activated immune cells, such as effector T cells, the TCA cycle is amphibolic, providing energy and anabolic precursors (Figure 1.5). Four and five

carbon intermediates are used to generate amino acids for protein synthesis and purines/pyrimidines for nucleotide synthesis. Whilst the six-carbon intermediate, citrate, provides cytosolic acetyl-CoA for fatty acid and sterol synthesis. To balance the loss of intermediates required for biosynthesis, the TCA cycle is replenished by anaplerotic pathways. Pyruvate and glutamine are particularly important for anaplerosis, feeding into oxaloacetate and alpha-ketoglutarate (αKG) respectively. Glutaminolysis supports immune cell function, such as NETosis in neutrophils and IL-2 production in T cells. Additionally, glutaminolysis is utilised to different extents depending on the nature of the immune response. For example, M1 macrophage antimicrobial responses preferentially require glutamine and metabolism of glutamine to aKG is a defining factor in Th1 over Treg differentiation (Klysz et al., 2015; Jiang et al., 2022)

1.2.4.3 Roles of the TCA cycle beyond metabolism

TCA intermediates demonstrate immunomodulatory effects thorough remodelling the chromatin landscape, post translational modification and regulation of transcription. As mentioned above citrate is exported to the cytosol where it provides cytosolic citrate through the action of ATP citrate lyase (ACYL). Cytosolic citrate is used for post translational acetylation of proteins including histones, via the action of HATs, which is required to promote IFN-γ production, for example. In DCs and macrophages a truncated TCA cycle, upon LPS stimulation, results in a build-up of citrate along with increased expression of ACYL and is associated with the production of proinflammatory mediators (Infantino et al., 2013). αKG is another TCA intermediate required for epigenetic modification by the histone demethylase Jumonji C domain containing lysine demethylases and DNA demethylases and ten-eleven translocation hydroxylases (TET)s. In macrophages, αKG derived from glutaminolysis, drives an anti-inflammatory phenotype through chromatin remodelling contrasting the proinflammatory role played by αKG in regulatory T cells (Liu et al., 2017; Matias et al., 2021). αKG is in careful equilibrium with succinate which acts as an allosteric inhibitor of αKG utilising enzymes, including TETs and 2-oxoglutarate-dependent dioxygenases (Laukka et al., 2016). Accumulation of succinate, by a perturbed TCA

cycle, stabilises hypoxia inducible factor (HIF)1α promoting the transcription of glycolytic and pro inflammatory IL-1β (Tannahill et al., 2013). Succinate also couples the TCA cycle directly with the electron transport chain and a in low ATP environment can drive reverse electron transfer generating ROS from complex I stabilising HIF1α and promoting proinflammatory responses (Garaude et al., 2016; Martinez-Reyes and Chandel, 2020). Itaconate, derived from decarboxylated TCA intermediate cis-aconitate, has an anti-inflammatory effect through inhibition of succinate dehydrogenase (SDH) preventing reverse electron transfer (Cordes et al., 2016; Lampropoulou et al., 2016). Interestingly this metabolite also has a direct antimicrobial role through inhibition of the glyoxylate shunt (Kim et al., 2023).

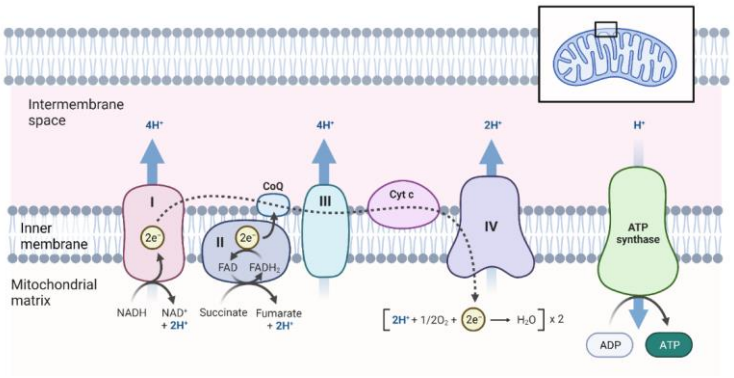

Figure 1.6 The electron transport chain couples cellular catabolism to ATP production.

The electron transport chain consists of four protein complexes, accepting electrons from NADH and $FADH_2$, that couple redox reactions, creating an electrochemical gradient, through pumping protons across the inner membrane, that leads to the creation of ATP in a system termed oxidative phosphorylation. Figure made using Biorender.com.

1.2.5 Oxidative phosphorylation

Oxidative phosphorylation (OXPHOS) generates ATP from the catabolic processes of the cell and is carried out across the inner mitochondrial membrane. A series of

oxidation-reduction reactions (redox) transfer electrons from glycolysis, TCA cycle and FAO, in the form of NADH and $FADH_2$, to oxygen by a series of protein, metal and lipid complexes known as the electron transport chain (ETC) (Figure 1.6). NADH supplies electrons to complex I (NADH:ubiquinone oxidoreductase) reducing flavin mononucleotide, and then through an iron-sulphate carrier to the ubiquinone pool. $FADH_2$ reduces the ubiquinone pool through complex II (SDH). Ubiquinone is a small lipid soluble mobile carrier able to transfer electrons from complex I and II through the inner mitochondrial membrane to complex III (cytochrome c reductase). The ubiquinone Q cycle transfers a net of 2 electrons to cytochrome c through the intermediate cytochrome b in complex III. Cytochrome c carries electrons along the periphery of the membrane to complex IV (cytochrome c oxidase) where they are finally transferred to oxygen. The free energy released from these redox reactions is used to pump protons across the inner mitochondrial membrane to the intermembrane space, at complex I, III and IV which establishes an energy potential across the membrane in the form of a proton gradient. ATP synthesis is coupled to the electron transport chain through chemiosmosis, whereby the electrical potential and pH gradient generated across the inner membrane is used to generate ATP from ADP. Movement of protons back into the mitochondrial matrix is restricted to transmembrane proteins, allowing complex IV (ATP synthase) to harness this gradient to drive ATP production. ATP synthase consists of two major components, F0, the channel though which protons pass through the membrane and F1, which uses the flow of proteins through F1 to mechanically drive the production of ATP. Thus, electrons and protons from NADH and $FADH_2$ are coupled to the production of ATP via the ETC.

Controlling the flow of electrons through the ETC and its chemiosmotic gradient is utilised by immune cells to direct cell fate and function. The uncoupling protein (UCP)2 is linked with the reduction of ROS generation and is more highly expressed in M2 macrophages then M1 which require ROS for proinflammatory functions. Additionally, UCP2 is required for M2 macrophages differentiation in response to IL-4 cytokine (De Simone et al., 2015). Loss of complex III in murine Treg cells impairs their

suppressive function, highlighting the importance of a functioning ETC in these cells (Weinberg et al., 2019).

1.2.6 Amino acid metabolism

As alluded to earlier, amino acids are essential for immune cell catabolic function through glucogenic and anaplerotic reactions and as direct precursors for bio synthesis. Despite glucose being the most abundant metabolite in circulation, amino acids make up the majority of the biomass of rapidly dividing cells (Hosios et al., 2016). Carbons from amino acids, particularly glutamine, primarily contribute to protein synthesis whilst glucose has a more diverse fate within the cell. De novo synthesis of purines, required by T cells for proliferation, is supported by extracellular serine but can also be supplemented by glycolysis, as mentioned earlier (Hosios et al., 2016). Additionally, serine is required by macrophages to suppress aberrant cytokine production (Kurita et al., 2021). Arginine is another key metabolite for immune function, providing NO for neutrophils and macrophages. In fact, arginine metabolism is central to macrophage phenotype, with metabolism via nitric oxide synthase (NOS) defining M1 phenotypes and arginase-1 metabolism defining M2 phenotypes (Rath et al., 2014). In M2 macrophages, metabolism of arginine to spermidine allows for hypusination of the eukaryotic initiation factor 5A (eIF5a), a protein required for the translation of some proteins including many of those associated with mitochondrial metabolism that characterises the M2 phenotype (Puleston et al., 2019). The same polyamine metabolic pathway is crucial for T cell lineage commitment through remodelling of the chromatin landscape (Puleston et al., 2021). Some amino acids, termed essential amino acids, cannot be synthesised by the body including tryptophan, which is known to have immunomodulatory effects, suppressing T cell proliferation through metabolism to kynurenine by APCs (Pour et al., 2019; Siska et al., 2021). Additionally, metabolism of tryptophan to NAD via kynurenine maintains the glycolytic phenotype of embryonic stem cells and could potentially play a similar role in immune cell metabolism (Liu et al., 2019a).

1.2.7 Integrating cell signalling and metabolism

As immune responses require considerable metabolic rewiring to exit the initial quiescent state, effective immune activation necessitates the successful integration of external stimuli and nutrients with intracellular cell state and function. Fulfilling this requirement, the mechanistic target of rapamycin (mTOR) containing complexes, (mTORC) 1 and 2, acts as a central hub integrating the external environment and cellular metabolism (Figure 1.7). Immune signalling, such as T cell receptor (TCR) or Toll-like receptor (TLR) engagement, and downstream signalling via cytokines, such as IL-2 and IL-7, trigger the activation of mTOR (Marzec et al., 2008; Wofford et al., 2008; Imanishi et al., 2020). In T cells, mTOR signalling is largely induced through TCR engagement and co-stimulation via CD28 in a PI3K-AKT dependent signalling axis. This series of signalling events results in the inhibition of the tuberous sclerosis complex (TSC) which reverses the inhibition of the Ras homolog enriched in brain (RHEB) which binds and promotes mTORC1 function. mTORC2 is also activated by TCR and costimulatory engagement, through a separate mechanism involving phosphatidylinositol 3 kinase (Chi, 2012; Huang et al., 2020).

Glucose, which is vital for maintain the energy balance of the cell acts through AMP sensing protein AMP-activated protein kinase (AMPK). In this mechanism, when the ATP/AMP ratio decreases, due to low glucose availability, AMPK promotes the inhibition of mTOR through TSC (Figure 1.7) (Leprivier and Rotblat, 2020). Additionally, lower rates of glycolysis allow aldolase to promote AMPK signalling (Zhang et al., 2017). Amino acids, including leucine, arginine and glutamine, regulate mTOR activation via the Rag complex and RHEB (Duran et al., 2012; Carroll et al., 2016; Wolfson et al., 2016). Transport of these amino acids into the cell are a known important factor in naïve T cell activation (Sinclair et al., 2013; Geiger et al., 2016).

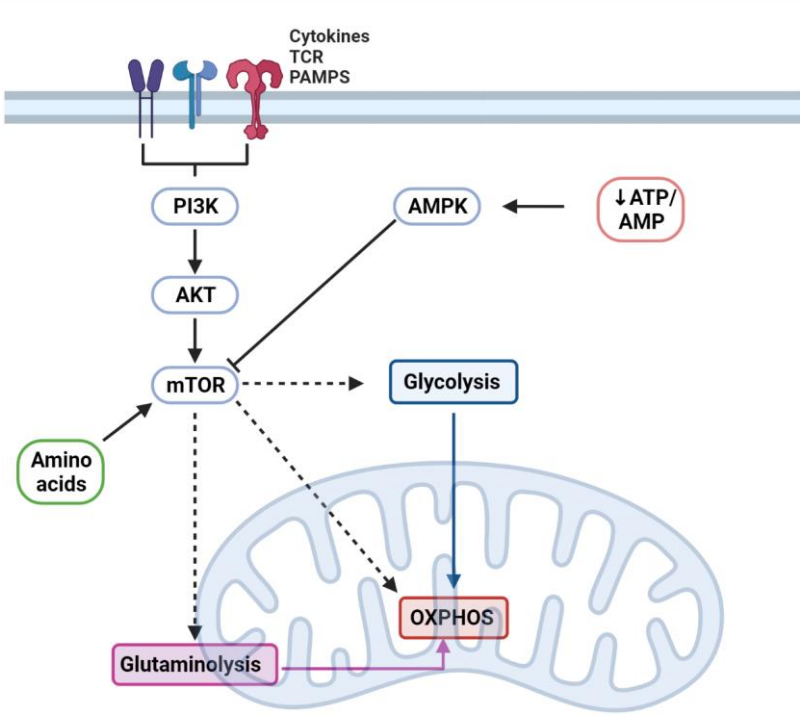

Figure 1.7 Metabolic signalling is integrated through mTOR

The mammalian target of rapamycin (mTOR) is a central signalling node controlling cellular metabolism by integrating cell extrinsic factors with metabolite availability and energy status. Signalling via cytokine receptors, Toll-like receptors and the T cell receptor can induce mTOR signalling, often through the PI3K-AKT signalling axis. Once activated mTOR drives the cellular metabolic programme to support growth, proliferation and function by upregulating key glycolytic pathways, glycolysis and glutaminolysis, required for rapid energy production. mTOR is inhibited by AMPK, when the ATP/AMP ratio decreases indicating a low energy state, whilst amino acid availability supports mTOR signalling. Thus, mTOR driven metabolic reprogramming is regulated by energy status and metabolite availability. Figure made using Biorender.com.

Signalling via mTOR is critical for cell growth, proliferation, survival and differentiation. mTORC1 and mTORC2 act via differing mechanisms to promote cellular metabolism and anabolic processes needed for growth and proliferation (Delgoffe et al., 2011; Zeng et al., 2016). mTORC1 promotes metabolic processes through the transcription factors c-Myc, sterol regulatory element binding proteins (SREBPs) and HIF1α. c-Myc and HIF1α both support glycolysis by transcribing genes for glycolytic enzymes and transporters whilst SREBPs support lipid synthesis (Huang et al., 2020). In addition to its role in glycolysis, c-Myc supports anaplerosis of the TCA cycle via glutaminolysis (Wang et al., 2011; Jones et al., 2019). Mitochondrial oxidative function is also supported directly by mTORC1 through recruitment of a peroxisome proliferator-activated receptor gamma coactivator 1-alpha (PGC-1α) and inhibition of eukaryotic translation initiation factor 4E-binding protein (4E-BP)s (Summer et al., 2019). Furthermore, inhibition of 4E-BPs and activation of the ribosomal protein S6 by S6 kinase (S6K) supports protein translation essential not only to cell growth and proliferation but also for production of effector molecules (Magnuson et al., 2012). On the reciprocal side, mTORC1 signalling inhibits processes related to autophagy by negatively regulating associated protein function and inhibiting their transcription (Jiang et al., 2019).

mTORC2 primarily supports metabolism through phosphorylation and activation of AKT which can activate mTOR and support glycolytic function. In synergy with mTORC1's function preventing autophagy and promoting cell growth, apoptosis is inhibited by an mTOC2-AKT mediated inactivation of forkhead box transcription factors (FOXO) and BCL2 associated agonist of cell death (BAD) (Datta et al., 1997; Jacinto et al., 2006). mTORC2-AKT regulation of FOXOs also controls cellular trafficking to lymph nodes via transcription of CCR7 and CD62L (Kerdiles et al., 2009; Kerdiles et al., 2010). The combined effects of mTORC1 and mTORC2 neatly integrate extracellular signals with intracellular metabolism to drive cell growth, proliferation, survival and function. Interestingly, there is growing evidence that the balance between these two signalling pathways is an important factor for differentiation (Chi, 2012). mTORC1 is essential for Th1, Th2 and Th17 differentiation however, some evidence suggests that mTORC2 might be largely dispensable for Th1 and Th17

differentiation (Lee et al., 2010; Yang et al., 2013a). Conversely, T follicular helper cells are less metabolically active and do not require metabolic reprogramming through mTORC1 for differentiation (Ray et al., 2015). Similarly, both mTORC1 and mTORC2 are antagonistic to iTreg differentiation (Delgoffe et al., 2009).

Factors other than those related to mTOR also integrate cell signalling and metabolism. Store operate calcium entry (SOCE) is essential to T cell activation allowing translocation of the nuclear factor of T cell activation (NFAT) to the nucleus needed for transcription of IFN-γ (Kiani et al., 2001). Sarco/ER Ca2+-ATPase (SERCA) channels mediated termination of calcium flux is dependent on the glycolytic metabolite PEP, precisely integrating effector function, metabolism and TCR signalling (Ho et al., 2015). SREBPs sense intracellular sterol stores and are essential for exiting quiescence through supporting the lipid cholesterol and lipid metabolism required for rapid proliferation (Bensinger et al., 2008; Kidani et al., 2013). Beyond the general requirement of cholesterol for membrane stability, high density regions of cholesterol in the membrane, termed lipid rafts, facilitate strong TCR signalling (Yang et al., 2016).

1.3 Neonatal immunometabolism

Thus far, the vast majority of studies into immune cell metabolism in humans has been conducted in adults. This work has been instrumental in advancing our understanding of how these cells function, their environmental requirements and the mechanisms underpinning these parameters. However, cells of the neonatal immune system are known to differ in significant ways from their adult counterparts potentially serving in different roles and performing separate functions. Naturally, this raises the question “is neonatal immune metabolic function comparable to adults or specifically adapted to support time of life specific functions?”. At present, this is a difficult question to answer as little to no work has been performed to characterise the metabolic phenotype of neonatal immune cells or ascertain impact on effector functions. This section explores the current understanding of neonatal immune function and sets this against the backdrop of the immunometabolism.

1.3.1 Innate immune responses

The innate immune system provides front line cellular and humoral defence, through the release of cytokines and other mediators that amplify the immune response, recruitment of first responders and education of the adaptive immune response to help counter the threat and develop immunological memory. These processes demand energy and biosynthetic intermediates that are generated via cellular metabolic pathways (as above).

1.3.1.1 Neutrophils

Neutrophils comprise 70% of the leukocytes in human blood. They extravasate from the blood and quickly travel to the site of insult along a chemokine gradient typically released by tissue resident macrophages. Once in the tissues, neutrophils engulf and kill pathogens before undergoing controlled apoptosis. In neonates, there is a transient rise in neutrophil frequency shortly before birth, as measured by neutrophil derived soluble FcRIII (CD16) levels in plasma of preterm and term infants. However, neutrophil frequency reduces again shortly after birth to levels below that of adults, contributing to diminished first responder function (Carr et al., 1992; Basha et al., 2014). Neonatal neutrophils also have reduced functional capacity; their chemotaxis response is reduced through slower velocities and lower expression of the surface adhesion molecules L-selectin and Mac1, contributing to a near 50% reduction in neutrophil transmigration to the site of infection (Kim et al., 2003; Raymond et al., 2018). Lower expression of TLR4 and defective downstream signalling by myeloid differentiation primary response 88 (MyD88) and p38 MAPK from TLR4 and TLR2 impair neutrophil response (Al-Hertani et al., 2007). High levels of adenosine in neonatal blood increases cyclic adenosine monophosphate (cAMP) leading to protein kinase A (PKA)-dependent/ TLR-independent inhibition of tumour necrosis factor (TNF)α (Levy et al., 2006).

Some reports also show reduced capacity, or entire loss, of the primary effector functions of phagocytosis, neutrophilic oxidative burst and formation of neutrophil extracellular traps in neonatal neutophils (Yost et al., 2009; Basha et al., 2014). These are all energetically demanding requiring high levels of glycolysis, the main metabolic

pathway in neutrophils and, to a lesser extent, glutaminolysis to support them (Borregaard and Herlin, 1982; Rodriguez-Espinosa et al., 2015). Inhibition of these metabolic pathways can entirely prevent effector functions of adult neutrophils (Borregaard and Herlin, 1982; Rodriguez-Espinosa et al., 2015). For instance, NETosis is suggested to be dependent on lactate derived from glycolysis in both NOX-dependent and independent pathways (Awasthi et al., 2019) and, the key metabolic modulator AKT is implicated in driving chemotaxis along a chemoattractant gradient (Baruah et al., 2019). Cell polarised activation of the downstream target of AKT, mTOR, and subsequent activation of mitochondrial function is required to drive directional chemotaxis (Bao et al., 2015). Thus, mitochondria are required to perform essential neutrophil functions. Interestingly mitochondrial function in neutrophils is linked with developmental stage, as mature neutrophil precursors are more reliant on glycolysis and neutrophil immaturity is correlated with early neonatal sepsis (Riffelmacher et al., 2017; Saboohi et al., 2019). Whether changes in neonatal neutrophil metabolism are responsible for their decreased effector functions has not been elucidated but clearly warrants investigation.

1.3.1.2 Eosinophils

Elevated eosinophil counts, compared to the already high eosinophil count in the neonatal period, have been reported with infection in preterm infants and have been linked to later development of atopy (Juul et al., 2005). Little is known about the metabolic functions of eosinophils in general though experiments in adults show that eosinophils use glycolytic metabolism (Porter et al., 2018). However, eosinophil metabolic plasticity was demonstrated recently with both increased glucose derived lactate production, when reactive oxygen species are inhibited, and generation of TCA intermediates from both glucose and glutamine, on cytokine stimulation (Jones et al., 2020b). Although beyond the scope of this thesis, further work is needed to explore the role of metabolism in determining eosinophil function and to evaluate if there is any role for altered metabolism in eosinophilia in neonates.

1.3.1.3 Innate lymphoid cells

Innate lymphoid cells (ILC) are a group of innate immune cells that functionally mirror the CD4+ T helper populations, much the same way that natural killer cells mirror CD8+ cytotoxic function (Eberl et al., 2015). In humans type 2 ILC (ILC2) is the most functionally mature subset compared to ILC1 and ILC3 (Bennstein et al., 2021). ILC2 are found at epithelial barriers such as in the lung and are a major source of IL-5 that can induce eosinophilia. In mouse models ILC2 numbers rapidly increase in the lungs after birth, peaking at 3 times that of adults by day 10 but quickly decreasing to adult levels (Steer et al., 2017). The alarmin IL-33, produced by epithelial cells, recruits eosinophils and ILC2 to the lungs and acts as a potent activator of ILC2s (Steer et al., 2017). Despite higher IL-33 levels in the neonatal lung, ILC2 activation is not as potent as in adults. The high levels of endogenous IL-33 in the neonatal lung are suggested to train the ILC2 response for a more efficient response to challenges in later life (Steer et al., 2020). It is also worth noting that IL-33 signalling via ST2 under neonatal hypoxia is important for the expression of asthma related genes (Cheon et al., 2018). Given that HIF1α strongly induces glycolysis, this suggests that a highly glycolytic programme of ILC2s in early life might have harmful effects.

In adults, ILC2s have the capacity to augment mitochondrial respiration above basal conditions when activated with IL-33. Arg1 is suggested as key to the function of ILC2s as inhibition leads to decreased production of effector cytokines such as IL-5 and IL-13 accompanied by significantly reduced glycolytic capacity (Monticelli et al., 2016). Evidence indicating a glycolytic programme in ILC2 comes from experiments inhibiting glycolysis via PD1 which resulted in decreased expression of effector cytokines and reduced proliferation and cell survival (Helou et al., 2020). Conflicting evidence using helminth infection in mouse models suggests fatty acid oxidation, rather than glycolysis, is necessary for expansion and cytokine production by ILC2 (Wilhelm et al., 2016). Differing methods of ILC2 activation as well as differences between mouse and human responses may account for the conflicting results with further experiments needed to clarify this. Furthermore, given that neonates exhibit less potent responses than adults, despite increased IL-33 signalling, and the emerging role of metabolism

in ILC2 effector cytokine production, an investigation into the metabolic function of neonatal ILC2s is well warranted.

1.3.1.4 Monocytes/macrophages

Monocytes and macrophages perform key innate roles, clearing threats through phagocytosis and oxidative killing and contribute to adaptive responses through antigen presentation to T cells. Monocytes are better studied in neonates compared to macrophages as they can be isolated from blood. Studies of pattern recognition receptors (PRRs) are essentially restricted to TLRs and neonates have similar expression levels compared to adults. However, depending on the TLR target, neonatal monocytes demonstrate impaired TLR-mediated production of TNFα protein and other pro-inflammatory cytokines (Levy et al., 2004). Reduced expression of TNFα has been associated with high levels of adenosine, a metabolite with immunomodulatory properties. Adenosine acts via the A3 adenosine receptor inducing production of the secondary messenger cAMP which inhibits TLR-mediated TNFα production (Levy et al., 2006). Reduced MyD88 expression has also been implicated in failure to produce pro-inflammatory cytokines such as TNFα and IL-12p70. Whilst limiting innate immune responses, this reduced capacity to produce key cytokines along with reduced expression of human leukocyte antigen (HLA)-DR and co-stimulatory molecules such as CD40, at the basal state, also affect the ability to activate T cells (Han et al., 2004; Hegge et al., 2019). However, after LPS treatment, expression of co-stimulatory molecules, MHC-II and CD80, do not differ significantly to adults (Hikita et al., 2019).

Altered cellular metabolism is now emerging as a critical regulator of neonatal monocyte function, especially cytokine production. Whole blood transcriptomic data suggests significantly increased activity of glucose and cholesterol metabolic pathways. Three glycolytic regulatory nodes - glucose transporter GLUT3, glycolytic enzymes 6 phosphofructo-2-kinase and hexokinase 3 - were upregulated in response to infection, but the cellular provenance of these was not identified (Smith et al., 2014a). Examination of the epigenetic landscape on monocytes revealed unique histone modifications in the neonatal period with large differences in methylation at

points associated with metabolic genes (Bermick et al., 2016). Monocytes isolated from term and preterm umbilical cord blood have reduced glycolysis compared to adults. Glycolysis was required for cytokine production but not for phagocytosis which was unaffected by inhibition of glycolysis using 2-deoxy-D-glucose (2DG) (Kan et al., 2018). In another study monocytes derived from cord blood showed greater cytokine response one day post exposure to the BCG vaccine. However, by day 7 most cytokines were much lower in cord derived monocyte supernatants, excluding IL-10, and significantly less lactate was present. These findings suggest neonatal monocytes underwent tolerisation rather than effective trained innate immunity (Angelidou et al., 2021). More recently, umbilical cord blood monocyte derived macrophages were also shown to be broadly defective in glycolysis and to exhibit reduced oxidative phosphorylation compared to adult peripheral blood monocyte-derived macrophages (Dreschers et al., 2019). IL-10 polarised umbilical cord blood derived macrophages had adult-like levels of OXPHOS but reduced glycolysis. Recent evidence suggests, that reduced glycolysis may impair trained innate immunity which potentially utilises aerobic glycolysis for epigenetic reprogramming in marcrophages, enhancing future protective function (Fang et al., 2024). As for adenosine, circulating factors in umbilical cord blood seem to mediate this effect as treating adult peripheral blood derived macrophages with cord blood plasma dramatically inhibited glycolysis. This was attributed to high expression of the S100 proteins S100A8/A9 in neonates (Dreschers et al., 2019). Furthermore, cord blood monocyte derived macrophages have reduced expression of costimulatory CD80 and CD86 and reduced capacity to stimulate T cells (Dreschers et al., 2020).

Mammalian target of rapamycin (mTOR) and its downstream targets are essential for metabolic reprogramming of macrophages, with signalling through this pathway required for glycolytic reprogramming (Covarrubias et al., 2015). Surprisingly, mTOR transcripts are elevated in cord blood compared to adult blood derived macrophages but total mTOR protein expression and mTOR phosphorylation are both reduced compared to adults. This disparity suggests post-transcriptional regulation of mTOR expression in neonates. Downstream targets of mTORC1, ribosomal protein s6 and eukaryotic translation initiation factor 4E-binding protein 1 also showed reduced

expression and phosphorylation respectively compared to adults (Dreschers et al., 2019).

The findings summarised above highlight that monocyte metabolism is critical to regulating the neonatal immune response. As variation in TLR-mediated cytokine production is linked to the development of allergic disease by the child (Prescott et al., 2008; Tulic et al., 2011; Zhang et al., 2016) identifying possible metabolic determinants of this might provide insight into why this occurs and how it might be prevented or rectified. Therefore, links between metabolic control of innate cell function in neonates and immediate and long-term health outcomes deserve further investigation.

1.3.1.5 Natural Killer (NK) cells

Natural killer (NK) cells are crucial to the resolution of acute respiratory viral infections such as those caused by influenza or respiratory syncytial virus. Mature NK cells can be sub-divided into two main subsets, a CD56bright CD16dim subset which produces high amounts of inflammatory cytokines and CD56dim CD16bright, which are a highly cytotoxic subset (Vivier et al., 2008). NK cell function is regulated by the balance of inhibitory and activating receptors expressed on the cell surface, especially HLA-E binding members of the CD94/NKG2 family such as inhibitory NKG2A and stimulatory NKG2C and NKG2D (Shereck et al., 2019). Neonatal NK cells have been shown to consistently have reduced degranulation and cytotoxicity as well as reduced IFNγ production (Luevano et al., 2012; Strauss-Albee et al., 2017). This seems to be despite high degrees of similarity in phenotypic markers in comparison to adults, though upregulated expression of inhibitory NKG2A on cord blood CD56dim NK cells has been suggested to contribute to these reduced responses although this might be counterbalanced by upregulated NKG2D (Sundstrom et al., 2007; Shereck et al., 2019).

Emerging data about the role of metabolism in NK cell function identifies key pathways that are influenced by metabolic phenotype. Murine NK cells rely on OXPHOS for homeostatic function and acute responses such as cytokine production, following short-term activation (Keppel et al., 2015). In human NK cells, early cytokine responses can occur independent of glucose (Velasquez et al., 2020). Long-term activation of NK cells upregulates both OXPHOS and glycolysis to meet the metabolic demands of effector function (Keating et al., 2016), supported by increased expression of nutrient transporters such as GLUT1, CD98 and CD71 following stimulation (Keating et al., 2016; Jensen et al., 2017). Inhibition of OXPHOS limits NK cell IFN-γ production and degranulation, whereas glycolytic inhibition impairs cytotoxic functions such as target cell killing and degranulation (Keating et al., 2016; Wang et al., 2020). Regulatory factor mTORC1 is required for successful NK cell function – inhibition of its activity in murine NK cells prevents the upregulation of glycolysis needed for granzyme B and IFNγ production (Donnelly et al., 2014). mTORC1 activity is also needed for NKG2D-mediated IFNγ production in human NK cell subsets (Jensen et al., 2017). Given the importance of metabolic reprogramming for the function of NK cells as summarised here, metabolic differences may be a key determinant of altered function of neonatal NK cells.

Given the possibility that metabolism might underpin changes in neonatal NK cell function, this leads to the question of what local environmental factors might regulate NK cell metabolism in early life. Various factors abundant in the neonatal circulation like adenosine and S100A8/A9, as discussed above, might contribute to this along with TGF-β which is a candidate for regulating NK cell metabolism. TGFβ is abundant *in utero* and during early life (Power et al., 2002; Singh et al., 2013; Frost et al., 2014) and is known to affect NK cell function including inhibition of cytotoxicity (Trotta et al., 2008; Wilson et al., 2011) and of CD16-induced IFNγ production through SMAD3 repression of transcription (Trotta et al., 2008). These inhibitory effects of TGF-β have been attributed to its role in inhibiting cellular metabolism. In short term activation assays, IL-15-stimulated mouse and human NK cells treated with TGFβ had reduced mTOR signalling (primarily mTORC1), impaired cellular metabolism and reduced cytokine production (Viel et al., 2016). While this also might be mTORC1 independent

(Zaiatz-Bittencourt et al., 2018) it seems that TGFβ inhibits metabolic pathways, such as glycolysis and OXPHOS, in human NK cells. As efforts are made to understand neonatal NK cell metabolism, parallel efforts should consider the role of TGFβ and similar immunomodulatory cytokines.

1.3.1.6 Dendritic cells

Dendritic cells (DCs) have a critical role in educating and priming the adaptive immune response through integrating signals from the local microenvironment to modulate MHC, co-stimulatory molecules and cytokine expression, thereby orchestrating T cell activation and effector function. The two major groups of DCs in humans are classical (cDCs) and plasmacytoid (pDCs). These are typically found in a ratio of around 3:1 in adult peripheral blood but occur at a ratio of 1:3 (cDCs to pDCs) in umbilical cord blood (Borras et al., 2001). Neonatal monocyte derived DCs have been described to favour the Th2 biased cytokine effector function of neonates (Langrish et al., 2002). This might reflect that, despite similar expression of TLRs to adult DCs, neonatal DCs have altered cytokine responses after TLR stimulation. Reduced secretion of the Th1 inducing cytokine IL-12p70, along with decreased IFNγ secretion (Langrish et al., 2002) might underpin this. T cell activation by neonatal dendritic cells is further limited by high expression of IL-27, in response to antigens such as those present in the BCG vaccine (Bradford et al., 2023).

Upon stimulation with LPS, neonatal DCs also have attenuated expression of HLA-DR CD86, CD80 and CD40 that might contribute to their reduced capacity to activate naïve cord blood T cells (De Wit et al., 2003). Similarly, in murine neonatal models, DCs have been shown to efficiently migrate and be capable of antigen presentation but fail to upregulate co-stimulatory molecules in response to IFNγ (Lau-Kilby et al., 2020). Indeed, early colonisation of tissues by regulatory dendritic cells might also contribute to a tolerising environment whereby dendritic cells inhibit IFN-γ production and CD8+ T cell expansion (Silva-Sanchez et al., 2023).

In human adults, metabolic rewiring supports DC activation. During differentiation from monocytes and from bone marrow progenitor cells, DCs use OXPHOS as the

primary means of energy production (Wculek et al., 2019). On activation, DCs switch to a glycolytic metabolism and inhibition of glycolysis decreases surface expression of IL-12p70, MHC class I and class II as well as costimulatory CD40 and CD86 (Everts et al., 2014). When looking at specific subsets of DCs, pDCs use both glycolysis and glutaminolysis fuelled OXPHOS to support activation with inhibition of these pathways resulting in decreased expression of HLA-DR, CD80, CD86 and IFNα (Bajwa et al., 2016; Basit et al., 2018). However, cDCs rely more exclusively on glycolysis which is crucial for CD40 and IL-12 expression. In contrast to pDCs TLR stimulation reduces OXPHOS in cDCs (Basit et al., 2018). Given the known down regulation of co-stimulatory molecules and reduced cytokine production in neonatal DCs and the established links between these features and metabolism, it seems reasonable to conclude altered metabolism in neonatal DCs has a significant role to play.

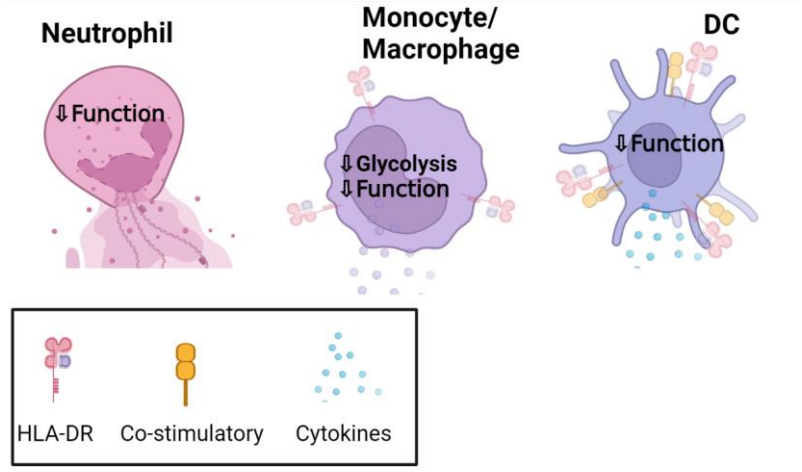

Figure 1.8 Neonatal immune function and metabolism in selected innate cells.

In general, neonatal innate cells show reduced functional capacity compared to adults. NET function in neutrophils is absent in the first days of life whilst monocytes/ macrophages and dendritic cells produce less inflammatory cytokines and express fewer HLA-DR and co-stimulatory molecules required for T cell activation. The function of these cells is dependent on the glycolytic pathway which is already known to be diminished in neonatal monocytes and macrophages; naturally, raising the question

of whether glycolysis plays a similar role in limiting the function of other neonatal innate cells. Figure made using Biorender.com.

1.3.1.7 Myeloid derived suppressor cells (MDSC)

MDSC are a heterogeneous population of early myeloid derived progenitor cells which share an immature state and the ability to suppress T cell activation. While dichotomised into monocytic MDSC (M-MDSC) and granulocytic MDSC (G-MDSC) subsets, in humans these phenotypes are poorly established. However, general consensus defines these subsets as CD11b+ CD14+ HLA-DR-/low CD15- and CD11b+ CD14-CD15+, respectively (Sica and Strauss, 2017). In adults, MDSC are typically associated with the proinflammatory environment of tumours and other chronic inflammatory conditions. As such, MDSC have been studied primarily for their immune suppressive role in the tumour microenvironment where they potently suppress T cell expansion and effector functions.

Recently in humans, the suppressive capacity of M-MDSC has been linked to specific metabolic adaptations. Compared to monocytes, the dicarbonyl metabolite methylglyoxal is 30-fold higher in M-MDSC inhibiting glycolysis in these cells (Baumann et al., 2020). M-MDSC also transfer cytoplasmic methylglyoxal to T cells in a contact dependent manner and inhibit T cell metabolic reprogramming to suppress their expansion and effector functions (Baumann et al., 2020). Methylglyoxal also selectively depletes L-arginine and L-glutamine (Baumann et al., 2020), which are both amino acids required for T cell function and might explain reports of depletion of L-arginine by MDSC (Rodriguez and Ochoa, 2008). Other studies have demonstrated that fatty acid uptake and FAO mediated by STAT3, STAT5 and lipid uptake by CD36 is required for generation of highly suppressive MDSC in the tumour microenvironment (Hossain et al., 2015; Al-Khami et al., 2017).

Compared to healthy adults, G-MDSC are transiently increased at birth with cord blood levels equivalent to those of cancer patients (Gervassi et al., 2014). G-MDSC frequency in neonates positively correlates with birth weight (Liu et al., 2019b). MDSC from healthy weight neonates have greater suppressive capacity than those from very low weight neonates, potentially indicating a link between nutrient availability and

MDSC function. Interestingly, breast milk lactoferrin is key to generating M-MDSC and G-MDSC able to suppress neonatal T cells, however, the same effect is not observed in adult MDSC (Gervassi et al., 2014; He et al., 2018). Additionally, lactoferrin treatment induced potent bacterial killing function in neonatal MDSC (Gervassi et al., 2014) demonstrating potential roles beyond immune suppression. In mouse models of neonatal necrotising enterocolitis lactoferrin treated MDSC are currently being investigated as a potential therapeutic due to their ability to suppress T cell activation and inflammation (Gervassi et al., 2014; Liu et al., 2019b).

1.3.2 Adaptive immune responses

The adaptive immune system of neonates is commonly described as immature. While memory T cells populations can be identified within the fetus, possibly arising from the fetal intestine (Zhang et al., 2014; Li et al., 2019b), nearly all neonatal T and B lymphocytes display markers of antigen inexperienced naïve cells (Basha et al., 2014; Zhang et al., 2014; Li et al., 2019b). Recent studies have also revealed the failure of human and mouse neonatal lymphocytes to differentiate into long lived memory cells and their reduced secondary responses upon antigen re-exposure (Cossarizza et al., 1996; Morbach et al., 2010; Tabilas et al., 2019).

1.3.2.1 B Cells

Neonatal B lymphocytes are almost exclusively antigen inexperienced naïve B cells. Neonates have reduced class switched antibody production, with almost no IgG or IgA antibody production on activation compared to adults which has been suggested to contribute to greater susceptibility to infection of neonates (Glaesener et al., 2018). Depending on the method of activation used, neonatal B cells exhibit either enhanced or reduced proliferation, leading researchers to conclude that whilst reduction in B cell proliferation may be observed in some settings; neonatal B cells do not have a general defect in proliferation. However, survival of neonatal B cells, across various subsets, is decreased across a range of activation methods using CpG-

oligodeoxynucleotides in combination with cytokines, such as IL-4, or with anti-CD40 antibodies (Glaesener et al., 2018). While much less is known about the immunometabolic features of B cells compared to other immune cells, we do know that unlike most other immune cells the upregulation of glycolysis does not appear to be crucial for their activation, proliferation or differentiation, despite increased import of glucose after activation (Waters et al., 2018). Rather, B cells appear to rely on OXPHOS to meet the demands of activation and proliferation, likely supported by glutaminolysis rather than glucose metabolism (Waters et al., 2018). Recent work has even demonstrated that germinal centre B cells can sustain proliferation through fatty acid oxidation without the need for aerobic glycolysis (Weisel et al., 2020). However, lactate dehydrogenase-A driven aerobic glycolysis is still a requirement for generation of germinal centre B cells from their naïve origins, demonstrating unique metabolic requirements for transition between these two cells states (Sharma et al., 2023). Additionally, glucose does seem to be required for class switch recombination which is known to be impaired in neonates (Glaesener et al., 2018; Waters et al., 2018). When assessing B cell subsets for enzymes related to glycolytic and oxidative metabolic pathways, naïve B cells were found to have the lowest expression across all enzymes examined. Memory subsets had higher expression of metabolic enzymes whilst plasma cells had the highest expression of all enzymes (Glass et al., 2020). A recently identified subset of B cells, now termed regulatory B cells (Bregs), characterised as $CD25^{hi}$ $CD38^{hi}$ perform important regulatory functions, promoting tolerance during pregnancy (Lima et al., 2016). Bregs suppress the immune system through direct cell to cell signalling via CD80/CD86, IL-10 and adenosine generation by the purine ecto-enzyme CD73. Bregs preferentially down-regulate IFNγ production along with the differentiation of Th1 and Th17 cells but not regulatory T cells (Tregs) (Blair et al., 2010; Flores-Borja et al., 2013). Increased frequency of Bregs in cord blood of neonates has been suggested to play a role in the altered immune response of neonates, with their suppressive role postulated to be primarily through production of IL-10 and costimulatory CD80/CD86 signalling to T cells (Sarvaria et al., 2016; Esteve-Sole et al., 2017). Alternatively, immune suppression can be achieved through the activity of CD73 which generates immune suppressive adenosine from ATP, in conjunction with CD39 (de Leve et al., 2019). However, adenosine production

is unlikely to be a mechanism used by neonatal Bregs for immune suppression as CD73 is markedly and selectively downregulated (Pettengill and Levy, 2016).

1.3.2.2 T cells

T cells are highly diverse and perform a multitude of specialised functions contributing to and orchestrating the immune response. Here the focus will be primarily on CD4+ (T helper), CD8+ (cytotoxic T cells) and CD4+FoxP3+ regulatory T cells.

1.3.2.3 CD4+ T helper cells

While the neonate is not devoid of memory CD4+ T cells, as already noted, neonatal CD4+ T cells are predominantly naïve (CD45RA+ CCR7+) and overwhelmingly display characteristics of recent thymic emigrants (RTEs) (Hassan and Reen, 2001). Neonatal CD4+ T cells that do not receive signals from IL-7 or other common γ chain cytokines are more susceptible to apoptosis leading to a high cell turnover rate (Hassan and Reen, 2001; Thornton et al., 2004). IL-7 promotes the survival and maturation of CD4+ RTEs without inducing differentiation (Soares et al., 1998) and this is supported by higher telomerase expression in neonates, which prevents shortening of the telomeres in this early stage of development (Schonland et al., 2003). This high IL-7 induced proliferative capacity is suggested to help maintain diversity in the T cell repertoire (Hassan and Reen, 1998) and, at least in mice, IL-7-induced neonatal T cell proliferation is linked to higher STAT5 activation, a signalling pathway shared with humans (Opiela et al., 2009). The metabolic requirements to support rapid T cell proliferation in neonates is unknown however, in adults, aerobic glycolysis and OXPHOS drive proliferation and differentiation of CD4+ T cells (Macintyre et al., 2014). Jones et al (2019) have previously shown a requirement for STAT5 signalling in very early adult naïve T cell activation. Inhibiting STAT5 in naïve but not effector or central memory CD4+ T cells resulted in reduced glutamine-dependent anaplerosis and loss of IL-2 production (Jones et al., 2019), highlighting the critical role of metabolic reprogramming and the use of glutamine in the very earliest stages of T cell activation in the periphery.

As mentioned earlier, CD4+ T cell cytokine responses are considered to be Th2 skewed in neonates in part due to altered functions of innate immune cells such as DCs. Additional to antigen presenting cells influencing neonate T cell phenotype through diminished IL-12-p70 (as discussed previously), monocyte derived pro-inflammatory cytokines have been shown to suppress IL-2 production inducing non-classical Th2 cells (Zhang et al., 2016). However, characteristic interleukin production of naïve CD4+ T cells also has been linked to epigenetic modification. Hypermethylation at CpG and non-CpG sites occurs within and adjacent to the IFNγ promoter region in neonatal naive CD4+ T cells and is accompanied by markedly reduced IFNγ production by neonates upon T cell activation (White et al., 2002). Although reduced IFNγ production is often reported in neonatal $\alpha\beta$ T cells it is however worth noting that neonatal $\gamma\delta$ T cells do not exhibit the same defect (Gibbons et al., 2009). Upon activation substantial metabolic rewiring is required for differentiation into effector cells capable of secreting lineage specific cytokines. Specifically, polyamine metabolism is an essential requirement for increased translation of enzymes required for the Krebs cycle. Loss of function in this pathway limits oxidative metabolism and prevents the chromatin remodelling needed for T helper lineage commitment (Puleston et al., 2021). This seminal study revealed a direct link between T helper lineage commitment and metabolism potentially revealing a mechanisms by which neonatal T cells might exhibit skewed helper functions.

In mice, neonates are poised for a Th2 type response. They exhibit pre-existing CpG hypomethylation at the CNS-1 locus when resting and CpG methylation at the CNS-1 locus remains lower than in adult mice after 5 days, under Th2 polarising conditions (Rose et al., 2007). In human neonates, the Th2 locus is extensively remodelled, with hypomethylation and permissive histone modifications selectively in Th2 cells cultured under Th2 polarising conditions (Webster et al., 2007). A novel subset of neonatal naïve CD31+ CD4+ T cells storing an unglycosylated isoform of IL-4, not present in adults, has also been described however any unique function of these cells has not yet been identified (Hebel et al., 2014). The relative balance of cytokines has implications in early life programming of later immune function and allergic disease risk in particular (Campbell et al., 2015). Greater expression of IL-13 at birth, along

with other epigenetic variations in metabolic genes such as *RPTOR, PIK3D and MAPK1*, have been linked with subsequent susceptibility to atopic disease in childhood (Webster et al., 2007; Martino et al., 2018). Reduced IFNγ at this time is a long-recognised hallmark of allergic disease risk (Tang et al., 1994). Therefore, there is much value in elucidating the immunometabolic regulation of T cell effector cytokine production at this stage of development to provide mechanistic insight and therapeutic targets for mitigating non-communicable disease risk.

T cell effector function has been linked closely with metabolism in various studies (Geltink et al., 2018) and may have a role to play in skewed T cell responses of neonates. Glycolysis is a specific requirement for IFNγ production in humans and in mice through post transcriptional regulation by the glycolysis enzyme GAPDH (Chang et al., 2013; Gubser et al., 2013; Jones et al., 2017). In vitro and in vivo blockade of glycolysis is also known to reduce expression of Th2 cytokines, IL-4 and IL-13 whether GAPDH has a role to play here too is still unknown (Tibbitt et al., 2019). Additionally, inhibition of PDH also blocked Th2 cytokine production by inhibiting post translational protein prenylation (Yagi et al., 2020). Furthermore, TGFβ signalling significantly inhibits mitochondrial complex V resulting in decreased ATP production and impaired IFNγ production in human CD4+ T cells (Dimeloe et al., 2019). Some work has begun to explore how altered mitochondrial respiration in neonates might contribute to altered T cell activity. So far, mitochondrial mass of neonatal CD4+ T cells has been shown to be lower than adults and accompanied by reduced levels of ATP (Meszaros et al., 2015; Aquilano et al., 2016). However, on activation of T cells from preterm infants higher calcium flux into the mitochondria than adults is observed along with increased ERK phosphorylation suggesting enhanced signalling for metabolic reprogramming (Palin et al., 2013). Calcium signalling itself is regulated by the glycolytic switch on TCR stimulation by PEP mediated inhibition of sarcoendoplasmic reticulum calcium ATPase (SERCA) leading to calcium accumulation in the cytoplasm and resultant NFAT signalling (Ho et al., 2015). However, despite greater calcium flux from the ER on activation nuclear translocation of NFAT still failed resulting in diminished IL-2 production (Schmiedeberg et al., 2016). Finally, nutritional regulation of T cell development has been shown in mice where oligosaccharide diets were

found to have a role in regulating neonatal Th1 type responses in respiratory syncytial virus infection models (Schijf et al., 2012). Such approaches might offer therapeutic strategies should immunometabolic signatures be found associated with disease outcomes.

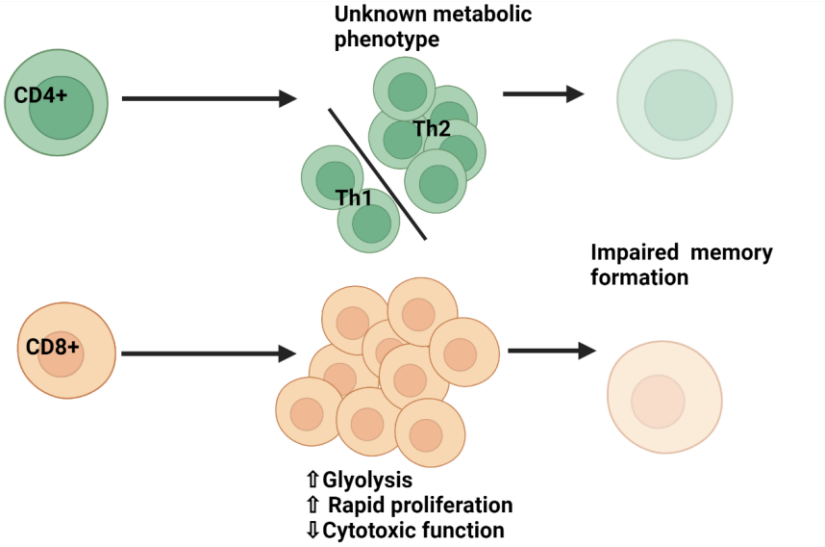

Figure 1.9 CD4+ and CD8+ T cell function and metabolism in neonates.

Neonatal T cells show are distinctly different from their adult counterparts. The circulating T cell compartment is comprised predominantly of naïve antigen inexperienced cells. On antigen encounter CD4+ (T-helper) responses are often described as diminished and Th2 skewed. Little is known about the metabolic characteristics of CD4+ cells in neonates but CD8+ T cells are more glycolytic which fuels rapid division but not cytolytic function. Figure made using Biorender.com.

1.3.2.4 CD8+ cytotoxic T cells

A number of features of neonatal CD8+ T cells have been associated with increased susceptibility of neonates to infection. CD8+ T cell responses in neonates are described as innate-like, with reduced cytotoxic capability and increased expression of anti-microbial protein transcripts (Galindo-Albarran et al., 2016). Exploration of the epigenomic landscape has revealed changes associated with lower TCR signalling and

cytotoxicity but higher expression of genes involved in cell cycle (Galindo-Albarran et al., 2016). In line with these findings, it is widely reported that neonatal CD8+ T cells are highly proliferative through homeostatic proliferation (Le Campion et al., 2002; Schonland et al., 2003; Schuler et al., 2004). This highly proliferative programme extends into activation (Smith et al., 2014b). Neonatal CD8+ T cells divide more than their adult counterparts over the first three days of activation with the cells entering division sooner after initial activation and each division then happening faster in neonates. Differentiation, measured by CD62L and Ly6C expression, also occurs faster in neonates yet they become terminally differentiated, shown by CD127 downregulation and KLRG1 upregulation, and fail to differentiate into long lived memory cells producing weak CD8+ T cell expansion on secondary challenge (Smith et al., 2014b; Reynaldi et al., 2016). Rapid proliferation and differentiation in neonates is suggested to impair the development of memory CD8+ T cells (Smith et al., 2014b). Studies in mice suggests a role for the inhibitor of let-7 microRNA, lin28b, in maintaining a naive-like phenotype by CD8+ T cells (Wang et al., 2016).

Carbon for de novo nucleotide synthesis is largely provided through metabolism of glucose to serine (Ma et al., 2019). Hence, murine neonatal CD8+ T cells preferentially rely on glycolysis to support their highly proliferative phenotype (Tabilas et al., 2019). Indeed, neonatal mice exhibit higher glycolytic metabolism than adults, a response attributable to functional programming by lin28b. High glycolytic metabolism was also linked directly to the inability of neonates to form memory populations with pharmacological inhibition of glycolysis with 2DG able to restore formation of memory cells (Tabilas et al., 2019). In comparison to mice, our understanding of human neonatal CD8+ T cell metabolism is not as well developed and what little evidence there is contradictory. For example, human umbilical cord blood CD8+ T cells have a propensity to differentiate into non classical T cytotoxic (Tc)2 cells when activated and this was associated with a decrease in glycolysis and an increase in fatty acid metabolism of Tc2 cells (Zhang et al., 2018). Much more work is needed to properly understand the role metabolism has to play in the fate of human neonatal CD8+ T cells.

1.3.2.5 Regulatory T cells

Regulatory T cells (Tregs) are crucial in preventing immune dysregulation and promoting peripheral tolerance and the subset defined by expression of the transcription factor forkhead box (FOX)P3 will be the focus here. It is also first worth mentioning that CD4+FOXP3+ non Tregs exist in humans which are suppressed but do not possess suppressor function (Miyara et al., 2009; Sada et al., 2016). Tregs have emerged as critical to the success of pregnancy playing a vital role in maternal tolerance of the fetus and immunoregulation more generally at the fetal-maternal interface (Jorgensen et al., 2019). Furthermore, maternal factors such as allergy have been suggested to reduce Treg suppressive function in the offspring (Cerny et al., 2018). IL-2R-STAT5 and TGFβ-SMAD signalling promote Treg differentiation through recruitment to CNS2 and CNS1 of the FOXP3 locus, respectively (Xu et al., 2010; Feng et al., 2014). Tregs have high mitochondrial mass, relying on OXPHOS via mitochondrial oxidation of pyruvate and lipids upon activation, unlike conventional T cells that primarily rely on aerobic glycolysis (Michalek et al., 2011; Beier et al., 2015). While proliferation of Tregs is fuelled primarily through OXPHOS, glycolysis appears to be crucial to the suppressor function of and migration of Tregs (Kishore et al., 2017). Enolase-1, a glycolytic enzyme, functions as a regulator of conserved non-coding sequence (CNS)2, preventing the transcription of a FOXP3 splice isoform containing exon-2 (FOXP3-E2) (De Rosa et al., 2015). Exogenous metabolites might also affect the stability of Tregs. Tregs have increased cell surface expression of ecto-nucleotidases CD39 and CD73, which convert ATP into immunosuppressive adenosine (Borsellino et al., 2007). In neonatal T cells CD39 expression is highest on activated Tregs, demonstrating the importance of their immunomodulatory function; the frequency of this population of Tregs correlates inversely with clinical severity of sepsis in neonates (Timperi et al., 2016). Intriguingly, neonatal CD4+FOXP3- T cells display a natural propensity to differentiate into Tregs (Thornton et al., 2004) likely reflecting suboptimal stimulation via TCR (Wang et al., 2010). Given the role metabolism has in determining T cell fate, an intrinsic metabolic programme in naïve neonatal CD4+ cells linked to early post-TCR activation events might favour the preferential generation of Tregs contributing to the development of immune tolerance at this time.

1.4 Thesis outline

As explored above, there is a growing understanding of immune cell metabolism and how it relates to phenotype and function. Key metabolic pathways have been identified in support of many of the functions of immune cells such as the dependence of NETosis on glycolysis or the requirement of glutaminolysis for T cell exit of quiescence (Awasthi et al., 2019; Jones et al., 2019). Furthermore, many of the functions of neonatal immune cells differ significantly from adults, with these functions often being diminished or entirely absent. Given the evident role of metabolism in many of these functions it seems highly plausible that difference between adults and neonates in many of these functions might be underpinned by differences in metabolic pathways. However, immunometabolism of neonatal cells is poorly understood. It is also worth considering that metabolic demands by the body in early life are drastically different from those of adults, as they must support a high growth rate and constant tissue remodelling. Thus, the metabolic function of neonatal immune cells might be adapted to compensate for these high energy demands. Indeed, differing metabolic profiles might even be necessary to support immune cell function geared toward growth and tissue remodelling. Improving our understanding of neonatal immune function and neonatal immunometabolism could provide valuable insights into potential therapies to reduce neonatal mortality as a result of disease and potentially elucidate new mechanisms for controlling adult immune function in health and disease.

This thesis will explore the T cell compartment of neonates in which naïve CD4+ T cells are highly abundant, in comparison to adults, and for the first time characterise the metabolic reprogramming of neonatal naïve CD4+ T cells on immediate, early and late stages of activation. The role of metabolite availability in defining CD4+ T cell phenotype and how this might influence T-helper function will also be explored, challenging the commonly held belief that neonatal T cells are poor IFNγ producers. Finally, this thesis will discuss differences in adult and neonatal neutrophil phenotype and function, which are thought to play a role an important role in early neonatal

health and disease, highlighting metabolism as key factor underlying impaired neutrophil function in neonates.

Chapter Two

2 Experimental procedures

2.1 Adult human blood collection

Human venous blood samples were collected between from healthy non-fasted volunteers, into heparinated Vacuettes™ (Greiner Bio-one, Frickenhausen, Germany) and immediately processed ex vivo. All samples were collected with informed written consent; ethical approval was obtained from Wales Research Ethics Committee 6 (13/WA/0190). Inclusion criteria were defined as healthy individuals aged 18-75 years of age who proved informed written consent. Exclusion criteria were defined as any blood borne infection; current cancer; pregnant breast feeding; diagnosed anaemia; evidence or history of clinically relevant disease such as any autoimmune diseases or type II diabetes.

2.2 Cord Blood collection

Blood samples from the umbilical cord, of healthy women delivering by elective Caesarean section, were collected into heparinated Vacuettes™ and immediately processed ex vivo. All samples were collected with informed written consent and ethical approval was obtained from Wales Research Ethics Committee 6 (11/WA/0140). Inclusion criteria were defined as healthy term women over the age of 18 who provided informed written consent. Exclusion criteria were defined as any blood borne infection; current cancer; diagnosed anaemia; evidence or history of clinically relevant disease such as any autoimmune diseases or type II diabetes.

2.3 Cell Isolation

Cell populations were isolated from peripheral adult whole blood and umbilical cord whole blood analysis using density gradient and magnetic associated cell sorting.

2.3.1 Mononuclear cell isolation

Mononuclear cells (MNC)s were isolated by diluting whole blood 1:4 with phosphate buffered saline (PBS; ThermoFisher, Massachusetts). 25-35 mL diluted whole blood was layered onto 15 mL sterile Lymphoprep™ (STEMCELL Technologies, Cambridge,

UK), before centrifugation at 400 x g for 40 min at room temperature. Separation by density centrifugation results in four distinct layers; plasma/PBS, MNC layer, Lymphoprep™ and red blood cells/ polymorphonuclear cells. Plasma/PBS was removed with a sterile plastic Pasteur pipette prior to carefully removing the MNC layer with a Pasteur pipette. Haemolysed samples, determined red colouration of the plasma fraction, were discarded. MNCs were washed twice with RPMI 1640 GlutaMAX™ (ThermoFisher Scientific, Massachusetts, USA) by centrifugation at 515 x g at room temperature. The resulting MNC pellet was resuspended in media appropriate for the downstream assay and cell density and viability determined using the Countess® automated cell counter (Life Technologies). Cell viability typically exceeded 95% but accurate counts from umbilical cord blood samples was hindered by the high abundance of red blood cells post density centrifugation.

2.3.2 Glycophorin depletion

Erythrocytes were depleted from isolated MNCs by positive selection using magnetic activated cells sorting (MACS). Erythrocytes are labelled with microbeads against glycophorin (CD235a). Counted MNCs were centrifuged at 300 x g for 10 min at room temperature. MNCS were resuspended in 80 µL MACS buffer (2% (V/V) fetal calf serum in PBS) per 10^7 cells and 10 µL, for adults, or 30 µL for neonates, per 10^7 cells of glycophorin microbeads (Miltenyi) were added. The cell microbead mixture was incubated for 15 min at 4°C then washed in MACS buffer by centrifugation at 300 x g for 10 min at 4°C. Washed cells were completely aspirated and resuspended in 500 µL MACS buffer, before loading onto the autoMACS® Pro separator (Miltenyi) and running a depletes separation whereby, the cell mixture is passed through two magenteic MACS® Columns which trap labelled cells whilst the negative (unlabelled) fraction is eluted (Miltenyi Biotech, 2024). Density and viability were again determined as in 2.4 with viability typically exceeding 95% for both adults and umbilical cords. Cell count for adults was usually in the range of 0.6 – 0.8 million cells per mL of starting whole blood volume. MNC count from umbilical cord blood varied substantially, depending on the quality of the sample but was typically between 2 million per mL of starting material.

2.3.3 Naïve CD4+ T cell isolation

CD4+ T cells were isolated via a negative selection MACS method. All other cell types are labelled with a cocktail of microbeads against CD8, CD14, CD15, CD16, CD19, CD25, CD34, CD36, CD45RO, CD56, CD123, TCRγ/δ, HLA-DR, and CD235a. Counted glycophorin-depleted MNCs were centrifuged at 300 x g for 10 min at room temperature. MNCs were resuspended in 40 µL of MACS buffer per 10^7 cells and 10 µL of CD4+ T cell biotin-antibody cocktail (Miltenyi) per 10^7 cells and incubated at 4°C for 5 min. Following the first incubation, 30 µL of MACS buffer per 10^7 cells and 20 µL of CD4+ T cell microbead cocktail (Miltenyi) per 10^7 and incubated at 4°C for 10 min, before loading cells onto the autoMACS® Pro separator and running a depletes separation. The unlabelled eluted fraction was centrifuged at 300 x g for 10 min at room temperature, before discarding the supernatant and resuspending in 1 mL PBS or growth medium for cell counting and counted as described in 2.4). Viability exceeded 95% and typical count for adults was around 90,000 naïve CD4+ T cells per mL of whole blood whilst the number was considerably higher from umbilical cord blood which was typically around 300,000 per mL of starting material although, this varied depending on the quality of the starting material.

2.3.4 Neutrophil isolation

Neutrophils were isolated using the MACSxpress® Whole blood Neutrophil Isolation kit (Miltenyi) via untouched negative selection. Firstly, lyophilized magnetic beads conjugated to monoclonal antibodies were reconstituted in 2 mL of buffer A. Reconstituted beads were either used immediately or kept for up to one week at 4°C. For labelling 4 mL of whole blood, 1 mL of reconstituted beads was mixed with an equal volume of buffer B before incubating at room temperature for 5 min with gentle mixing. The whole blood – magnetic bead mixture was then placed in the magnetic field of MACSxpress® Separator (Miltenyi) for 15 min. Unlabelled cells were recovered by carefully pipetting the supernatant into a new 15 mL falcon tube.

2.3.5 Erythrocyte depletion

After neutrophil isolation any remaining erythrocytes were removed by positive selection using MACSxpress® Erythrocyte Depletion Kit. Following collection of supernatant from neutrophil isolation, 20 µL of magnetic beads were added per 1 mL of supernatant and incubated for 5 min at room temperature with gentle mixing. The falcon was then placed in the magnetic field of the MACSxpress® Separator for 10 min before carefully pipetting of the supernatant into a new 15 mL falcon. The cell suspension was centrifuged at 300 x g for 10 min at room temperature and resuspended in 1 mL RPMI 1640 GlutaMAX™, or appropriate assay media, and cell counting was performed (2.4). Viability exceeded 95% and typical retrieval was 1 -2 million neutrophils per mL of whole blood for both adult and umbilical cord samples.

2.4 Counting Cells

Determination of cell count and viability were conducted using the Countess™ automated cell counter (Life Technologies). 10 µL of isolated cells were diluted appropriately and mixed with 10 µL of trypan blue (0.4%; Life Technologies). Cell suspension/ trypan blue mixture as applied to a Countess™ cell counting slide (Life Technologies); the image was focused, and density determined via equivalent counting of four 1 mm x 1mm squares on a standard haemocytometer. Exclusion of trypan blue was used for determining total live cell count. Downstream experimentation used live cell count multiplied by dilution factor used.

2.5 Bioenergetic analysis

To examine various metabolic parameters of isolated leukocyte populations Seahorse XFe24, XFe96, and XF HS mini analysers (Seahorse Bioscience) was used to measure extracellular flux. The ATP producing metabolic pathways, oxidative phosphorylation (OXPHOS) and glycolysis directly relate to two defined and measurable parameters, oxygen consumption rate (OCR; pmol/min) and extracellular acidification rate (ECAR; mpH/min) respectively. ECAR and OCR measurement was performed using an adherent cell monolayer with a transient microchamber. Using a series of metabolic

enhancer and inhibitor injections over time accompanied by measurements of dissolved oxygen and pH change enabled calculation of metabolic parameters. 24 h prior to the assay, the sensor cartridge was hydrated by the addition of XF calibrant solution to each well and incubated in a 37 °C non-CO_2 oven. 15 min before cells were ready for use in an assay, the calibration plate was loaded into the Seahorse analyser and calibration measurements made. The calibration plate contains both oxygen and pH sensors, linked to a fibre optic waveguide. Excitation signals are read as a fluorescent signal which is transmitted to a photodetector, enabling dual measurement of OCR and ECAR.

2.5.1 Adhesion to the Bioflux culture plate and initialisation of bioenergetic assays

The polyphenolic protein secreted by Mytilus edulis, Cell-Tak (Corning, Massachusettes, USA) diluted in 0.1 M sodium bicarbonate ($NaHCO_3$; Life technologies) was used at 22.4 μM per well, to attach isolated leukocytes to the bioflux plate (Seahorse, Bioscience, Copenhagen, Denmark). Cell-Tak was left to adsorb to the plate for 20 min where upon each well was washed twice with 200 μL of cell sterile, endotoxin free, water. All liquid was then removed from the plate and the plate left to dry completely. Each prepared plate was used immediately or stored for up to two weeks before use. Alternatively, a poly-D-lysine pre-coated 8 well plate was used (Agilent).

On the day of the assay, the cell culture plate was pre-warmed in a non-CO_2 incubator at 37°C. Assay media was prepared by supplementing either XF assay minimal media DMEM or XF assay media RPMI to a concentration of 5.5 mM glucose (Agilent), 1 mM pyruvate (Agilent) and 2 mM glutamine (Sigma), unless otherwise specified in each chapter. Assay media was then warmed to 37°C in water bath and brought to a pH of 7.4 by titrating with 1 M sodium hydroxide (NaOH; Sigma), before filtering (Millex® 33 mm sterile filter unit with Millipore Express® PES membrane with 0.22 mM pore, Ireland) and returning to the water bath. Isolated cells were resuspended in warm assay media counted (as in chapter 2.4) and seeded onto the warmed cell culture plate, leaving some wells to be filled with only assay media, as specified in each chapter. The plate was centrifuged at 200 x g for 1 min at room temperature with no

brake, to encourage the cells to adhere to the plate in a monolayer. Adhesion was visually inspected by light microscopy. Additional assay media was added to each well and the plate was transferred to a non-CO_2 incubator at 37°C for 45 min. At this time assay injections were added to the injection ports in the sensor cartridge, as specified in each chapter.

15 min prior to loading the cell culture plate, the calibration plate was loaded into the machine and calibration/ quality control measurements were performed. On passing calibration and quality control, the cell culture plate was loaded into the machine and cells were acclimatised for 15 min.

2.5.2 Oxidative phosphorylation

Metabolic parameters of the mitochondria were determined using a mitochondrial stress test. Firstly, oligomycin (Sigma) was added, at 1 μM, to block ATP synthase. This was followed by the injection of 1 μM carbonyl cyanide-p-trifluoromethoxyphenylhydrazone (FCCP; Sigma) an uncoupler of mitochondrial oxidative phosphorylation, enabling the maximum rate of respiration to be determined. Finally, 1 μM rotenone (Sigma), a complex I inhibitor, and 1 μM antimycin A (Sigmal), a complex III inhibitor were added to completely inhibit the electron transport chain. Mitochondrial parameters, basal respiration, ATP production, maximal respiration, spare respiratory capacity, proton leak and non-mitochondrial respiration were calculated according to Table 1.

Table 1 Calculations for mitochondrial stress assay

Table shows the mitochondrial parameters assessed by the mitochondrial stress assay and the formulas used to calculate each parameter.

Parameters	Equation
Basal respiration	$[OCR_{initial}]$mean - $[OCR_{rotenone/AA}]$median
ATP linked respiration	$[OCR_{initial}]$mean - $[OCR_{oligo}]$median

Maximal respiration	$[OCR_{FCCP}]$max - $[OCR_{rotenone/AA}]$median
Non-mitochondrial respiration	$[OCR_{rotenone/AA}]$medain
Proton Leak	$[OCR_{oligo}]$mean - $[OCR_{rotenone/AA}]$median
Spare respiratory capacity	$[OCR_{FCCP}]$max - $[OCR_{initial}]$mean

2.6 Flow cytometry

Flow cytometry was used to phenotype isolated MNCs and lymphocytes; determine purity of isolated lymphocytes; measure expression of surface and intracellular proteins and for functional assays. Experiments used either the Novocyte3000 or CytekAroura. Quality controsl were performed on both machines every day before use to ensure proper functional performance within expected parameters using NovoCyte QC particles (Agilent) and SpectroFlo® QC Beads (Cytek) respectively.

Both cytometers use a three lasers system, consisting of an ultraviolet (405 nm), blue (488 nm) and red (633 nm) laser, to excite antibody bound fluorophores, fluorescent dyes and other fluorescent molecules. In the Novocyte3000 the emission spectra are passed through dichromic mirrors to photo multiplier tube detectors to give a total of eight fluorescent channels plus forward and side scatter. In contrast, the Cytek aroura uses course wavelength multiplexing semiconductor detector arrays for a continuous measure of the emission spectra.

2.6.1 Surface marker staining

Surface marker immunofluorescent staining was performed by aliquoting 100,000 cells to 5 mL FACS tubes. Appropriate fluorescently tagged antibodies were added along with FACS buffer (0.2% (W/V) bovine serum albumin (BSA), 0.05% (w/v) sodium azide (Sigma-Aldrich) in PBS) to bring the final volume of each FACS tube to 100 µL which was then vortexed to mix the contents thoroughly. Additionally, unstained controls without the addition of antibody were also prepared by adding 100 µL of FACS buffer per tube. After incubating on ice for 30 min in the dark the cells were washed by adding 2 mL of FACS buffer and centrifuging at 515 x g for 7 min at 4°C.

Supernatant was tipped off and the tubes blotted on blue roll before being vortexed and analysed on the Novocyte3000 or CytekAroura.

2.6.2 Cell purity monitoring

Flow cytometry was used to determine the purity of MACS isolated naive CD4+ T cells and neutrophils. For purity monitoring of naïve CD4+ T cells, isolated cells were stained with Alexa Fluor™ 647 anti-CD4 (OKT4; Biolegend); FITC anti-CD45RO (UCHL1; Biolegend); Brilliant Violet™ 605 anti-CD45RA (HI100; Bioleged) and anti-CCR7, as described in chapter 2.6.1. In flow cytometry analysis, CD4+ cells were gated on and the percentage of CD4+CCR7+CD45RA+ (naïve CD4+ T cells) was determined with purity >90% deemed satisfactory.

For neutrophil purity monitoring, isolated cells were stained with CD15-FITC (as above). Followed by cell staining DRAQ7 staining (Chapter 2.6.3 below) and analysed on the Novocyte3000. Debris was gated out and live cells were assessed for expression of CD15. Purity of over 90% was deemed satisfactory.

2.6.3 Cell Death

Cell viability was determined by staining with DRAQ7™ (ThermoFisher) a membrane impermeable dye that stains double stranded DNA of dead or permeabilised cells, excited by a red (633 nm) laser with emission maxima at 678/697 nm. Post staining of surface markers (as described above) cells were resuspended in 100 μL of FACS buffer and DRAQ7™ was added at a concentration of 1 mM and the contents mixed thoroughly by vortexing. Cells incubated in the dark at room temperature for 15 min before washing in 2 mL of FACS buffer, centrifuging at 515 x g for 7 min at 4°C and tipping of the supernatant.

2.6.4 Intracellular staining

Intracellular proteins can be assessed by flow cytometry by first fixing and then permeabilising cells followed by staining with fluorescently tagged antibodies in permeabilising conditions. Here, intracellular proteins were examined using the True-

Nuclear™ buffer set (BioLegend®). Firstly, $1x10^5$ cells were aliquoted to 1 mL of True-Nuclear™ fix buffer in 5 mL FACS tubes, vortexed and incubated at room temperature in the dark for 45 min. Next, 2 mL of True-Nuclear™ permeabilisation buffer was added and the tubes were centrifuged at 300 x g for 5 min at room temperature. After centrifugation, supernatant was discarded and the cells were washed in 2 mL of True-Nuclear™ permeablisation buffer, as before. Supernatant was discarded and the cell pellet was resuspended in 100 µL of True-Nuclear™ permeabilisation buffer before adding the appropriate fluorochrome conjugated antibodies and incubating in the dark at room temperature for 30 min. After staining, cells were washed once in True-Nuclear™ permeablisation buffer and then a second time in FACS buffer. Prior to analysis on the Novocyte3000 the cell pellet was resuspended in 100 µL of FACS buffer and vortexed.

2.6.5 Mitochondrial mass

Mitochondrial content of cells was interrogated using the cell permanent mitochondrial specific dye MitoTracker™ Green (ThermoFisher). To stain mitochondria, 100,000 cells were incubated with 25 nM Mitotracker™ Green in 100 µL RPMI for 30 min in a CO_2 incubator at 37 °C. Cells were then washed twice by adding FACS buffer and centrifuging at 515 x g for 7 min at 4°C and discarding the supernatant. The cell pellet was resuspended in 100 µL of FACS buffer and emission spectra in the FITC channel analysed on the Novocyte3000.

2.6.6 Mitochondrial superoxide stain

The mitochondrial superoxide stain MitoSox™ red (ThermoFisher) was used as an indicator of mitochondrial activity. To stain mitochondrial superoxide, 100,000 cells in 100 µL were incubated with 1 µM of MitoSOX™ red for 15 min in a 5% CO_2 incubator at 37 °C for before being washed twice by addition of FACS buffer and centrifuging at 515 x g for 7 min at 4°C followed by discarding the supernatant. The cell pellet was resuspended in 100 µL of FACS buffer and emission spectra in the PE channel analysed on the Novocyte3000.

2.7 T cell culture

Cell culture plates were prepared in advance by coating with anti-CD3 antibodies (OKT). Anti-CD3 was diluted in PBS to a final concentration of 2 μg/mL and 200 μL was added to each well of a tissue culture treated 96 well flat bottom plate. Prior to addition of cell suspension anti-CD3 coating solution was removed, and wells were washed twice with PBS. Isolated naïve CD4+ T cells (described above) were washed into the appropriate culture medium, typically RPMI 1640 GlutaMAX™ or human plasma-like medium, by filling the falcon tube with media and centrifuging at 300 x g for 10 min at room temperature and counting as described above. Cells were added to the wells of the 96 well plate with media and anti-CD28 (diluted in matching culture media) to a final concentration of $1x10^6$ cells per mL in a total volume of 200 μL after addition of fetal calf serum 3 hours after initial plating. Cells were cultured in a 5% CO_2 incubator at 37°C incubator.

2.8 Protein immunoblotting

Semi quantitative analysis of protein expression was achieved by sodium dodecyl sulphate-polyacrylamide gel electrophoresis (SDS-PAGE) and western blot. In this process mixed protein samples are first separated by mass using SDS-PAGE. Proteins are denatured by heat in the presence of SDS which coats the denatured protein with a uniform negative charge. Negatively charged proteins can be separated in a polyacrylamide gel with a charge applied across it. Proteins migrate down the gel away from the negative cathode with the smallest mass proteins able to progress through the gel matrix at a faster rate than the more massive proteins thus separating the mixture of proteins by size. The negatively charged proteins in the gel can be transferred to a membrane for interrogation by antibodies. A primary antibody is used to target the protein of interest whilst a secondary antibody, conjugated to an enzyme, recognises the primary antibody and is used to generate a measurable chemiluminescent signal, on addition of enzyme substrates.

2.8.1 Sample preparation

Cell lysates were prepared from isolated cell populations for later analysis by western blot. Isolated cells were aliquoted into eppendorfs on ice and centrifuged at 515 x g for 7 min in a pre-chilled (4°C) centrifuge, to pellet cells. Supernatant was removed by pipette and 100 μL of phosphosafe™ (Sigma) was added per million cells to lyse the cells whilst preventing degradation of the sample. Cell lysates were stored at -20°C.

2.8.2 Protein quantification

A detergent compatible (DC) protein assay (Bio-Rad, Hemel Hempstead, UK) was used to quantify protein content of cell lysates. Cell lysates were defrosted on ice and centrifuged at 4°C for 5 min at 10000 x g and then returned to ice. A serial dilution of a 2mg/ml protein standard (TheroFisher) was added in duplicate at 5 μL per well in a flat bottom 96 well plate. 5 μl of cell lysate supernatant was added in duplicate to sample wells. 25 μL of a 2% v/v mixture of reagent A and reagent S were added to each well. Finally, 200 μL of reagent B was added to each well before incubating in the dark at room temperature with gentle agitation for 15 min. Absorbance was measured at 750 nm using a plate reader (POLARstar Omega). A linear regression was fit to the standard curve and used to determine protein content in the samples.

2.8.3 Sodium dodecyl sulphate-polyacrylamide gel electrophoresis (SDS-PAGE)

10 μg of protein lysates were added to x5 loading buffer (10% w/v SDS, 10mM β-mercaptoethanol, 20% v/v glycerol, 0.2 M Tris-HCL (pH 6.8) and 0.05% w/v bromophenolblue) and heated for 5 min at 95°C. Gel electrophoresis was performed by submerging the Bio-Rad mini_PROTEAN Tetra system (Bio-Rad) in x1 SDS-PAGE running buffer (25 mM Tris-HCL, 200 mM glycine and 0.1% w/v SDS; Sigma-Aldrich) and loading samples into the gel. To aid cutting of the membranes, a Precision Plus Protein All Blue Standard (Bio-Rad) molecular weight marker was added in parallel lanes. Gel electrophoresis was performed at performed at 120 V for an hour using a PowerpPack 300 (Bio-Rad).

2.8.4 Semi-dry membrane transfer

Before completion of the gel electrophoresis, Amersham Hybond-P polyvinylidene difloride (PVDF) membrane (GE Healthcare, Chicago, USA) was activated in methanol for at least 20 seconds then transferred to x1 transfer buffer (10% x10 Tris-glycine and 20% methanol). Blot absorbent filter paper was soaked in transfer buffer for 10 min. The SDS-PAGE gel was placed on the PVDF and sandwiched between the two pieces of filter paper. A Trans-Blot Turbo transfer system (Bio-Rad) was used to transfer the protein from the gel to the PVDF membrane at 25 V for 30 min. To prevent non-specific binding the PVDF was blocked using 5% (w/v) bovine serum albumin (BSA, Sigma-Aldrich) in Tris-buffered saline (TBS; Sigma-Aldrich) with 0.1% Tween 20 (pH 7.6; Sigma-Aldrich) at room temperature for an hour with gentle agitation.

2.8.5 Immunoblotting

Glycolytic proteins were examined by probing the membrane with antibodies against hexokinase I (HKI; C35C4), hexokinase II (HKII; C64G5), pyruvate kinase (PKM2; D78A4) and lactate dehydrogenase A (LDHA; C4B5). β-actin (8H10D10) was used to assess protein loading and to normalise expression. Blocked PVDF membranes were incubated with primary antibodies (diluted 1:1000 in block buffer) overnight at 4°C, with gentle agitation. The following day PVDF membranes were washed three times in TBST then incubated with either streptavidin-horse radish peroxidase (HRP) linked anti-rabbit (7074S; Cell Signaling) or anti-mouse secondary antibody (7076S; Cell Signalling), diluted 1:1000 in TBST, at room temperature for one hour. After incubation with secondary antibody, membranes were washed three times with TBST. Blots were imaged using the enhanced chemiluminescence (ECL; ChemiDoc XRS, Bio-Rad) by applying a 1:1 mixture of Amersham™ ECL Select™ Western blotting detection reagents A (luminol) and B (peroxide solution, Cytiva) to the membranes and exposing the blots for a period of 0.5 to 240 seconds, depending on the expression levels if the protein.

In some instances, typically for β-actin, antibodies were stripped from the blot with stripping buffer (Thermofisher) for no longer than 10 min at room temperature. The

PVDF membrane was washed three times with TBST, for 5 min each, before incubating with blocking buffer for 1 hour at room temperature. Proteins were then labelled with antibodies as described above.

2.8.6 Densitometry

Densitometry was used for semi-quantification of immune labelled proteins. Immunoblots were exposed to maximise exposure without saturation of the sensor and were then analysed with the Image Lab software (Bio-Rad). Lanes and bands were gated on manually and background noise removed before determining the histogram area and comparing to that of β-Actin loading control.

2.9 Microscopy

Cellular characteristics were assessed visually by microscopy using conventional chemical dyes and fluorescent dyes for high contrast images.

2.9.1 Slide preparation

Cell-Tak (Corning, Massachusettes, USA) was used to adhere the suspension cells to the surface of the glass slides. Initially Cell-Tak was diluted in 0.1 M sodium bicarbonate ($CHNaO_3$; Life technologies) to achieve a 22.4 μM solution and applied to the slides. Cell-Tak was allowed to coat the surface at room temperature for 20 min before the slides were washed three times by flooding with endotoxin free sterile water (ThermoFisher). Cell-Tak coated slides were left to dry completely before use.

2.9.2 Fluorescence dye staining

To stain cell structures using fluorescent dyes, $1x10^5$ cells were seeded onto Cell-Tak coated slides (2.5.1), in RPMI or assay appropriate media. Cells were fixed on the chamber slide in 10% formalin (Sigma) for 15 min at room temperature. Each chamber was washed twice by flooding with PBS before adding 200 μL of 100 ng/mL DAPI (4',6-diamidino-2-phenylindole; ThermoFisher) and incubating for 15 min at room

temperature. After washing the chambers, a further three times by flooding each well with PBS, the chamber compartment was removed from the glass slide and VECTASHEILD® mounting medium (Vector laboratories, California, USA) was added. A glass over slip was mounted onto the slide and the edges sealed.

2.9.3 Mitochondrial content staining

To image mitochondrial content $1x10^5$ cells were seeded onto Cell-Tak coated slides (2.5.1) in RPMI 1640 GlutaMAX™ and stained with MitoTracker™ Green in a 5% CO_2 incubator at 37 °C. Following incubation, each chamber well was washed twice by flooding with PBS before fixation and further staining as described in 2.9.2.

2.9.4 Mitochondrial superoxide staining

The mitochondrial specific superoxide stain, MitoSOX™ was used to image ROS produced by mitochondria. Firstly, $1x10^5$ cells were seeded onto Cell-Tak coated slides (2.8.1) in RPMI 1640 GlutaMAX™ and stained with MitoSox™ for 15 min, in a 5% CO_2 incubator at 37 °C. Following incubation, each chamber well was washed twice by flooding with PBS before fixation and further staining as described in 2.9.2.

2.9.5 Light Microscopy

For imaging of neutrophil nuclear structure, $1x10^5$ isolated neutrophils from adults or cords were seeded onto glass slides by cytospin centrifugation at 800 x g for 2 min. Cells prepared by cytospin were then stained with Kwik-Diff by briefly dipping the slides into reagent 1 five times and blotting the excess on absorbent paper. This procedure was repeated for reagents two and three before rinsing, by briefly dipping into distilled water. Slides were air dried at stored at 4 °C until imaging. Slides were imaged with the EVOS imaging system in the visible spectrum (ThermoFisher).

2.10 Enzyme linked immunosorbent assay (ELISA)

Specific cytokines or chemokines were measured in cell free culture supernatants using a sandwich ELISA in accordance with manufacturer's instructions. In a half area 96 well plate, capture antibody of interest was diluted to a working concentration in PBS. On the morrow, excess capture antibody was tipped off and 150 µL block buffer (1% BSA in PBS) was added to each well, for 1 h at room temperature with gentle agitation, to block the remaining protein binding sites. Block buffer was then discarded, and the plate washed three times with 200 µL/well washing buffer (0.05% Tween (Sigma-Aldrich) in PBS). Shortly before washing, samples and standards were thawed. Samples were diluted appropriately, and a serial dilution was made of the standard. Standards and samples were applied to individual wells and incubated at room temperature for 2 h with gentle agitation. After which, the plate was washed four times with washing buffer and detection antibody, diluted appropriately to a working concentration was added to each well. Again, the plate was incubated a room temperature for 2 h with gentle agitation. The plate was then washed four times with washing buffer and an appropriately diluted working concentration of HRP was applied to the plate for 20 min at room temperature with gentle agitation. After washing the plate thoroughly six times, a 50 µL 1:1 mixture of hydrogen peroxide and tetramethylbenzidine (TMB; BD Biosciences) was added to each well. The plate was left to incubate, in the dark at room temperature, until a blue colour developed then 1M sulphuric acid (H_2SO_4) was added 50 µL per well stopping the enzymatic function and turning the solution yellow. Absorbance was measured at 450 nm using a plate reader (POLARstar Omega, BMG, Germany) and the protein content calculated using the standard curve.

2.11 Data analysis, presentation and statistics.

Data were processed and statistics calculated using the tidyverse (version 2.0.0) and tidymodels (version 1.1) packages in RStudio (version 4.3.1) and graphs were produced using the ggplot2 package (version 3.4.3). As the number of samples tested did not reach a threshold for testing normality, the data could not be assumed to be normal. Therefore, non-parametric tests were used for statistical comparisons. For

comparing two unrelated groups, a Wilcoxon Rank Sum Test (also known as a Mann-Whitney U Test) was employed using the R stats function (version 3.6.2) wilcox.test. in cases where the data are paired, a Wilcoxon signed-rank test was employed using the wilcox_test function from rstatrix (version 0.7.2).

Chapter Three

3 Ex vivo characterisation of T cells in neonates and a detailed exploration of neonatal naïve CD4+ T cell metabolism

3.1 Introduction

T cells are an extremely diverse group of lymphocytes that perform a wide variety of functions throughout the body. Broadly, T cells can be categorised into two distinct groups TCR$\alpha\beta$ T cells, which comprise the vast majority of T cells in circulation, and TCR$\gamma\delta$ T cells (Morath and Schamel, 2020). However, within these categories there is a plethora of diversity for example mucosal associated invariant T cells, CD8+ cytotoxic T cells and invariant natural killer T cells are all examples of TCR$\alpha\beta$ cells (Kaminski et al., 2021). This chapter will focus on conventional HLA restricted TCR$\alpha\beta$ T cells. All T cells begin life as a haematopoietic stem cell originating in the bone marrow which differentiates into the common lymphoid progenitor and migrates to the thymus becoming a lymphoid progenitor before becoming a committed T cell progenitor, identifiable by the expression of CD1a (Cante-Barrett et al., 2017). As these progenitor CD4-/CD8-, double negative, cells develop through various stages the TCR-β loci are rearranged generating a pre-TCR. β-selection selects only those cells that have successfully rearranged their TCR-β chain which is paired with the pre TCR-α chain to make a pre-TCR that complexes with CD3 promoting survival and halting β-chain rearrangement. After maturation into double positive (CD8+ CD4+) cells, rearrangement of the TCR-α chain occurs, producing TCR$\alpha\beta$ T double positive cells (vonBoehmer and Fehling, 1997). At this stage cells are positively selected by interaction with peptides from self-antigens presented in major histocompatibility complexes (MHC) I and II. Cells that do not interact strongly enough with peptide in MHC die via apoptosis (Spits, 2002). This is followed by a negative selection in the medulla whereby antigen presenting cells (APC)s negatively select for TCR with overly strong response to peptides from self-antigens presented in MHC (Spits, 2002). Whilst the vast majority of self-reactive T cells die via apoptosis at this stage, a small but important fraction of self-reactive T cells survive, some of which will go on to become regulatory T cells, identified as CD25hi CD127lo FOXP3hi cells (Owen et al., 2019). Surviving non-self-reactive T cells down regulate one or other of the MHC restrictive co-receptors to become single positive - CD4+ or CD8+ naïve (CD45RA+ CCR7+) T (Tn) cell that enter the circulation and traffic to secondary lymphoid organs where they

await activation by APCs from peripheral tissues to initiate an antigen-specific immune response (Spits, 2002).

On activation T cells differentiate into effector cells (CD45RA+ CCR7-) that rapidly divide and are capable of producing effector molecules such as cytokines that are required for clearance of the initiating threat. This is followed by a contraction phase where the effector cells die off by apoptosis, but some T cells will have differentiated into long lived effector memory (CD45RA- CCR7-) or central memory (CD45RA- CCR7+) T cells (Sallusto et al., 1999). The exact path of this differentiation is still debated but strong in vivo evidence demonstrates a clear trajectory of differentiation to terminally differentiated effector cells (Berger et al., 2008; Gattinoni et al., 2011; Cano-Gamez et al., 2020) . The proportion of memory cells increases over the hosts lifespan as fewer naïve T cells are generated as thymic involution progresses with age and more memory cells are generated from antigen encounter. At birth, nearly all conventional T cells are antigen inexperienced naïve cells and Tregs form the majority of the memory T cell compartment (Kumar et al., 2018).

During differentiation T cells also take on a further set of functionally distinct programs each suited to a different mode of defence. The most well characterised of these are the T-helper phenotypes Th1, Th2, Th17 and Th22. These helper phenotypes are characterised by distinct transcription factors, cytokines and chemokines aiding separate functions (Szabo et al., 2000; Corripio-Miyar et al., 2022). Th1 cells aid the clearance of intracellular pathogens and are defined by the expression of transcription factor T-bet, IFNγ production and the chemokine receptor CXCR3. Th2 cells support humoral immunity, promoting B cell responses and are identified by the expression of GATA3 transcription factor, IL-4 and IL-13 production and the chemokine receptor CCR4 (Kim et al., 2001; Pai et al., 2004; Corripio-Miyar et al., 2022). Th17 cells help with the clearance of large extracellular pathogens like fungi but are also heavily involved in auto immune responses. RORγT and interferon regulatory factor 4 (IRF4) are master transcription factors for Th17 cells; IL-17 is a defining cytokine whilst co expression of CCR4 and CCR6 chemokine receptors can

also be used to identify them (Szabo et al., 2000; Brustle et al., 2007; Annunziato et al., 2012). Finally, Th22 cells support barrier integrity but are also implicated in allergic responses. Aryl hydrocarbon receptor is the key transcription factor controlling differentiation and IL-22 is a key cytokine product. Th22 cells can also be identified by surface co expression of CCR4, CCR6 and CCR10 (Trifari et al., 2009; Jiang et al., 2021). The ability to commit to one of these lineages is dependent on epigenetic remodelling fuelled by metabolic reprogramming and upregulation of TCA enzymes (Puleston et al., 2021). Interestingly, Tregs also show similar groupings of chemokine receptors leading to the suggestion of Th-like Tregs (Duhen et al., 2012; Halim et al., 2017). The distribution of Th-like Tregs has not been investigated in neonates though in general Th2 cells are suggested to dominate the T cell response in neonates (Debock and Flamand, 2014).

All of these T cell populations are fuelled by unique metabolic programmes that aid the specific functional demands of the cell type. Regulatory T cells are the most unique of these, relying primarily on fatty acid oxidation (FAO) and mitochondrial metabolism to support survival proliferation and some effector functions (Newton et al., 2016; Pacella et al., 2018; Field et al., 2020). However, Tregs still require glycolysis for effective trafficking and during early activation, glycolysis might be required to stabilise FOXP3 transcription (Sauer et al., 2008; Zeng et al., 2013). Likewise, memory T cells utilise fatty acid oxidation to meet much of their energy demand but are still dependent on other fuel sources such as glucose and glutamine to fuel expansion or re-exposure to antigen (Pearce et al., 2009; Taub et al., 2013; van der Windt et al., 2013). Naïve T cells are the most reliant on glycolysis and the least metabolically prepared for generating effector responses. All T cells are relatively metabolically inactive when in a quiescent state. However, on antigen presentation TCR and costimulatory receptors such as CD28 and 4-1BB induce metabolic reprogramming to exit the quiescent state and provide the necessary energy and precursors for rapid expansion (Gubser et al., 2013; Choi et al., 2017). Tcm and Tem have significantly greater mitochondrial mass than naïve T cells which supports a faster exit of quiescence into proliferation enhancing the rapid recall response and accelerated

pathogen clearance of memory responses (Jones et al., 2019). Naïve T cells on the other hand are more reliant on glycolysis, requiring a significantly greater glycolytic switch on activation but also rapidly inducing glutamine anaplerosis of the TCA cycle required for early IL-2 production (Gubser et al., 2013; Jones et al., 2019). Furthermore, emerging evidence indicates that individual T helper phenotypes are also underpinned by unique metabolic programmes driven by different metabolic signalling pathways. mTORC1 signalling may favour Th1 differentiation whilst highly glycolytic Th2 cells might be induced by greater mTORC2 signalling (Lee et al., 2010; Delgoffe et al., 2011; Ray et al., 2015). Sophisticated algorithms have been developed to take advantage of these distinct metabolic, and accompanying transcriptional differences, to link function and phenotype of T cells in health and disease as well as highlighting regulatory nodes (Wagner et al., 2021). Such tools exemplify the importance and impact of understanding T cell metabolism and its relation to cell function.

Despite its evident role in defining phenotype and function in adults little is known about the metabolic characteristics of human neonatal CD4+ T helper cells, which are known to exhibit a unique activation profile to adults (Holm et al., 2021). This chapter explores the T cell compartment in neonates and distribution of T helper cells in conventional and regulatory CD4+ populations. For the first time in the literature this chapter characterises the metabolic switch, for neonatal naive CD4+ T cells immediately on activation, the metabolic signalling pathways involved and the unique factors governing these responses. Additionally, early metabolic reprogramming, as naive cells exit quiescence is also explored here, for the first time.

3.1.1 Rationale

Neonatal T cells are predominantly naïve with most of the memory population emanating from the regulatory T cell compartment. Some evidence suggests that neonatal CD4+ T cells are programmed to be Th2 skewed however, it is unknown if the same holds true for regulatory T cells at this stage of development. Understanding the distribution of T-helper phenotypes could provide a better understanding of the

extent of Th skewing in neonates and whether this phenomenon is present before birth, as reflected though the memory compartment. Furthermore, early metabolic reprogramming of naïve T cells is essential for exiting quiescence and the production of effector molecules. However, the nature and extent of metabolic reprogramming in neonates is mostly unknown. This chapter explores the early response to TCR/CD28 signalling including mTOR signalling events and metabolic reprogramming, with the aim of shedding light on the mechanisms underpinning differences in neonatal versus adult T cell responses.

3.1.2 Hypotheses

1) Th2 skewing is a feature of the total neonatal CD4+ population reflected in the regulatory T cell population.
2) Metabolism is a distinctive feature differentiating adult and neonatal naïve CD4+ T cells.
3) Differences in early activation drive distinct metabolic programmes.
4) Metabolism underpins a unique functional profile of neonatal naive CD4+ T cells, post activation.

3.2 Methods

3.2.1 MNC isolation

Non-pregnant adult human peripheral blood, from healthy non-fasted donors, or umbilical cord blood from elective caesarean sections was collected into heparinised Vacuettes™ (Greiner Bio-one. Frickenhausen, Germany), as described in sections 2.1 and 2.3. MNCs were isolated by density centrifugation, as in chapter 2.3.1, washed and resuspended in PBS. MNC cell number was determined, as in chapter 2.4.

3.2.2 Characterisation of CD4+ and CD8+ T cells from MNCs by flow cytometry

0.5 x 10^6 MNCs in suspension were stained in 200 μL FACS buffer (as described in 2.6.1) with anti-CD4, anti-CD8, anti-CD45RA, anti-CCR7, anti-CXCR3, anti-CCR4, anti-CCR6 and anti-CCR10 as detailed in Table 3.1. Stained cells were acquired with the ACEA Biosciences Novocyte 3000 and data analysed in FlowJo version 10.9. To aid

with placement of gates, initial fluorescence minus one experiments (FMO) for the chemokine markers (CXCR3, CCR4, CCR6 and CCR10) were conducted in healthy adult samples.

Table 2 Total T cell antibody panel

Indicating the antibody target, clone and fluorophores used.

Antibody	Clone	Fluorophore	Supplier
Anti-CD4	REA623	VioGreen	Miltenyi
Anti-CD8	BW135/80	VioBlue	Miltenyi
Anti-CD45RA	REA562	APC vio-770	Miltenyi
Anti-CCR7	REA108	PE	Miltenyi
Anti-CXCR3	REA232	Viobright FITC	Miltenyi
Anti-CCR4	L291H4	Brilliant violet 605	BioLegend
Anti-CCR6	REA190	PE vio-615	Miltenyi
Anti CCR10	REA326	APC	Miltenyi

3.2.3 Characterisation of CD4+CD25^{hi}CD127^{lo} (Treg) cell populations from MNCs by flow cytometry

0.5 x 10^6 MNCs in suspension were stained in 200 µL FACS buffer (as described in 2.6.1) with anti-CD4, anti-CD8, anti-CD45RA, anti-CCR7, anti-CXCR3, anti-CCR4, anti-CCR6 and anti-CCR10 as detailed in Table 3.1. Stained cells were acquired with the ACEA Biosciences Novocyte 3000 and data analysed in FLowJo version 10.9. To aid with placement of gates, initial FMO for the chemokine markers (CXCR3, CCR4, CCR6 and CCR10) were conducted in healthy adult samples.

Table 2 Antibody panel for Treg cells.

Indicating the antibody target, clone and fluorophores used.

Antibody	Clone	Fluorophore	Supplier
Anti-CD4	REA623	VioGreen	Miltenyi
Anti-CD45RO	REA611	VioBlue	Miltenyi
Anti-CD127	REA614	APC vio-770	Miltenyi
Anti-CD25	REA945	PE	Miltenyi
Anti-CXCR3	REA232	Viobright FITC	Miltenyi
Anti-CCR4	L291H4	Brilliant violet 605	Biolegend
Anti-CCR6	REA190	PE vio-615	Miltenyi
Anti CCR10	REA326	APC	Miltenyi

3.2.4 Analysis of naïve CD4+ T cell transcriptomics

Data from published transcriptomic data of 12 adult and 12 umbilical cord blood naïve CD4+ T cells were accessed from the NCBI gene expression omnibus (GSE) repository accession GSE135467. Data were read into R (version 4.3.1) using GEOquery (Bioconductor 3.17). Raw counts were log2 transformed and examined for normalisation using Biobase (version 2.32.0). Intra group correlation was determined by Pearson correlation coefficient with the package stats (version 3.6.2). Following the removal of background expression, determined as expression levels in the lower quartile and/or expressed by two or less donors, and identification of unique identifiable transcripts, a linear model was fit to the data to determine differentially expressed genes (Limma; Bioconductor 3.17).

The KEGG database was accessed via the R package KEGGREST, to curate a list of genes associated with the following KEGG metabolic pathways and selected T cell signalling pathways "04010", "04350", "04630", "04066", "04020", "04070", "04024", "04024", "04151", "04152", "04150", "00510", "00515", "00250", "00260", "00270", "00280", "00290", "00300", "00310", "00220", "00330", "00340", "00350", "00360", "00380", "00190", "00061", "00062", "00071", "00230", "00240", "00010", "00020", "00030",

"00051", "00052", "00053", "000570", "000620", "000630", "000640", "000650", "00562", "04110", "04660", "04648". Over representation of this gene set, in the differentially expressed genes, was assessed in the total gene set using Fisher's exact test (stats version 3.6.2).

Gene set enrichment analysis (GSEA) was conducted using the set of differentially expressed genes, ranked by log fold change and p value, present in the curated list of genes described above. The WikiPathways repository, along with the rWikiPathways (Bioconductor 3.17) and ClusterProfiler (Bioconductor 3.17) (Wu et al., 2021) R packages were used to perform GSEA.

3.2.5 Naïve CD4+ T cell isolation, purity monitoring and cell culture

Following Mononuclear cells (MNC) isolation (section 2.3.1), CD235a antibody labelled magnetic microbeads were used to deplete erythrocytes (autoMACS; Miltenyi Biotech; see section 2.3.2). Here, 10 μL of beads were used per 10^7 adult MNCs whilst 30 μL of beads were used per 10^7 umbilical cord blood (UBC) MNCs. CD235a depleted MNCs were resuspended in PBS before cell density was determined (Chapter 2.4). Naïve CD4+ T cells were isolated from MNCs by negative selection with antibody labelled magnetic microbeads from Miltenyi's Naive CD4+ T cell isolation kit II (autoMACS; Miltenyi Biotech; see chapter 2.3.3). Isolated naïve CD4+ T cells were resuspended in PBS and purity was determined using flow cytometry for Alexa Fluor™ 647 anti-CD4 (OKT4; BioLegend); FITC anti-CD45RO (UCHL1; BioLegend); Brilliant Violet™ 605 anti-CD45RA (HI100; BioLegend) and BV421 anti-CCR7 (G043H7; BioLegend) (see section 2.6.2).

Naïve CD4+ T cells counted in PBS were washed into RPMI GlutaMAX media and cultured at 1 x 10^6 cells/ mL with or with 2 μg/mL plate bound anti-CD3 (OKT3; Biolegend) and 20 μg/mL soluble anti-CD28 (CD28.2; BioLegend) in a 24 well tissue culture treated plate with a total volume of 1 mL after supplementation with 20% fetal calf serum after 3 hours. Cells were cultured for 16 h at 37°C in 5% CO_2 before

harvesting by gentle pipetting and centrifuged at 515 x g for 7 min at 4°C to separate cells and supernatant. Cells were stained with 1 μM DRAQ7 (Thermofisher) and PE anti-CD25 (REA945; Miltenyi), to determine cell death and activation by flow cytometry (staining detailed in section 2.6.2) whilst culture supernatant was stored at -20°C for later analysis.

3.2.6 Immunoblotting

Determination of protein by western blot was carried out as described in section 2.7. In brief 1 x 10^6 ex vivo or cultured (section 2.2.5) naïve CD4+ T cells were lysed in Phosphosafe™ and stored at -20°C. Protein content was determined by DC assay (chapter 2.7.2) and 10 μg of protein from each donor was separated by SDS-PAGE (Chapter 2.7.3). Separated proteins were transferred to PVDF membrane through a semi dry transfer (chapter 2.7.4). Glycolysis proteins of ex vivo and cultured cells were examined by probing the membrane with antibodies against hexokinase I (HKI; C35C4), hexokinase II (HKII; C64G5), pyruvate kinase (PKM2; D78A4) and lactate dehydrogenase A (LDHA; C4B5). For 16 h cultured cell lysates, blots were probed with HKII (C64G5), LDHA (C4B5), mitochondrial pyruvate carrier protein (MPCP) 1 (D2L9I), MCP2 (D4I7G), glutaminase (GLS) 1 (E4T9Q) and peroxisome proliferator-activated receptor gamma coactivator 1-alpha (PGC-1α) (3G6). β-actin was used to assess protein loading and to normalise expression. All antibodies were purchased from Cell Signalling Technology.

3.2.7 Flow cytometry of naïve CD4+ T cells

Cell death ex vivo was determined by 1 μM DRAQ7 staining and dead cells were excluded when determining cell activation, as monitored by surface staining (see chapter 2.6.1) of Pacific blue anti-CD25 (M-A251; Biolegend), FITC anti-CD44 (REA690; Miltenyi Biotech) and PE anti-CD69 (FN50; Biolegend). Additionally isolated nCD4+ T cells were stained separately with APC anti-CD98 (REA387; Miltenyi), to determine surface expression of the large neutral amino acid transporter, or jointly with FITC

anti-CD3 (OKT3; Biolegend) and APC anti-CD28 (REA612), to assess surface expression of the target stimulatory markers, as described in section 2.6.1.

One hour post activation with plate bound anti-CD3 (2 μg/mL) and anti-CD28 (20 μg/mL), naïve CD4+ T cells were fixed and permeabilised using the True-Nuclear™ buffer set (BioLegend®) and stained with intracellular Vio® B515 anti-pS473-AKT (REAfinity™; Miltenyi), PE anti-Hu/Mo Phospho-mTOR-Ser2448 (MRRBY; Invitrogen) and APC anti-pS235/pS236-S6 (REA454; Miltenyi), as described in chapter 2.6.4.

Mitochondrial mass of ex vivo and 16 h cultured cells was measured with the cell permanent mitochondrial specific dye MitoTracker™ Green (ThermoFisher) by incubating cells with the dye at 37°C for 30 min at 5% CO_2 (See chapter 2.6.5). Mitochondrial superoxide production was determined, in naïve CD4+ T cells ex vivo and after 1 hour culture with or without anti-CD3 (2 μg/mL) and anti-CD28 (20 μg/mL) with the stain MitoSox™ Red (ThermoFisher); cells were incubated with 1 μM of MitoSOX™ Red for 15 min in a 5% CO_2 incubator at 37 °C and washed before analysis by flow cytometry (see section 2.6.6)

Activity of the large neutral amino acid transporter 1 (SLC7A5) was assessed via uptake of auto-fluorescent kynurenine (Sinclair et al., 2018). To begin, $2x10^5$ freshly isolated naïve CD4+ T cells were aliquoted to each of five FACS tubes and washed with 2mL phenol red free Hanks buffered salt solution (HBSS; Gibco) by centrifugation at 515 x g for 7 min at room temp. Cells in each FACS tube were resuspended in 200 μL HBSS at 37°C. Reagents were added to each FACS tube according to the Table 4, with kynurenine being added last, all reagents were kept at 37°C.

Table 4 Reagent combinations for Kynurenine uptake assay

Table showing the different conditions/ controls and the amounts of each reagent used in the kynurenine assay.

	HBSS	Kynurenine (800 µM)	BCH (40 mM)	Lysine (20 mM)
Negative control	200 µL	-	-	-
Kynurenine uptake	100 µL	100 µL	-	-
Non-competitive Inhibitor control	-	100 µL	100 µL	-
Competitive inhibitor control	-	100 µL	-	100 µL
Kinetic (temperature) control	100 µL	100 µL	-	-

The kinetic (temperature) control was placed immediately on ice. All tubes were incubated for 4 min before 125 µL of Paraformaldehyde (37°C) was added to each FACS tube, stopping the uptake of kynurenine. After incubation at room temperature in the dark for 30 min, cells were washed twice with 0.5% BSA in PBS by centrifugation at 515 x g for 7 min. Washed cells were resuspended in 200 µL and analysed on the Novocyte3000 (ACEA biosciences) data was processed using FlowJo version 10.9.

3.2.8 Confocal microscopy

Mitochondria were visualised after MitoTracker™ and MitoSox™ staining by confocal microscopy as described in sections 2.9.3 and 2.9.4. Briefly, 100,000 cells were seeded in RPMI GlutaMAX™ onto Cell-Tak™ coated 8 well chamber slides. For mitochondrial biomass staining, directly ex vivo cells were incubated with 25 nM MitoTracker™ Green for 30 min at 37°C and 5% CO_2. For mitochondrial superoxide staining cells were either left unstimulated or activated with 2 µg anti-CD3 and 20 µg anti-CD28 for 1 h at 37°C and 5% CO2, before 1 mM MitoSox™ Red was added for an additional 15 min. Following stimulation, cells were fixed with 10% formalin and washed twice with PBS, followed by staining with DAPI (100nM; ThermoFisher) for 10 min at room

temperature. Wells were washed thoroughly with PBS before adding mounting media and cover slips for imaging at ×63 magnification using a laser scanning confocal microscope (Zeiss LSM710). Captured images were analysed using the Zen 3.4 software (Zeiss).

3.2.9 Bioenergetic assays

Bioenergetic analysis of nCD4+ T cells was conducted using the XFe8 and XFe96 Seahorse Extracellular Flux Analysers (Seahorse Bioscience), as detailed in chapter 2.5. For base line ex vivo experiments, freshly isolated naïve CD4+ T cells were resuspended in Seahorse XF RPMI assay medium supplemented with 5.5 mM glucose (Sigma), 1 mM pyruvate (Sigma) and 2 mM L-glutamine (Sigma) and 70,000 cells seeded onto a PDL coated XF microplate (Agilent). OCR (pmoles/min) and ECAR (mpH/min) were measured simultaneously. Mitochondrial and glycolytic parameters were determined by injections of oligomycin (0.75 µM; Sigma), FCCP (1 µM; Sigma) and rotenone and antimycin A (both 1 µM; Sigma). Alternatively, to measure the change in metabolic flux on in situ activation and assess the role of glutamine, ex vivo naïve CD4+ T cells were resuspended in Seahorse XF RPMI assay medium supplemented with 5.5 mM glucose (Sigma), 1 mM pyruvate (Sigma) with or without 2 mM L-glutamine and seeded onto PDL microplates. ECAR/OCR were measured simultaneously continuously for 15 min before injection of anti-CD3 (2 µg/mL; HIT3a, BioLegend) and anti-CD28 (20 µg/mL; CD28.2, BioLegend) and thereafter for 2 h. Immediately following this, mitochondrial and glycolytic parameters were determined by injection of oligomycin, FCCP and rotenone/antimycin A, as described above.

Realtime assessment of metabolite requirements for glycolysis and mitochondrial respiration were determined after 16 h culture with anti-CD3 (2 µg/mL) and anti-CD28 (20 µg/mL). Harvested cells were counted (section 2.4) and resuspended in Seahorse XF RPMI assay medium supplemented with 5.5 mM glucose (Sigma), 1 mM pyruvate (Sigma) and 2 mM L-glutamine (Sigma) and 2 x 10^5 cells were seeded onto Cell-Tak coated microplates (section 2.5.1). Baseline measurements of ECAR and OCR were

recorded, continuously for 15 min before injection of UK5099 (2 μM; Sigma), BPTES (3 μM; Sigma) or etomoxir (3 μM; Sigma), which inhibit MCP, GLS1 and CPT1a respectively, and continuously measured for 40 min which was followed by injections of oligomycin, FCCP and rotenone/antimycin A to determine glycolytic and mitochondrial parameters.

3.2.10 Extracellular lactate assay

L-Lactate in cell culture supernatant was measured by colorimetric assay according to the manufacturer's instructions (L-Lactate assay Kit; abcam). Naïve CD4+ T cells were cultured with or without anti-CD3/28, described in chapter 3.3.5. Culture supernatant was harvested by resuspending cells in culture and centrifuging at 300 x g for 10 min and removing the supernatant for storage at -20°C for later analysis. On the day of analysis, supernatant was defrosted on ice and centrifuged at 10,000 x g, 4°C for 10 min to remove any debris. To conduct the assay, the resulting culture supernatant was diluted 10x with assay buffer and added to a reaction mix. A standard curve and background wells were prepared at the same time. Samples and standards were incubated at room temperature for 30 min, protected from light. The plate was read at OD570nm, using the FLUORstar Omega Microplate Reader (BMG Labtech).

3.2.11 Protein array

43 proteins were assessed simultaneously in the culture supernatant using the RayBio® C-Series human Angiogenesis antibody array C100 (RayBiotch; Georgia), according to the manufacturer's instructions (RayBiotech; Georgia), In brief, antibody array membranes were blocked in blocking buffer for 30 min at room temperature. After removing the blocking reagent, antibody array membranes were incubated with culture supernatant overnight at 4 °C. The following day, supernatant was removed, and membranes were washed four times in wash buffer, 5 min at room temperature each time. Biotinylated antibody cocktail was added to each membrane and incubated at 4°C overnight. The following morning, membranes were washed four times in wash buffer for 5 minutes each at room temperature which was followed by the addition of *HRP-Streptavidin* for 2 hours at room temperature and another 4

washes in wash buffer for 5 min at room temperature. Following these procedures, membranes were transferred printed side up to a blotting paper and a 1:1 mixture of Amersham™ ECL Select™ Western blotting detection reagents A (luminol) and B (peroxide solution, Cytiva) were added to the membranes and the membranes were imaged using the ChemiDoc system (Model details; BioRad). Using Image Lab (BioRad), intensity values were determined by densitometry and normalised to the positive control and background reading was subtracted from all targets.

3.2.12 ELISA

IL-2, IL-10, CXCL8 and IFNγ were measured in supernatants of naïve CD4+ T cells cultured for 16 h with or without anti CD3/28 (Chapter 3.3.5) by ELISA, as described in chapter 2.9. Culture supernatant was harvested by resuspending cells in culture and centrifuging at 300 x g for 10 min at 4 °C and removing the supernatant for storage at -20°C for later analysis. On the day of analysis, supernatant was defrosted on ice and cytokines determined separately by specific ELISAs for IL-2, IL-10, CXCL8, IFNγ (DuoSet; R&D Systems)

3.3 Results

3.3.1 The T cell compartment in adults and neonates

To assess the memory populations of CD4+ T helper and CD8+ cytotoxic PMCs from adults and cord blood (representative of neonates) were stained for CD4, CD8, CD45RA and CCR7 and analysed by flow cytometry. Duplets were removed before gating on lymphocytes followed by gating on CD4 and CD8 single positive populations. (Figure 3.1A-C). Naïve cells were identified as CD45RA+ CCR7+, central memory (CM) as CD45RA- CCR7+ effector memory (EM) as CD45RA- CCR7- and effectors (EMRA) (Figure3.1D). Similar CD4/CD8 ratios ($p = 0.95$) were seen in adults and cords with larger CD4+ populations than CD8+ (Figure 3.1E). As expected, naïve cells dominated both CD4+ (93% ± 1.6) and CD8+ (83% ± 1.5) T cell compartments in neonates however there was a noticeable population of CD8+ EMRA cells (7.8% ± 0.8). Naïve T cells also represented the largest single population in adult CD4+ (61% ± 3.4) and

CD8+ (58% ± 5.1) cells however adults also exhibited EM populations in both T cell populations. Similar to cords the CD8+ fraction also contained a notable EMRA population (11% ± 2.7) and a very small CM compartment (4.4% ± 0.5) (Figure 3.1F).

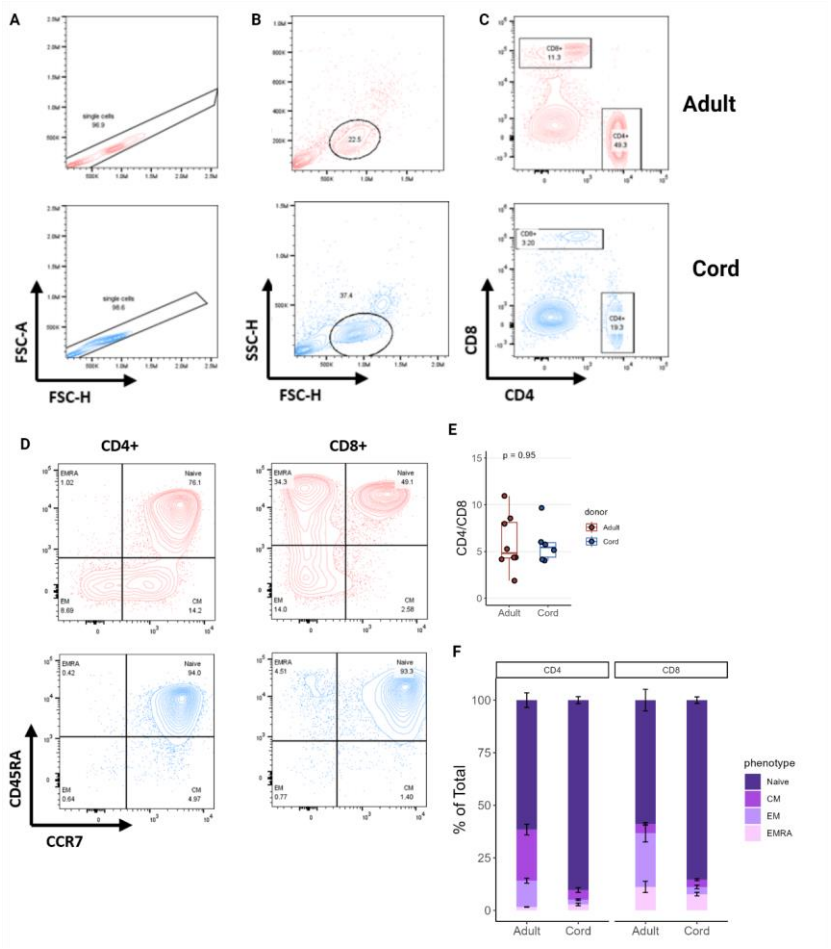

Figure 3.1 The T cell compartment human adult peripheral and umbilical cord blood.

MNCs from human adult peripheral blood and umbilical cord blood were analysed using flow cytometry. Gating was determined manually for identification of cell populations. A) Doublet cells were removed by comparing FSC-H and FSC-A and B) total lymphocytes were gated on. C) Single positive CD4

and CD8 cells were identified and gated. D) Naïve, effector and memory populations of CD4+ and CD8+ T cells were determined by expression of CD45RA and CCR7. E) Summary plots of CD4+/CD8+ ratio. F) Summary plots showing naïve, CM, EM and EMRA as a percentage of total CD4+ or CD8+ population with mean ± SEM. n = 10 adult and n = 6 cord. p value determined by Wilcoxon rank sum test; p < 0.05 was deemed significant.

As neonates are thought to have a Th2 skewed helper phenotype (Hebel et al., 2014), the CD4+ naïve and memory compartments were further analysed for the chemokine receptors CXCR3, CCR4, CCR6 and CCR10 to identify Th1 (CXCR3+ CCR4- CCR6- CCR10-), Th2 (CXCR3- CCR4+ CCR6- CCR10-), Th17 (CXCR3- CCR4+ CCR6+ CCR10-) and Th22 (CXCR3- CCR4+ CCR6+ CCR10+) (Duhen et al., 2012; Halim et al., 2017). After gating on CD4 single positive cells, naïve, CM, EM and EMRA fractions were assessed separately for chemokine receptor expression with the aid of FMO controls to guide placements of threshold gates (Figure 3.2A). First, CXCR3+ CCR4- and CXCR3- CCR4+ positive populations were gated ahead of determination of Th1, Th2, Th17 and Th22, according to CCR6 and CCR10 expression, as such Th helper phenotypes are reported as a percentage of the total grandparent population, for which the lowest number of defined cells was 305 (Cord CD4+ EM; Figure 3.2B-E). As expected, helper phenotypes were nearly exclusively present in the memory compartments meaning that few defined helper cells were seen in neonates (Figure 3.1E). Of the defined helper phenotypes, Th1 was the largest sub-population present in all the adult subsets whilst Th2 cells were the most frequently identified population of defined helper cells in cords and Th1 cells formed only a very small fraction in each memory population (Figure 3.1E). Th17 cells were observed most commonly in CM and EM populations for both donor groups and Th22 cells were the least common in all fractions for both groups (Figure 3.1E).

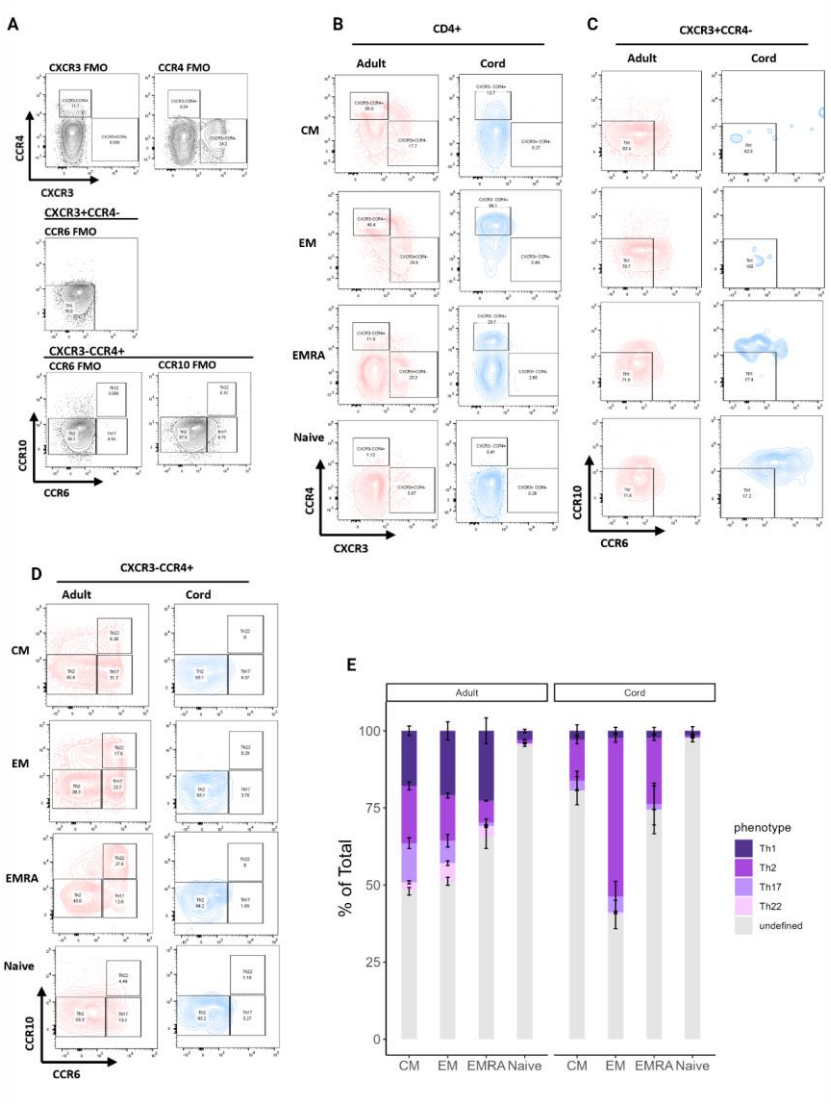

Figure 3.2 T helper phenotypes in naïve and memory CD4+ T cell populations in adult peripheral and umbilical cord blood.

MNCs from human adult peripheral blood and umbilical cord blood were analysed using flow cytometry. T-helper phenotypes in naïve, CM, EM and EMRA CD4+ populations were determined by expression of chemokine

receptors. A) Representative FMO controls, here showing cells from an adult effector memory population, used to set threshold gates for both adult and cord chemokine markers. B) CXCR3+ CCR4- and CXCR3- CCR4+ cells gated for naïve, CM, EM and EMRA populations. C) Th1 cells identified in the CXCR3+ CCR4- fraction of naïve, CM, EM and EMRA populations. D) Th2, Th17 and Th22 cells identified in the CXCR3- CCR4+ fraction of naïve, CM, EM and EMRA populations. E) Summary plots showing percentage of helper phenotypes in each naïve and memory population (grandparent population). Summary plot shows mean ± SEM, n = 10 adult and n = 6 cord. p value determined by Wilcoxon rank sum test; p < 0.05 was deemed significant.

Regulatory cells are the first to gain a memory population, forming relatively early in fetal development and representing a substantial portion of the total memory population in neonates. As T helper phenotypes are mostly confined to memory populations, it stands to reason that regulatory T cells are a primary source of T helper phenotypes in neonates. Duhen et. al. have previously described the presence of Th-like regulatory T cell populations in adults, identified through the same chemokine receptors used above, providing a basis to investigate T helper like phenotypes in the regulatory T cell population of neonates (Duhen et al., 2012). To investigate this, adult and cord MNCs were stained for memory CD4+ regulatory T cells and chemokine receptors to identify Th-like Tregs. Doublets were removed before gating on total lymphocytes and selecting CD4+ cells (Figure 3.3A-C). Regulatory T cells were identified through a limited approach using surface markers $CD25^{high}CD127^{low}$ whilst memory T cells were identified as CD45RO+ (Figure 3.3D-E). Regulatory T cells, as a fraction of total CD4+ cells, were comparable between adults and neonates (p = 0.75; Figure 3.3F), although more adult donors showed frequencies in the higher ranges. The frequency of memory Tregs was significantly greater in adults (52% ± 6.2 %; n = 10,) than cords (18.0 ± 1.2 %; n = 6; p = 0.0006) revealing a reasonably large population of memory Tregs in cords.

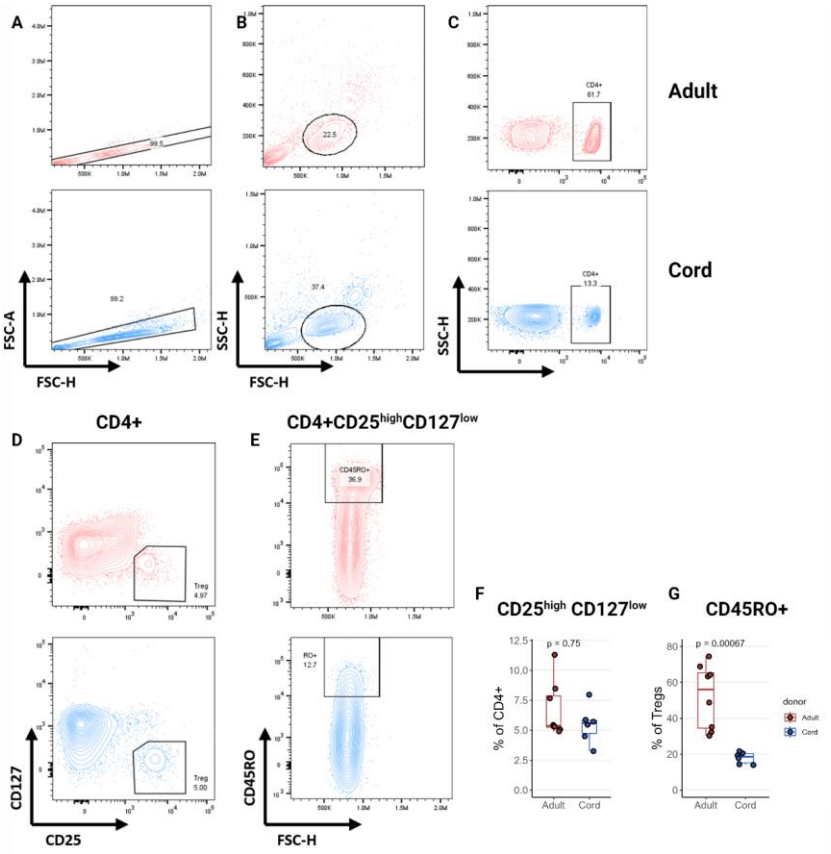

Figure 3.3 CD4+ regulatory T cells in adult peripheral blood and umbilical cord blood.

MNCs from adult human peripheral blood and umbilical cord blood were analysed using flow cytometry. A) doublet cells were removed by comparing FSC-H and FSC-A and B) gating on total lymphocytes. C) Gating of CD4+ T cells. D) Gating on $CD25^{high}CD127^{low}$ regulatory T cells, in total CD4+ fraction. E) Gating on CD45RO+ memory fraction of regulatory T cells. F) Summary plot showing frequency of regulatory T cells ($CD25^{high}CD127^{low}$) in total CD4+ population. G) Frequency of memory (CD45RO+) regulatory T cells. n = 8 adults and n = 6 cords. p value determined by Wilcoxon rank sum test; $p < 0.05$ was deemed significant.

Th-like Tregs were identified by expression of chemokine receptors, using an FMO gating strategy as follows, Th1-like (CXCR3+ CCR4- CCR6- CCR10-), Th2-like (CXCR3- CCR4+ CCR6- CCR10-), Th17-like (CXCR3- CCR4+ CCR6+ CCR10-) and Th22-like (CXCR3- CCR4+ CCR6+ CCR10+). Using the gating strategy shown in Figure 3.4A-C, Th-like phenotypes defined 58.0 ± 0.8% of adult memory Tregs and 43.0 ± 4.1% of cords memory Tregs. Unlike in total CD4+ conventional T cells the Th2-like phenotype did not dominate the Th-like subsets of Treg cells in adults and Th-like cells are a substantially larger fraction of the total Treg pool (Figure 3.4D). In neonates, the Th2-like phenotype was still the most dominant (19% ± 5.1), but Th17-like cells were more similar in frequency (15.0 ± 2.8%) and again only a tiny fraction of cells were identified as Th22-like (1.5 ± 0.5%) (Figure 3.4D).

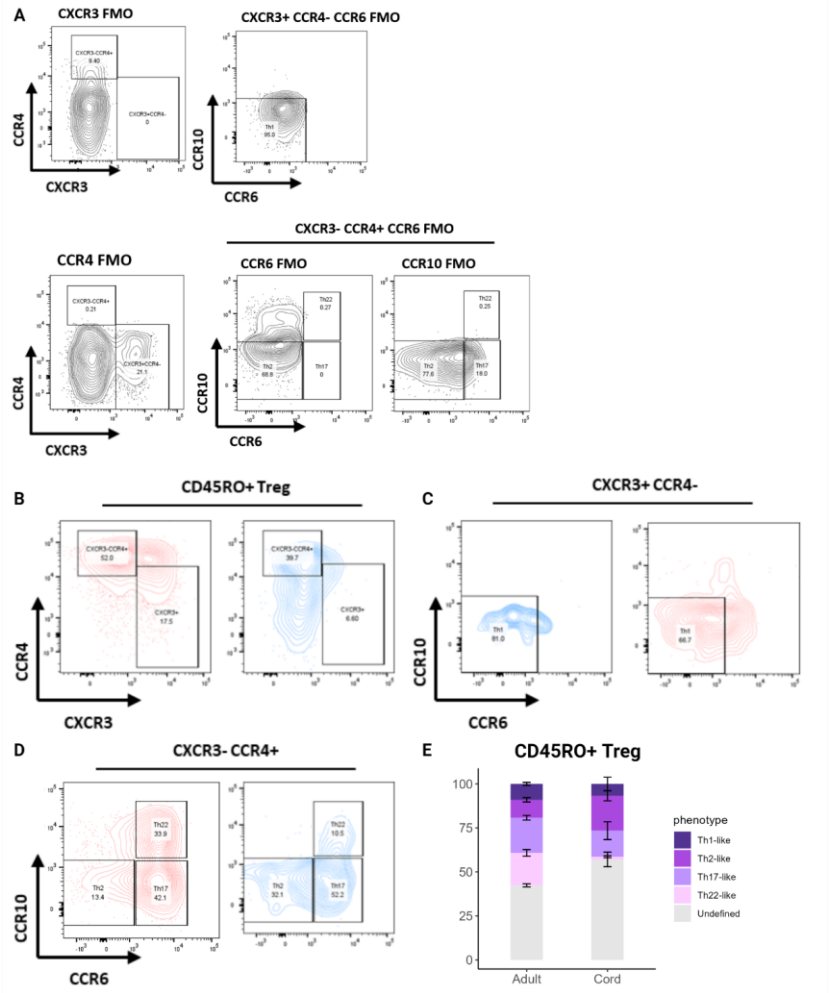

Figure 3.4 Th-like regulatory CD4+ T cells in adult peripheral blood and umbilical cord blood.

Th-like phenotypes were assessed in the CD45RO+ Treg fraction of MNCs isolated from human adult peripheral blood umbilical cord blood .A) Showing FMO controls used as guides for setting threshold gates of chemokine receptors in B-D. B) Gating for CXCR3+ CCR4- and CXCR3- CCR4+ cells. C) Th1 cells identified in the CXCR3+ CCR4- fraction. D) Th2, Th17 and Th22 cells identified in the CXCR3- CCR4+ fraction. E) Summary plots showing percentage of Th-like

phenotypes in CD435RO+ Tregs (Grandparent population). Summary plot shows mean ± SEM, n = 10 adult and n = 6 cord.

3.3.2 The transcription profile of ex vivo adult and cord naïve CD4+ T cells

The nCD4+ T cell compartment from neonates form a unique time of life specific phenotype, however, the factors driving this unique phenotype are still poorly understood. Metabolism plays a decisive role in defining T cell phenotype and it was hypothesised that it might play an important role in defining the unique nCD4+ phenotype of neonates. To explore the potential of this hypothesis the contribution of metabolic genes to differences in T cell metabolism was assessed using a freely accessible transcriptomic dataset of umbilical cord blood and adult nCD4+ T cells accessed from the NCBI GSE repository (GSE135467). Firstly, data were log2 transformed and assessed for normalisation (Figure 3.5A). Then an initial clustering of donors was performed by Pearson correlation and hierarchical clustering which showed distinct clustering between donor groups (Figure 3.B), confirming the unique phenotype of neonatal nCD4+ cells.

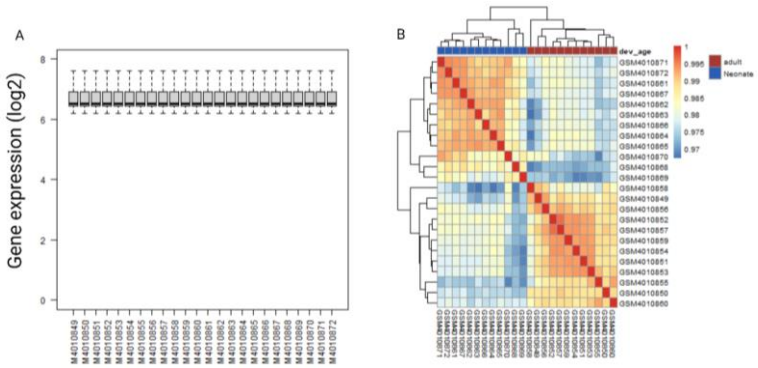

Figure 3.5 Normalised data from transcriptomics of naïve CD4+ T cells show clustering on donor group.

Transcriptomic data of nCD4+ T cells from human adult peripheral and umbilical cord blood , accessed via GSE135467, was assessed for normalisation and

donor correlation determined by Pearsons tests *A) Transcriptomic data of nCD4+ T cells from 12 umbilical cord blood donors and 12 healthy adult donors were log2 transformed and visually assessed for normalisation. B) Correlation between donors is determined by Pearson correlation's test and displayed in a clustered heatmap.*

A total of 47,323 probes were present in the data set. Background expression, defined as expression below the bottom quartile and/or not expressed by more 2 or less donors, was excluded and the remaining 35,933 probes were matched to 17,261 unique known gene transcripts. A linear model fitted to these 17,261 genes determined there are 4,830 significantly (adjusted p value <0.05) differentially expressed genes. To determine whether metabolic genes were overrepresented in these significantly differentially expressed genes a list of 1,214 metabolically associated genes was curated from KEGG of which 1,034 genes were expressed in the total 17,261 genes identified in the data (Figure 3.6A). A contingency table (Table 5) of metabolic genes present in the differentially expressed and non-differentially expressed genes used with Fisher's exact test (Table 6) determined that metabolic genes were overrepresented (p = 0.000007) in the list of differentially expressed genes. Similarly, when principal component analysis (PCA) was performed using the list of metabolic genes expressed in the dataset, adult and cord samples clearly separated along PC1 (Figure 3.6B). Closer inspection of the loading scores for the principal components explaining the majority of the variance in the data did not reveal any individual genes responsible for the clustering (Figure 3.6C-D).

Table 5 Contingency table for differentially expressed metabolic genes in the total set of genes.

Table shows the number of genes present in the total gene set and differentially expressed genes from the list of metabolically associated genes.

	In Differentially Expressed Gene List	**Not In Differentially Expressed Gene List**

In Metabolic Gene List	352	682
Not In Metabolic Genes List	4,478	11,731

Table 6 Fisher's exact test for over representation.

P values and descriptive statistics for Fisher's exact test for over representation of metabolic genes in total differentially expressed genes.

	P value	**Odds ratio**	**95% CI**
Fishers Exact Test	$7x10^{-6}$	1.35	1.20

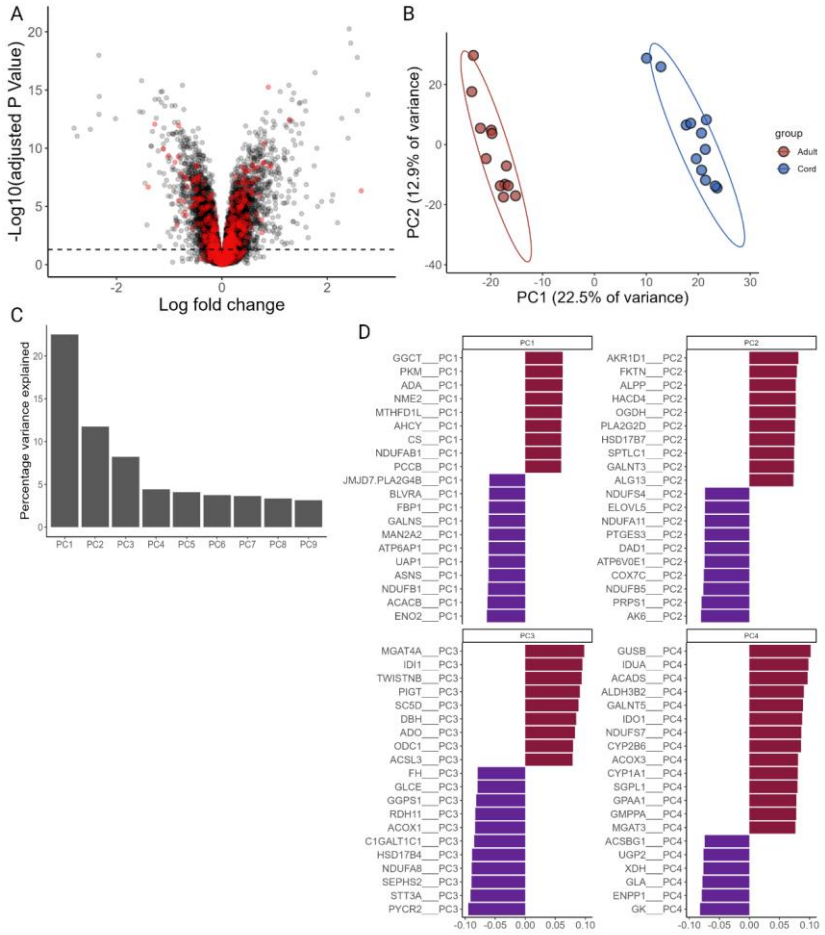

Figure 3.6 Umbilical cord blood nCD4+ T cells show a unique metabolic transcriptome. *The metabolic transcriptome of neonatal nCD4+ T cells was assessed within the total transcriptomic data set. A) Volcano plot of differential expression of genes with metabolically associated genes highlighted in red. B) Adult and cord donors plotted in principal component space. C) Elbow plot showing the variance explained by each principal component. D) Plot of loading scores showing the contribution of each gene to each principal component. n = 12 adult and n = 12 cord.*

Given no single gene or genes was clearly responsible for explaining the metabolic transcriptomic differences between adult and cords, next gene set enrichment analysis (GSEA) was performed. The list of 1,034 metabolic genes were ranked according to log2 fold change and significance and compared against the WikiPathways repository to identify enriched pathways. The top 15 most significantly enriched pathways included aerobic glycolysis ($p = 0.003$), purine metabolism related disorders and purine metabolism ($p = 0.004$, $p = 0.014$) and fatty acid metabolism ($p = 0.015$) (Figure 3.7A-E). Most of the top pathways were enriched in cords (Figure 3.7B) including aerobic glycolysis and purine metabolism, which both showed a number of several genes in the pathways that were highly differentially expressed (Figure 3.7C-D). Additionally, the IL-7 signalling pathway, is among the top significantly enriched pathways in neonates, matching already established experimental data in the field (Schonland et al., 2003) (Figure 3.7A-B).

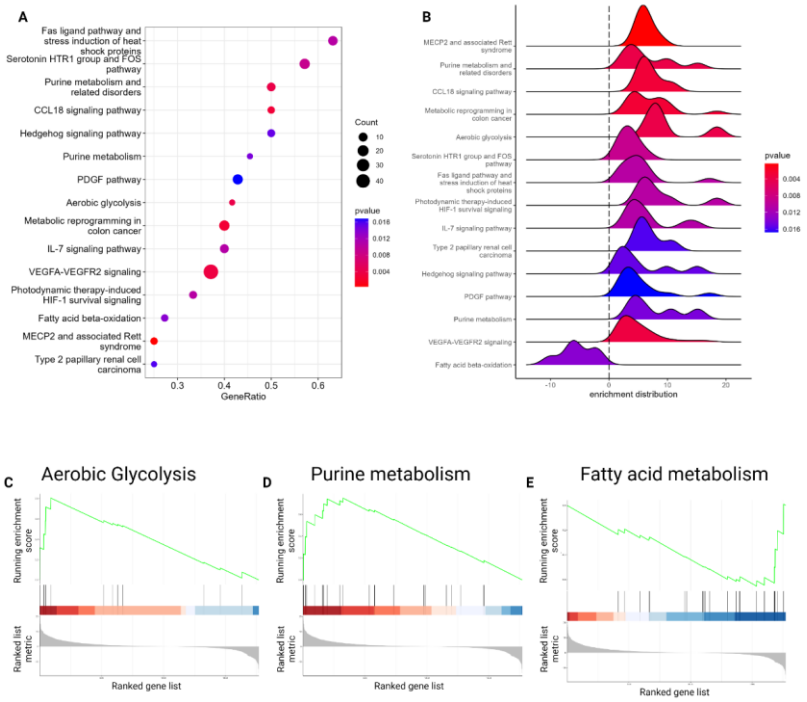

Figure 3.7 Key metabolic pathways are enriched in cord naïve CD4+ T cells.

Metabolic associated genes were ranked according to log2 fold change and significance and GSEA was performed using the WikiPathways repository. A) The top 15 most significantly enriched pathways are shown along with the number of genes present in the pathway and the gene ratio. B) Histograms of the enrichment distribution of the 15 most significantly enriched pathways in the ranked gene list. C-E) Running enrichment scores for aerobic glycolysis, purine metabolism and fatty acid metabolism, respectively.

3.3.3 Ex vivo neonatal naïve CD4+ T cells are more glycolytic

As GSEA highlighted central metabolism of glucose as a defining feature of neonatal nCD4+ T cells, real time extracellular flux assays that measure glycolysis alongside oxidative phosphorylation were employed to determine the metabolic profile of directly ex vivo nCD4+ isolated from adult peripheral blood and umbilical cord blood.

Cells were left to equilibrate for approximately 2 h after in the XF bioanalyzer at 37°C in assay RPMI media supplemented with 5.5 mM glucose 2mM glutamine and 1mM pyruvate. After which ECAR and OCR were measured at baseline and in response to injections of oligomycin, FCCP, rotenone and antimycin A to assess mitochondrial respiration parameters (Figure 3.8A-B). Basal respiration and ATP production were not significantly different between adults and cords (Figure 3.8C-D), although injection of the uncoupler FCCP resulted in a significantly greater maximal respiration in cords ($p = 0.044$) and consequently a greater spare respiratory capacity, potentially suggesting greater metabolic flexibility in cord nCD4+ T cells (Figure 3.8E-F). Cord nCD4+ T cells showed greater baseline extra-cellular acidification rate ($p = 0.027$; Figure 3.8G-H) and maximal ECAR ($p = 0.01$; Figure3.8), indicating a higher rate of glycolysis. However, analysis of protein expression for key glycolytic enzymes HKI, HKII, PMK2 and LDHA did not show any significant differences between adults and neonates (Figure 3.8I-M).

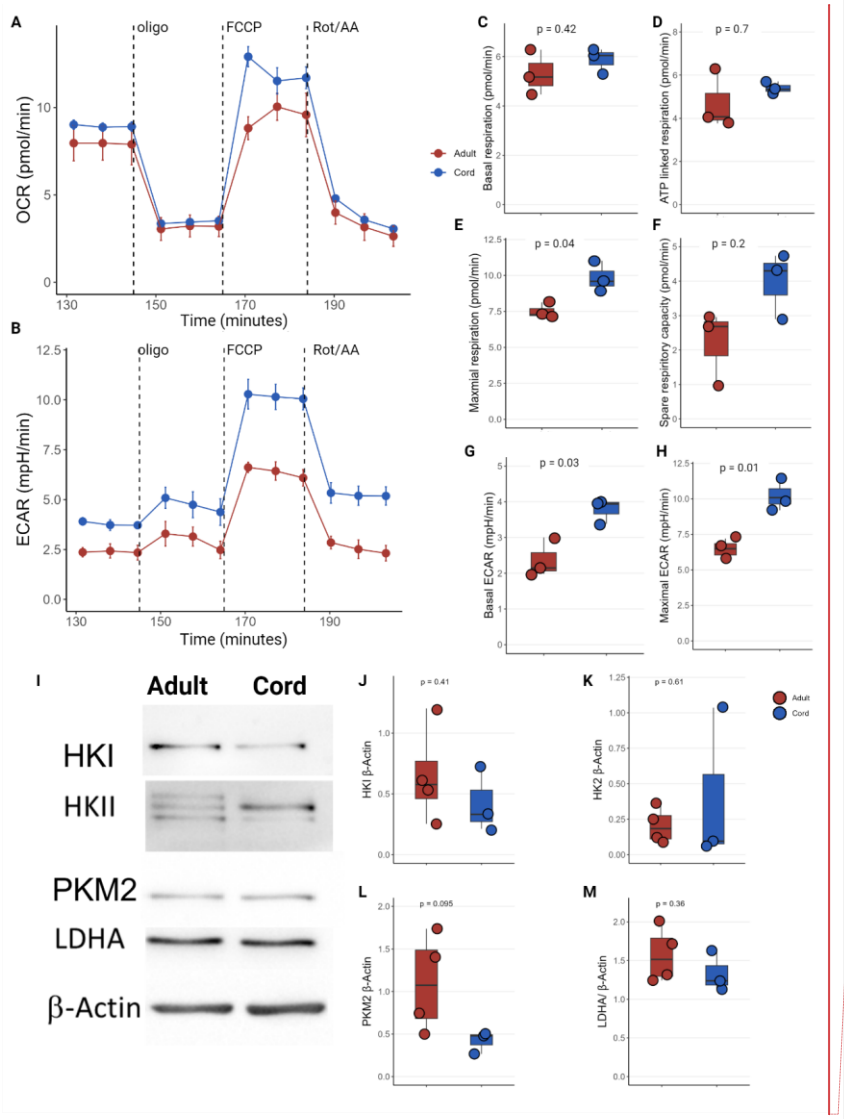

Figure 3.8 Ex vivo umbilical cord blood nCD4+ T cells are more glycolytic.

A,B) Mitochondrial and glycolytic stress profiles of freshly isolated ex vivo naïve CD4+ T cells isolated from human adults peripheral blood and umbilical cord blood were determined by simultaneous measurements of OCR and ECAR, before and after injections of oligomycin (0.75 µM), FCCP (1 µM) and antimycin

Commented [SH2]: Spelling mistake change figures

A and rotenone (1 μM). C) Basal respiration, D) ATP linked respiration, E) maximal respiration, F) spare respiratory capacity, G) basal ECAR and H) maximal ECAR parameters were calculated for adults and cords. Data are representative of n = 6-7 independent experiments. I) Representative immunoblots from each donor group for HKI, HKII, PKM2, LDHA, and β-Actin and (J-M) respective densitometry normalised to β-actin. n = 3-4 adults and 3 cords. statistical comparison was performed using Wilcoxon rank sum test and p values are as indicated on each figure; p < 0.05 was deemed significant.

Mitochondrial mass, determined by MitoTracker™ Green staining, showed no difference in mitochondrial content with both donor groups showing homogenous mitochondrial content across the population. Confocal images of MitoTracker™ Green cells found similar results with diffuse small mitochondria sparsely populating the cell (Figure 3.9A-C). Mitochondrial super-oxide is another indicator of mitochondrial respiration. Staining with the mitochondrial superoxide specific dye MitoSox™ Red suggested similarly low levels of mitochondrial respiration in quiescent adults and cords nCD4+ T cells (Figure 3.9D-E).

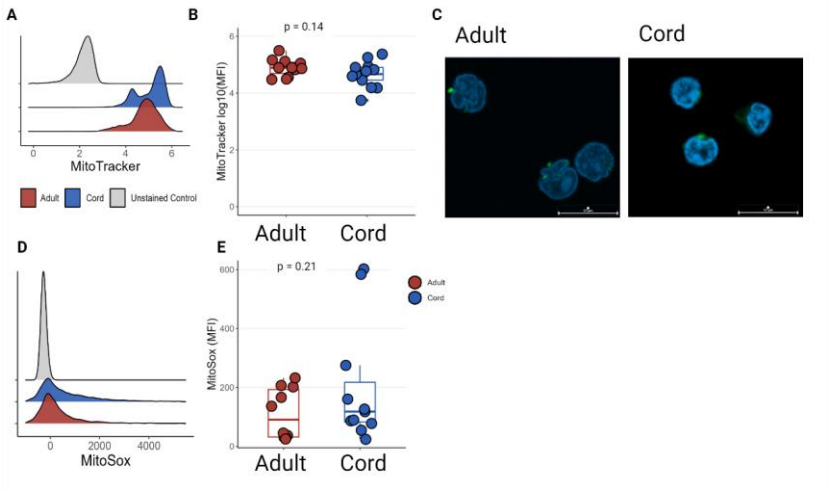

Figure 3.9 Mitochondrial mass does not differ between adult peripheral and umbilical cord blood nCD4+ T cells.

A) ex vivo nCD4+ T cells from human adult and umbilical cord donors stained with MitoTracker with representative histograms from flow cytometry including unstained controls shown in grey, B) summary data from flow cytometry and C) representative confocal images of mitochondria stained with the nuclear stain DAPI (Blue) and the mitochondrial stain MitoTracker Green (Green). Alternatively, nCD4+ T cells were stained with MitoSox™ Red and measured by flow cytometry with D) showing representative histograms and E) summary plots. A-B) n = 11 adult and 13 cord, C) n = 2 adult and 2 cord, D-E) n = 8 adult and n = 9 cord. P values determined by Wilcoxon rank test sum; p < 0.05 was deemed significant.

As nCD4+ T cells from cord donors exhibited increased basal glycolysis directly ex vivo it was hypothesised nCD4+ T cells from umbilical cord blood might exist in a more active resting state poised for antigen encounter. To assess this ex vivo nCD4+ T cells from adult and cord donors were stained for the surface expression of classical activation markers CD25, CD69 and CD44 (Figure 3.10A-F). CD25 (IL-2Ra) is the high affinity receptor of IL-2 and supports T cell survival and proliferation but no difference

in CD25 expression was seen between ex vivo adult and cord nCD4+ T cells (Figure 3.10). However, significantly increased expression of the adhesion molecule CD44 (p=0.047, Figure 3.10C-D) and near significantly increased expression of the galectin-1 receptor CD69 (p=0.054; Figure E-F) were observed in cords (Figure 3.10). As these activation markers were not uniformly upregulated in cords it is difficult to determine whether these differences are representative of activation or if cord nCD4+ T cells are more readily poised for activation.

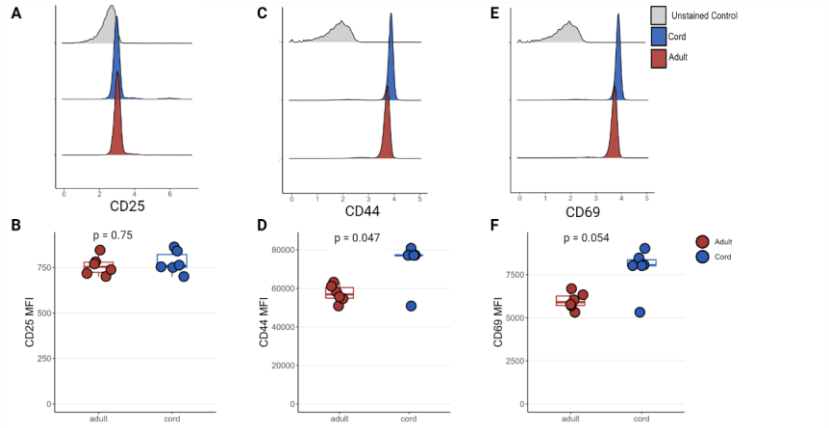

Figure 3.10 Activation status of ex vivo nCD4+ T cells from adult peripheral blood and umbilical cord blood, determined by flow cytometry of activation markers.

Ex vivo nCD4+ T cells, isolated from human adult peripheral blood and umbilical cord blood were examined for activation markers by flow cytometry. Representative histograms and summary plots, with unstained controls in grey, are shown for A-B) CD25, C-D) CD44 and E-F) CD69. n= 6 adult and 6 cord. p values determined by Wilcoxon rank sum test; $p < 0.05$ was deemed significant.

3.3.4 Greater glycolytic switch in cord nCD4+ T cells on CD3/28 stimulation.

Metabolic reprogramming to aerobic glycolysis on cognate antigen encounter is an essential requirement for T cells to exit quiescence, proliferate and produce effector molecules. On stimulation with CD3/28 an immediate switch to a glycolytic metabolism is induced in T cells through the phosphorylation of pyruvate dehydrogenase (PDH) by pyruvate dehydrogenase kinase (PDHK), preventing

pyruvate from entering the TCA cycle through acetyl-CoA and leading to a build-up of glycolytic intermediates and increased conversion to lactate (Menk et al., 2018). This glycolytic switch appears specifically important to the activation of naive T cells however, whether this switch is also induced in neonatal naive T cells is unknown. To determine if the same metabolic switch is seen in cord nCD4+ T cells, directly isolated ex vivo naïve CD4+ T cells from adult and cords were activated in situ with simultaneous injection of anti CD3 (2 μg/mL) and anti CD28 (20 μg/mL) during real time monitoring of extracellular flux (Figure 3.11A-B). To measure the glycolytic switch, baseline measurements of ECAR and OCR were taken for 15 min before injection of anti-CD3/28 (Pre) and compared with the first 15 min peak measurements after injection (Post). For the first time, these data show that umbilical cord naive CD4+ T cells induce a glycolytic switch on activation with anti-CD3/28. ECAR and OCR both increased immediately on injection of anti-CD3/28 but not the vehicle and most notably the increase in ECAR for cords was much more prominent (Figure 3.11A-B). Additionally, both donor groups maintained elevated ECAR and OCR for the remainder of the ~2 h assay (Figure 3.11A-B). The increase in ECAR was significant for both donor groups however, comparing the ECAR fold change in adults and cords clearly shows a greater glycolytic switch in cords ($p = 0.026$; Figure 3.11C-D). Together these data illustrate an immediate switch to increased glycolysis for naïve CD4+ T cells of a greater magnitude for umbilical cord derived cells (Figure 3.11).

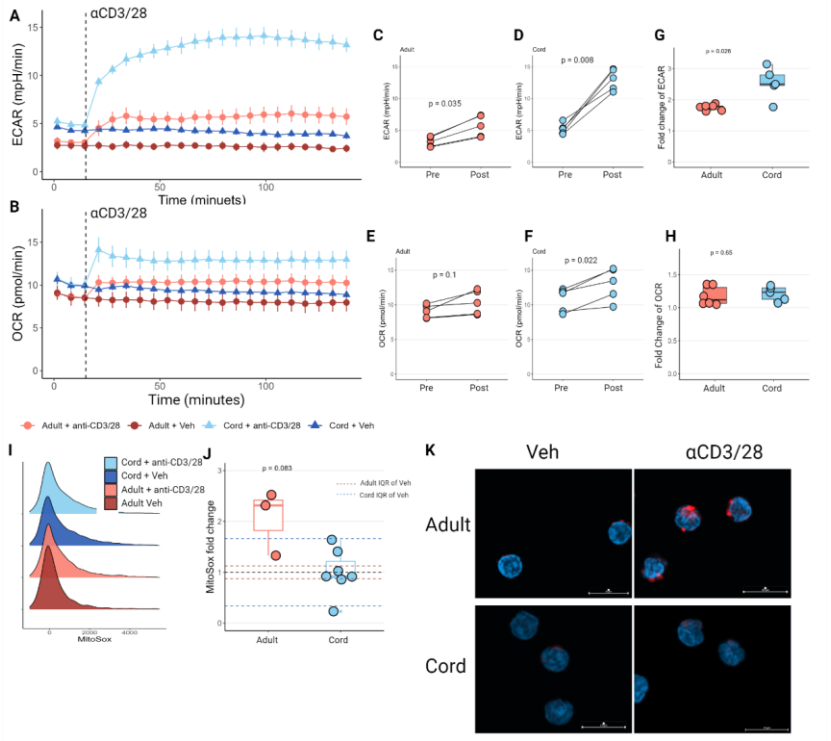

Figure 3.11 Bioenergetic analysis for in situ activation of nCD4+ T cells from adult peripheral and umbilical cord blood.

A-B) Ex vivo nCD4+ T cells isolated from human adult peripheral blood and umbilical cords were activated with anti-CD3/28 or vehicle in situ and changes in ECAR and OCR were continuously measured. Pre and Post activation C-D) ECAR, and E-f) OCR. G-H) Fold change in ECAR and OCR post activation. I-J) representative and relative summary plots for MitoSox™ Red of nCD4+ T cells activated for 1 hr with anti-CD3/28 or vehicle. K) Confocal images of activated nCD4+ T cells with DAPI DNA staining (blue) and MitoSox™ Red. A-H) Data are representative of 11 independent experiments n = 6 adult and 5 cord. I-K) n = 3 adult and 7 cord. C-F) p values were determined by Wilcoxon signed rank test, (G,H) p values determined by Wilcoxon rank sum test; $p < 0.05$ was deemed significant.

Unlike ECAR, OCR fold change was comparable (p = 0.65) between both groups (Figure 3.11E-H). Mitochondrial superoxide production is often used as another measure of mitochondrial activity and production of mitochondrial superoxide has been reported previously as an important factor in T cell activation. Intriguingly, despite comparable increases in OCR on stimulation, mitochondrial superoxide production after 1 h anti CD3/28 stimulation measured using Mitosox™ Red was increased, relative to unstimulated controls, in adults but neonates, suggesting unique mitochondrial respiration in cords independent of OCR (Figure 3.11I-J). The same finding was further validated by confocal microscopy imaging of MitoSox stained cells (Figure 3.11K).

At 2 hours post activation another glycolytic/mitostress test was conducted by injection of oligomycin, FCCP, rotenone and antimycin A (Figure 3.12A-B). Post activation basal respiration and ATP linked respiration was greater in cords, though this did not reach significance for basal respiration (p = 0.063; p = 0.029, Figure 3.12C-D). However, maximal respiration and spare respiratory capacity were greatly increased in cords (p = 0.016; p = 0.016, Figure 3.12E-F). Furthermore, due to the greater glycolytic switch, basal ECAR and maximal ECAR were both significantly greater in cords (p = 0.01; p = 0.016; Figure 3.12G-H). Together these data show nCD4+ T cells from cords are significantly more metabolically active than adults immediately upon and shortly after activation.

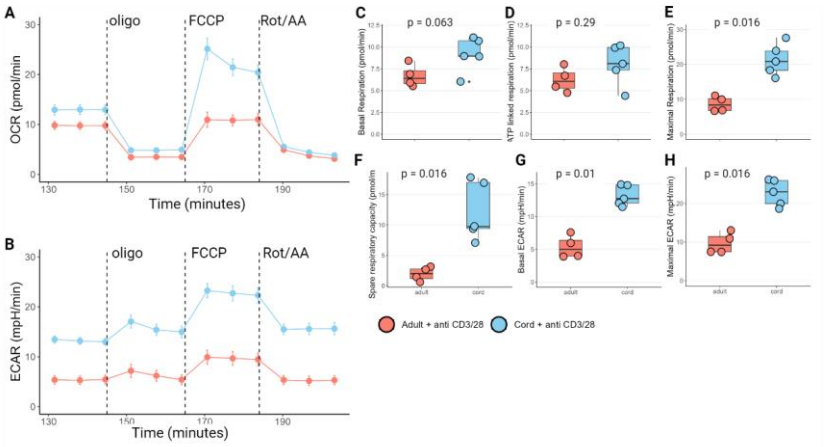

Figure 3.12 Umbilical cord blood nCD4+ T cells are more metabolically active early post activation.

Metabolic parameters of nCD4+ T cells isolated from human adult peripheral blood and umbilical cord blood were assessed A-B) ~2 hours post in situ anti-CD3/28 activation mitochondrial and glycolytic parameters were determined by injections of oligomycin (1 µM), FCCP (1 µM) and antimycin A and rotenone (1 µM). C) Basal respiration, D) ATP linked respiration, E) maximal respiration, F) spare respiratory capacity, G) basal ECAR and H) maximum ECAR for adults and cords. Data are representative of 9 independent experiments, n = 4 adults and 5 cords. p values determined by Wilcoxon rank sum test; p < 0.05 was deemed significant.

To ensure that the greater glycolytic switch induced by stimulating with anti-CD3/28 was not simply due to greater expression either CD3 or CD28, ex vivo nCD4+ T cells from both donor groups were examined for surface expression of these two antigens using flow cytometry. CD3 and CD28 was homogenously expressed by cells in both donor groups (Figure 3.12A,C) and no difference in expression was seen (Figure 3.13B,D), suggesting that the difference in glycolytic switch on activation is not explained by increased expression of these molecules.

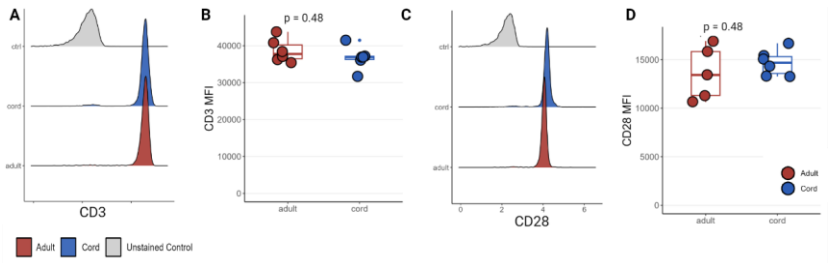

Figure 3.13 Surface expression of CD3 and CD28 on adult peripheral and umbilical cord blood naïve CD4+ T cells ex vivo.

nCD4 + T cells isolated from human adult peripheral blood umbilical cord blood were assessed by flow cytometry for CD3 and CD28 surface receptors. Representative histograms and summary plots of A-B) CD3 and C-D) CD28 surface receptors on and cord ex vivo Tn. n = 5 adult and n = 6 cord. p value determined by Wilcoxon rank sum test; $p < 0.05$ was deemed significant.

3.3.5 The glycolytic switch in cords is accompanied by greater mTOR signalling.

Thus far, the data indicated a more prominent metabolic switch in cord nCD4+ T cells and as it well documented that reprogramming in T cells is driven by the PI3K-AKT-mTOR signalling axis (Finlay et al., 2012; Jones et al., 2019; Shyer et al., 2020) it was hypothesised that this pathway might be more strongly induced on activation in cords. On anti-CD3/28 stimulation mTOR is phosphorylated, at serine 2448 via a signalling cascade involving PI3K and AKT (de Souza et al., 2016). mTOR integrates nutrient availability with metabolic function by acting as an ATP and amino acid sensor, only activating when the environment is sufficient to meet the energetic and metabolite demands of the cell. As such, mTOR signalling can be repressed by inhibition of glycolysis or amino acid deprivation. To measure the phosphorylation of mTOR, nCD4+ T cells isolated from adults and cords were treated with vehicle or anti-CD3/28, as well as the inhibitors 2DG or BCH, for 1 hour before determination of phosphorylated proteins, compared to vehicle controls, using intracellular flow cytometry (Figure3.14).

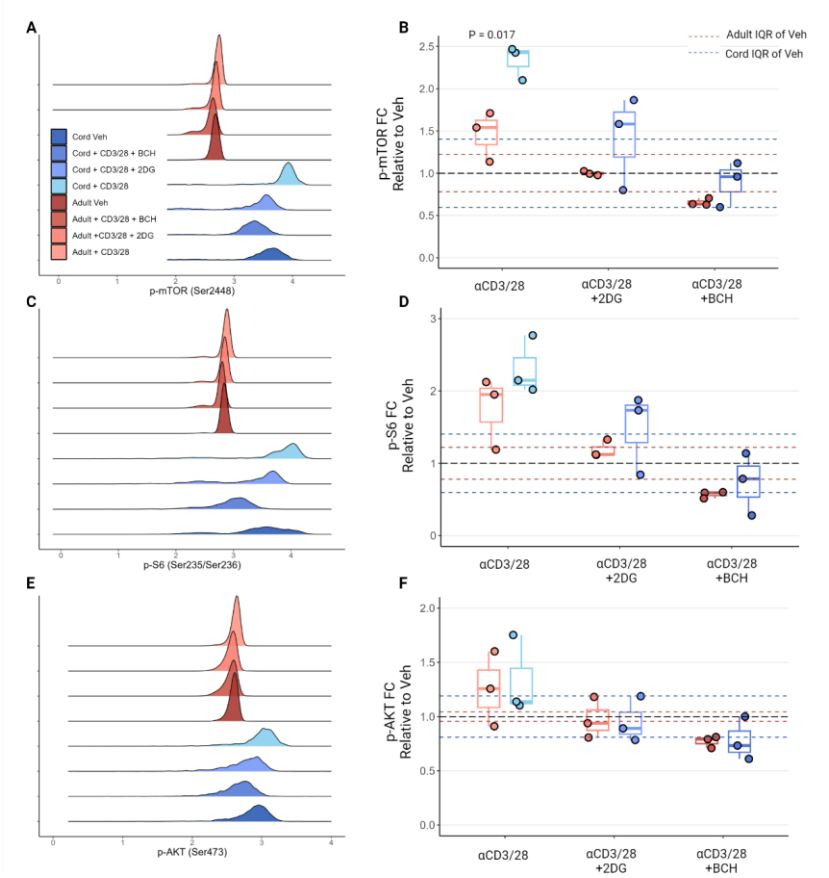

Figure 3.14 Greater induction of mTOR in umbilical cord blood naïve CD4+ T cells.

Phosphorylation of intracellular proteins, assessed by flow cytometry, in nCD4+ T cells isolated from human adult peripheral blood and umbilical cord blood. Plots showing Intracellular flow cytometry measuring phosphorylated proteins after 1 h activation with anti-CD3/28 with representative histograms and summary plots relative to vehicle controls for A-B) p-mTOR (Ser2448), C-D) pS6 (Ser235/Ser236) and p-AKT (ser473). Interquartile range (IQR) for vehicle controls are shown by dashed lines red for adult and blue for cord. n = 3 adult and n = 3 cord. p value determined by Wilcoxon rank sum test; $p < 0.05$ was deemed significant.

Phosphorylated mTOR increased, slightly for adults (p = 0.22) and significantly for cords (= 0.023) on activation (Figure 3.14A-B) and a greater increase above vehicle control was seen in neonates (p = 0.017) (Figure 3.14B). mTOR phosphorylation was totally impaired in adults by 2DG inhibition however inhibition was only partial in cords. Inhibition by BCH was more potent for both adults and cords with complete inhibition in both cases (Figure3.14B) (Dennis et al., 2001; Nicklin et al., 2009). Phosphorylated S6, a phosphorylation target of mTOR, in the mTORC1 complex, was used as a measure of downstream mTOR signalling (Dieterlen et al., 2012). Again, both donor groups showed increased phosphorylation of S6 on activation as expected, although there was no significant difference between them (Figure 3.14C-D). The same trends in inhibition with 2DG and BCH were observed as were seen with mTOR phosphorylation (Figure 3.14C-D). mTORC2 is the other mTOR containing signalling complex potentially induced on T cell activation and is known to phosphorylate AKT at serine 473 (Pollizzi et al., 2015). Unlike mTOR and S6, there was minimal phosphorylation of AKT indicating that mTORC2 did not increase significantly compared to vehicle control though a small increase was seen for both groups which was completely inhibited by 2DG and BCH (Figure 3.14E-F).

As BCH was a more potent inhibitor of mTOR signalling and its target LAT1/CD98 is known to modulate metabolic reprogramming and immune function, the activity of this amino acid transporter was investigated (Hodge et al., 2022; Kedia-Mehta et al., 2023). Firstly, surface expression was examined using flow cytometry of CD98 and found to increased dramatically in cords (p = 0.002; Figure 3.15A-B). Secondly the activity of the transporter was assessed by measuring the specific uptake of the auto fluorescent amino acid, kynurenine, using flow cytometry (Sinclair et al., 2018) to reveal significantly greater kynurenine uptake in cords (p = 0.0045, Figure 3.15C-D). Furthermore, uptake was inhibited by the addition of BCH as well as competitive inhibition with lysine and kinetic inhibition at 4^{o}C, (p < 0.002 for all comparisons)

indicating that changes in fluorescence were indeed due to CD98 mediated uptake of kynurenine.

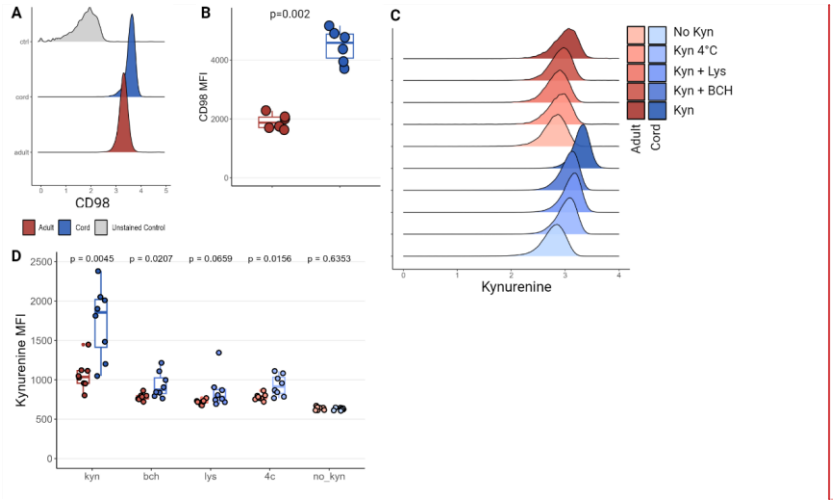

Commented [SH3]: Not MFI

Figure 3.15

CD98 expression and kynurenine uptake is greater in umbilical cord blood naïve CD4+ T cells.

A-B) Representative histogram and summary plots of CD98 surface expression on ex vivo human adult and umbilical cord nCD4+ T cells. C-D) Representative histograms and summary box plot of median fluorescence intensity, showing of kynurenine uptake determined by kynurenine fluorescence in the presence of inhibitors indicated. A-B) n= 6 adult and 6 cord. C-D) n= 8 adult and 8 cord. p value determined by Wilcoxon rank sum test; $p < 0.05$ was deemed significant.

3.3.6 Differential requirements of glutamine in umbilical cord blood nCD4+ T cells metabolic reprogramming.

Interestingly 2DG was more effective at inhibiting mTOR signalling in adults than cords (Figure 3.14B). As inhibition by 2DG blunts glycolysis to decrease in the ATP/ADP ratio thereby activating AMPK mediated inhibition of mTOR it seems plausible that nCD4+ T cells from cords are able to derive more ATP from a source other than glucose

metabolism. As OCR is greater in cords post activation, mitochondrial metabolism might supply the ATP required to maintain a higher ATP/ADP ratio. Glutamine is a major source of carbon for the TCA cycle and metabolic reprogramming after T cell activation is known to be driven by mTOR signalling in human naïve T cells (Jones et al., 2019). To examine the role of glutamine in sustaining metabolic reprogramming on activation, nCD4+ T cells from adult and cord donors were activated in situ with or without glutamine present in the media and OCR/ECAR was recorded (Figure3.16A-D).

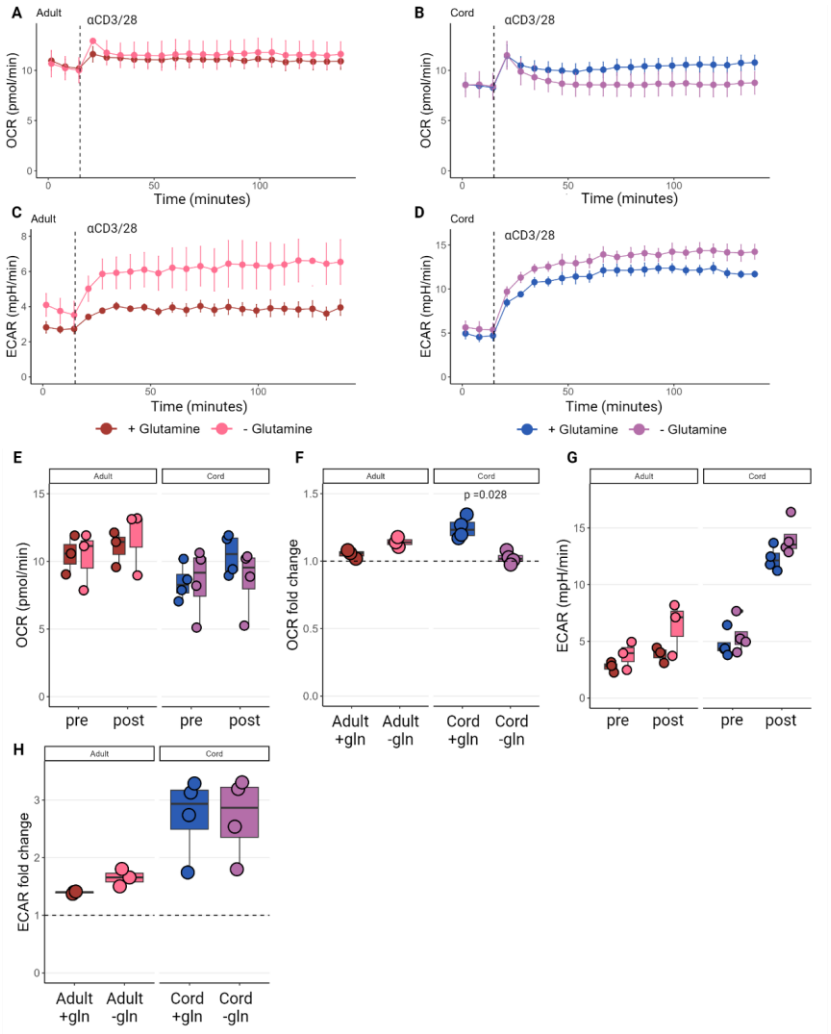

Figure 3.16 Glutamine fuels oxidative phosphorylation in umbilical cord blood nCD4+ T cells.

A-D) OCR and OCR measurement of ex vivo nCD4+ T cells, from human adult peripheral blood and umbilical cord blood, activated in situ with anti-CD3/28 with or without glutamine. E-H) OCR and ECAR measurements Pre and Post injection of anti-CD3/28 and fold change 2 h post injection. Data are representative of 7 independent experiments n = 3 adult and 4 cord. p values

comparing glutamine supplementation within donor groups was determined by Wilcoxon signed rank test and comparisons between donor groups were made by Wilcoxon rank sum test; $p < 0.05$ was deemed significant.

As seen earlier in this chapter, ECAR and OCR increased on in situ activation with anti-CD3/28 (Figure3.11). Activation in the absence of glutamine did not appear to affect OCR in adults but a slight decrease in OCR after activation was seen in cords compared to glutamine containing media where the increase in OCR diminished to basal levels over the course of the assay, although this did not reach significance ($p = 0.16$; Figure3.16B,E). However, when adjusting for donor variability by comparing fold change in OCR activation on an individual basis no fold change increase in OCR was seen in cords activated without glutamine, resulting in a significantly reduced OCR fold change compared to donor matched cells activated in the presence of glutamine ($p = 0.028$, Figure 3.16F). No difference in OCR fold change was seen for adults (Figure 3.16F). Inversely, ECAR was slightly increased for adults when glutamine was absent although this difference did not reach significance either in direct comparison of ECAR or when comparing fold change (Figure 3.16G-H). The same trend was observed for cords, although even less pronounced (Figure 3.16G-H).

3.3.7 Metabolic and activation profile of nCD4+ T cells 16 hours post initial activation.

Following on from these experiments, phenotype and fuel requirements of nCD4+ T cells activated for 16 h in adults and neonates were examined. By this time point significant metabolic reprogramming has occurred and many proteins associated with metabolism and mitochondrial function have been significantly upregulated (Ron-Harel et al., 2016; Tan et al., 2017; Mocholi et al., 2023). Additionally, T cells will have begun to produce their first effector cytokines and activation related markers, which at this stage are predominantly IL-2, CD69 and the IL-2 receptor CD25 (Sojka et al., 2004; Soskic et al., 2022). There for changes to some of these markers and cytokines were assessed by flow cytometry and ELSIA. CD25, IL-2 and IL-10 were chosen due to their known relationship with cell growth and proliferation CD25 expression is known

to correlate to glycolytic expression and IL-2 production is dependent on glutamine metabolism (Jones et al., 2019; Ahl et al., 2020). The cytokine IFNγ and chemokine CXCL8 were included as previous work has demonstrated differing capabilities to produce these cytokines between adults and neonates potentially indicating divergent functions (Gibbons et al., 2014; Razzaghian et al., 2021).

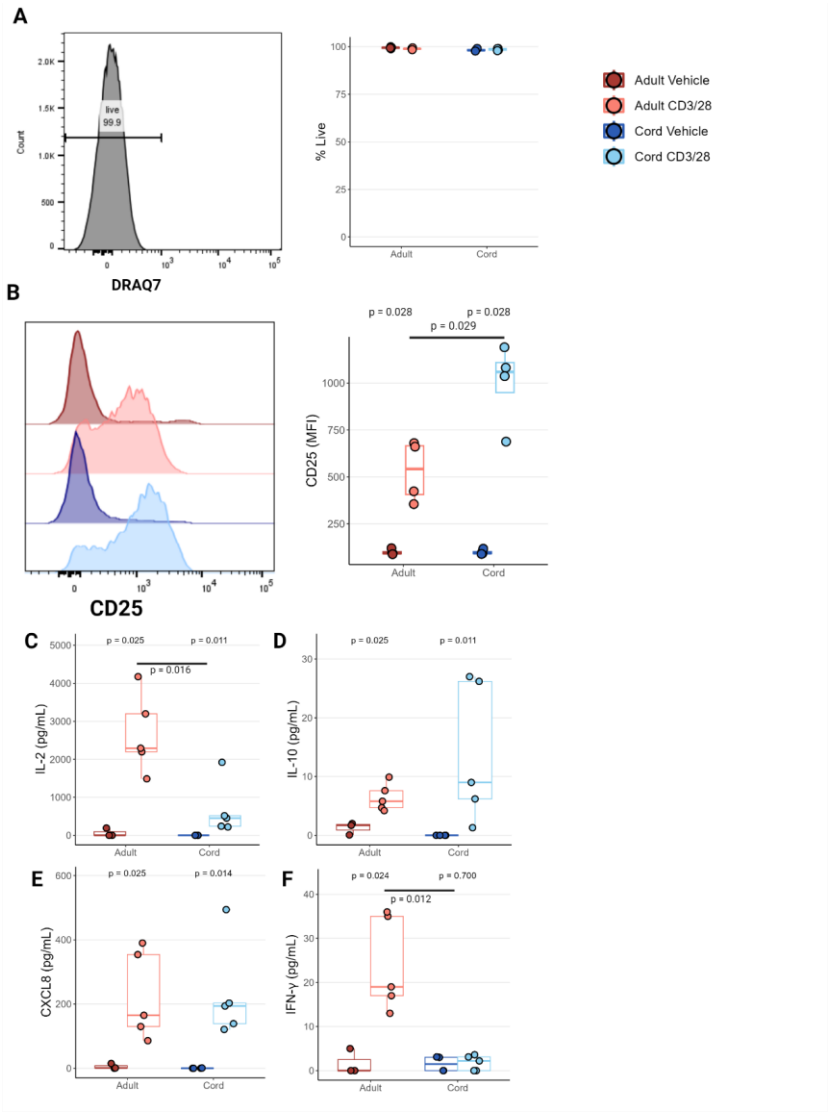

Figure 3.17 Activation profile of adult peripheral and umbilical cord blood naïve CD4+ T cells at 16 h.

The early activation profile of human adult and umbilical cord naïve CD4+ T cells cultured with anti-CD3/28 or vehicle was assessed at 16 h. A) Representative histogram of DRAQ7 live dead staining and summary plot of percentage live cells. B) Representative histogram of CD25 and summary plots

of CD25 MFI. Cytokines in culture supernatant C-F) IL-2, IL-10, CXCL8, IFNγ, respectively. A-B n = 4 adults and n = 4 cords. C-F) n= 5-6 adults and 6 cords. when comparing adults and cords p value determined by Wilcoxon rank sum test and when comparing Vehicle to αCD3/28 treatment, within each donor group, Wilcoxon signed rank test was used; p < 0.05 was deemed significant.

After 16 h culture in RPMI + 10% FCS with or without anti-CD3 (2 μg/mL) and anti-CD28 (20 μg/mL), minimal cell death was seen in both anti-CD3/28 and unstimulated controls for both donor groups (Figure 3.17A). Both donor groups saw significant increases in CD25 expression on the cell surface when stimulated (p = 0.028 adult and p = 0.028 cord; Figure 3.17B) with CD25 expression significantly greater in cords (p = 0.029; Figure 3.17B). Examining known important cytokines (IL-2, IL-10, CXCL8 and IFNγ) by ELISA found little secretion in supernatants, except for IL-2 (Figure 3.17C-F). However, both adults and cords secreted significantly more cytokines when stimulated with anti-CD3/28 apart from IFNγ in cord nCD4+ T cells where there was no difference compared to unstimulated controls (Figure 3.17F). Adults secreted significantly more IL-2 (p = 0.016; Figure 3.17C) and IFNγ (p = 0.012; Figure 3.17F) than cords, in keeping with other studies (Rudd, 2020; Razzaghian et al., 2021). Contrary to this, cord nCD4+ T cells secreted more IL-10 then adults however, this did not reach significance (p = 0.23; Figure 3.17D) whilst there was no noticeable trend for CXCL8 (Figure 3.17E).

The three inhibitors UK5099, BPTES and etomoxir impair the usage of common metabolic fuels, glucose, glutamine and fatty acids, respectively. UK5099 is a mitochondrial pyruvate carrier inhibitor, preventing further metabolism of glucose derived pyruvate in the TCA cycle, by halting its entry into the mitochondria. BPTES inhibits the activity of glutaminase 1 (GLS1) impairing glutaminolysis and etomoxir inhibits carnitine palmitoyltransferase-1 (CPT1A), the primary entry point of fatty acids into the TCA cycle. To examine the oxidative utilisation of the glucose, glutamine

and fatty acids, anti-CD3/28 treated cells were harvested at 16 h, resuspended in Seahorse XF RPMI assay media and real time bioenergetic parameters measured at base line and following injections of UK5099 (2 μM), Bis-2-(5-phenylacetamido-1,3,4-thiadiazol-2-yl)ethyl sulphide (BPTES; 3 μM), 2[6(4-chlorophenoxy)hexyl]oxirane-2-carboxylate (etomoxir; 3 μM) and vehicle control as well as injections of oligomycin (1 μM), FCCP (1 μM) and antimycin (1 μM) and rotenone (1 μM), for a mito-stress assay (Figure 3.18A).

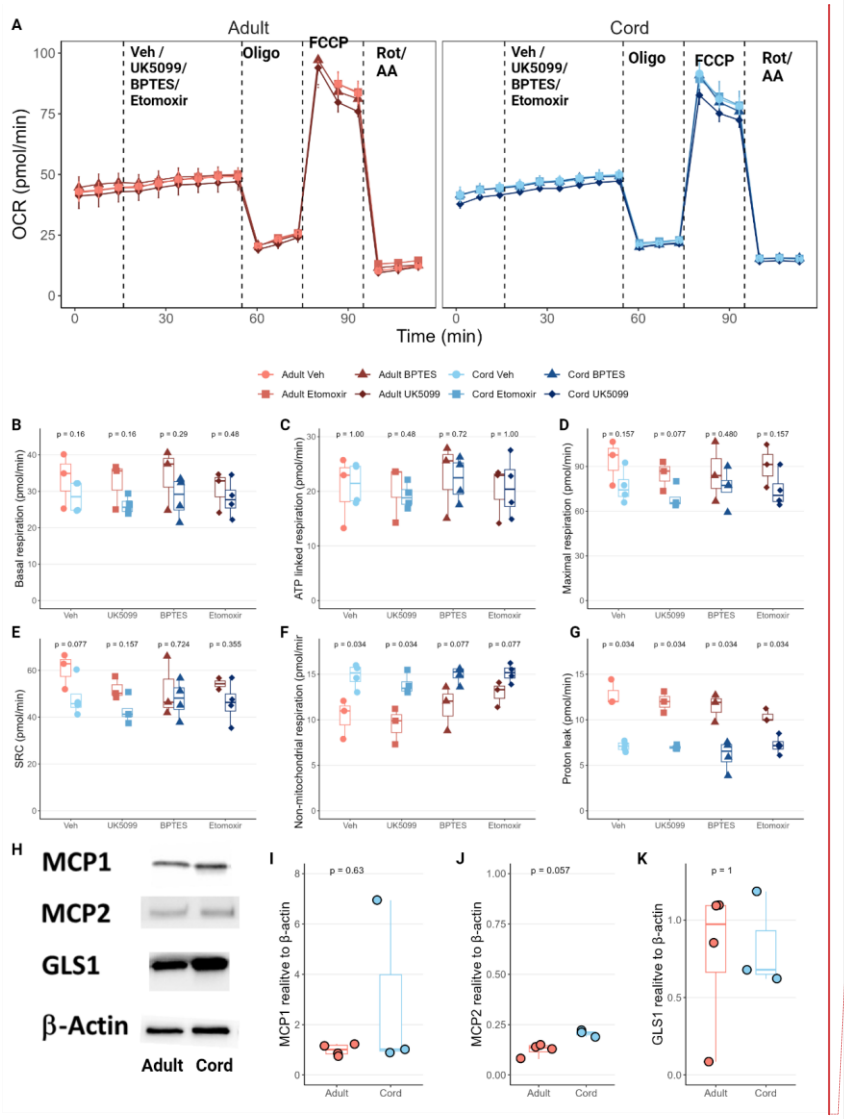

Figure 3.18 Mitochondrial respiration of c adult and umbilical cord nCD4+ T cells is comparable 16 h post stimulation.

Naïve CD4+ T cells from human adults and umbilical cords were activated for 16 h with anti-CD3/28 and mitochondrial parameters were assessed. A) Trace of mitostress test in the after in situ inhibition of MCP with UK5099 (2 µM), GLSI1 with BPTES (3 µM) and CPT1a with Etomoxir (3 µM). Mitochondrial parameters determined by injections

Commented [SH4]: Labels on blots

of oligomycin (1 µM), FCCP (1 µM) and antimycin (1 µM) and rotenone (1 µM) following injections of UK5099, BPTES and Etomoxir. B) Basal respiration, C) ATP linked respiration, D) maximal respiration, E) spare respiratory capacity, F) non-mitochondrial respiration, G) proton leak. H) Representative western blots of MPCP1, MPC2, GLS1 and β-actin loading control. Summary densitometry plots normalised to β-actin, I) MCP1, J) MCP2, K) GLS1. Data are representative of 5 independent experiments. n = 4 adults and 3 cords. p value determined by Wilcoxon rank sum test; p < 0.05 was deemed significant.

Firstly, comparing adult and cord vehicle controls, barring non-mitochondrial respiration and proton leak, no significant differences in most mitochondrial metabolic parameters was seen between the donor groups (Figure 3.18B-G). The same trends held true when cells were treated with the inhibitors UK5099, BPTES and etomoxir suggesting similar reliance on these metabolic fuels for adult and cord nCD4+ T cells (Figure 3.18B-G). To be sure these observations were not a result of different expression of the enzymes targeted by the inhibitors, MPC1, MPC2 and GLS1 proteins were determined by western blot (Figure 3.18H). No significant difference was seen between donor groups for any of the proteins examined (3.18I-K). Exploring the fuel requirements of Tn, no significant differences were seen in any of the mitochondrial parameters measured, compared to vehicle control, for adults or cords (Figure 3.18B-G).

Figure 3.19 Mitochondrial biogenesis of activated nCD4+ T cells from adult peripheral and umbilical cord blood.

Mitochondrial content was assessed in nCD4+ T cells, isolated from human adult peripheral blood and umbilical cords, after 16 h culture with anti-CD3/28 or vehicle. A) Mitochondrial mass determined by MitoTracker® MFI. B) Representative western blot of PGC1α and β-actin loading control. C) Summary plots of PGC1α densitometry normalised to β-actin. n = 4 adults and 3 cords. For comparisons between donor groups p value determined by Wilcoxon rank sum test and for comparisons between vehicle and αCD3/28 treatment within donor groups a Wilcoxon signed rank test was used; p < 0.05 was deemed significant.

Compared to ex vivo (Figure 3.8), a much greater OCR was observed at 16 h (Figure 3.18) suggesting that mitochondrial mass may have increased to support the increased metabolic demand. Surprisingly, on examining mitochondrial mass of anti-CD3/28 treated and vehicle controls with MitoTracker™ Green, there was evidence of significant mitochondrial biogenesis in cords but not adults (p = 0.01), resulting in a greater mitochondrial mass for activated cord T, although this did not reach significance (p = 0.4; Figure 3.19A). However, blotting for peroxisome proliferator-activated receptor gamma coactivator 1-alpha (PGC1α), the master regulator of mitochondrial biogenesis, did not show any significant difference between adults and cords (p = 0.63; Figure 3.19B-C).

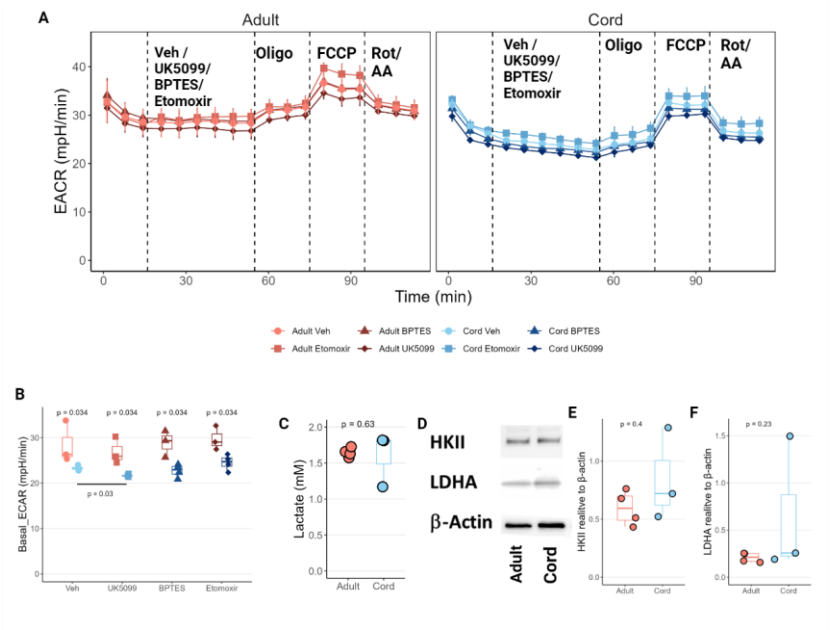

Figure 3.20 Glycolysis of nCD4+ T cells from adult peripheral and umbilical cord blood 16 h post activation.

Naive CD4+ T cells from adults and cords were activated for 16 h with anti-CD3/28 and glycolytic parameters were assessed. A) Trace of ECAR with in situ inhibition of with UK5099 (2 µM), BPTES (3 µM) and Etomoxir (3 µM) followed by injections of injections of oligomycin (1 µM), FCCP (1 µM) and antimycin (1 µM) and rotenone (1 µM). B) Basal ECAR, C) maximal ECAR. Lactate in culture supernatant after 16 h activation. D) Representative western blots of HKII and LDHA compared to β-actin loading control. Summary plots of densitometry normalised to β-actin, E) HKII and F) LDHA. Data are representative of 5 independent experiments. n = 4 adult and 3 cord. p value determined by Wilcoxon rank sum test and for comparisons between vehicle and inhibitor treatment within donor groups a Wilcoxon signed rank test was used ; p < 0.05 was deemed significant.

Additionally, to determining mitochondrial metabolism, ECAR was simultaneously measured and used as a determinant of glycolysis (Figure 3.20A). Contrary to the

finding directly ex vivo, at 16 h cords showed significantly reduced ECAR, in situ compared to adults in the vehicle control and on addition of UK5099, BPTES and etomoxir ($p = 0.034$; Figure 3.20B). Additionally, treatment with UK5099 in situ resulted in a significant decrease in ECAR, compared to vehicle, for cords but not adults ($p = 0.03$; Figure 3.20B). Despite the decreased basal ECAR measured in situ, total lactate in culture media supernatant at 16 h was comparable between adults and cords ($p = 0.63$; Figure 3.20C) and no significant difference was seen in the expression of glycolytic enzymes HKII and LDHA, as determined by western plot ($p = 0.4$ and 0.23; Figure 3.20D-F)

The significantly different metabolic profile after ex vivo activation and at 16 hours post activation, prompted measurement of a wider array of cytokines, to consider if altered metabolic adaptation was associated with a differential cytokine response tailored toward a unique role for umbilical cord blood T cells, in keeping with other observations made around CXCL8 and IL-4 (Gibbons et al., 2014; Hebel et al., 2014). To assess other potential roles of umbilical cord blood naïve CD4+ T cells, a proteome approach was taken using the Human Angiogenesis Array C1000 (RayBiotech). Along with conventional cytokines such as IL-2 and TNFα this panel included any signalling factors associated with tissue repair and wound healing and was used to test the hypothesis that naïve CD4+ T cells from the umbilical cord may have an enhanced time of life specific role in this area (Li et al., 2019a; Chen et al., 2022; Dolejsi et al., 2022).

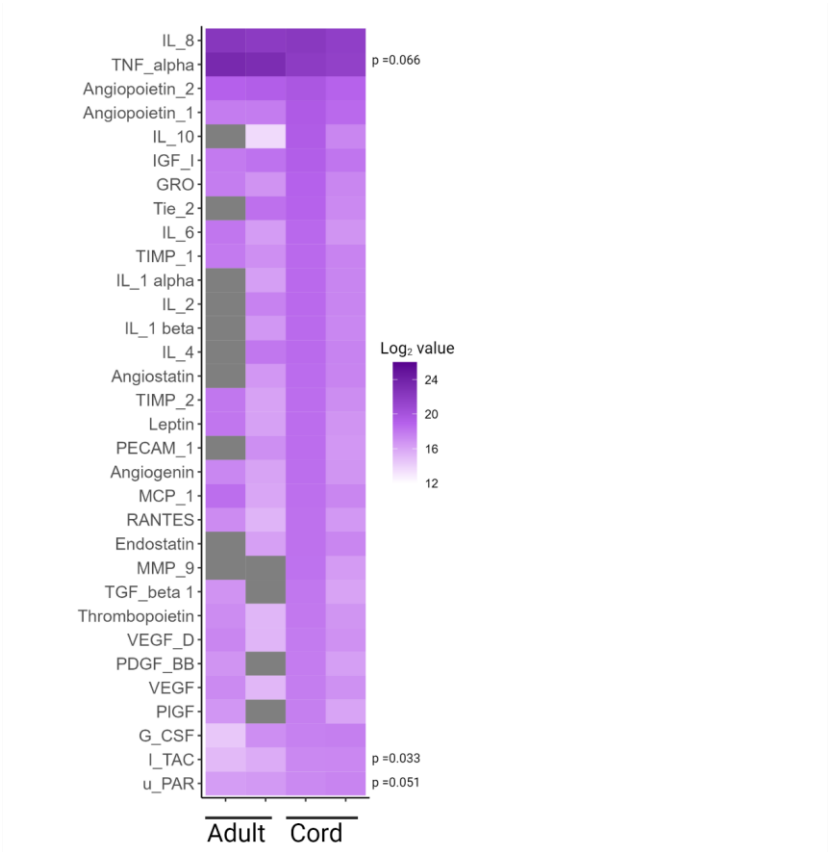

Figure 3.21 Proteome analysis of angiogenesis factors in adult peripheral umbilical cord blood nCD4+ T cells activated for 16 hours.

nCD4+ T cells from adult peripheral and umbilical cord blood were activated with anti CD3/28 for 16 h and the presence of angiogenesis related factors was assessed in the culture supernatant. Data shows log_2 transformed values minus background reading. n = 2 adult and 2 cord. p value determined by Wilcoxon rank sum test; $p < 0.05$ was deemed significant.

43 targets were simultaneously detected in adult and cord naïve CD4+ T cell supernatant after 16 h in culture of which 9 targets (EGF, ENA-78, bFGF, I-309, MCP-3, MCP-4, MMP-1, VEGF-R2 and VEGF-R3) were not detected above background levels

in any of the samples measured. IL-8, TNFα and Angiopoietin were the most highly secreted targets in cord supernatant however, only I-TAC was significantly different between the two donor groups which was higher in cords ($p = 0.033$). u-PAR and TNFα both neared significance ($p = 0.051$ and $p = 0.066$) with u-PAR higher in cords and TNFα higher in adults. It also appears that other targets such as IL-10, MMP-9, G-SCF may also be higher in cords although, the high degree of individual donor variability makes this hard to determine.

3.4 Discussion

At birth, the T cell repertoire is dominated by the naïve compartment with only a small fraction of memory cells at birth, which likely impacts the kinetics of the immune response and pathogen clearance as the number of fast reacting antigen experienced memory cells are greatly diminished compared to adults. Metabolic reprogramming on antigen encounter is vital to exiting the quiescent state, expanding cell number and producing effector molecules to perform their intended functions (Bailis et al., 2019; Jones et al., 2019; Nastasi et al., 2021). For the first time, this chapter explores the early activation events in neonatal umbilical cord blood derived naïve CD4+ T cells and finds a more strongly glycolytic switch induced on activation and greater mTOR activation supported by increased uptake of leucine when compared to adults. However, this comparatively elevated energetic state did not extend into the later hours of activation (16 hours), where metabolic parameters were largely comparable to adults.

Total T cells were first examined and similar ratios of CD4+:CD8+ cells were found and both the CD4+ and CD8+ T cell populations were predominantly naïve in cord blood (~90%), in line with previous reports (Prabhu et al., 2016; Jacks et al., 2018). Compared to other finding in the literature, a higher ratio of CD4 to CD8+ cells for adults was reported here (Wikby et al., 2008). This result may have been caused by not including the T cell lineage marker CD3 in the panel which would have excluded CD4 expressing cell types such as dendritic cells, thus limiting the overall specificity of the panel (Jardine et al., 2013). Of the few CD4+ memory cells present in cord, CM cells were the most frequent with terminally differentiated EMRA cells being the least

frequent, implying that the CD4+ compartment is in a mostly inactive and undifferentiated state at birth. Contrary to others, a comparable population of CD8+ EMRA cells were seen in cords and adults (Prabhu et al., 2016). The discrepancies in CD4+ and CD8+ effector gradients observed here might reflect the innate like function of neonatal CD8+ T cells enabling more rapid responses (Galindo-Albarran et al., 2016). A more detailed consideration of different T helper lineages was enabled by examining the expression of chemokine receptors associated with these different T helper lineages which are mostly confined to the memory compartment. Although only a small fraction of the total cord CD4+ T lymphocytes, a distinctively Th2 skewed phenotype was seen across all cord memory populations. However, the true validity of these cell as Th2 differentiated cells is still up for debate here, as transcription the lineage defining transcription factor GATA3 was not stained for and the low frequencies of these populations confounds accurate determination of populations (Halim et al., 2017). Whether or not human neonates are Th2 skewed is still under debate with various conflicting pieces of evidence and much of the early foundational evidence coming from mice (Chen and Field, 1995; Forsthuber et al., 1996; Halonen et al., 2009; Jacks et al., 2018; Rudd, 2020). Obvious Th2 skewing at the time of birth, at least in the memory compartment as shown here, might indicate a biased response favouring the Th2 phenotype rather than a programmed cell intrinsic bias for Th2 differentiation and might reflect the repertoire of antigen experience at this point of development. Another consideration is that the relatively antigen poor environment during gestation provides little opportunity for the generation of antigen experienced conventional memory T cells. On the other hand, regulatory T cells are generated early in gestational development and go on to form a long-lived memory population (Mold et al., 2008; Li et al., 2019b; Peterson et al., 2021). Here T-helper-like chemokine phenotype was assessed in $CD25^{high}CD127^{low}$ population which are indicative of regulatory T cells although limited by lack of intracellular FOXP3 staining which can lead to an impure population or failure to capture the full population (Klein et al., 2010). When using the same chemokine receptor expression, as used with total CD4+, Th2-like Tregs were still the most abundant Th phenotype but the Tregs were not overwhelmingly Th2 skewed suggesting that Th2 skewing may be confined to conventional T cells. It must also be considered that these results are limited by the

very small number of Th-like events recorded in some cord blood samples. Additionally, further research would benefit from higher throughput and more specific approaches, such as single cell sequencing, to more accurately and definitively define T-helper and T-helper-like Tregs populations by also examining the expression of master transcription factors known to be involved in the T-helper lineages of T cells (Halim et al., 2017). One should also consider that these chemokine receptors also govern trafficking of T cells to separate locations in the body so it stands to reason that Tregs and conventional T cells are not distributed equally throughout tissues. Uniquely in cords, there was a distinct lack of Th22-like Tregs, which perhaps contributes to greater susceptibility of neonates to allergic immune reactions as fewer regulatory T cells will traffic to epithelial sites (Koning et al., 1996; Prescott et al., 2003; Smith et al., 2008).

Given that naïve CD4+ T cells formed the largest T cell population in umbilical cord blood collected at term birth further investigation focused on this subset. Although the details of neonatal nCD4+ T cell activation differ by report it is commonly agreed that the activation phenotype is distinct from adults (Rudd, 2020). There is now a fairly broad consensus that metabolism has a defining role in T cell phenotype and function, leading to the hypothesis tested here that the reported in differences in adult and neonatal nCD4+ T cell activation are underpinned by distinct metabolic profiles (Holm et al., 2021). Initial hypothesis testing used a freely available and published transcriptomic data set which revealed differences in key metabolic pathways associated with T cell activation, including glycolysis which is an essential pathway required for exiting T cell quiescence on activation. Increased ECAR in neonatal ex vivo nCD4+ T cells corroborated the in-silico findings. Although, elevated levels of key glycolytic proteins were not seen in cords which may indicate that these differences are instead due to differences the modulation of glycolytic rate through modification of enzyme kinetics. This slightly elevated glycolytic rate when resting might be indicative of a higher readiness state in neonatal nCD4+ T cell as early activation markers CD69 and CD44 were also elevated, suggesting neonatal nCD4+ T cells are poised for rapid responses. Supporting this possibility, the metabolic switch, measured by in situ activation with anti-CD3/28, was considerably greater in

neonates. This was accompanied by considerably greater spare respiratory capacity in the hours immediately following activation providing neonatal nCD4+ T cells with greater metabolic flexibility to meet growing demand as the immune response ensues and might be fuelled by increased glutaminolysis (Matias et al., 2021). Interestingly, despite increased mitochondrial activity in both groups, this was not accompanied by increased mitochondrial superoxide production in the neonates in stark contrast to the adult. The lack of mitochondrial superoxide signalling might have significant ramifications for T cell activation as it supports NFAT translocation to the nucleus and subsequent production of IL-2 (Sena et al., 2013) which was found to be reduced in neonates at 16 h.

Matching the heightened metabolic switch in neonates, increased phosphorylation of mTOR, a key metabolic regulator, and its downstream targets was also observed. As there was no difference in AKT phosphorylation at ser473, it seems most likely that mTORC1 is the key differentially regulated signalling protein. Mechanistically, greater mTOR signalling might be supported by greater amino acid uptake through increased surface expression of CD98, as inhibition of CD98 with BCH abrogated the increase in mTOR phosphorylation. Similar mechanisms for controlling mTOR activation and subsequent cell function have been reported in other cells including murine ILCs (Panda et al., 2022). Furthermore, increased mTOR signalling may have resulted in enhanced glutaminolysis, which fuels oxidative phosphorylation and spare respiratory capacity through αKG entering the TCA cycle, (Jones et al., 2019) leading neonatal nCD4+ T cells to be more sensitive to glutamine depravation on activation.

Going beyond the immediate hours after activation and examining nCD4+ T cell characteristics at 16 h, a more conflicting story emerged. By this time ELISAs showed a distinct activation profile of cord nCD4+ T cells with reduced IL-2 and IFNγ secretion and some donors showing much greater IL-10 secretion, which could result in reduced functional and proliferative capacity (Canto et al., 2005). As it is currently not established here whether the differences in early neonatal nCD4+ T cell responses are a or whether some behave more like adults whilst another population behaves differently, additional experiments examining cytokine production on a single cell

basis, by staining intracellularly for flow cytometry, would provide more granular detail of the differences in cytokine production seen between adults and cords.

It has also been suggested that neonatal T cells have a unique role in tissue regeneration and homeostasis with evidence demonstrating an important role in heart neonatal heart regeneration, not seen in adults, as well as the unique ability to traffic in and out of non-lymphoid tissues (Mackay et al., 1988; Dolejsi et al., 2022). However, in this chapter an initial analysis of this role, by examining over 40 targets associated with angiogenesis, is inconclusive, potentially due to the small number of samples studied. Although some factors associated with tissue remodelling and repair appeared to be secreted in greater amounts by cord nCD4+ T cells such as MMP-9 (which was only secreted in cords), as well as angiopoietin and u-PAR. Further experiments using more quantitative methods and larger sample numbers are required to provide more clarity.

In comparison to the first hours of activation, mitochondrial parameters such as basal respiration and spare respiratory capacity no longer differed between adults and neonates, after 16 hours despite apparently greater mitochondrial biogenesis in cords. Although, as there is no difference in PGC1α between donor groups and ex vivo analysis had found comparable mitochondrial content between adults and cords, it may be that mitochondrial content dropped in unstimulated controls, leading to the appearance of increased biogenesis. Use of inhibitors, UK5099, BPTES and etomoxir suggested that there are minimal differing fuel requirements in adults and neonates although, glycolysis in neonates might be more sensitive to accumulation of pyruvate. The results of these assays may also demonstrate the degree of metabolic flexibility in both adult and cord naïve T cells. This leaves increased ECAR in adults as the only metabolic parameter measured here that differs dramatically between adults and neonates. Whether this is sufficient to explain the differing cytokine production of adults and cords is not clear and requires further investigation. However, there is some supporting evidence in the literature that could support this outcome such as the known reliance on glycolysis for IFNγ secretion which is significantly reduced in cords (Chang et al., 2013; Peng et al., 2016). Other metabolic pathways, not interrogated here, are likely to also play a role in creating the unique activation profile

of neonatal naïve CD4+ T cells. In particular, time course analysis of adult T cell proteomics during activation revealed one carbon metabolism as amongst the most upregulated in the early stages of activation whilst the more commonly assessed pathways of glycolysis and glutaminolysis were amongst the lowest upregulated (Ron-Harel et al., 2016; Tan et al., 2017).

3.5 Conclusions

This chapter finds that neonatal T cells are primarily naïve and that the CD4 compartment in particular exists in a highly undifferentiated state. The small fraction of memory T cells in the total CD4+ population is distinctly Th2 skewed although the same skewing is not evident in regulatory T cells, suggesting differing antigen specificity and trafficking potential to separate sites of the body. Investigation of immediate metabolic reprogramming of neonatal naïve CD4+ T cells on activation revealed a strong glycolytic switch and greater mTOR signalling driven by increased amino acid uptake likely through CD98. However, the comparatively heightened energetic state was not sustained by 16 h, at which point a lower glycolytic rate might have contributed to a differing activation phenotype, defined by lower IL-2 and IFNγ production. The importance of this enhanced early metabolic switch in neonates remains unclear and further work is required to elucidate how this initial metabolic enhancement is diminished in the first hours post activation and how this relates to altered T cell function.

Chapter 4

4 The Effects of Physiologic Media on Adult and Umbilical Cord Blood Naïve CD4+ T Cell Responses

4.1 Introduction

A substantial body of literature demonstrates several differences in the T cell compartment of neonates, usually represented by umbilical cord blood (UCB) T cells. Perhaps most obviously, circulating human neonatal T cells are comprised almost entirely of naïve, antigen inexperienced, cells with more recent thymic emigrants (Lorenzini and Toldi, 2023). Understanding the functions and mechanistic underpinnings of human neonatal naïve T cells has been confounded by limited neonatal material leading the field to be largely driven by murine models which demonstrate Th2 skewing in neonates (Adkins and Du, 1998; Rose et al., 2007). However, it is unclear whether this phenomenon is true in humans as some reports have shown no global Th2 skewing in human infants (Jacks et al., 2018). Ex vivo studies of human neonatal naïve T cells have revealed reduced chromatin accessibility and increased hypermethylation at Th1 associated transcription sites (White et al., 2002; Yu et al., 2021; Bermick et al., 2022). Furthermore, the highly permissive IL-13 locus of neonatal naïve T cells, even under Th1 skewing conditions suggests that human neonatal naïve T cells may also be Th2 skewed (Webster et al., 2007; Jacks et al., 2018).

In vitro models of T cell activation utilising mammalian cell culture techniques have enabled studies to further probe the intrinsic characteristics of neonatal T cells; although, the findings from such studies vary considerably. Some early work reported broad defects in neonatal T cell responses with decreased expression of both IL-4 and IFN-γ but similar expression of IL-2 (Lewis et al., 1991). In a later study, human neonates were found to exhibit reduced activation markers and IFN-γ production when stimulated with anti-CD3 antibodies alone, however, when used in combination with anti-CD28 this gap was reduced to the point of insignificance (Canto et al., 2005). These data suggest that increased reliance on co-stimulatory signals might explain previously reported defects in neonatal T cell function, although, subsequent studies using anti-CD3/28 also have reported conflicting results. Some evidence increased type 2 cytokine responses or diminished type 1 responses whilst others show little to no differences in cytokine production (Lesniewski et al., 2008; Hebel et al., 2014; Schmiedeberg et al., 2016; Yu et al., 2021; Bermick et al., 2022). Under skewing

conditions, neonates are consistently able to generate Th1 and Th2 cells with some studies noting greater propensity for type 2 cytokine secreting cells under Th1 skewing conditions than seen in adults (Webster et al., 2007; Jacks et al., 2018; Razzaghian et al., 2021). It has been suggested that neonatal T cells are as intrinsically functional as their adult counterparts and the fault instead lies with altered priming by DCs (Zaghouani et al., 2009). However, altered cytokine production can only partially be explained by DC function, as illustrated by studies using adult DCs or cross treatments of adult and umbilical cord blood APCs (Chen et al., 2006; Razzaghian et al., 2021).

In recent years a growing body of evidence has begun to highlight the importance of metabolism for cell function. In adult T cells, central metabolic programmes, such as glycolysis and oxidative phosphorylation, are essential for exit of quiescence, rapid expansion and production of effector molecules (Wang et al., 2011; Jones et al., 2019). Metabolic control of cell function is facilitated through a number of mechanisms including energy and anabolic precursor generation, post transcriptional regulation and epigenetic regulation of the chromatin landscape (Peng et al., 2016; Puleston et al., 2021). Whilst neonatal T cell metabolism is very poorly defined, studies providing fish oil supplementation to mothers during pregnancy or increasing arginine supplementation in cord blood CD4+ T cell culture have hinted at a role for metabolism in defining the neonatal T cell responses (Harb et al., 2017; Yu et al., 2021).

Given the evident role of metabolism in shaping T cell function, the metabolite content of commonly used cell culture media has come under close scrutiny. Modern culture techniques derived from the need to produce lower cost and more standardised growth media than natural biological fluids. Animal cell culture was pioneered in the early 20th century, often using reptilian or amphibian embryos. By the mid-1900s the first continuous cell cultures were established with a cervical cancer biopsy from Henrietta Lacks, establishing the first human tumour cell lines HeLa, still in use to this day. Harry Eagle then described the essential nutrient requirements of the HeLa cells as well as a mouse fibroblast cell line L929, culminating in the creation of Eagle's Medium Base (Eagle, 1955b; c; d; a). This was shortly

followed by Eagle's Minimal Essential Media, which enabled longer culture times and contained glucose, 13 amino acids, six inorganic salts, eight water-soluble vitamins and dialyzed blood serum (Eagle, 1959). Numerous variations have since been developed for more specialised use cases including Dulbecco's Modified Eagle Medium, Ham's F12 Medium and other complete media which do not require serum supplementation (Ham, 1965; Cantor, 2019). Among the many new media formulations, in 1967, the Cell Laboratory at Roswell Park Memorial Institute (RPMI) defined a cell culture medium for human leukocyte culture RPMI 1640 (Moore et al., 1967). This media formulation, supplemented with fetal calf serum or fetal bovine serum, is still commonly used today for a wide range of cell cultures, including T cells.

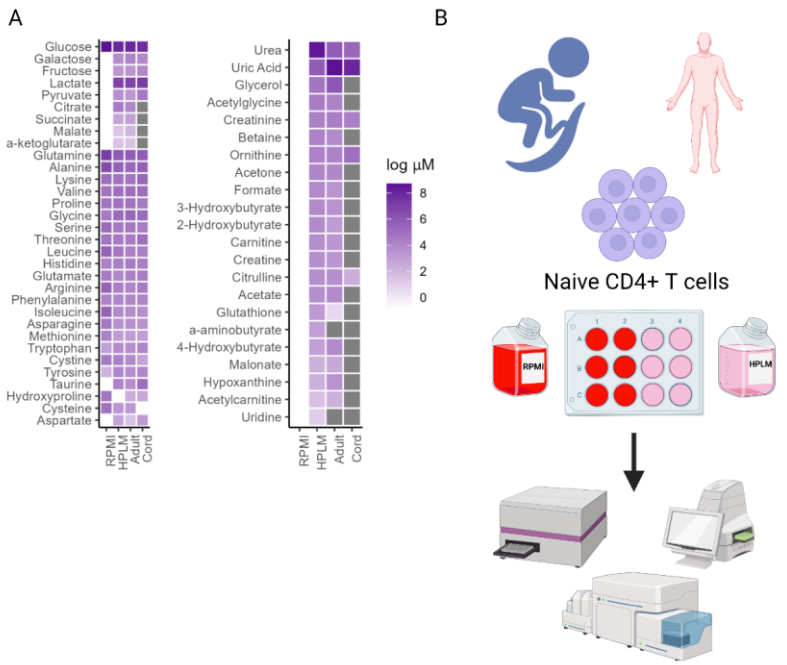

Figure 4.1 Comparing culture media and plasma metabolites.

A) A comparison of metabolites present in RPMI, HPLM, adult human plasma and umbilical cord blood plasma. White cells indicate non presence of the metabolite and grey indicates no standard value identified in the literature. B) Schematic of

experimental design to compare the effects of culture media on the activation of adult and cord blood naïve CD4+ (nCD4+) T cells. Figure made using Biorender.com.

Nearly 70 years later, most multipurpose culture medias are based on the original observations by Harry Eagle and are designed to meet the needs of a handful of specific cell lines. Given the pervasive role of metabolism in cell function efforts have now been made to produce physiologic culture media, in hopes of creating better in vitro models. Human Plasma Like Media (HPLM) and Plasmax are examples of commercialised physiologic media that closely resemble human plasma in metabolite, vitamin and ion concentrations (Cantor et al., 2017; Voorde et al., 2019). It is worth noting, neither HPLM or Plasmax is a complete media and still requires supplementation with dialysed serum to provide the other factors required for healthy cell growth. Compared to RPMI, HPLM contains considerably less glucose and glutamine however, HPLM contains other sugars, carbohydrates and amnio acids not present at all in RPMI (Figure 4.1A). Work focusing on adult T cells has already found significant differences in many aspects of CD4+ T cell activation, including metabolic features proliferation and cytokine production, when cultured in HPLM compared to RPMI 1640, (Leney-Greene et al., 2020; MacPherson et al., 2022). However, little is known about the metabolic requirements of neonatal T cells or how physiologically relevant media may affect their activation profile. To address this gap in the literature, this study compared and contrasted nCD4+ T cell activation, from adults and umbilical cords, in conventional culture media (RPMI 1640) and HPLM which more closely replicates adult and umbilical cord blood plasma (Figure 4.1B).

4.1.1 Rationale

T cell culture is a vital tool in the study of neonatal immune responses. However, the effects of recently developed physiologically relevant media have not been investigated. The purpose of this study is to compare and contrast activation responses of human nCD4+ T cells from adults and umbilical cord blood (UCB) cultured in HPLM or RPMI 1640 and to better understand their metabolic function and requirements. The results of this study will provide valuable insights into the use

of physiologically relevant media for T cell culture and its potential applications in neonatal immune response research.

4.1.2 Hypothesis

1. The use of more physiologically relevant media will significantly alter the activation profiles of adult and cord derived nCD4+ T cells.
2. Adult and cord derived nCD4+ T cells are fuelled by distinctly different metabolic phenotypes and culture in physiologic media will significantly alter the metabolic phenotype.
3. Differing metabolic requirements of adult and cord derived nCD4+ T cells will drive distinct activation profiles in response to physiologic media.

4.2 Experimental procedures

4.2.1 nCD4+ T cell isolation

Adult human peripheral blood, from healthy nonfasted donors, or umbilical cord blood was collected onto heparinised Vacuettes™ (Greiner Bio-one. Frickenhausen, Germany), as described in 2.1 and 2.3. MNCs were isolated by density centrifugation, as in chapter 2.3.1, washed and resuspended in PBS. MNC density was determined (see chapter 2.4), prior to depletion of CD235a-bearing cells by antibody labelled magnetic microbeads (autoMACS; Miltenyi Biotech; see chapter 2.3.2). Here, 10 μL of beads were used per 10^7 adult MNCs whilst 30 μL of beads were used per 10^7 umbilical cord blood MNCs. CD235a depleted MNCs were resuspended in PBS before cell density was determined. nCD4+ T cells were isolated from MNCs by negative selection with antibody labelled magnetic microbeads (autoMACS; Miltenyi Biotech, see chapter 2.3.3). Isolated nCD4+ T cells were resuspended in PBS and purity was determined by flow cytometry (see chapter 2.6.2).

4.2.2 T cell culture in HPLM and RPMI

nCD4+ T cell counted in PBS were washed into either HPLM (ThermoFisher) or RPMI GlutaMAX™ (ThermoFisher) by filling with the appropriate media and centrifugation at 300 x g for 10 min at room temperature media. Cells were cultured at 1 x 10^6 cells/ mL in a total volume of 200 μL in a flat bottom 96 well tissue culture treated plate with 2 μg/mL plate bound anti-CD3 (OKT3; BioLegend) and 20 μg/mL soluble anti-CD28 (CD28.2; BioLegend). Cultures were supplemented with 10% dialysed FCS (ThermoFisher) 3 hours after initial plating (Chapter 2.7). Cells were cultured for 24 h or 48 h at 37°C in 5% CO_2 before harvesting by gentle pipetting. Cell death (DRAQ7) and activation (CD25, CD44 and CD69) were determined by flow cytometry whilst culture supernatant was stored at -20°C for later cytokine analysis by LEGENDplex™ and ELISA.

4.2.3 Flow cytometry

nCD4+ T cell purity was determined, as described in chapter 2.6.2, using Alexa Fluor™ 647 anti-CD4 (OKT4; Biolegend); FITC anti-CD45RO (UCHL1; Biolegend); Brilliant Violet™ 605 anti-CD45RA (HI100; BioLegend) and anti-CCR7. T cell death was determined using 1 μM DRAQ7 staining and excluded when determining cell activation, as monitored by surface staining (see chapter 2.6.1) using Pacific blue anti-CD25 (M-A251; Biolegend), FITC anti-CD44 (REA690; Miltenyi Biotech) and PE anti-CD69 (FN50; Biolegend). Intracellular signalling of select pathways was determined by intracellular flow cytometry with Vio® B515 anti-pS473-AKT (REA359™; Miltenyi), PE anti-pSTAT5-Tyr694 (A1701B; Biolegend) and APC anti-pS235/pS236-S6 (REA454; Miltenyi). Briefly, cells stimulated from 48 hours (as above) were fixed for 1 hour and permeabilised before adding the antibodies under permeabilising conditions for 30 min in the dark at room temperature. Stained cells were washed, and staining assessed using the NovoCyte3000, as detailed in chapter 2.6.4. Data were analysed in FlowJo version 10.8.1.

4.2.4 Cell proliferation assay

Cell proliferation in culture was determined over 72 h using CellTrace™ violet (ThermoFisher), according to the manufacturer's instructions. Isolated nCD4+ T cells were resuspended in PBS at 0.5 x 10^6 cells/mL and stained with CellTrace™ violet at 5 μM for 20 min at 37°C temperature protected from light. The stained cells were split across two tubes and excess dye was quenched by washing in either HPLM or RPMI media containing 1% FBS. Quenched cells were rested for 10 min before plating at 1 x 10^6 cells/mL in HPLM or RPMI for a total volume of 200 μL in a flat bottom 96 well tissue culture treated plate. Cultured cells were activated with precoated anti-CD3 (2 μg/mL) and soluble anti-CD28 (2 μg/mL) or left unactivated. After 3 h of incubation at 37°C and 5% CO_2 cultures were supplemented with 10% FBS. After 72 h of culture, cells were harvested by gentle pipetting and CellTrace violet intensity examined by flow cytometry. Cell proliferation was analysed in FlowJo version 10.8.1.

4.2.5 Bioenergetic analysis

Bioenergetic analysis was conducted using an Extracellular Flux Analyzer XF^e96 (Seahorse Biosciences), as described in detail in chapter 2.5.1 and 2.5.2. In brief, nCD4+ T cells cultured in different media for 48 h (as described above) were harvested from the culture plate by gentle pipetting. Harvested cells where then washed and resuspended in PBS before cell density was determined. After counting, cells were divided and washed into XF assay media supplemented with 5.5 mM glucose, 0.05 mM pyruvate, and 0.55 mM glutamine (HPLM-like) or supplemented with 11 mM glucose and 3 mM glutamine (RPMI-like). 0.15 x 10^6 cells were seeded into each well of a Cell-Tak (Corning) coated culture plate. A mitochondrial stress assay was performed using of oligomycin (1 μM), FCCP (1 μM), rotenone (1 μM) and antimycin A (1 μM) prepared in HPLM-like or RPMI-like assay media.

4.2.6 LEGENDplex™

The LEGENDplex™ HU Th cytokine panel (Biolegend) was used to measure concentration of IL-2, 4, 5, 6, 9, 10, 13, 17A, 17F, IFN-γ and TNFα in cell culture

supernatants, according to manufacturer's instructions as summarised below. To begin, a 1:4 serial dilution of standards was prepared from the lyophilised human cytokine panel 2 standard bead mix. Standards and samples were added to a v-bottom 96 well plate, together with LEGENDplex™ assay buffer and premixed capture beads. The plate was sealed and incubated on a plate shaker set to 800 rpm for 2 h protected from light. The beads were pellet by centrifugation at 250 x g for 5 min and the supernatant carefully removed. Next, the beads were washed twice by resuspending in LEGENDplex™ wash buffer and centrifuging at 250 x g for 5 min. After washing detection antibody was added to each well and the plate was sealed, protected from light and incubated at room temperature for 1 h, on a plate shaker set to 800. LEGENDPLEX™ SA-PE was added to each well and the plate was incubated, as detailed before, for 30 min. Following this incubation, the beads were pelleted and washed, as described above, before resuspending in LEGENDplex™ wash buffer and acquiring by flow cytometry (Novocyte3000, Agilent). Data were analysed in FlowJo version 10.8.1.

4.2.7 Enzyme linked immunosorbent assay

Secretion of CXCL8 in cell culture was measured by specific ELISA as per the manufacturer's instructions (DuoSets; R&D Systems; as in chapter 2.9).

4.2.8 Data analysis

Flow cytometry data analysis was performed using FlowJo version 10.8.1. Further data analysis was performed in R using the Tidy verse and Tidy models packages.

4.3 Results

To understand the effects of using physiologically relevant media on early activation, nCD4+ T cells were isolated from the peripheral blood of adults and from the umbilical cord (to represent neonates). Isolated cells were cultured in HPLM or RPMI for 24 or 48 h with or without plate bound anti-CD3 (2 μg/mL) and soluble anti-CD28 (20 μg/mL). After culture cells were harvested and viability, proliferation, activation

markers, metabolic parameters and cytokine profile were determined. These readouts were compared between the medias and differences between adults and neonates compared and contrasted. Additionally, unstimulated controls were used to assess the differences in impact of CD3/28 stimulation between the medias and between adults and neonates, providing a baseline comparison.

4.3.1 HPLM improves cell survival in culture.

Growth medium is specially formulated to allow continued survival and growth of cells, once removed from the host organism. Whilst RPMI is known to perform this role well for adult nCD4+ T cells others have previously reported poor survival of unstimulated cord blood nCD4+ T cells in culture(Thornton et al., 2004). To assess if the non-physiologic conditions of cell culture is a contributing factor to increased cell death of cord blood nCD4+ T cells, cell death was determined ex vivo and after culture in HPLM or RPMI (Figure. 4.2). Cell death was determined by flow cytometry, using the non-membrane permeable DNA dye DRAQ7. Firstly, debris and doublets (Figure 4.2a-b) were gated out followed by gating on live DRAQ7 negative and dead DRAQ7 positive cells (Fig 4.2D). Little to no cell death was seen ex vivo for both adults and cords at first isolation, however, cell death increased with the length of unstimulated culture for cords whilst there was only a moderate increase in cell death observed for adults (Figure 4.2D). HPLM culture reduced cell death for unstimulated cords and adults with cell survival becoming significantly greater by 48 h (Figure 4.2D; $p = 0.003$ and $p = 0.01$ in adults and cords respectively). When stimulated with anti-CD3/28, cell death became comparable between the donor groups as both showed little death in anti-CD3/CD28 stimulated culture (Figure 4.2E).

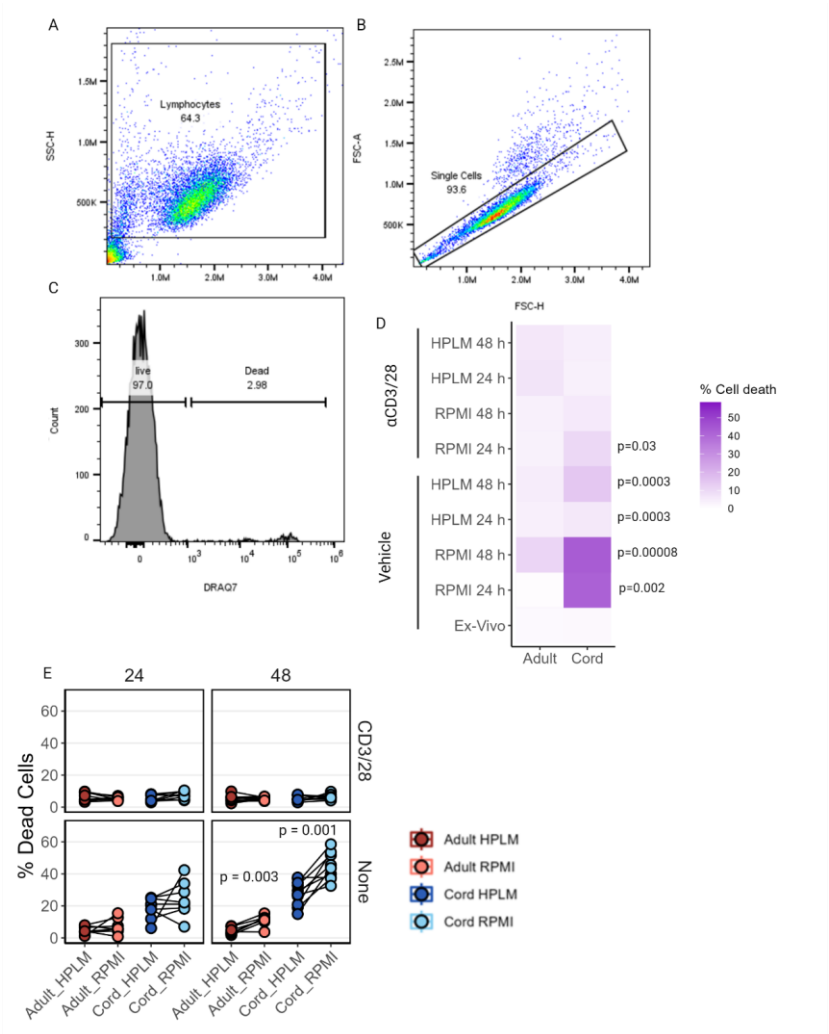

Figure 4.2 HPLM improves survival in cell culture.

Isolated nCD4+ T cells from human adult and umbilical cord blood were stimulated with anti-CD3/CD28 or left unstimulated. Cell viability at 24 and 48 h was determined using DRAQ7 staining with assessment by flow cytometry. (A) Gate applied to plot excluding debris. (B) Gate applied to exclude doublets. (C) Representative histogram plot of DRAQ7 stained cells with gates on DRAQ7 positive and DRAQ7 negative cells. (D) Summary of cell DRAQ7 positive cells ex vivo immediately on isolation of nCD4+ T

cells or after culture, compared between adults and cords. (E) Percentage DRAQ7 positive cells compared between different culture medias. n = 8 adult and 8-11 cords. For comparisons made between donor groups p-values were determined by Wilcoxon rank sum test (D) and comparisons of paired donors in different media conditions were determined by Wilcoxon signed rank test (E). p < 0.05 was deemed significant.

4.3.2 Growth and proliferation of adults and cords in HPLM and RPMI

Growth medium provides the essential molecules required for the catabolic and anabolic processes that drive cell growth and proliferation. Previous studies have demonstrated that various extracellular metabolites are necessary for T cell proliferation including glucose and glutamine, which are present at considerably lower concentration in HPLM (Carr et al., 2010; Ma et al., 2017; Ma et al., 2019). This raised the question of how growth and proliferation may differ in HPLM and RPMI cultures. To address this, cell growth was determined by forward scatter at 24 and 48 hours and proliferation was examined using cell trace violet (CTV) at 72 h. Cells only grew in size when stimulated with anti CD3/28 and continued to increase in size from 24 to 48 hours ($p = 0.01$for adult HPLM; $p = 0.01$ for adult RPMI, $p = 0.00028$ for cord HPLM and $p = 0.00027$ for cord RPMI). No significant differences in cell size were observed between stimulated HPLM and RPMI cultures nor between adults and cords (Figure.4.3A-C). However, proliferation at 72 h was profoundly reduced in HPLM cultures in both adults and cords with only a single division observed in most HPLM cultures compared to at least three division in RPMI. When comparing proliferation between adults and cords, a similar distribution across the generations was observed in HPLM. In RPMI cultures the percentage of cells seen in generations 2 and 3 were slightly higher in cords but this difference was not significant ($p = 0.4$ for generation 2 and $p = 0.7$ for generation 3) (Fig 4.3D-E)

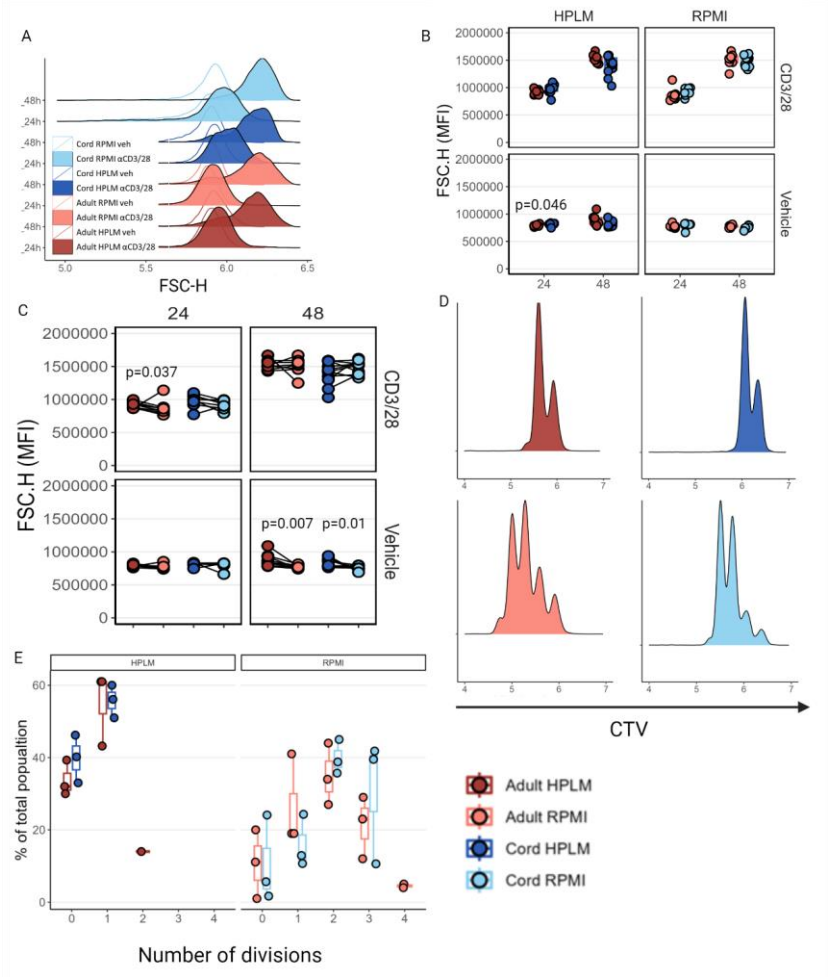

Figure 4.3 HPLM culture media restricts cell proliferation.

Human adult peripheral and umbilical cord blood naïve CD4+ T cells were assessed for cell growth and proliferation. (A) Size of naïve CD4+ T cells cultured with or without anti-CD3/28 for 24 and 48 hours was determined by flow cytometry forward scatter (FSC) representative histograms are shown in (B) summary graphs, represented as box and whisker plots, comparing median FSC values in adults and cords (C) comparing cells median FSC values for HPLM and RPMI cultured cells within each donor group. Cellular proliferation as determined with cell trace violet shown in representative histogram (D) and summary box plots showing each cell division as a percentage of

the total number of cells. n = 8 adults and 8-11 cords (A-C); n = 3 adults and 3 cords (D-E). For comparisons made between donor groups p-values were determined by Wilcoxon rank sum test (B,E) and comparisons of paired donors in different media conditions were determined by Wilcoxon signed rank test (C). p < 0.05 was deemed significant.

4.3.3 Activation profile of adults and cords in HPLM and RPMI

To assess how culture in HPLM and RPMI affected nCD4+ T cell activation and how activation might differ between adults and cords, a selection of surface activation markers was examined on live (DRAQ7-negative) cells harvested after culture at 24 and 48 hours with or without anti-CD3/28. When stimulated with anti-CD3/28, there was a noticeable increase in CD25 expression compared to unstimulated controls. MFI of CD25 increased between 24 and 48 hours, in all groups and expression was consistently higher in cords ($p = 0.009$ in HPLM at 24 h; 0.006 for RPMI at 24 h and 0.02 for RPMI at 48 h; Figure 4.4A-B). Anti-CD3/28 treated cultures increased expression of CD44 (compared to unstimulated controls) which increased over time in adults but remained constant in cords. When left unstimulated CD44 expression was comparable for both media conditions in adults, but in cord RPMI culture CD44 expression was significantly decreased by 48 hours compared to adults ($p = 0.002$). No difference in expression between adults and cords was seen at 24 hours. However, unlike adults, expression of CD44 did not increase in cords by 48 hours resulting in significantly greater expression in adults by this time point (Figure 4.4C-D; $p = 0.0003$ for HPLM and $p = 0.001$ for RPMI). Like the other activation markers, CD69 expression increased when cells were stimulated with anti-CD3/28 but no significant differences in median expression were observed between adults and cords. However, when left unstimulated expression decreased in cords, compared to the 24 hour timepoint, leading to a significantly lower expression than adults at 48 h although, this was not significant (Figure 4.4E-F).

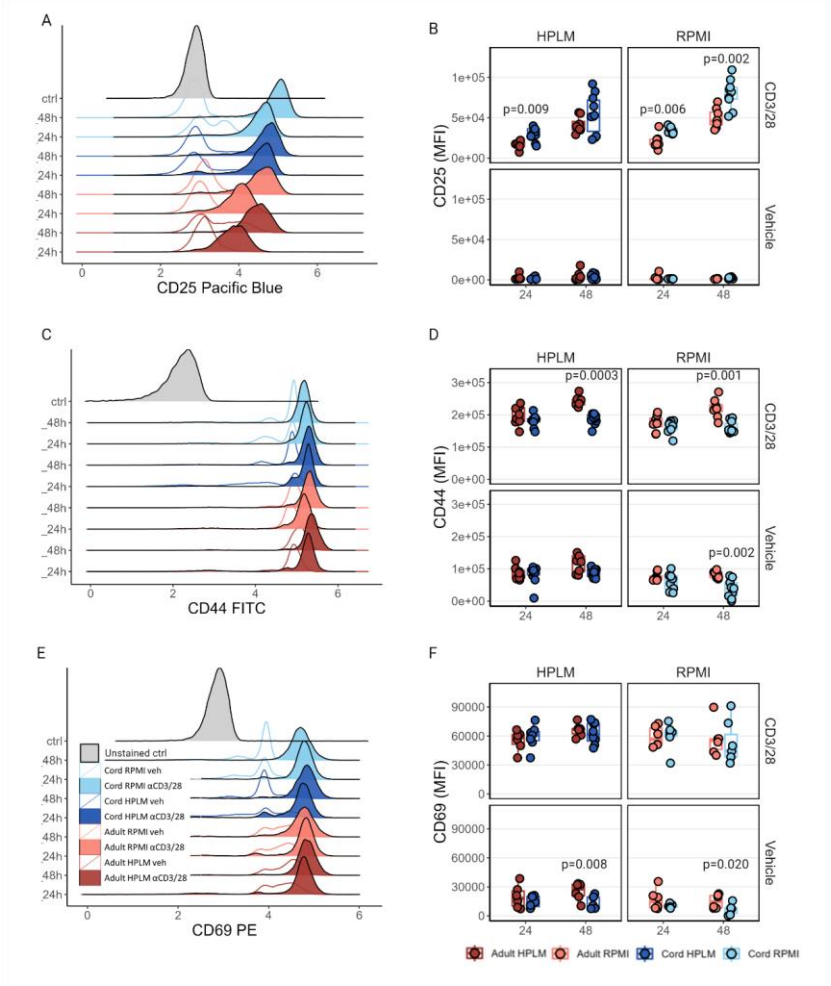

Figure 4.4 Adults and cords exhibit different activation profiles.

Activation of nCD4+ T cells from adult peripheral and umbilical cord blood, cultured in HPLM or RPMI with or without anti-CD3/28, determined by flow cytometry analysis at 24 and 48 hours. CD25 showing (A) example histogram and (B) summary box plots comparing CD25 MFI for adult and cord samples rested or activated in HPLM or RPMI for 24 and 48 hours. CD44 showing (C) example histogram and (D) summary box plots comparing CD44 MFI for adult and cord samples rested or activated in HPLM or RPMI for 24 and 48 hours. CD69 showing (E) example histogram and (F) summary box plots comparing CD69 MFI for adult and cord samples rested or activated in HPLM or RPMI

for 24 and 48 hours. n = 8 adults and 8-10 cords (A-D); n = 6 adults and n = 6-8 cords (E-F). Comparisons made between donor groups, p-values were determined by Wilcoxon rank sum test (B,D,F). p < 0.05 was deemed significant.

When directly comparing culture media conditions for each donor group at both 24 and 48 hours it can be seen that culture media has consistent effects on both adults and cords despite significant differences in expression markers between the two groups. Culture and activation in RPMI increased the expression of CD25 for both donor groups, with the effect becoming more prominent by 48 hours (p = 0.03 and 0.04 for adults and cords respectively at 24 hours and p = 0.02 at 48 hours for cords). The reverse was true for unstimulated cultures where a general trend to slightly greater CD25 expression in HPLM cultures, although this was significance at 24 hours for cords (Figure 4.5A; p = 0.02 at 24 hours for cords). CD44 and CD69 expression were generally greater in stimulated HPLM cultures reaching significance in cords for CD44 at 24 and 48 hours (p = 0.004 and p = 0.006, for 25 and 48 hours respectively; Figure 4.5B-C). Unstimulated RPMI cultures also showed reduced CD44 and CD69 expression from 24 to 48 hours, resulting in significantly greater expression in HPLM cultures by 48 hours for both donor groups (Figure 4.5C; for CD44 p = 0.007 for cords and p = 0.01 for adults. for CD69 p = 0.007 for adult and p = 0.03 for cords).

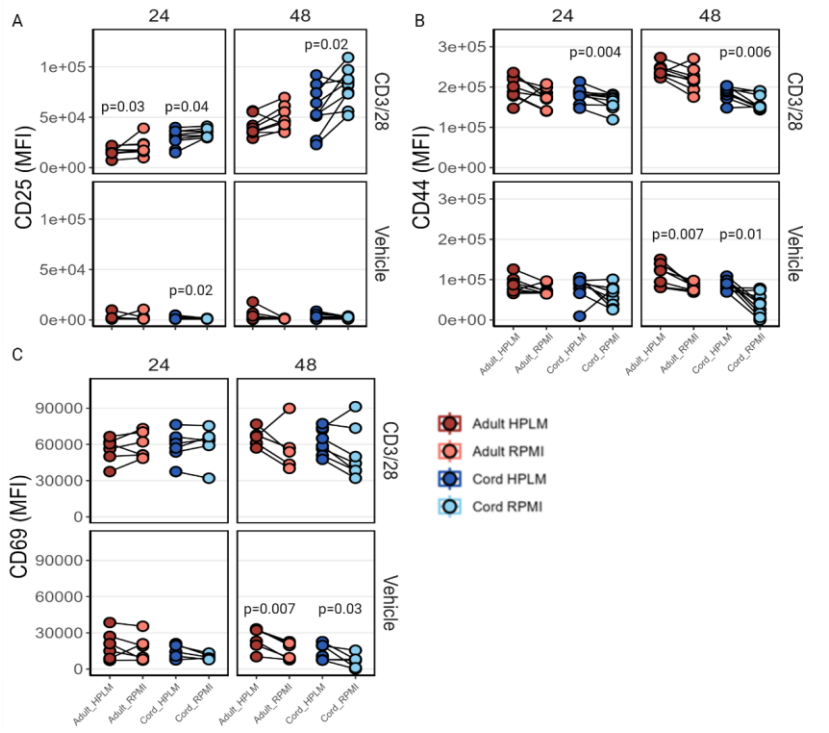

Figure 4.5 Surface marker activation profile comparison of HPLM and RPMI.

Comparison of nCD4+ T cell activation from adult peripheral and umbilical cord blood, cultured in HPLM or RPMI with or without anti-CD3/28. Summary graphs showing donor matched MFI values for (A) CD25, (B) CD44 and (C) CD69, cultured in HPLM or RPMI. n = 8 adults and 8-10 cords (A-B); n = 6 adults and n = 6-8 cords (C). Comparisons of paired donors in different media conditions were determined by Wilcoxon signed rank test (A-C). p < 0.05 was deemed significant.

4.3.4 Cytokine production of adults and cords in HPLM and RPMI

Cytokines direct the immune response, and their production is a key effector function of CD4+ T cells. Cytokines perform many functions such as promotion of cell growth by IL-2 or priming immune responses in the case of IFNγ and IL-4 and their production

is dependent on metabolic processes and the availability of specific metabolites including such as the requirement of glutamine for IL-2 production or glucose for IFNγ (Chang et al., 2013; Jones et al., 2019; Qiu et al., 2019). However, to date the vast majority of studies looking at cytokine production of human nCD4+ T cells have used non-physiologic media containing highly elevated levels of metabolites like glucose whilst lacking all other sugars. Additionally, specific cytokines are associated with distinct programmes of immune response such as IFNγ and IL-4 with type one and type-II responses respectively. Increasing evidence suggests metabolism has a central role in determining nCD4+ T cell fate and cytokine production (Kouidhi et al., 2016; Puleston et al., 2021). Differences in metabolism have also been postulated to explain differences in cytokine production between adults and cords (Holm et al., 2021).

To examine how cytokine production is affected by physiologic media and how this might differ between adults and neonates, secreted cytokines in culture supernatants, of stimulated or unstimulated nCD4+ T cells, were measured at 24 and 48 hours. Here a multiplexed cytokine detection approach was used to maximize the data generation from limited sample volume.

In general, greater cytokine secretion was measured in HPLM cultures at 24 hours and this effect was more pronounced in cords than adults. However, by 48 hours cytokine production was generally lower in HPLM with IFNγ and CXCL8 in cords being notable exceptions (Figure 4.6; $p = 0.039$ and $p = 0.0009$ for IFNγ and CXCL8 respectively).

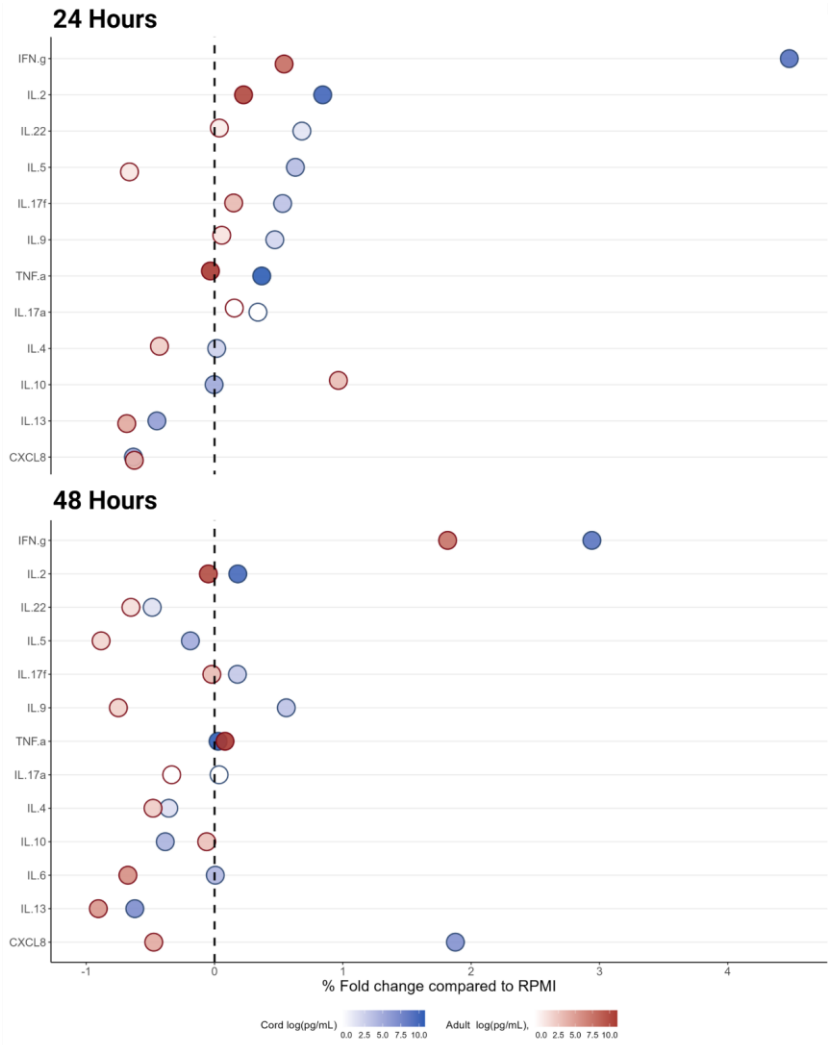

Figure 4.6 Cytokine production differs in CD4+ T cells when cultured in HPLM.

Summary plot showing fold change in cytokine production of HPLM cultures compared to RPMI, for nCD4+ T cells from adults or umbilical cords, stimulated with CD3/28 for 24 or 48 hours. Data are representative of n = 4-5 adults and 4-5 cords.

Cord blood nCD4+ T cells are often cited as poor producers of Th1 associated cytokines, responsible for driving cell mediated immunity against intracellular

pathogens. Here, these data show a reduction in TNFα in both medias, in cords compared to adults at 48 hours (Figure 4.7A). However, more secreted IFN-γ was measured in cord supernatant with this increase being significant in HPLM cultures (p = 0.03 and p = 0.03 at 24 and 48 hours respectively; Figure 4.7B). Culture in HPLM significantly increased anti-CD3/CD28 stimulated IFNγ production for cords compared to RPMI (p = 0.02 and p = 0.03 for 24 and 48 hours respectively). The same trend was generally true for adults, though, this did not reach significance. No discernible trends for differing TNFα secretion were observed between HPLM and RPMI cultures. Unstimulated cells did not secrete TNFα or IFNγ at any meaningful level (Figure 4.7A, B).

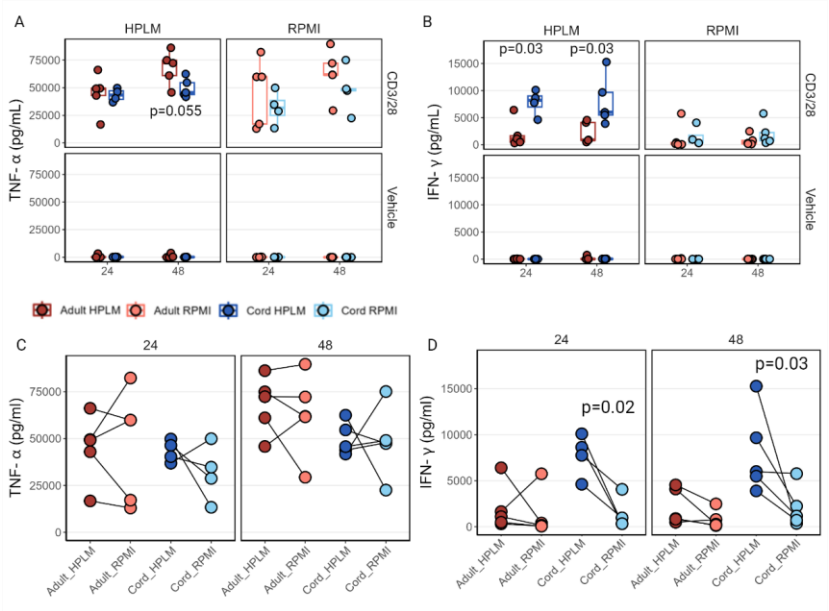

Figure 4.7 Culturing in HPLM increases IFNγ production.

Th1 associated cytokine production of nCD4+ T cells, from human adult peripheral or umbilical cord blood, cultured in HPLM or RPMI with or without anti-CD3/28 for 24 or 48 hours showing (A-B) summary box plots comparing cytokine secretion in adults and cords and (C-D) showing data as donor matched cytokine secretion in HPLM and RPMI

culture media. n = 4-5 adults and 4-5 cords. For comparisons made between donor groups p-values were determined by Wilcoxon rank sum test (A-B) and comparisons of paired donors in different media conditions were determined by Wilcoxon signed rank test (C-D). p < 0.05 was deemed significant.

nCD4+ T cells from cord blood are suggested to be preprogramed for production of Th2 cytokines, IL-4 and IL-13, with the literature often citing them as Th2 skewed (Debock and Flamand, 2014). Additionally, neonatal nCD4+ T cells possess a unique IL-4 variant in secretory granules allowing for rapid IL-4 secretion however, this IL-4 variant is not assessed in this panel(Hebel et al., 2014). This study finds increased expression of some Th2 cytokines in cords; however, this difference is often only slight and only sometimes significant. These data, show no difference in adult and cord IL-4 secretion with neither group secreting substantial amounts of this cytokine at either time point (Figure 4.8A). However, increased secretion of IL-5, IL-9 and IL-13 was often measured in cord supernatants with this often being more significant for HPLM cultures (Figure 4.8B-D). E.g. IL-13 secretion is significantly increased in cord HPLM cultures, compared to adults, but not in RPMI cultures ($p = 0.01$ and 0.007 for HPLM cultures at 24 and 48 hours respectively). For the most part, culture media did not significantly alter secretion of type 2 cytokines and what effects were observed differed by cytokine (Figure 4.8E-H). No type 2 cytokines were measured in unstimulated cultures (Figure 4.8A-D).

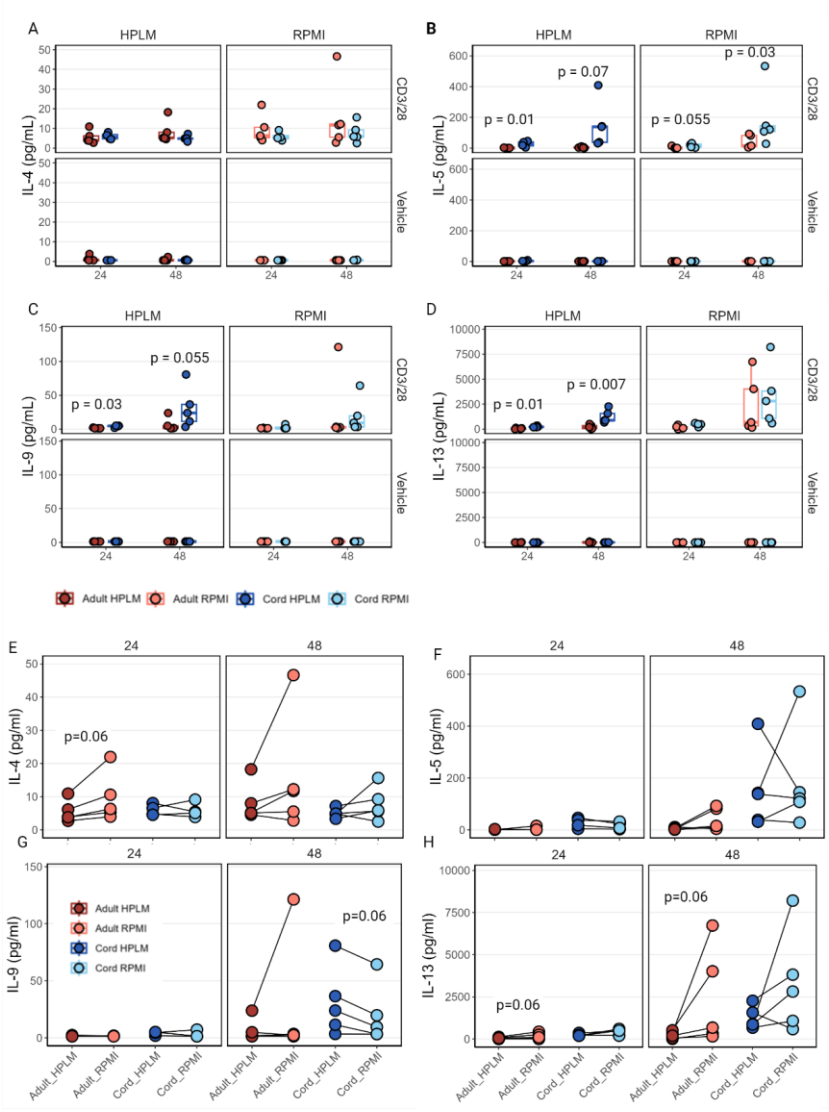

Figure 4.8 nCD4+ T cells from cord blood produce more Th2 associated cytokines than adults.

Th2 associated cytokine production of nCD4+ T cells, from human adult peripheral and umbilical cord blood, cultured in HPLM or RPMI with or without anti-CD3/28 for 24 and 48 hours showing (A-D) box plots comparing cytokine secretion of adults and cords and (E-H) showing data as donor matched cytokine secretion in HPLM and RPMI

culture media. n = 4-5 adults and 4-5 cords. For comparisons made between donor groups p-values were determined by Wilcoxon rank sum test (A, D) and comparisons of paired donors in different media conditions were determined by Wilcoxon signed rank test (E-H). $p < 0.05$ was deemed significant.

Little to no secretion of type 3 associated cytokines, typically linked with Th17 and Th22 cells in support of barrier immunity, was detected in culture supernatant. Secretion of IL-17a was negligible across all groups, with only three samples showing secreted cytokine levels above the limit of quantification (1.22 pg/mL), whilst small amounts of IL-17f and IL-22 were detected in some samples (Figure 4.9A-C). IL-17f secretion was generally lower for cords, where secretion was also reduced in RPMI cultures at 24 hours (Figure 4.9B-H; $p = 0.028$).

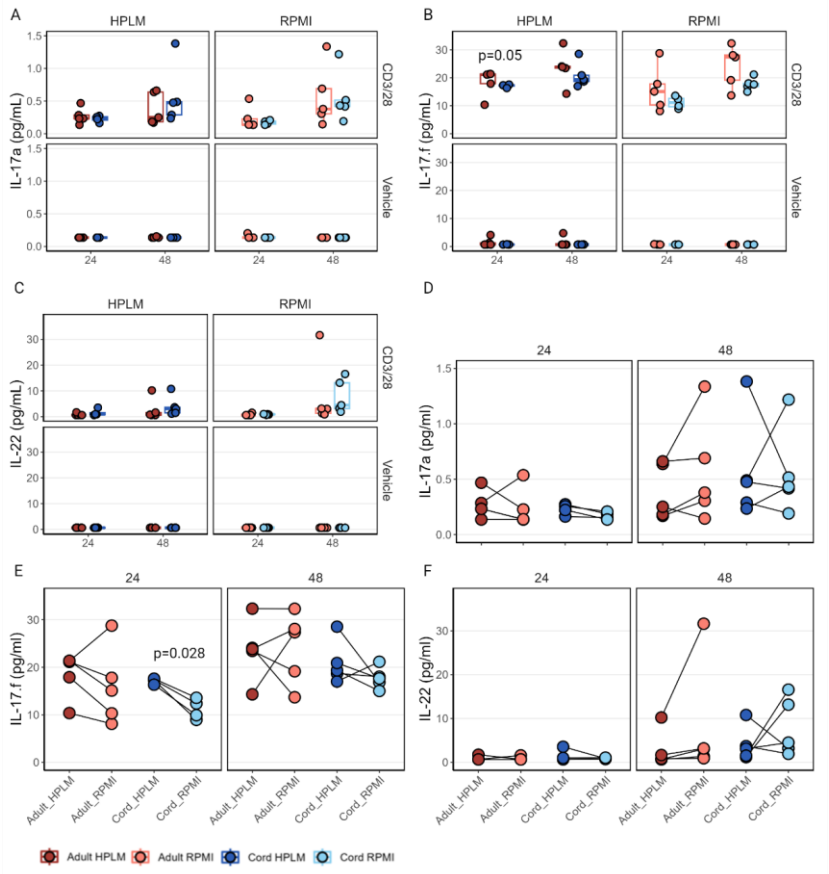

Figure 4.9 Little type 3 associated cytokines are secreted during early activation.

Th 17 associated cytokine production of nCD4+ T cells, from human adult peripheral and umbilical cord blood, cultured in HPLM or RPMI with or without anti-CD3/28 for 24 and 48 hours, showing (A-C) summary box plots comparing cytokine production by adults and cords and (D-F) showing data as donor matched cytokine production in HPLM and RPMI culture media. n = 4-5 adults and 4-5 cords. For comparisons made between donor groups p-values were determined by Wilcoxon rank sum test (A,C) and comparisons of paired donors in different media conditions were determined by Wilcoxon signed rank test (D-F). $p < 0.05$ was deemed significant.

Anti-CD3/28 resulted in expression of IL-2, a positive regulator of growth and proliferation, in all groups. Less IL-2 was measured in cord RPMI supernatant than their adult counterparts though this only neared significance at 48 hours ($p = 0.09$) and no notable differences were observed in HPLM cultures (Figure 4.10A). This might be as a result of increased IL-2 secretion in HPLM which is most pronounced at the earlier stages of cord activation (Figure 4.10D; $p = 0.03$ for cords at 24 hours). As is reported in the literature (Canto et al., 2005), these data show increased secretion of proliferation antagonist, IL-10, in cords and almost no IL-10 secreted in adult cultures (Figure 4.10B). Culture media had no discernible effect on IL-10 secretion (Figure 4.10E).

CXCL8 is another cytokine uniquely associated with cord blood nCD4+ T cells and acts a potent chemoattractant for neutrophils (Gibbons et al., 2014). Data here shows increased CXCL8 secretion in cord cultures with this effect being considerably more exaggerated when cultured in HPLM ($p = 0.01$ and $p = 0.007$ of HPLM cultures at 24 and 48 hours respectively and $p = 0.03$ in RPMI cultures at 24 hours; Figure 4.10C). At 24 hours, more CXCL8 was secreted by cords in RPMI than HPLM ($p = 0.02$; Figure 4.10F); however, this was dramatically reversed by 48 hours where CXCL8 expression had increased several fold in HPLM but remained roughly the same in RPMI cultures ($p = 0.03$; Figure 4.10F). As expected, unstimulated cells did not secrete IL-2, IL-10 or CXCL8 (Figure 4.10A-C).

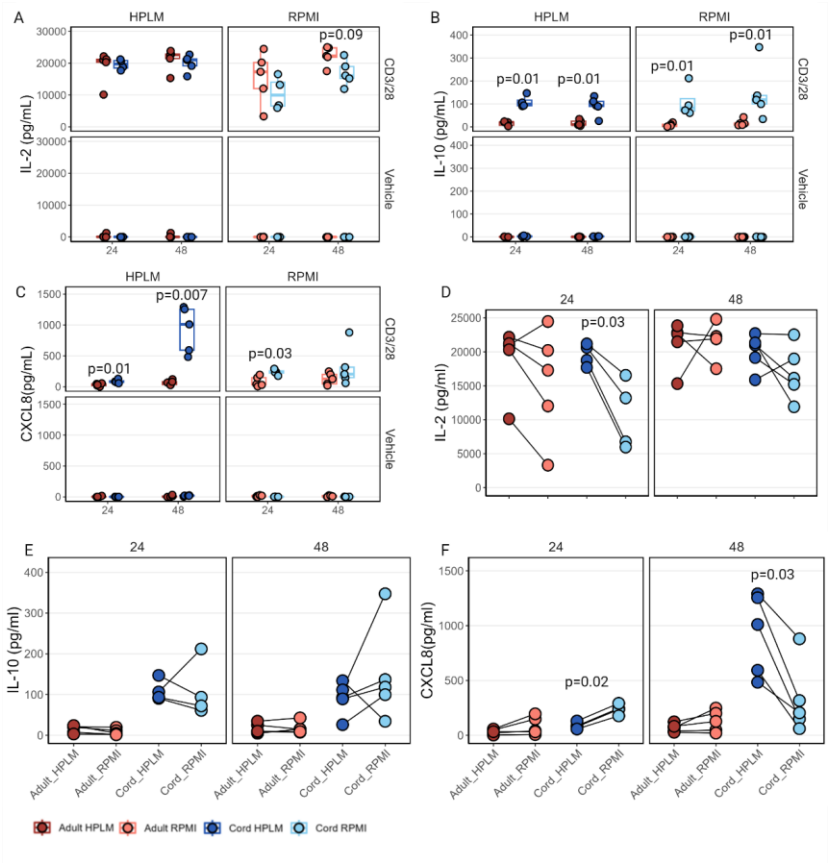

Figure 4.10 nCD4+ T cells from cord blood favour the production of different cytokines.

Other associated cytokine production of nCD4+ T cells, from human adult peripheral and umbilical cord blood, cultured in HPLM or RPMI with or without anti-CD3/28 for 24 and 48 hours showing (A-C) summary box plots comparing cytokine production by adults and cords and (D-F) showing data as donor matched cytokine production in HPLM and RPMI culture media. n = 4-5 adults and 4-5 cords. For comparisons made between donor groups p-values were determined by Wilcoxon rank sum test (A, C) and comparisons of paired donors in different media conditions were determined by Wilcoxon signed rank test (D-F). $p < 0.05$ was deemed significant.

To assess the overall difference for nCD4+ T cell activation between adults and cords and the effect of culture media, PCA was used across all the parameters measured excluding the cytokine IL-17a as there was no detectable secretion of this cytokine in culture. PCA dimensionality reduction was carried out separately for samples at 24 and 48 hours (Figure 4.11).

At 24 hours, PC1 and PC2 explained the majority of the variance in the data with donor samples separating predominantly across PC1 which was driven by a mostly uniform difference in cord nCD4+ T cell activation response. Culture media separated across PC2 and was much more distinct for cord donors, being driven largely by differences in IL-2, TNF, IFNγ and IL-17F secretion, however actual levels of IL-17f secreted in culture media was very low (Fig4.11A-D; Figure 4.9B). At 48 hours, PC1 explained the majority of the variance in the data however, the donor and culture media groups clustered on PC1 and PC3 respectively, indicating that PC2 likely accounted for donor variability. Differences between adults and cords at 48 hours were explained by many factors including CD25/CD44 expression and IL-2/IL-5 secretion whilst differences in media groups were driven largely by IFNγ production and cell death (Figure 4.11E-H).

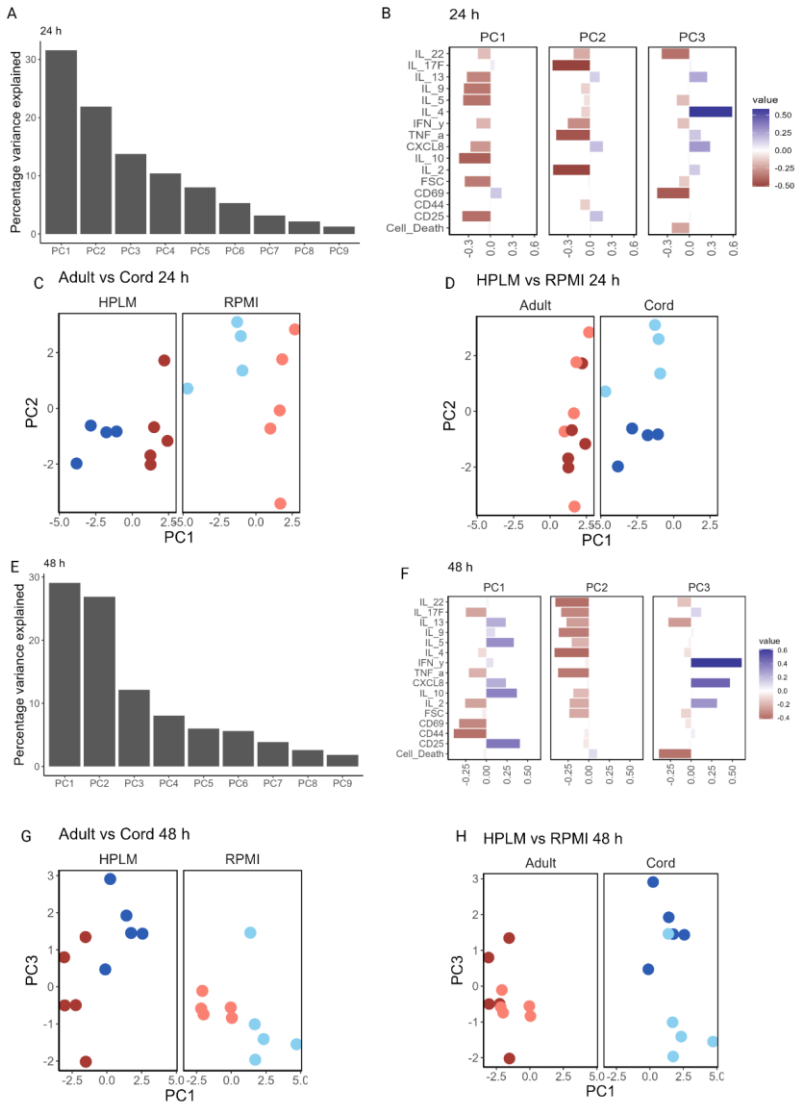

Figure 4.11 Culture media has a greater effect on nCD4+ T cells from cord blood.

The overall difference between nCD4+ T cell activation, from human adult peripheral and umbilical cord blood, and the effect of culture media was assessed by PCA analysis, of cytokines, cell death and surface activation markers, at 24 and 48 hours. Scree plot, loading scores and PCA plots are shown for samples at 24 hours (A-D) and 48 hours (E-H)

4.3.5 Metabolic characterisation of adult and cord nCD4+ T cells cultured in HPLM or RPMI

Given the many differences in metabolite concentrations between HPLM and RPMI and the key role metabolism plays in shaping phenotype and function, metabolic characteristics were assessed after 48 hours in RPMI or HPLM. Determination of glycolytic and oxidative metabolism was made using a real time extra-cellular flux assay and mitochondrial function was interrogated with a Mito Stress test (Figure 4.12A). To better replicate culture conditions during the assay, XF culture media was supplemented with glucose, glutamine, and pyruvate to match the media the cells were cultured in.

In Chapter 3 cord blood derived nCD4+ T cells initially showed greater ECAR and OCR on activation but by 16 hours there was no significant difference between adults and cords. Here, after 48 hours in culture, basal respiration ($p = 0.07$ and $p = 0.050$ for HPLM and RPMI respectively) and ATP linked respiration ($p = 0.05$ and $p = 0.05$)were considerably lower in cords for both HPLM ($p = 0.07$ and $p = 0.05$ for basal respiration and ATP linked respiration, respectively) and RPMI ($p = 0.05$ and $p = 0.05$ for basal respiration and ATP linked respiration, respectively) cultures (Figure 4.12B-C). In HPLM, adults showed consistently higher maximal respiration rates ($p = 0.05$) whilst in RPMI maximal respiration varied considerably between cord blood donors and no significant difference was seen between adults and neonates (Figure 4.12D). Interestingly, adults showed a severely limited capacity for spare respiratory capacity in RPMI cultures, which was not seen in cords (Figure 4.12E). Other sources of oxygen consumption were fairly low for all groups though slightly greater in cords than adults when cultured in RPMI (Figure 4.12F). Finally, proton leak was lower in cords but only nearing significance in the RPMI culture group ($p = 0.05$) (Figure 4.12G).

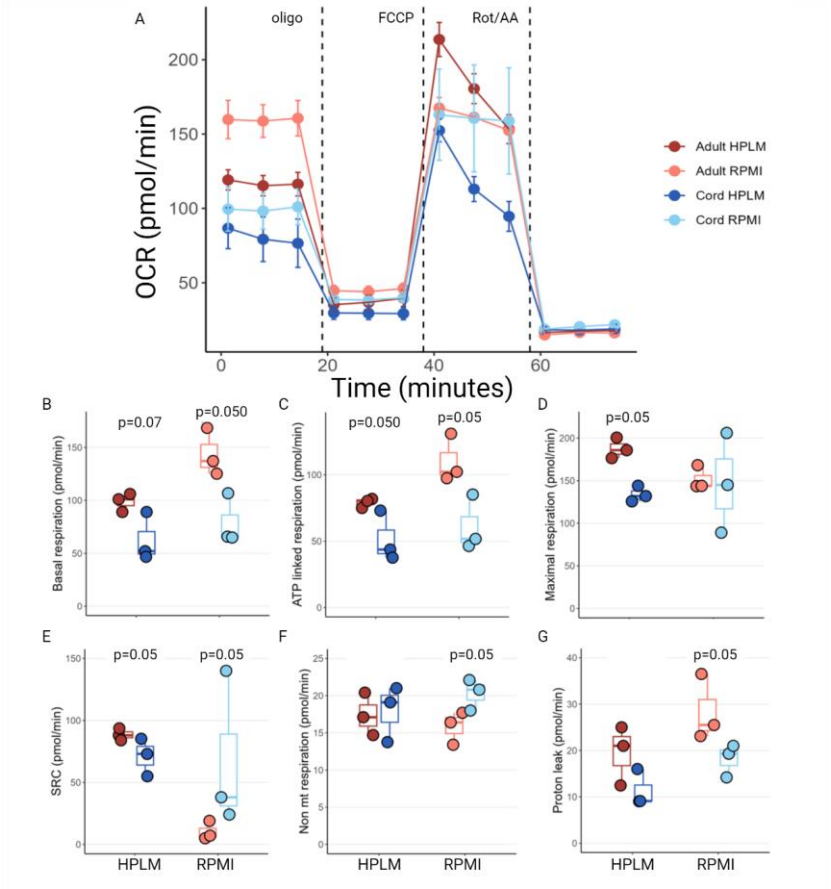

Figure 4.12 Oxidative metabolism is reduced in cord blood nCD4+ T cells.

nCD4+ T cells, from human adult peripheral and umbilical cord blood, were activated for with anti-CD3/28 for 48 hours in HPLM or RPMI, before metabolic flux and mitochondrial parameters were determined by real time extra-cellular flux. (A) Oxidative phosphorylation of adult and neonatal nCD4+ T cells cultured in HPLM or RPMI for 48 h was measured at baseline and in response to oligo (1 μM), FCCP (1 μM) and rot (1 μM) and AA (1 μM). (B) Basal respiration, (C) ATP linked respiration, (D) maximal respiration, (E) spare respiratory capacity, (F) non mitochondrial respiration and (G) proton leak parameters were compared between adults and cords. Data are representative of 6 independent experiments; n = 3 adults and 3 cords. For

comparisons made between donor groups p-values were determined by Wilcoxon rank sum test (B-G). p < 0.05 was deemed significant.

Contrary to what was seen at on activation and at 16 h (Chapter 3) cord blood derived nCD4+ T cells cultured for 48 h are more glycolytic than adults (Figure 4.13A). This effect is more prominent for RPMI cultures as basal ECAR was equivalent between adults and cords in HPLM cultures (Figure 4.13B; p = 0.05). Overall, cords were less oxidative than adults but with RPMI cultured cords being particularly glycolytic whilst HPLM cultured cords were the most quiescent (Figure 4.13C).

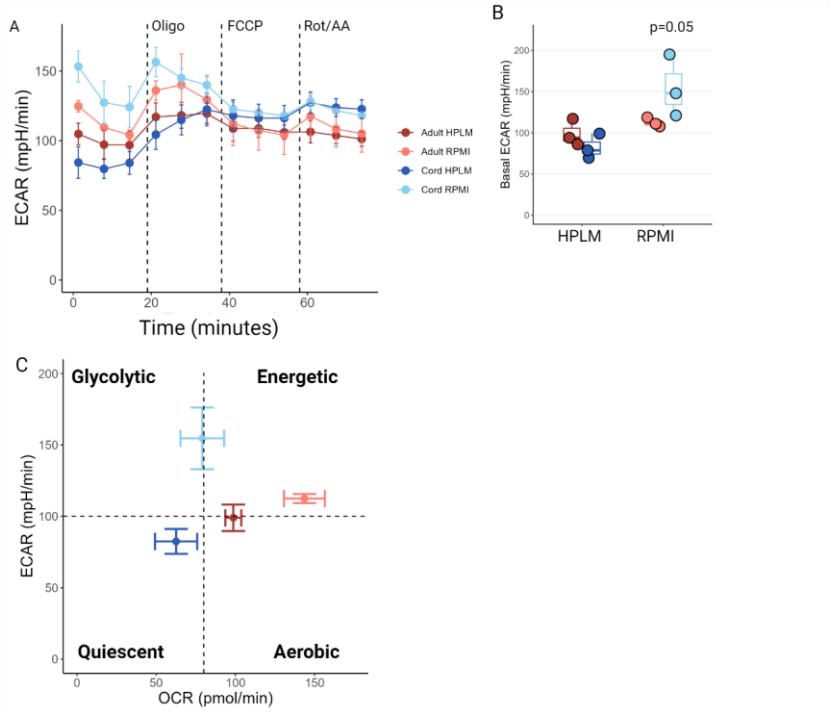

Figure 4.13 Cord blood nCD4+ T cells are more glycolytic than adults.

nCD4+ T cells, from adult peripheral and umbilical cord blood, were activated for with anti-CD3/28 for 48 hours in HPLM or RPMI, before metabolic flux and mitochondrial parameters were determined by real time extra-cellular flux. (A) Extracellular acidification of adult and neonatal nCD4+ T cells cultured in HPLM or RPMI for 48 h

was measured at baseline and in response to oligo (1 μM), FCCP (1 μM) and rot (1 μM) and AA (1 μM). (B) Basal ECAR and (C) OCR and ECAR were plotted against each other for adults and cords in a quadrant plot. Data are representative of 6 independent experiments; n = 3 adults and 3. For comparisons made between donor groups p-values were determined by Wilcoxon rank sum test (B). $p < 0.05$ was deemed significant.

Alongside the differences in adult and cord nCD4+ T cell metabolism these data also highlight the metabolic programming effect of culture medium composition. Basal oxidative metabolism, ATP production and glycolysis are all slightly but not significantly greater, for both adults and cords, when cultured in RPMI (Figure 4.14A-B, G). On the other hand, metabolic plasticity, as indicated by spare respiratory capacity, was reduced in adult RPMI cultures (Figure 4.14C-D; $p = 0.0003$). It is also worth noting, these metabolic differences were usually more pronounced in adults than cords (except in the case of basal ECAR) although the same trends were seen for both. Culture medium did not seem to appear to affect other cellular oxidative processes but did slightly increase proton leak for cords (Figure 4.14E-F). Overall, culture media affected the glycolytic to oxidative metabolic balance differently in adults and cords. In adults, a general trend toward favouring glycolytic metabolism was seen in HPLM whilst the reverse was seen for cords; although, neither difference reached significance (Figure 4.14H).

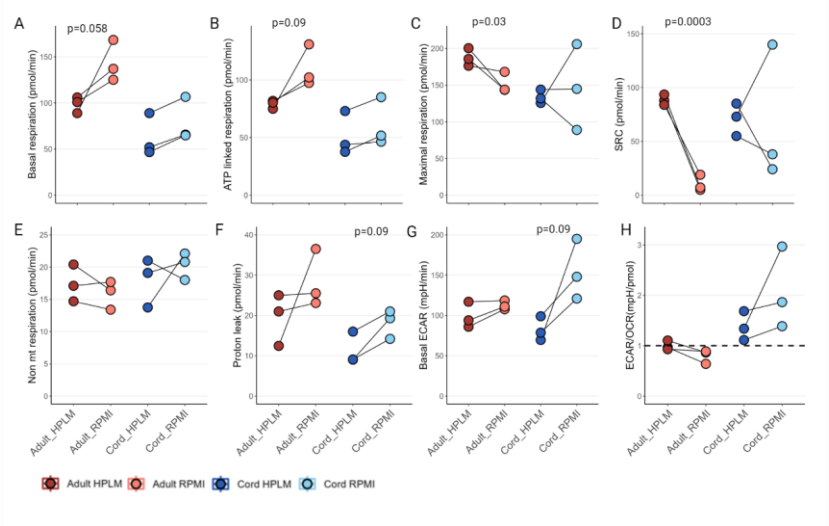

Figure 4.14 Culture media alters metabolic parameters.

nCD4+ T cells, from adult peripheral and umbilical cord blood, were activated for with anti-CD3/28 for 48 hours in HPLM or RPMI, before metabolic flux and mitochondrial parameters were determined by real time extra-cellular flux. (A) Basal respiration, (B) ATP linked respiration, (C) maximal respiration, (D) spare respiratory capacity, (E) non-mitochondrial respiration and (F) proton leak parameters were compared between culture medias for adults and cords. Data are representative of 6 independent experiments; n = 3 adults and 3 cords. Comparisons of paired donors in different media conditions were determined by Wilcoxon signed rank test (A-H). $p < 0.05$ was deemed significant.

As other studies had demonstrated different metabolic parameters, measured by extra-cellular flux assays, in response to altered metabolite availability (Zhu et al., 2021), it was possible that differences between the two culture medias were not representative of a programmed metabolic phenotype but rather a result of environmental factors. To assess the contributions of culture medium and assay medium to metabolic parameters a cross treatment experiment was devised. In this

experiment, HPLM and RPMI cultures were divided after harvesting, with half washed into HPLM-like assay media and the other half washed into RPMI-like assay media, before running the XF assay. To illustrate the effect assay media metabolic parameters of cells cultured and assayed in alternate medias are plotted relative to the same donor cultured and assayed in matching medias (Figure 4.15A-D).

Overall, significant differences in metabolism as a result of assay media were not seen for either adults or cords. Basal OCR, ATP production and ECAR were comparable when cells were assayed in matching or alternate media (Figure 4.15E-F,I). However, assaying RPMI cultured adult cells in HPLM-like media increased maximal respiration and spare respiratory capacity although not significantly (Figure 4.15G,J; $p = 0.06$). Additionally, cords cultured in HPLM and assayed in RPMI consistently favoured a less glycolytic program which neared significance (Figure 4.15H; $p = 0.07$).

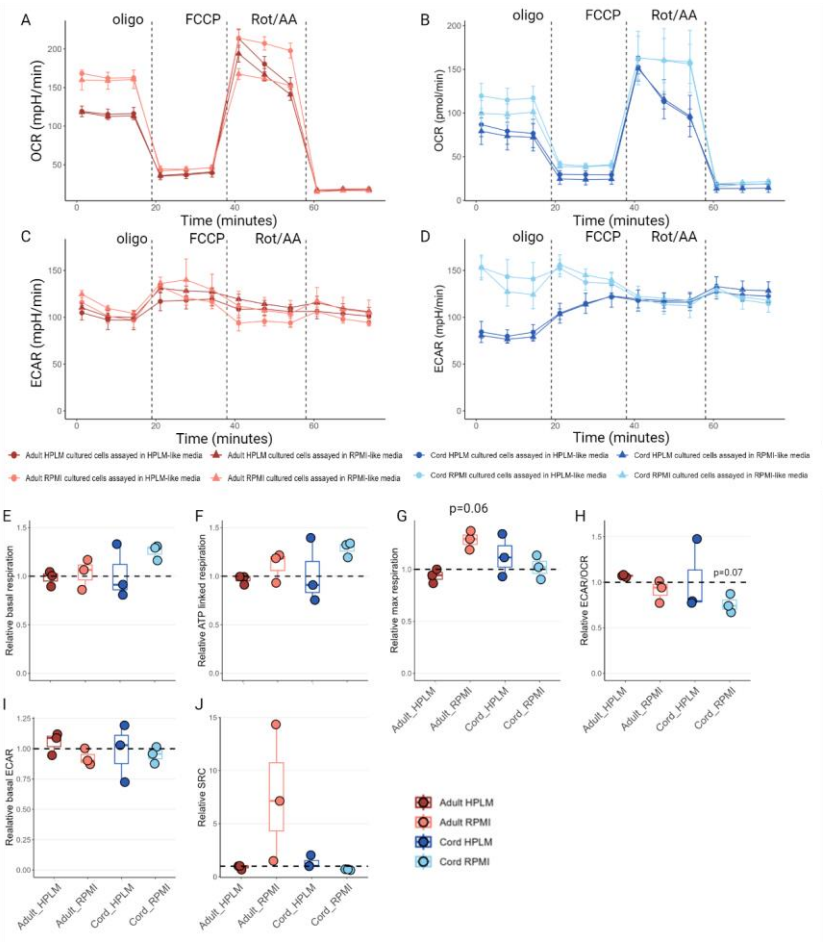

Figure 4.15 Metabolic differences are not explained by assay media.

nCD4+ T cells, from adult peripheral and umbilical cord blood, were activated for with anti-CD3/28 for 48 hours in HPLM or RPMI, before metabolic flux and mitochondrial parameters were determined by real time extra-cellular flux in closely matching assay media or opposing assay media. (A-D) Oxidative phosphorylation and ECAR of adult and neonatal nCD4+ T cells cultured in HPLM or RPMI for 48 h and assayed in HPLM-like or RPMI-like media, was measured at baseline and in response to oligo (1 μM), FCCP (1 μM) and rot (1 μM) and AA (1 μM)). Relative (E) basal respiration, (F) ATP linked respiration, (G) maximal respiration, (H) spare respiratory capacity, (I) Basal ECAR and (J) ECAR/OCR ratio were compared to matching culture and assay media

conditions. Data are representative of 6 independent experiments; n = 3 adults and 3 cords. Comparisons of paired donors in different media pre-conditions, relative to assay conditions, were determined by Wilcoxon signed rank test (E-J). p < 0.05 was deemed significant.

Alongside, measurements of physical metabolic parameters key metabolic signalling pathways were interrogated by intracellular flow cytometry. Phosphorylation of signal transducers like ATK and functional proteins, STAT5 and ribosomal protein S6 act like on off switches in circuity and provide valuable information on the current functional status of the cell (Shyer et al., 2020). Phosphorylated S6, indicative of mTOR signalling (Iwenofu et al., 2008; Scholz et al., 2016), showed no significant differences between adults and cords for either culture media (p = 0.3 for HPLM and p = 0.4 for RPMI), and culture media had no significant effect either donor group (p = 0.14 for adults and b = 0.8 for cords). In HPLM, cords exhibited consistent but non-significant increased AKT phosphorylation, compared to adults, (p = 0.09) whilst no difference was observed in RPMI cultures (p = 0.7). Again, culture media had no significant effect (p = 0.2 for adults and p = 0.8 for cords). Cords also showed increased phosphorylated STAT5, which is known to be induced by IL-2 signalling (Jones et al., 2020a) reaching significance in HPLM cultures (Figure 4.16A-E; p = 0.01).

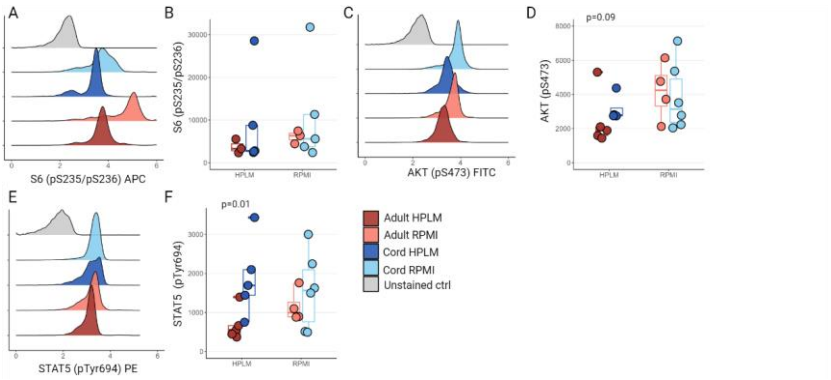

Figure 4.16 HPLM does not significantly alter central metabolic signalling pathways.

Adult peripheral and umbilical cord nCD4+ T cells cultured for 48h with anti-CD3/28 were assessed by intracellular flow cytometry for (A-B) representative histogram and summary plots of phospho-S6 (pS3245/pS236), (C-D) representative histogram and summary plots of phospho-AKT (pS473) and (E-F) representative histogram and summary plots of phospho-STAT5 (pTyr694). Data are representative of 3-5 adults and 5-6 cords. For comparisons made between donor groups p-values were determined by Wilcoxon rank sum test (B, D, F). $p < 0.05$ was deemed significant.

4.3.6 Assessing the contribution of altered glucose and calcium concentrations in RPMI to cord blood nCD4+ T cell activation.

Much of the data above showed an altered activation profile when cultured in HPLM, compared to conventional RPMI. Perhaps most interestingly in cords this alternate activation profile appeared to break with the conventional wisdom that neonatal naïve CD4+ T cells are poor IFN-γ producers. Both calcium dependent NFAT and the glycolytic metabolism of glucose are implicated in regulating IFNγ production, and both differ greatly between HPLM and RPMI (Table 7) (Palmer et al., 2015; Klein-Hessling et al., 2017; Menk et al., 2018). To assess how these two media components contribute to the altered activation profile seen in cord HPLM, cord cells were activated and cultured in RPMI media, supplemented to 5.5mM glucose or 2.39 mM Ca^{2+} as found in HPLM or a combination of both, along with standard RPMI and HPLM

controls. After 24 hours activation, surface markers were assessed by flow cytometry and cytokine secretion in culture determined by ELISA.

Table 7 Glucose and Calcium ion concentration in HPLM and RPMI.

Table showing the concentration in mM for glucose and Ca^{2+} in HPLM and RPMI media.

	HPLM	RPMI
Glucose	5.5 mM	11 mM
Ca^{2+}	2.39 mM	0.424 mM

Relative to HPLM there was no significant difference in CD25 expression for any of the culture media groups (Figure 4.17A; p = 0.38, p = 0.076, p = 0.82, p = 0.79 for RPMI, 2.29mM Ca^{2+}, 5.5 mM glucose and combined 2.29mM Ca^{2+}; 5.5 mM glucose, respectively). Supplementation of RPMI with either Ca^{2+} and or glucose appeared to partially increase expression of CD44 relative to HPLM, showing considerably less significant difference than RPMI (Fig4.17C, D; p = 0.07, p = 0.21, p = 0.35 and p = 0.19 for RPMI, 2.29mM Ca^{2+}, 5.5 mM glucose and combined 2.29mM Ca^{2+}; 5.5 mM glucose, respectively). Glucose and Ca^{2+} supplementation differentially effect the secretion of cytokines IL-2 and IFN-γ. Lower glucose appears to increase relative IL-2 compared to RPMI although not significantly (Figure4.17E). Ca^{2+}, but not in combination with lower glucose, increased relative secretion of IFNγ (p = 0.07) compared to RPMI (Fig4.17F). However, IFNγ secretion, in RPMI when supplemented with additional calcium, was still not equivalent to culture in HPLM (p = 0.021; Figure 4.17F).

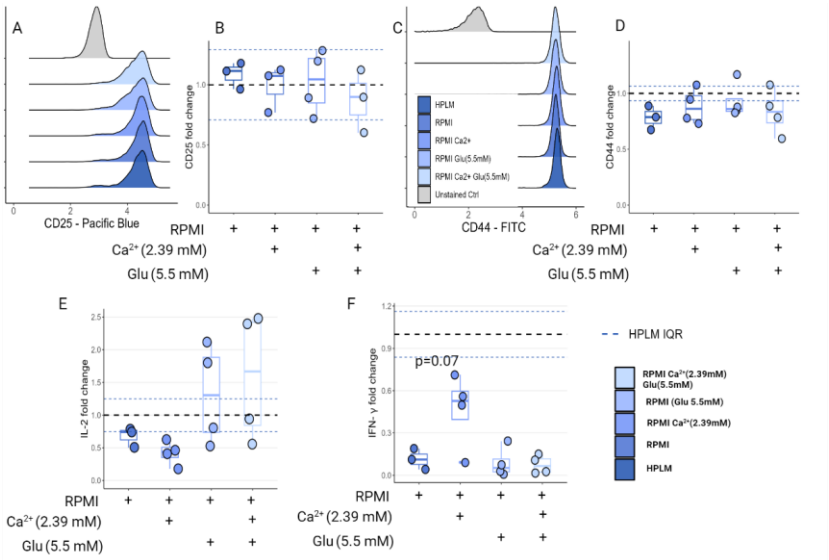

Figure 4.17 IFNγ production is dependent on extra-cellular calcium.

Anti-CD3/28 activation of nCD4+ T cells, from umbilical cord blood, cultured for 24 h in HPLM, RPMI or RPMI modified with 5.5 mM glucose, Ca^{2+} or both as measured by (A-B) CD25 expression and (C-D) CD44 expression. n = 3. (E-F) IL-2 and IFNγ cytokine production in culture supernatant. n = 3-4 cytokine. Summary data are plotted relative to the donor matched HPLM group. Comparisons, of donor matched relative fold change, between different RPMI supplemented media were determined by Wilcoxon signed rank test (D-F). $p < 0.05$ was deemed significant.

4.4 Discussion

CD4+ T cells direct effective and appropriate immune responses and a growing body of evidence highlights the importance of metabolic function in relation to the ability of T cells to perform this function (Shyer et al., 2020). To date, the vast majority of T cell immune metabolism research has been conducted in adults with little to no understanding of how metabolism may govern neonatal T cell responses which are often reported to vary from their adult counter parts (Holm et al., 2021). Furthermore, the majority of this work, in humans, has been conducted through in vitro cell culture using non physiologically relevant culture media such as RPMI 1640.

This study aimed to characterise and compare naïve CD4+ T cell responses from adults and neonates when using physiologic and non-physiologic media and, assess the metabolic activation profile for neonatal naïve CD4+ T cells. These data reveal significantly different activation profiles of adult and cord derived nCD4+ T cells accompanied by differing metabolic phenotypes and provide useful insights into the use of physiologic media in T cell culture.

Interestingly, even without anti CD3/28 stimulation, when cells were rested in culture, growth medium had significant effects on cell survival and maintenance of surface activation markers CD25, CD44 and CD69 between 24 and 48 hours, especially for cord blood derived cells where survival improved dramatically. Despite the typical focus on metabolite requirements post activation, these data showcase the importance of metabolite availability in resting T cell homeostasis. Such observations may be of consequence to modern technologies such as gene editing which might require in vitro culture without activation. When examining the phenotype of anti-CD3/28 stimulated cells, principle component analysis, across the 16 included parameters, revealed clearly distinct activation profiles with adults and cords clustering separately in PCA space regardless of the culture media used. At both 24 and 48 hours donor groups separated along PC1, which explains the most variance of any principle competent in the data set, showcasing the unique activation profile of neonatal nCD4+ T cells. Expression of surface activation markers increased on activation compared to rested cells however, neither donor group or culture media exhibited a clearly enhanced or diminished activation profile as no group displayed consistently higher or lower expression of activation markers. CD25 expression, part of the IL-2 receptor complex and driver of cell growth and proliferation, was among the largest factors contributing to differing nCD4+ T cell activation profiles. Increased CD25 expression was not strongly reflected in the growth and proliferation profile which exhibited only subtle differences on activation. However, as has been reported elsewhere IL-2 secretion was equivalent between the donor groups with further expansion from cord donors possibly hampered by heightened IL-10 secretion (Canto et al., 2005; Lesniewski et al., 2008) although this was not formally tested here.

Culture media appeared to have a more discernible overall effect on cord nCD4+ T cells in culture, as these clustered more clearly than their adult counterparts. At 24 hours culture media was the second largest contributor to variance in the data however, by 48 hours its effect was trumped by donor variability as groups did not cluster along PC2. Again, IL-2 was a notable contributor to group clustering. IL-2 secretion inversely correlated with CD25 expression, which was greater in RPMI cultures though, it is unclear whether this is due to reduced IL-2 secretion or increased autocrine uptake promoting greater proliferation in RPMI cultures (Redeker et al., 2015; Toumi et al., 2022). Reduced proliferation in HPLM might be attributed to the IL-2/CD25 axis, but it is also plausible that the reduced quantities of essential metabolites, such as glucose and glutamine, in HPLM are inadequate to support continued T cell expansion. Studies have shown that T cell proliferation is impaired in nutrient-limiting conditions and that T cells can rapidly deplete media of glucose upon activation (MacPherson et al., 2022). The impaired expansion of T cells in HPLM might be of particular concern to novel therapeutics such as CAR T cells that require in vitro expansion but aim to balance expansion with desired phenotypic characteristics. To more accurately determine the effect of HPLM on T cell expansion, further experiments with regular media changes are required to reduce the effect of metabolite depletion (Quinn et al., 2020).

Cytokine secretion by nCD4+ T cells is a central tool in their arsenal to direct effective immune responses and the types of cytokines they secrete can be used to categorise the responses. It is often stated that neonatal T cells favour type 2 responses, producing cytokines such as IL-4 and IL-13, but fail to produce effective type 1 IFNγ responses. Evidence for this is largely based on mouse models with conflicting reports in humans (Zaghouani et al., 2009; Rudd, 2020). Data in this study finds no evidence for impaired type 1 responses from cord donors. Indeed, when cultured in HPLM, IFN-γ secretion was greater in cords compared to adults. This might be explained by the relatively calcium deficient composition of RPMI, as cord blood nCD4+ T cells may require greater exogenous calcium influx for activation (Schmiedeberg et al., 2016). This study goes further to show RPMI supplemented with additional calcium

increases IFN-γ secretion considerably, even nearing HPLM culture levels. Some evidence was found to support reports of cord blood nCD4+ T cells exhibiting greater type 2 responses. However, secretion of type 2 associated cytokines was very low with the exception of IL-13, which is known to have a very accessible chromatin landscape in ex vivo cord blood nCD4+ T cells (Webster et al., 2007). These data did not show substantial IL-4 secretion, despite IL-4 containing nCD4+ T cells in cord blood having been previously reported. This is likely due to these cells containing a non-classical isoform not measured by this study. Unlike type 1 responses culture media did not substantially or consistently affect the production of type 2 cytokines. The same held true for type 3 cytokines which were only secreted in small quantities. Additionally, the neutrophil chemoattractant CXCL8 is suggested to play a uniquely important role in neonatal nCD4+ T cell responses, as it is secreted in significantly greater quantities compared to adults (Gibbons et al., 2014). This study shows similar results and highlights a metabolic axis to regulating secretion of CXCL8, as significantly more CXCL8 was secreted in HPLM cultures.

Given the ever-mounting body of evidence demonstrating a central role for metabolism in governing immune responses, this study, for the first time, characterises the bioenergetic profile of neonates during the days after initial activation (48 h) and the effects of culture in physiologic concentration of a broad range of metabolites. Perhaps unsurprisingly, considering the greater amounts of glucose and glutamine, baseline ECAR and mitochondrial respiration were both greater in RPMI cultured cells. Similarly, other studies using mouse models, comparing in vitro cultured T cells to ex vivo T cells, also found reduced metabolic parameters suggesting that metabolite availability can reprogram T cell metabolism (Ma et al., 2019). As greater CD25 expression has previously been correlated with increased glycolysis in T cells (Ahl et al., 2020). In the higher glucose concentrations of RPMI culture, greater glycolysis might have driven the increased expression of CD25, particularly in cord nCD4s which had greater CD25 expression than adults. This in turn may have maintained greater IL-2/STAT5 mediated signalling promoting proliferation, although this did not correlate with greater mTOR signalling at these

later time points, as determined by phosphorylation of the downstream target S6. Energy and anabolic precursors, from greater glycolysis and mitochondrial respiration, likely also supported greater proliferation in RPMI. Cytokine production was likely impacted by these differences in metabolism, as the role of both metabolic pathways in regulating cytokine production is well documented (Chang et al., 2013; Peng et al., 2016; Qiu et al., 2019; Soriano-Baguet and Brenner, 2023). Here, modification of RPMI with physiologic glucose resulted in greater IL-2 being present in the culture supernatant of cord nCD4s however the mechanism behind this requires further elucidation.

As these assay results were gathered using glucose, glutamine and pyruvate concentrations matching the those of the culture media there was a very real possibility that the differences observed were simply a result of metabolite availability during the course of the assay. To address this a cross culture and assay media experiment was devised whereby cells cultured in HPLM or RPMI were then assayed in DMEM either supplemented to match the original culture media or to match the culture media of the opposing group. As little difference was observed in most oxidative parameters it seems most plausible that culture media had a significant programming effect on cellular metabolism that could not be overcome by modifications to metabolite availability. This is with the exception of SRC, in adult RPMI cultured cells assayed in HPLM-like media, which was likely augmented by the addition of pyruvate, which is lacking in RPMI.

4.5 Conclusions

Together these data demonstrate the importance of physiologic media in activation models of human nCD4+ T cells. Physiologic culture media altered the bioenergetic program and subsequent production of effector molecules for both adult and cord derived cells, with this effect being more pronounced in cords. These findings add to the growing body of literature defining the distinct activation profile of umbilical cord blood derived nCD4+ T cells, highlighting their altered metabolic phenotype and

greater dependence on exogenous calcium for IFNγ production. Finally, this model of activation was limited to culture media representative of adult plasma, as no cord blood plasma analogue was available. Therefore, further studies should explore the effects of a more relevant culture media for cord derived nCD4+ T cells.

5 Impaired neutrophil metabolism prevents NETosis in neonates.

5.1 Introduction

Neutrophils are part of the innate immune response and are the most abundant leukocyte in circulation making up 50-70% of all the circulating lymphocytes. These vast numbers support the neutrophils as first responders, quickly trafficking to the site of insult to mount a rapid defence to stem the possibility of infection. Neutrophils also have a very high turnover rate, with an approximate half-life of around 6 – 19 hours, though some estimated put it at around 3 days (Lahoz-Beneytez et al., 2016; Rosales, 2018; Koenderman et al., 2022). To support such a rapid turnover of cells new neutrophils are generated in the bone marrow, originating from hematopoietic stem cells (Borregaard, 2010). The hematopoietic stem cells in bone marrow first differentiate into myeloblasts which retain the ability to differentiate into other polymorphonuclear cells (PMNCs) and monocytes (Hidalgo et al., 2019). In turn, myeloblasts differentiate through promyelocytes, myelocytes and metamyelocytes to form immature band neutrophils. In times of stress, stores of promyelocytes and myelocytes, formed through differential rates of cell division within the population, are able to support rapid mobilisation of neutrophils although this often leads to an increase in the number of immature circulating neutrophils. (Dresch et al., 1986; Manz and Boettcher, 2014; Daix et al., 2021). At the promyelocyte to metamyelocyte stages of development many of the essential components required for neutrophil function are acquired, such as myeloid peroxidase and neutrophil elastase, required for neutrophil extra-cellular trap (NET)s, and granule contents in readiness for degranulation (McKenna et al., 2021). At the point of band cell differentiation, cell division stops and differentiation into segmented neutrophils marks the final step in neutrophil maturation, whereon neutrophils exit the bone marrow and go into circulation (Lieschke et al., 1994; Summers et al., 2010; Evrard et al., 2018).

Neutrophils appear in the bone marrow of the developing fetus in the first trimester of pregnancy with mature neutrophils only seen in peripheral blood by the beginning of the second trimester and increasing exponentially with developmental age (Davies et al., 1992; Slayton et al., 1998). Following the rapid increase in neutrophil count in the lead up to birth, term neonates have neutrophil counts that are comparable to

adults but a lower total mass of neutrophils compared to total body mass (Erdman et al., 1982; Schmutz et al., 2008). Additionally, in the days following birth, neutrophil count decreases before stabilising around 5 days after birth and factors such as birth weight, sex and mode of delivery can all effect neutrophil count (Schmutz et al., 2008; Proytcheva, 2009).

Alongside differences in neutrophil content, neutrophils of term neonates are also functionally immature. Most functions essential to neutrophil function are deficient in neonates at the time of birth, including the ability to traffic, transmigrate and produce NETs (Lawrence et al., 2017). Specifically, reduction of adhesion molecules Mac-1 and L-selectin at the time of birth impair the ability of neutrophils to firmly adhere and transmigrate to sites where they are needed (Nussbaum et al., 2013). Trafficking in response to chemokines is also reduced compared to adults, which is thought to be a result of reduced chemoattractant signalling via phosphatidylinositol 3-kinase and NF-κB (Weinberger et al., 2001). Atop the impaired ability to move to the site of inflammation, neonatal neutrophils display a reduced capacity for pathogen clearance due to lower azurophil granule content and loss of NET function (Levy et al., 1999; Yost et al., 2009; Lawrence et al., 2017). Low neutrophil count and dysfunctional neutrophils are both risk factors for sepsis which is still one of the biggest killers in hospitalised patients, with a mortality rate of around 32 % in high income countries (Arraes et al., 2006; Sonego et al., 2016; Bauer et al., 2020; Michael et al., 2023). Along with pregnant women the elderly and patients receiving chemotherapy, neonates are a particularly at risk group for sepsis with an estimated worldwide incidence rate of 2824 neonatal sepsis cases per 100 000 live births (Greer et al., 2019; Kochanek et al., 2019; Martin-Loeches et al., 2019; Fleischmann et al., 2021). However, there is little evidence linking neutrophil activation markers with sepsis and some studies in mice have even suggested that NETosis in neonatal mice may exacerbate sepsis although, this work focused on the role of NETosis after induction of sepsis and did not consider the role of NETosis in preventing the initial infection (Stiel et al., 2020; Denorme et al., 2023). Despite the well-known

dysfunction of neonatal neutrophils and the associated risks, the mechanisms behind the loss of some functions such as NETs are poorly understood.

NETosis is a special form of programmed cells death separate from apoptosis, first described by Brinkmann et al in 2004 and is characterised by the release of unravelled DNA, coated in granule enzymes like neutrophil elastase, into the cytosol (Brinkmann et al., 2004). Now it is understood that there are two fundamentally distinct types of NETosis that can occur, lytic and non-lytic NETosis (Yipp and Kubes, 2013). Lytic NETs, also known as classical or ROS-induced NETs, are induced by PMA or IL-8 and formed around 3 h post activation, requiring the presence of strong ROS signals (Fuchs et al., 2007). The exact mechanisms underpinning lytic NET formation are not fully clear but it is commonly suggested that NE and myeloperoxidase (MPO) degrade the nuclear membrane and peptidylarginine deiminase 4 facilitates chromatin decondensation by converting histone arginine residues to positively charged citrulline (Wang et al., 2009; Papayannopoulos et al., 2010). Non-Lytic NETosis, also known as vital or ROS-independent NETosis, is non-terminal and much more rapid, occurring within 20-30 min post activation. It is triggered by some bacteria, lipopolysaccharide, granular macrophage colony stimulating factor (GM-CSF) and the complement factor C5a (Pilsczek et al., 2010; Amini et al., 2018). In adults both lytic and non-lytic NETs are largely dependent on glycolysis with stimulation increasing the surface expression of GLUT1 and increased influx of glucose and inhibition of glucose inhibiting NETosis (Rodriguez-Espinosa et al., 2015; Awasthi et al., 2019). However, there are multiple proposed mechanisms through which glycolysis supports NETosis, including through lactate production, ATP provision or fuelling the pentose phosphate pathway (Azevedo et al., 2015; Awasthi et al., 2019). Whilst all the mechanistic reasoning for why glycolysis is required for NETosis is still debated, the clear reliance of NETosis on this pathway provides a target that could potentially explain the failure of neonatal neutrophils to produce NETs.

5.1.1 Rational

Neutrophils are a critical first line of defence but many key functions of neutrophils, including NETs, are either diminished or absent in neonates. Impaired neutrophil

function is linked to increased sepsis susceptibility which is still a leading cause of neonatal mortality. Glycolytic metabolism fuels NETosis in adults although the underlying mechanisms for this are not fully elucidated. Little is known about the metabolic function of neonatal neutrophils, but studies of other neonatal innate immune cells have suggested that glycolytic metabolism may be impaired. Thus, glycolysis likely represents a good target for investigating impaired NET function in neonates.

5.1.2 Hypothesis

Impaired formation of NETs by neonatal neutrophils is a result of reduced glycolysis.

5.2 Methods

5.2.1 Neutrophil isolation

As detailed in chapter 2.34 neutrophils were isolated from adult and umbilical cord whole blood by an untouched magnetic associated cell sorting system (MACSxpress® Whole Blood Neutrophil isolation kit, human; Miltenyi). Whole blood was incubated with magnetically labelled beads and magnetically labelled cells were removed by placing the mixture in a strong magnetic field (MACSxpress® separator) and collecting off the supernatant. Remaining erythrocytes were removed from by magnetically labelling (MACSxpress® Erythrocyte depletion reagent) and placing the mixture in a strong magnetic field (MACSxpress® separator) to deplete labelled erythrocytes. Supernatant was collected and centrifuged at 300 x g for 10 min.

5.2.2 Flow cytometry

5.2.2.1 Purity monitoring and cell death

Neutrophils isolated from whole blood were stained with anti-CD15-FITC to check purity and DRAQ7 to monitor cell death. 100000 cells were stained with anti-CD15; FITC (W63D; BioLegend) for 30 min on ice in the dark before washing with FACS buffer (Chapter 2.5.3). Following staining with CD15 cells were stained with 1 μM DRAQ7 for 15 min at room temperature in the dark then washed in FACS buffer (detailed in

chapter2.5.4). Live, DRAQ7 negative cells, were gated on and assessed for CD15 expression. After gating on live, DRAQ7 negative cells, CD15 expression was assessed after acquisition on the NocoCyte3000.

5.2.2.2 Phenotyping

Isolated neutrophils were stained for surface markers with anti-CD10 VioBlue (REA877; Miltenyi), anti-CD16 (REA423; Miltenyi) VioGreen, anti-CD35 APC-Vio770(REA1133; Miltenyi) and anti-CD66b PE (REA306, Miltenyi), on ice for 30 min in the dark (as detailed in chapter 2.6.1). Stained cells were washed twice with FACS buffer and analysed by using flow cytometry (Cytek Aroura).

5.2.2.3 Mitochondrial mass.

Mitochondrial mass was determined by staining with 25 nM MitoTraker™ Green for 30 min in a dark incubator at 37°C and 5% CO_2 in RPMI GlutaMAX media. Cells were washed twice in FACS buffer and median fluorescence intensity (MFI) of MitoTracker™ Green determined using flow cytometry (detailed in chapter 2.6.5).

5.2.3 Microscopy

5.2.3.1 Light microscopy

For imaging of neutrophil structure, $1x10^5$ isolated neutrophils from adults or cords (5.2.1) were seeded onto glass slides by cytospin centrifugation at 800 x g for 2 min. Cytospun cells were then stained with Kwik-Diff by briefly dipping the slides into reagent 1 five times and blotting the excess on absorbent paper. This procedure was repeated for reagents 2 and three before rinsing, by briefly dipping into distilled water. Slides were air dried at stored at 4 °C until imaging. Slides were imaged with the EVOS imaging system in the visible spectrum (ThermoFisher).

5.2.3.2 *Fluorescence microscopy*

8 well glass microscopy chamber slides were prepared in advance by coating with 200 μL of Cell-tak (Corning) in 0.1 M sodium bicarbonate solution ($Na(CO)_2$; Life Technologies) at 22.5 μM per well for 20 min at room temperature, as described in chapter 2.8.1 and prepared slides were kept at 4 °C until use.

Isolated neutrophils from adults and cords (chapter 5.2.1) were seeded at 50,000 cells per well onto Cell-tak coated 8 well chamber slides and cultured in RPMI GlutaMAX, with vehicle control (DMSO), 2-deoxyglucose (2DG; 100 mM; Sigma), Glucose free RPMI, glycogen phosphorylase inhibitor CP-91149 (GPi; 10 μM; Sigma), RPMI – D-glucose and GPi, lactate dehydrogenase inhibitor GSK 2837808A (LDHi; 10 μM; Sigma), for 15 min in an incubator at 5 % CO_2, 37 °C. In other experiments Isolated neutrophils (chapter 5.2.1) were cultured in RPMI GlutaMAX with adenosine triphosphate (ATP; 200 μM; Sigma) or nicotinamide mononucleotide (NMN; 500 μM) for cords and oligomycin (1 μM; Sigma) or rotenone (1 μM; Sigma) for adults. Cells were cultured at in an incubator at 5 % CO_2, 37 °C for 30 min. Following the initial 15- or 30-min incubation, phorbol 12-myristate 13-acetate (PMA) was added at 50 nM to all wells or vehicle control. Cells were returned to a 5 % CO_2 incubator at 37 °C for 3 hours. Subsequently culture supernatant was removed by pipette from each well and cells were fixed by adding 10 % formalin (Sigma) to each well for 10 min at room temperature. After fixation, wells were washed twice with PBS before adding DAPI staining solution for 15 min at room temperature protected from light. Staining solution was removed, and wells were washed three times by flooding the wells with PBS. Finally, all remaining PBS was removed, and the chamber compartments disassembled before VECTASHEILD® mounting medium (Vector laboratories) was added and a cover slip applied on top. Prepared slides were imaged using a laser scanning confocal microscope (Zeiss LSM710) or the EVOS imaging system (ThermorFisher). Captured images were analysed using the Zen 3.4 software (Ziess).

Images of mitochondrial content were taken using confocal microscopy of MitoTracker™ Green stained neutrophils. Neutrophils from adults or cords were incubated in RPMI glutaMAX with 25 nM MitoTracker™ green for 30 min at 37°C and 5% CO_2. Following staining cells were stained with DAPI (Chapter 2.8.2). Cells were

fixed with 10% formalin (Sigma) and washed twice with PBS, followed by staining with DAPI for 10 min at room temperature. Wells were washed thoroughly with PBS before mounting cover slips with mounting media and imaged and at ×63 magnification using a laser scanning confocal microscope (Zeiss LSM710). Captured images were analysed using the Zen 3.4 software (Ziess).

5.2.4 Extracellular flux analysis

Extracellular acidification rate (ECAR) and oxygen consumption rate (OCR) were measured ex vivo in resting isolated neutrophils under mitostress conditions and on activation with PMA in the presence of various inhibitors.

5.2.4.1 Mitochondrial stress test

Ex vivo neutrophils were examined for mitochondrial function using the mitostress assay ECAR (chapter 2.5.2). $2x10^5$ neutrophils were seeded in assay media (5 mM glucose, 2 mM glutamine 2 mM pyruvate, pH7.4) onto a 24 well cell-tak coated plate. The plate was loaded into the Seahorse bioanalyzerXF24 (Agilent) and allowed to equilibrate for 15 min before starting the assay. During the assay simultaneous measurements of OCR and were made at baseline and on injections of oligomycin (1 μM), FCCP (1 μM), rotenone (1 μM) and antimycin-A (1 μM).

5.2.4.2 Activation assays

Isolated neutrophils were seeded at 2 x 10^5 cells per well onto Cell-Tak coated 24 well XF assay culture plates in minimal media supplemented with 5.5 mM glucose (unless otherwise stated), 2mM glutamine and 2mM pyruvate, adjusted to pH 7.4 with sodium bicarbonate ($Na(CO)_2$; Life Technologies) and incubated in a non-CO_2 oven at 37 °C for 1 hour prior to conducting the assay. Injections were also prepared and placed in the non-CO_2 oven. Injections were loaded into the injection ports before the assay plate was placed in the Seahorse bioanalyzerXF24 (Agilent) and allowed to equilibrate for 15 min before the first measurements were taken. Three baselined measurements were taken before injection of vehicle, 2DG (100 mM), GPi (10 μM) or

LDHi (10 μM), where on another three measurements were taken before injection of vehicle or 50 nM PMA. Measurements were recorded for a further 80 min before the plate was unloaded.

5.2.5 Lactate assay

L-Lactate in cell culture supernatant was measured by colorimetric assay (L-Lactate assay Kit; abcam) according to the manufacturer's instructions. 500,000 neutrophils, from adults or cords, were left untreated or activated with 50 nM PMA in 1 mL RPMI or RPMI without glucose or activated in the presence of 10 μM LDHi for 15 or 60 min, at 37°C 5% CO_2. At the designated time point, culture plates were placed immediately on ice and harvested by pipetting. Cell-free supernatant was collected by centrifugation at 300 x g for 10 min at 4°C and removing the supernatant from the cell pellet for storage at -20°C. On the day of analysis, supernatant was defrosted on ice and centrifuged at 10,000 x g, 4°C for 10 min to remove any debris. To conduct the assay, culture supernatant was appropriately diluted with assay buffer and added to reaction mix. A standard curve and background wells were prepared at the same time. Samples and standards were incubated at room temperature for 30 min, protected from light. The plate was read at OD570 nm.

5.3 Results

5.3.1 Isolation of viable neutrophils

Untouched magnetic activated cell sorting (MACS) was used to isolate neutrophils from whole peripheral adult blood and cord blood. Neutrophils are highly sensitive to mechanisms inducing cell death, as such cell death was determined after isolation to ensure the collection and isolation process had not caused excess cell stress and death. Total Isolated cells were stained with the lineage marker CD15, to determine purity and DRAQ7 as a measure of cell death. In the total cells population of MACS isolated neutrophils purity was very high for both adults and cords (Figure 5.1). All donors used had a purity of >90 %. Additionally, little to no cell death was observed in the CD15+ population of any donors (Figure 5.1).

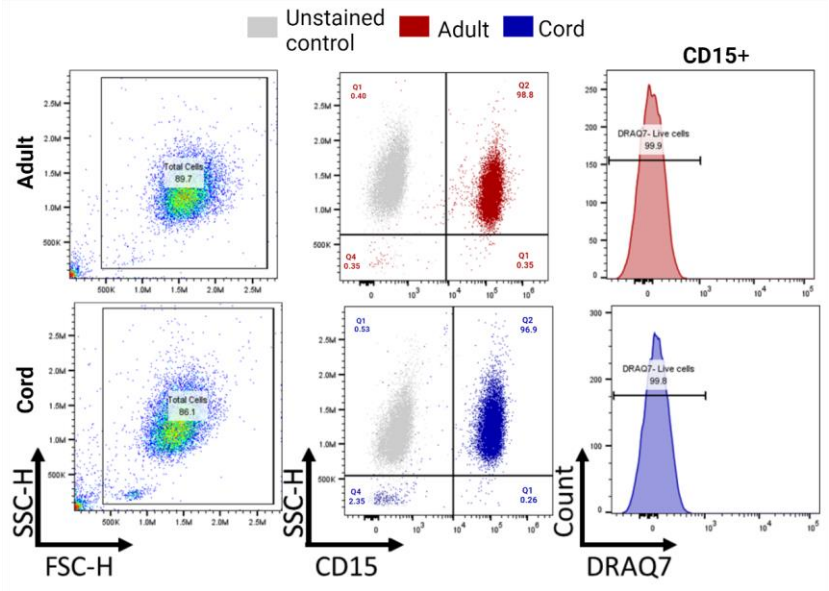

Figure 5.1 Isolated Neutrophils are viable.

CD15+ purity and cell viability were monitored by flow cytometry after MACS isolation from healthy adult or umbilical cord blood. Total cells were gated on (left column) and CD15 expression examined and compared to unstained controls (middle column). Cell death in CD15+ cells was assessed with DRAQ7 staining, with DRAQ7 negative cells considered to be live.

5.3.2 Neutrophils in cord blood represent a distinct intermediate population.

As early neonatal neutrophils are known to be impaired in their ability to perform some functions it seemed logical to first assess the maturation state of the cord blood neutrophils as there might be higher proportions of immature band neutrophils in circulation explaining these reported differences (Lawrence et al., 2017). Neutrophil maturation occurs primarily within the bone marrow starting from myeloblasts which are negative for most neutrophil markers but express CD15. This first stage of differentiation is followed by promyelocytes, myelocytes and metamyelocytes which

all express CD66b and CD15 but not CD35. These cells mature into band and mature neutrophils, of which mostly mature $CD16^{hi}$ $CD10^{hi}$ neutrophils exit the bone marrow into circulation (McKenna et al., 2021). In some circumstances such as severe disease and neonatal sepsis significantly greater proportions of the immature neutrophil populations are seen in circulation (Newman et al., 2010; Hornik et al., 2012). To assess the proportions of these neutrophil populations in adult and cord blood, MACS isolated neutrophils were stained with a panel containing CD66b, CD35, CD16 and CD10 and analysed by flow cytometry. Polymorphonuclear cell (PMNC)s were first gated on and then doublets excluded (Figure 5.2A). Gating of the following neutrophil differentiation markers were determined in adult samples and the same thresholds applied to cord blood samples. Next CD66b and CD35 expression was used to identify a mixed population of promyelocytes, myelocytes and metamyelocytes, defined as CD66b+CD35- (Figure 5.2A). The CD35+ fraction was gated on and further assessed for expression of CD10 and CD16. Band neutrophils were identified as $CD10^{lo}$ and $CD16^{lo}$ whilst mature neutrophils were defined as $CD10^{hi}$ and $CD16^{hi}$. In adults, nearly all cells were mature neutrophils (96.8% ± 0.8) with little to no promyelocytes myelocytes (0.9% ± 0.3) and metamyelocytes present (Figure 5.2B-C). Similarly, only a very small population (0.6% ± 0.2) of $CD10^{lo}$ and $CD16^{lo}$ band cells was seen. In cord however, there was a significantly larger population of promyelocytes, myelocytes and metamyelocytes ($p = 0.0019$) ranging from around 5 to 10 % of circulating PMNCs (Figure 5.2B). Additionally, a smaller fraction of the CD35+ cells were identified as mature $CD10^{hi}$ $CD16^{hi}$ neutrophils (55.5% ± 7.3; $p = 0.019$) and significantly more band neutrophils were seen ($p = 0.003$). Interestingly there also appears to be a large population with intermediate expression of CD10 and CD16 between band and mature neutrophils which is not seen in significant numbers in adults (36.6 % ± 7.6; $p = 0.0019$). To provide more clarity on the maturation state of this intermediate population identified in cords, isolated neutrophils from adults and cords, were prepared by cytospin for Kwik Diff™ staining. Mature neutrophils can be identified clearly by their highly segmented nucleus whilst band neutrophils contain a semi-circular band shaped nucleus (Marini et al., 2017). As expected, on visual inspection of Kwik Diff™ staining, adult neutrophils were highly segmented whilst some band

neutrophils were seen in cords most were still segmented suggesting the intermediate population may represent a unique maturation phenotype in cords.

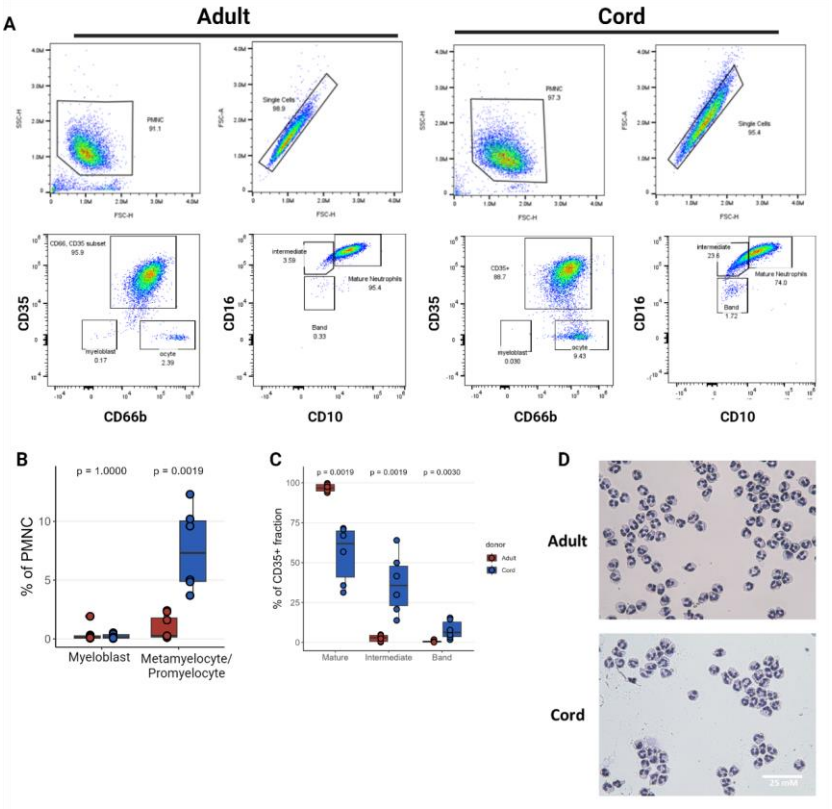

Figure 5.2 Developmental phenotype of cord blood neutrophils.

Developmental phenotype of MACS isolated neutrophils from human adult peripheral blood and umbilical cord blood was determined by flow cytometry and Kwik Diff™ staining. A) Manually determined gating for adult and cord neutrophils, top left panel shows gating on total PMNCs, top right panel shows single cell gating, bottom right panel shows identification of CD35+ myeloblasts (bottom left gate) combined promyelocytes, myeloblasts and metamyelocytes (bottom left gate) and the bottom right panel identifies band neutrophils, mature neutrophils and an intermediate population. B) summary plots of neutrophil populations. C) Summary plots of mature, intermediate and band

CD35+ neutrophil populations. D) Light microscopy images of Kwik Diff™ stained neutrophils prepared by cytospin. A-C) n = 8 adult and n = 6 cord; D) n = 3 adult and n = 3 cord. p-values were determined by Wilcoxon rank sum test (B, C). p < 0.05 was deemed significant.

5.3.3 Mitochondrial metabolism

As the neutrophil population was more diverse in cords and contained a large fraction of intermediately mature neutrophils it seemed reasonably likely that metabolic function might differ between adult and cord neutrophils. Realtime extracellular flux with a mitochondrial stress test was used to examine the metabolic parameters of ex vivo neutrophils. Baseline OCR and ECAR were recorded ahead of injections of oligomycin, FCCP and rotenone/antimycin A and metabolic parameters were calculated from these results (Figure 5.3A). Basal respiration and ATP linked respiration were very low and comparable between adults and cords (Figure 5.3B-C). However, maximal respiration and spare respiratory capacity were significantly greater in adults ($p = 0.0096$ and $p = 0.0019$ respectively) suggesting adults possess a significantly greater metabolic reserve able to meet greater demand when needed (Figure 5.3D-E). Additionally, a large amount of non-mitochondrial respiration was seen in both adults and cords with nearly equal OCR compared to basal respiration (Figure 5.3F). Basal ECAR was comparable between adults and cords and overall neutrophils from both donor groups were more glycolytic than oxidative (Figure 5.3G).

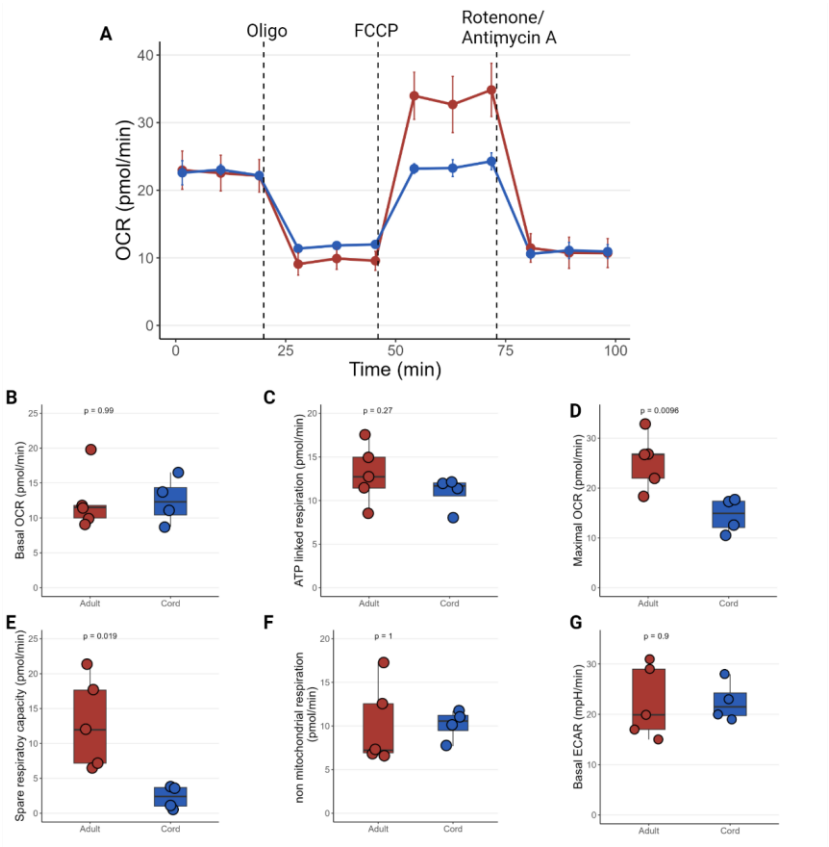

Figure 5.3 Basal mitochondrial metabolism is comparable between adult and cord neutrophils.

Metabolic function of 2 x 10^5 ex vivo neutrophils from human adult peripheral blood and umbilical cord blood were assessed by measuring OCR and ECAR in response to a mitochondrial stress test. A) Trace of OCR during mitostress test by injection of 1 μM oligomycin, 1 μM FCCP, 1 μM antimycin A and 1 μM rotenone. Summary plots of B) basal respiration, (C) ATP linked respiration, (D) maximal respiration, (F) spare respiratory capacity, (G) Basal ECAR calculated for adults and cords. n = 5 adults and 4 cords. p-values were determined by Wilcoxon rank sum test (B-G). $p < 0.05$ was deemed significant.

In concordance with the findings from extra-cellular flux analysis no differences were seen in mitochondrial content of adult and cord blood derived neutrophils. MitoTracker™ staining and analysis by flow cytometry found high and fairly uniform mitochondrial content across the neutrophil population in adults and cords which was comparable between the donor groups (Figure 5.4A-B). Furthermore, confocal images of neutrophils stained with DAPI (blue) and MitoTracker™ Green showed similar mitochondrial content spread throughout the cell (Figure 5.4C).

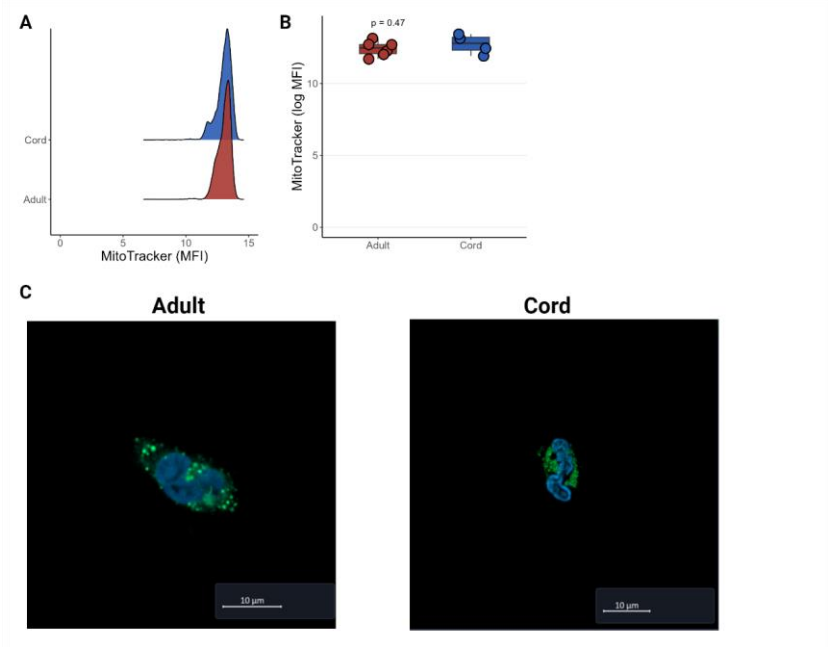

Figure 5.4 Mitochondrial content of adult and cord neutrophils.

Mitochondrial content of neutrophils from human adult peripheral blood and umbilical cord blood determined by MitoTracker™ Green staining using flow cytometry and confocal microscopy. A) Representative histograms of MitoTracker™ staining by flow cytometry with B) summary plots. C) Representative confocal microscopy images of neutrophils stained with

Mitotracker™ Green. A-B) n = 6 adult and 4 cord; C) n = 4 adult and 3 cord. p value determined by Wilcoxon rank sum test. $p < 0.05$ was deemed significant.

5.3.4 Neonatal neutrophils fail to produce NETs

NET formation is an essential mechanism of neutrophil mediated defence, able to trap and destroy invading pathogens (Yipp and Kubes, 2013). Neonates are particularly vulnerable to sepsis potentially due to reduced protective functionality such as trafficking and low expression of the Fc receptor CD16, as shown earlier (Yost et al., 2009; Melvan et al., 2010; Fleischmann et al., 2021). Furthermore, it has been reported that the ability to form lytic NETs is absent from cord blood neutrophils (Yost et al,. 2009). To validate this described lack of NET formation observed in the literature, neutrophils from adult and cord blood were isolated by MACS and activated with 50 nM PMA for 3 h in RPMI cultures. NETs were visualised using the DNA binding dye DAPI. DMSO vehicle was used as a negative control and 2DG, a known inhibitor of NETosis, was used as an additional control (Rodriguez-Espinosa et al., 2015). When left unstimulated (DMSO control) no NETs were seen in either adults or cords however, when stimulated with PMA NETs were observed only in adults (Figure 5.5). The formation of NETs in adults could be completely inhibited by pretreatment with 2DG (Figure 5.5).

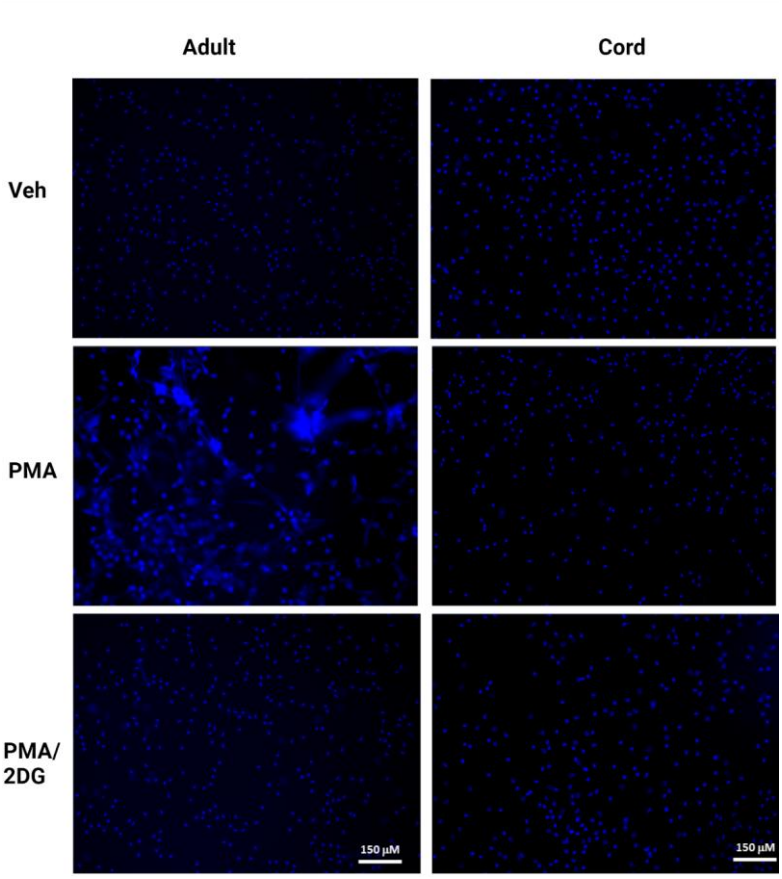

Figure 5.5 Cord neutrophils do not produce NETs in response to PMA.

Neutrophils isolated from human adult peripheral blood and cord blood stimulated with (top) vehicle control, (middle) PMA (50 nM) or (bottom) PMA after pre-treatment with 2DG (100 mM) for 3 h. Left column shows representative images from n = 5 adults and right column shows representative images from n = 5 cords

5.3.5 Oxidative and glycolytic burst is reduced in neonates.

Lytic NET formation is dependent on ROS production by the surface protein NOX2 which leads to the release of NE and MPO stored in granules and the breakdown of

the nuclear envelope followed by the release of extracellular DNA (Yipp and Kubes, 2013). On activation NOX2 rapidly consumes 0_2 and NADPH in a respiratory burst, which can be measured as the extracellular oxygen consumption rate (Rice et al., 2018; Awasthi et al., 2019). The oxidative burst of neutrophils is often measured by detection of reactive oxygen species with the aid chemiluminescent probes. Whilst in common use, these approaches suffer from a number of drawbacks including selectivity of ROS species and their ability to detect extra-cellular and intracellular ROS (Murphy et al., 2022). In this thesis, consumption of oxygen from the assay media, required by NOX2 for the formation of ROS, was utilised as an alternative method for assessing the oxidative burst of neutrophils. Oxygen consumption was measured in real time, using the seahorse extra-cellular flux platform which also provided the benefit of simultaneous measurements of extra-cellular acidification. Whilst, this method does provide some advantages over traditional chemiluminescent approaches, non-ROS specific sources of oxygen consumption, such as mitochondria, may impact on measurements of the oxidative burst. Although mitochondria are not thought to play a significant role in the oxidative burst of neutrophils (Grudzinska et. al., 2023).

As the ROS production via NOX2 is required for NET formation and NETs were distinctly absent in cord neutrophils it seemed likely that cord neutrophils may possess some deficiency in the oxidative burst. To test this, real time extra-cellular flux as measured in adult and cord neutrophils stimulated with 50 nM PMA. Additionally, as NETs also show a requirement for a functional glycolysis pathway (Rodriguez-Espinosa et al., 2015) some wells were also treated with 2DG. Baseline OCR and ECAR remained stable prior to the first injection with ECAR then decreasing, for cells treated with 2DG whilst the vehicle treated cells were unaffected (Figure 5.5A-B). Following injection of PMA, OCR and ECAR rapidly and dramatically increased before reaching a peak and dropping back down, whilst little to no increase in OCR or ECAR was seen in cell pre-treated with 2DG before PMA stimulation or unstimulated cells (Figure 5.5A-B). Whilst similar trends were seen across both adults and neonates in response to PMA and 2DG treatment the magnitude of the responses differed significantly. Maximum OCR was significantly reduced in cord PMA stimulated cells (p

= 0.014) and this maximum was reached around 10 min earlier (p = 0.061) and the total oxygen consumption was also significantly less in cords (p = 0.014; Figure 5.5C, E). Maximum OCR and total 0_2 consumption did not differ between adult and cord neutrophils when left untreated whilst both parameters were greater when stimulated after pre-treatment with 2DG with adults showing slightly greater basal OCR (p = 0.077) and total 0_2 consumption (p = 0.054). Similarly, maximum ECAR was significantly reduced in PMA stimulated cord neutrophils (p = 0.014) and peak ECAR was reached slightly faster. No differences were observed between adult and cord neutrophils that were left untreated or treated with 2DG prior to PMA stimulation. Although ECAR is often used as a measure of glycolysis there are also other sources of extracellular acidification some of which may come from degranulation of neutrophils. To determine if differences in ECAR were reflective of differing glycolytic rates lactate in supernatant was measured at 15 and 60 min after addition of PMA or vehicle (Figure 5.5H). At 15 min after addition of PMA lactate in culture supernatant was slightly but significantly increased compared to unstimulated controls (p =0.022) whilst only a slight difference was seen between unstimulated or stimulated cord neutrophils (Figure 5.5H). Interestingly, at this early time point post activation, more lactate was present in the culture supernatant of cord neutrophils (p = 0.063; Figure 5.5H). Lactate increased with time for all donor groups under unstimulated and stimulated conditions. Lactate in culture supernatant increased significantly between 15 and 60 min for both donors when left unstimulated; though, this only reached significance in adults (p = 0.006; Figure 5.6H). Showing that PMA stimulation increased aerobic glycolysis, at 60 min, significantly more lactate was present in stimulated culture supernatant, for both donor groups (p = 0.002 and 0.003 respectively) and there was significantly less lactate in cord culture supernatant (p = 0.021; Figure 5.5H).

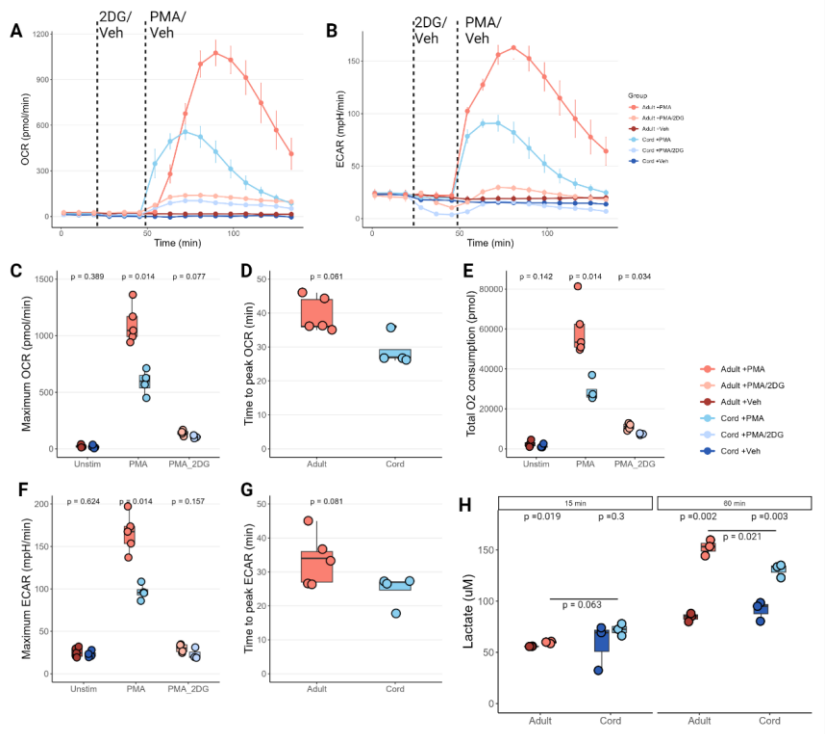

Figure 5.6 Cord neutrophils show reduced oxidative burst on activation with PMA.

The oxidative burst of 2 x 10^5 PMA activated neutrophils from adult peripheral blood and umbilical cord blood was measured in real time by extra-cellular flux analysis. A) OCR and B) ECAR traces at baseline, after injection of 2DG or vehicle and after injection of 50 nM PMA. Summary plots comparing C) maximum OCR, D) time to peak OCR, E) total 02 consumption, F) maximum ECAR and, G) time to peak ECAR for adults and cords. Measurement of lactate in supernatant after 15 and 60 minutes culture with or without 50 nM PMA. A-G) n = 5 adult and n = 4 cord; H) n = 3 adult and n = 3 cord. For comparisons between donor groups p values were determined by Wilcoxon rank sum test and for comparing donor matched treatments, p values were determined by Wilcoxon signed rank test. $p < 0.05$ was deemed significant.

5.3.6 Increased ECAR on activation is largely due to factors other than extracellular flux of lactate but LDHA activity is required for NETosis.

Next the role of lactate production and the activity of LDHA, in the formation of NETs was assessed, as some evidence in the literature suggests that lactate formation is sufficient for NETosis (Awasthi et al., 2019). The role of both LDHA and lactate were assessed separately by adding lactate to culture with neutrophils or activating neutrophils in the presence of the LDHA specific inhibitor GSK 2837808A (LDHi). Contrary to other published reports lactate alone was not sufficient to induce NETosis even at the highest concentration of 20 mM (Figure 5.7A). In contrast and confirming some aspects of the literature, inhibition of LDHi impaired the formation of NETs in adults (Figure 5.7B).

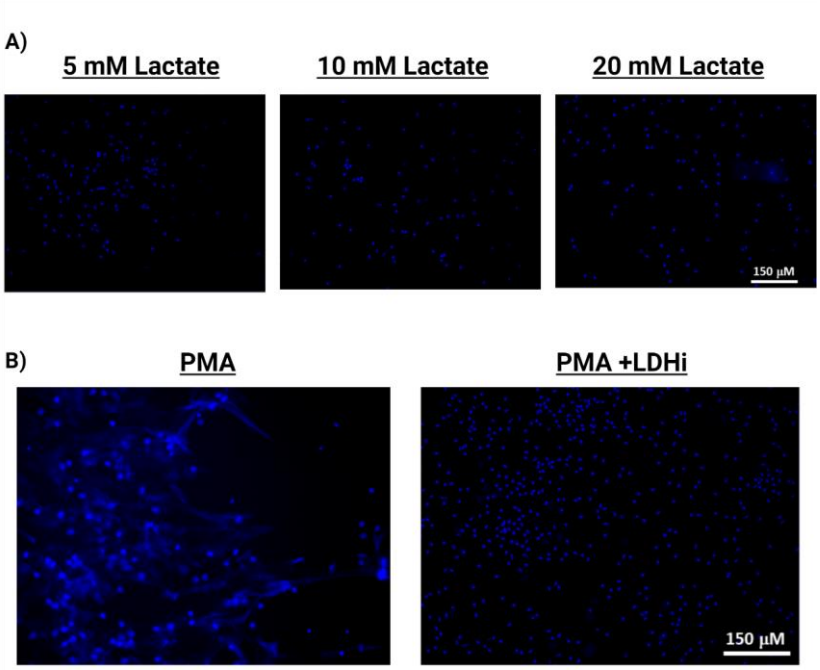

Figure 5.7 LDHA activity is required for NETosis in adults.

The role of lactate and the enzyme lactate dehydrogenase A was assessed using by fluorescence imaging. A) Adult neutrophils were cultured with 5-, 10- or 20-mM lactate and stimulated with PMA for 3 hours and NETosis assessed by DAPI staining (blue). B) Adult neutrophils were stimulated with PMA (50 nM) alone or pretreated with a lactate dehydrogenase inhibitor (GSK 2837808A; 10 µM) for 15 min followed by PMA stimulation. NET formation visualised by DAPI staining (blue). A) images representative of n= 2 donors and B) images representative of n= 7 donors.

The effect of LDH inhibition on the oxidative burst was also assessed in adults and neonates using real time measurements of OCR and ECAR before and after injections of LDHi/Veh and PMA (Figure 5.8A-D). Initially on injection of LDHi, OCR increased compared to vehicle for both adults and cords ($p = 0.009$ and $p = 0.052$, respectively;

Figure 5.8E). Despite inhibition of LDHA impairing NETosis the maximum oxidative burst, as measured by OCR, actually increased when cells were pretreated with LDHi although this, increase did not reach significance in either donor group ($p = 0.063$ for adults and $p = 0.1$ for cords; Figure 5.8F). The kinetic of the oxidative burst were also affected by pretreatment with LDHi, where peak OCR was reached later however, this was only significant in adults ($p = 0.013$; Figure 5.8G). As one would expect, injection of LDHi decreased initial ECAR for both adults and cords ($p = 0.01$ and $p = 0.0062$, respectively; Figure 5.8H) however, maximum ECAR was unaffected in either donor group (Figure 5.8I). And the time taken to reach peak ECAR was only decreased slightly (Figure 5.8J). As there are other sources of extracellular acidification, a lactate assay was also performed, at 15- and 60-min post PMA activation with or without LDHi, to more specifically consider glycolysis (Figure 5.8K). 15 min post activation lactate production was significantly reduced in both adults and cords ($p = 0.01$ and $p = 0.02$, respectively) and the same was true at 60 min ($p = 0.04$ and $p = 0.01$; Figure 5.8K). When treated with LDHi lactate in culture supernatant did not significantly increase, between 15 and 60 min, for either donor group ($p = 0.6$ for adults and $p = 0.2$ for cords), between 15 and 60 min (Figure 5.8K).

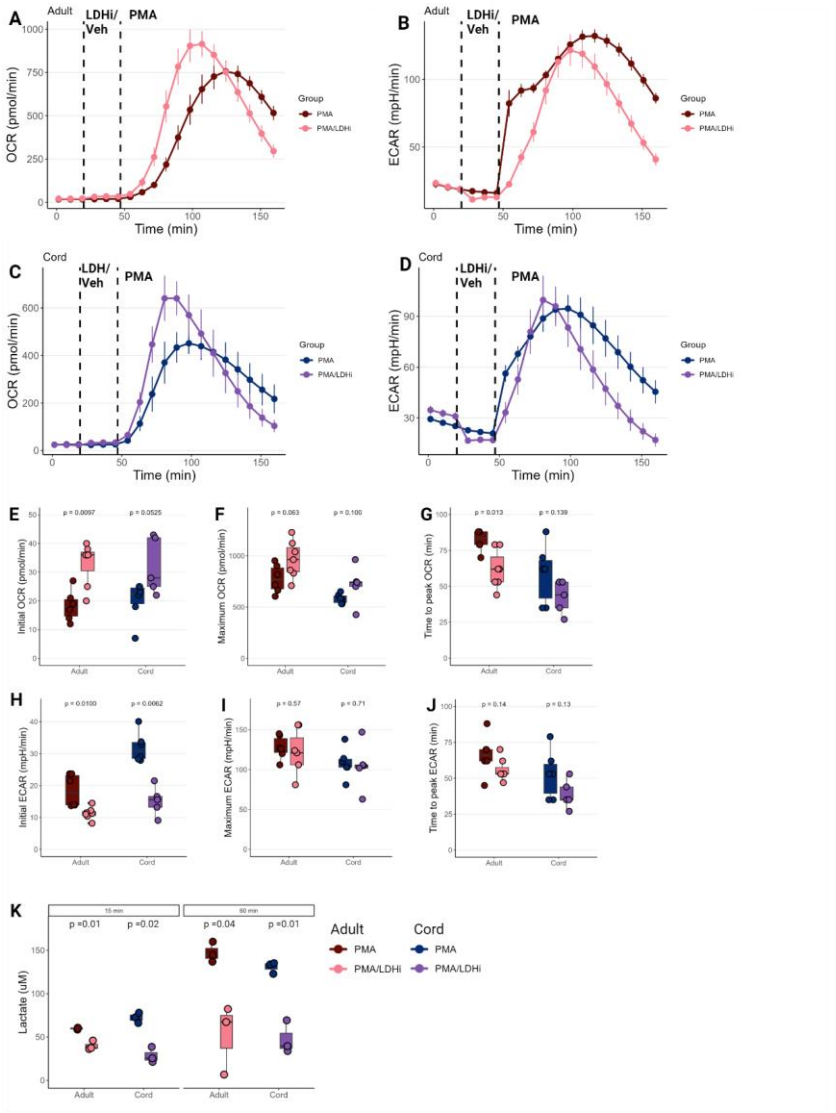

Figure 5.8 LDH inhibition reduces the oxidative burst but does not reduce ECAR.

Oxidative burst (OCR) of2 x 10^5 neutrophils per well isolated from adult peripheral blood and umbilical cord blood measured in real time on activation with or without lactate dehydrogenase inhibitor. A-D) OCR and EACR traces of neutrophils at baseline, after injection of LDHi (10 μM) vehicle and after

injection of 50 nM PMA for adult and cords. Summary plots comparing E) initial OCR (post injection of LDHi/vehicle), F) Maximum OCR, G) time to peak OCR, H) initial ECAR (post injection of LDHi/ vehicle), I) maximum ECAR and, J) time to peak ECAR. K) Measurement of Lactate in culture media after PMA stimulation +/- 10 μM LDHi for 15 or 60 minutes. A-J) n = 6 adult and n = 5-6 cord; K) n = 3 adult and n = 3 cord. For comparisons between donor groups p values were determined by Wilcoxon rank sum test and for comparisons of donor matched treatment conditions, p values were determined by Wilcoxon signed rank test. p < 0.05 was deemed significant.

5.3.7 NETosis is dependent on extracellular glucose.

It has already been established that lytic NETosis is dependent on glycolysis however the source of glucose fuelling NETosis is less clear (Awasthi et al., 2019). As well as expressing glucose transporters, neutrophils also contain large glycogen stores, likely to support function in low glucose environments such as wound sites (Rodriguez-Espinosa et al., 2015; Sadiku et al., 2021). Furthermore, on activation with LPS adult neutrophils begin generating more glycogen by running glycolysis in reverse (Sadiku et al., 2021). As glycogen clearly plays a significant role in neutrophil energy metabolism and function, the role of both extracellular glucose and glycogen were assessed in NETosis and the oxidative burst.

To examine the role of both intracellular and extracellular glucose sources in NETosis, adult neutrophils were stimulated with PMA in complete RPMI media, RPMI without glucose, pretreated with the glycogen phosphorylase inhibitor CP-91149 (GPi) or pretreated with GPi and cultured in RPMI without glucose. Removing exogenous glucose from the media completely impaired NETosis whilst inhibition of glycogen phosphorylase had no effect and a combination of glucose free media and GPi also completely impaired NETosis (Figure 5.9).

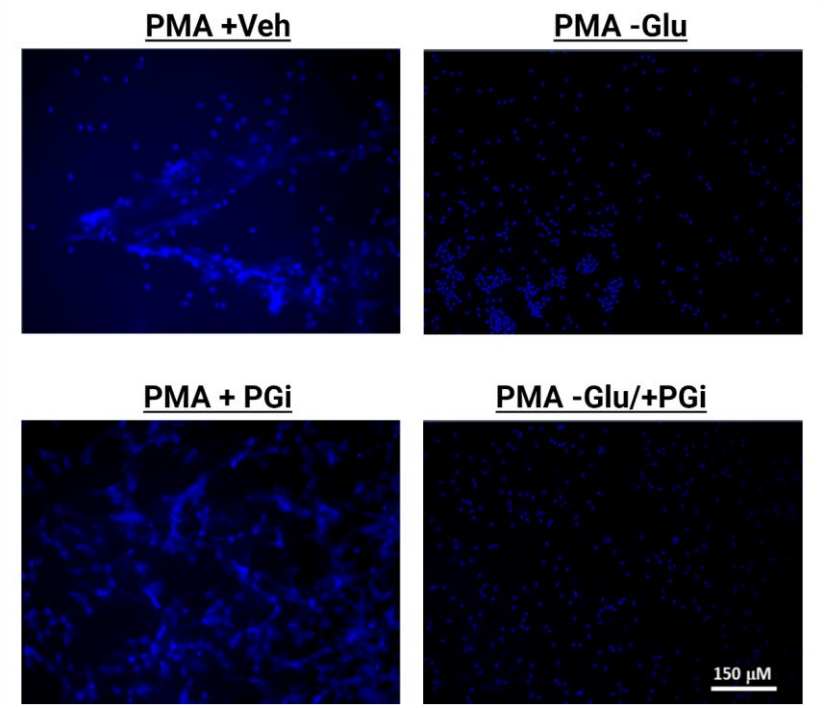

Figure 5.9 Exogenous glucose is required for NETosis.

The requirements of exogenous glucose and glucose from glycogen stores for NET formation were assessed by activating adult neutrophils with or without glucose and the glycogen phosphorylase inhibitor CP-91149. Neutrophils were cultured stimulated with PMA (50 nM) for 3 hours in RPMI or glucose free RPMI (-Glu) with or without GPi pretreatment for 15 min. NET formation was visualised by DAPI staining (blue). Images representative of n = 3-5 donors.

Next, to examine the role of these two glucose sources in the oxidative burst, real time OCR and ECAR were measured in neutrophils assayed in minimal assay media supplemented with 2 mM glutamine, 1 mM pyruvate and with or without 5.5 mM glucose. OCR and ECAR were measured in response to injections of GPi/Veh and PMA (Figure 5.10A-D). Lack of extracellular glucose or injection of GPi resulted in increased initial OCR for both adults and cords (In adults $p = 0.003$ for -Glu, $p = 0.02$ for +GPi,

and for cords -Glu p = 0.005 and +GPi p =0.05). However, removal of exogenous glucose and injection of GPi only increased initial OCR in adults (p = 0.009; Figure 5.10E). Maximum OCR, for both adults and cords, was reduced significantly whenever there was no exogenous glucose in the assay media (in adults, -Glu p = 0.001, -Glu/+GPi p = 0.004 and in cords -Glu 0.005 and -Glu/+GPi p = 0.01, Figure 5.10F) and the average maximum OCR was lowest in glucose free GPi treated conditions (Figure 5.10F). Kinetics of the oxidative burst were largely unaffected except in the glucose free condition for adults where peak OCR was reached earlier than in glucose supplemented media (p = 0.03; Figure 5.10G). Initial ECAR was decreased significantly in both adult and cord neutrophils assayed in glucose free media conditions (for adults -Glu p = 0.01, -Glu/+GPi 0.008 and for cords -Glu p = 0.002 and -Glu/+GPi p = 0.01; Figure 5.10H) and the average ECAR was lowest when neutrophils were cultured in glucose free media and treated with GPi. Injection of GPi, when glucose was present in the assay media, did not result in any change in ECAR for either donor group (Figure 5.10H). Similarly, maximum ECAR was reduced in all glucose free conditions (for adults -Glu p = 0.003, -Glu/+GPi p = 0.008, and for cords -Glu p = 0.008, -Glu/+GPi p = 0.01, respectively; Figure 5.10I) and the average maximum ECAR was lowest in GPi treated neutrophils assayed in glucose free media (Figure 5.10I). As with OCR, the kinetics were largely unaffected by glucose deprivation or GPi treatment (Figure 5.10J). As only exogenous glucose appeared to be required for NETosis and was largely responsible for reduced oxidative burst, the effects of exogenous glucose deprivation on metabolic function were further assessed using a lactate assay. Here, neutrophils were activated with PMA for 15 or 60 min with or without exogenous glucose in the media and lactate in the culture supernatant was measured. At both 15- and 60-min, adult and cord neutrophils activated in glucose free media produced significantly less lactate (p = 0.002 and 0.01 for adults and p = 0.01 and 0.02 for cords; Figure 5.10K). Adult neutrophils appeared better able to compensate for the lack of exogenous glucose as the amount of lactate increased significantly between 15 and 60 min (p = 0.002) whilst no significant increase was observed in cords (p = 0.8; Figure 5.10K). Glycogen content in resting adult and cord neutrophils was also measured, but no difference was observed (p = 0.69; Figure 5.10L).

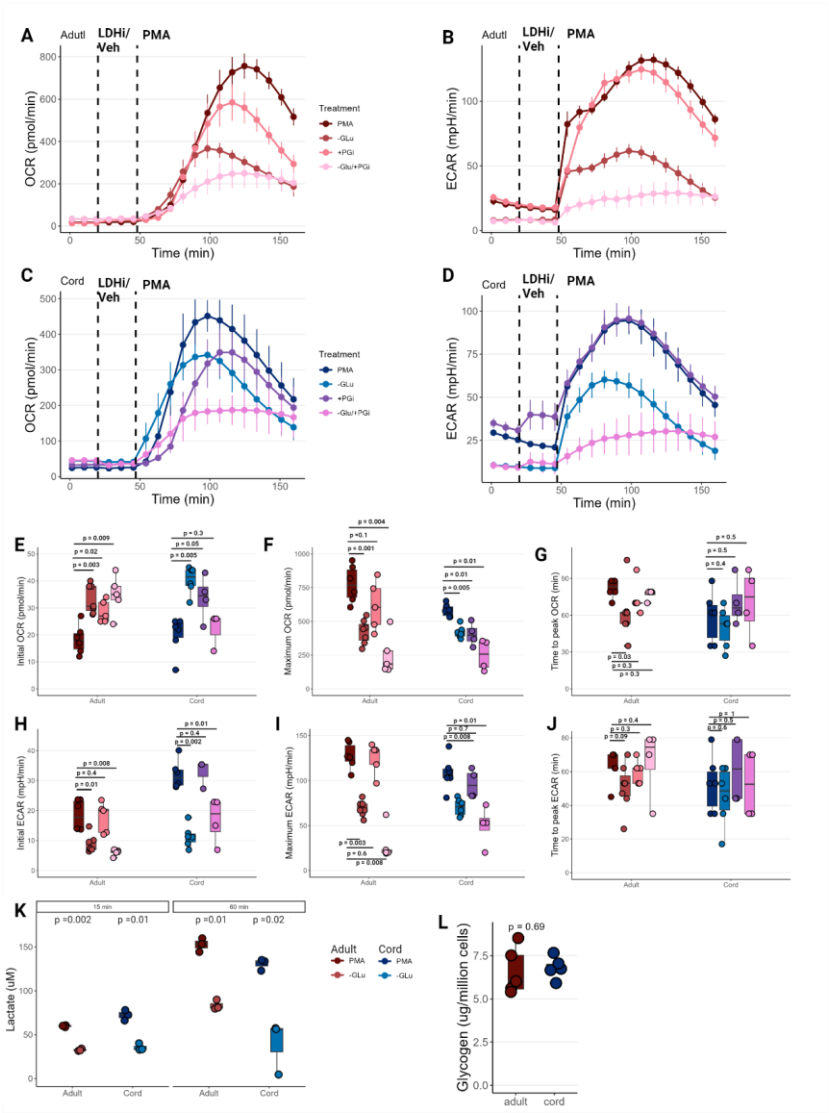

Figure 5.10 Exogenous glucose fuels the oxidative burst.

Oxidative burst, of 2 x 10^5 peripheral blood adult neutrophils and umbilical cord blood neutrophils, measured in real time on activation with or without glucose or in the presence of a glycogen phosphorylase inhibitor. A-D) Shows trace OCR

and ECAR traces for neutrophils in media +/- glucose (5.5mM) at baseline; after injection of GPi (10 mM)/vehicle and after injection of 50 nM PMA for adult and cords. Summary plots comparing treatment conditions across E) initial OCR (post injection of GPi/vehicle), F) Maximum OCR, G) time to peak OCR, H) initial ECAR (post injection of GPi/ vehicle), I) maximum ECAR and J) time to peak ECAR. k) summary plots of lactate in culture media after PMA stimulation in media +/- glucose (5.5mM) and/or 10 mM GPI, for 15 and 60 min. L) Glycogen content in mg/million cells. A-J) n = 5-6 adult and n = 4-6 cord; K) n = 3 adult and n = 3 cord and L) n = 5 adult and 5 cord. For comparisons between donor groups p values were determined by Wilcoxon rank sum test and for comparing donor matched treatment conditions, p values were determined by Wilcoxon signed rank test. p < 0.05 was deemed significant.

5.3.8 Restoring energy production in neonatal neutrophils restores NET function.

Thus far the exact mechanism linking glycolysis with NETosis remained elusive although a requirement for exogenous glucose and functioning LDHA had been demonstrated. Aerobic glycolysis is the very rapid conversion of glucose to lactate in the presence of oxygen, and whilst highly inefficient it is able to generate ATP at a faster rate than metabolism to pyruvate and subsequent mitochondrial oxidative phosphorylation (Desousa et al., 2023). LDHA serves as an important mechanism for regenerating NAD+ from NADH generated during glycolysis, maintaining the redox balance of the cell and enabling continued aerobic glycolysis (Xu et al., 2021). Complex I of the mitochondrial electron transport chain (ETC) performs the same function and therefore may show a similar effect on NETosis (Luengo et al., 2021). To determine whether complex I activity is required for NETosis neutrophils from adults were stimulated with PMA in the presence of the complex I inhibitor rotenone. To ensure that any differences observed were not due to impaired ATP production on disrupting the ETC, neutrophils were also activated in the presence of ATP synthase inhibitor oligomycin. Additionally, the ability of these inhibitors alone to generate

NETosis was also determined. Inhibition of complex I or ATP synthase did not impair NETosis in adults (Figure 5.11). Furthermore, the inhibitor compounds rotenone and oligomycin did not cause any spontaneous NETs (Figure 5.11).

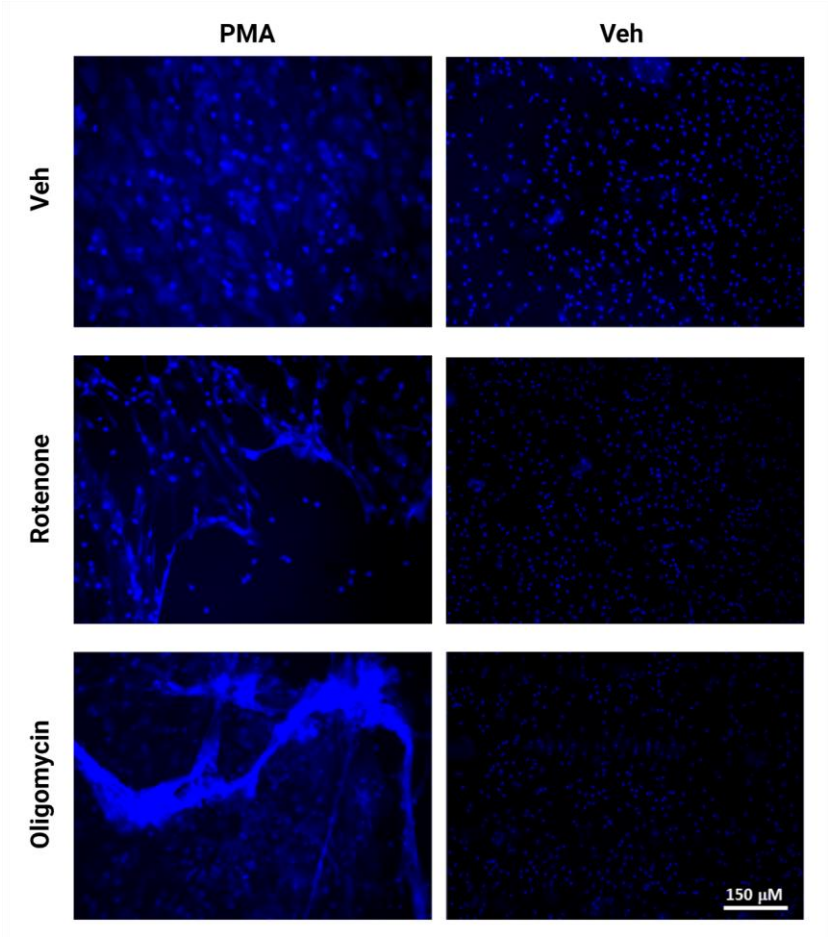

Figure 5.11 Complex I is not required for NETosis.

Dependence of NETosis on complex 1 and ATP synthase was determined by activating adult neutrophils in the presence of rotenone or oligomycin. Neutrophils were pretreated with vehicle, rotenone (1 µM) or oligomycin (1 µM) for 30 min before addition of PMA (50 nM; left column) or vehicle (right

column). Images representative of n = 5-6 donors for PMA treatment; n = 2 for vehicle treated Oligomycin and Rotenone conditions.

Impaired NETosis in adults with LDHA inhibition suggests that ATP, derived from aerobic glycolysis, is required for NET formation. This is likely due to reduced capacity to restore the NAD+ pool. Furthermore, reduced lactate, in the culture supernatant of activated cord neutrophils compared to adults, suggests that the rate of aerobic glycolysis is lower in cords. This led to the hypothesis that NET formation in cord neutrophils may be impaired due to insufficient ATP production from glycolysis which has already been shown in some other settings (Amini et al., 2018). To test if the slower rate of NAD regeneration in cords is responsible for failure to produce NETs, neutrophils from cords were stimulated for 3 h with PMA (50 nM) after pretreatment with extracellular ATP (200 μM) for 30 min. Additionally, neutrophils from cords were stimulated with PMA (50 nM) with or without extracellular nicotinamide mononucleotide (NMN; 500 μM). The ability of these compounds to induce spontaneous NETs was also assessed. As seen previously, neutrophils from cord blood did not produce NETs in response to PMA treatment alone. However, when pretreated with ATP or NMN for 30 min, before addition of PMA (50 nM), neutrophils from all cord blood donors produced NETs. (Figure 5.12). No NET formation was seen when neutrophils were cultured with ATP or NMN alone.

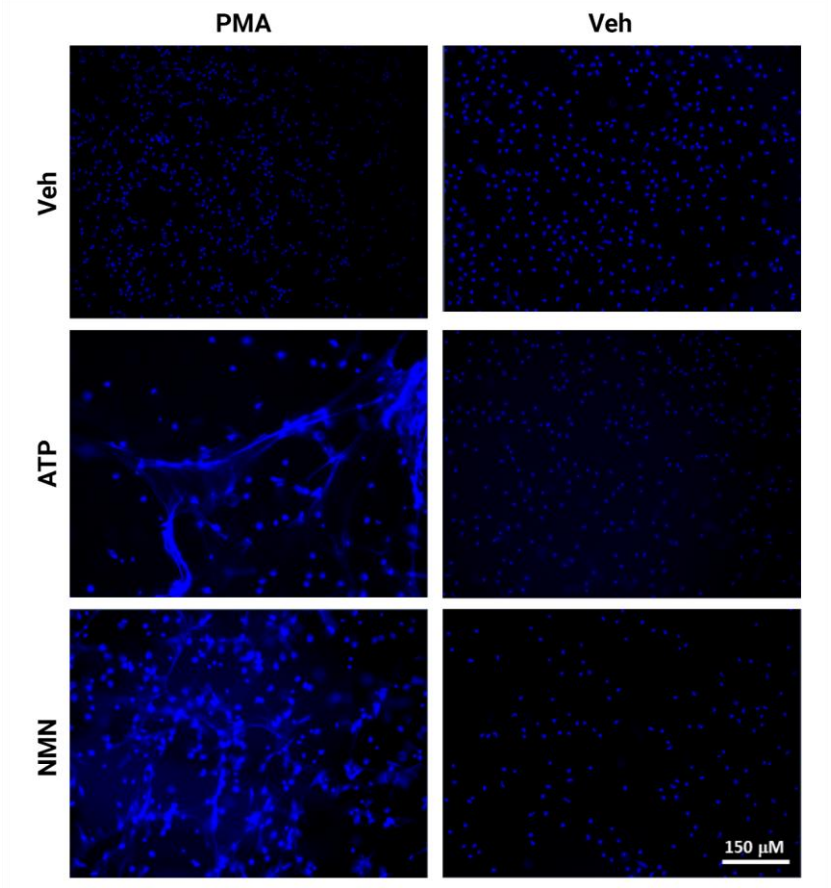

Figure 5.12 Increasing energy availability of cord neutrophils enables NET function.

Assessing the ability of umbilical cord blood neutrophils to produce NETs when given exogenous ATP or NMN when stimulated with PMA. Neutrophils were pretreated with vehicle, ATP (200 µM) or NMN (500 µM) for 30 min before addition of PMA (50 nM; left column) or vehicle (right column). Images representative of 5-6 donors for PMA treated conditions; n = 2 for vehicle treated NMN and ATP conditions .

5.4 Discussion

Neutrophil extracellular traps are an important feature of host defence, trapping and killing pathogens, thus limiting further infection. However, along with other functions that are diminished in the first days of life, the production of NETs is absent, potentially leaving neonates even more vulnerable to infection and sepsis (Yost et al., 2009; Melvan et al., 2010). In other published work, a link between the ability of adult neutrophils to form NETs and metabolic function has already been established (Awasthi et al., 2019). Specifically lytic NETosis is known to rely primarily on glycolysis, although the exact mechanism through which glycolysis supports NETosis is still debated with some evidence suggesting glycolysis supports NETosis via feeding into the pentose phosphate pathway and fuelling the oxidative burst whilst others have suggested that the end product of aerobic glycolysis, lactate, is a key requirement for NETosis (Awasthi et al., 2019; Britt et al., 2022). As the metabolic function of neonatal neutrophils is not well studied, but a link between metabolic function and NETosis had already been established in adults, this chapter sought to understand the metabolic characteristics of neonatal neutrophils and explore metabolism as an underpinning mechanism for lack of NET formation in neonates. As such this chapter finds that NETosis in neonatal neutrophils is impaired as a result of insufficient ATP generation from glycolysis due a reduced ability to regenerate the NAD+ pool needed for rapid glycolysis and the oxidative burst.

Firstly, analysis of the neutrophil content of cord blood, using a flow cytometry based maturation panel, revealed greater proportions of circulating neutrophil precursors and immature band neutrophils in cord blood compared with adult peripheral blood. Furthermore, “intermediately mature” neutrophils, characterised by intermediate expression of CD10 and CD16 were identified as a large proportion of circulating cord blood neutrophils which was not present to any significant degree in adults. As Kwik Diff™ stained images of cord blood neutrophils showed mostly segmented nuclei structures, indicative of mature neutrophils, it seems most likely that a large fraction of the cord blood neutrophil exists in an intermediary developmental phase and therefore may not possess the same functional characteristics as their mostly mature

adult counterparts. Similarly, low expression of CD16 and CD10 has been identified as a feature of immunosuppressive low density neutrophils in diseases settings, sepsis and pregnancy, further adding to the possibility that the function of neonatal neutrophils may differ significantly from that of adults however, whether these neutrophils were low density neutrophils was not determined here (Dumitru et al., 2012; Kostlin et al., 2014). Further experiments in this chapter utilised the whole neonatal neutrophil compartment, despite it differing significantly from adults. As this study aimed to characterise the metabolic function of neonatal neutrophils, with the aim of understanding how metabolic function may relate to effector function in neonates, it was reasoned that the whole neutrophil compartment would be most representative of what is seen in the neonate. Sorting of mature neutrophils from neonatal populations to make a like for like comparisons with adults was beyond the scope of this thesis but is likely worth future investigation to understand if differences in neonatal neutrophil function can be accounted for by a simple lack of maturity.

Exploring the basal metabolic status of adult and cord blood neutrophils did not show many significant differences, with basal respiration, ECAR and mitochondrial content all being comparable. However, reduced maximal respiration and almost no spare respiratory capacity in cord neutrophils indicates poor metabolic flexibility and suggests there is little scope for cord blood neutrophils to rapidly augment metabolic function to meet heightened demand (Marchetti et al., 2020).

One such function that likely requires significant augmentation of the resting metabolic state is NETosis which is driven by the oxidative burst and is an essential tool in the neutrophils arsenal of defensive capabilities. Here the oxidative burst of neutrophils was measured using the oxygen consumption rate from the media which provides some advantages over common use probe-based methods which often suffer from issues of specificity (Murphy et al., 2022).

Confirming the literature, no NET formation was observed in cord blood neutrophils on PMA stimulation which was accompanied by lower maximum OCR and total oxygen consumption suggesting a reduced oxidative burst, compared to adults. Glycolysis fuels the pentose phosphate pathway which generates NADPH consumed

by NOX2 in the oxidative burst causing lytic NETosis (Rice et al., 2018; Britt et al., 2022). The combined reduction in oxidative burst and lactate production suggested that cord blood neutrophils may be unable to form NETs due to a reduced capacity to augment glycolysis when stimulated.

To better understand the mechanisms linking glycolysis with NETosis, further experiments on were conducted on NETosis capable adult neutrophils. Glucose is a known requirement for NETosis however, neutrophils contain large glycogen stores that enable function in oxygen deprived environments or potentially low glucose environments but whether the use of glycogen stores has any impact on NET formation was not known (Sadiku et al., 2021). This chapter confirms that glucose and specifically exogenous glucose is an essential requirement for NETosis. Furthermore, real time metabolic flux analysis showed that exogenous glucose is the primary fuel source for the oxidative burst, for both adult and cord blood neutrophils, as removing glucose reduced maximum OCR but inhibition with a glycogen phosphorylase inhibitor did not affect the maximum OCR. These data suggest that glycogen might be able to fuel a reduced glycolytic burst as the oxidative burst was not blocked entirely by removing exogenous glucose and inhibition by GPi in glucose free conditions further reduced the maximum OCR and total oxygen consumption. Some of these differences in readings for oxidative burst, using OCR, may also have been impacted by other sources of oxygen consumption which were not properly controlled for in these experiments. Addition of mitochondrial inhibitors, rotenone and antimycin A in prior to PMA stimulation should be used in future experiments to provide clearer results and increase resolution by reducing background reading. Bearing this in mind, and as there was no difference in glycogen content between adults and neonates it seems unlikely that differences in glycogen metabolism could explain the failure of cord blood neutrophils to produce NETs. Additionally, impaired lactate production in both donor groups, when exogenous glucose was removed, suggest that glucose is the primary source fuelling aerobic glycolysis on PMA stimulation.

As cord blood neutrophils produced less lactate after PMA stimulation, the role of lactate dehydrogenase in NETosis and the oxidative burst was investigated in adults. Firstly, it is worth noting that no change in maximum ECAR was observed after PMA stimulation of LDHi treated neutrophils, compared to vehicle controls for either donor group. As LDHi treatment prevented significant increase in lactate production and ECAR initially dropped on injection of LDHi, before the addition of PMA, it was concluded that the inhibitor successfully impaired LDHA activity and that the increase in ECAR seen on PMA injection was largely due to sources other than lactate, such as degranulation or H_2O_2 produced from NOX2 activity during the oxidative burst. Surprisingly maximum OCR and total oxygen consumption of PMA stimulated neutrophils increased with LDHi treatment for both donor groups. The exact reason for this is still unclear though it may be that inhibiting the LDHA resulted in a build-up of glycolytic intermediates expanding the pool of metabolites (glucose-6-phosphate, fructose-6-phosphate and glyceraldehyde-3-phosphate) able to fuel the pentose phosphate pathway and hence the oxidative burst. Together with the evidence these LDHA activity is required for NETosis, these results suggest that a strong oxidative burst can occur independently from NETosis and that the oxidative burst is not the soul factor responsible for NETosis. Additionally, the product of LDHA activity, lactate, is not sufficient to induce NETosis despite contrary findings in the literature (Awasthi et al., 2019). However, this does not seem that unlikely given that high concentrations of lactate can often appear under normal physiological conditions such as heavy exercise and spontaneous NETosis under these conditions would not be advantageous (Li et al., 2023). It seems more likely that the role of lactate dehydrogenase in restoring NAD+ pools during rapid aerobic glycolysis is the mechanism underpinning the impaired NET formation observed in umbilical cord blood neutrophils. Furthermore, regeneration of NAD+ for NETosis is not dependent on complex I, another major source of NAD+ regeneration in the cell. Applying this understanding of NETosis to cord blood neutrophils revealed that reduced ATP production as a result of the inability to rapidly regenerate the NAD+ pool appears to be the mechanism impairing NETosis in cord blood neutrophils as supplementation with exogenous ATP or NMN was able to induce NETosis in PMA stimulated cord blood neutrophils.

5.5 Conclusion

In agreement with the literature, this chapter finds that lytic NETosis and the oxidative burst is indeed dependent on glycolysis, which is fuelled specifically by exogenous glucose although the oxidative burst can be partially sustained by mobilisation of glycogen stores. Additionally, this chapter finds a strong oxidative burst can occur independently of NETosis showing that this function of neutrophils has more complex requirements. The production of ATP from rapid aerobic glycolysis is one of these additional requirements and the ability to produce enough ATP through aerobic glycolysis is the limiting factor preventing NET formation in cord blood neutrophils. However, the factors resulting in reduced ATP production from aerobic glycolysis requires further exploration. These findings might provide valuable insight into the mechanisms behind the loss of neutrophil function seen in sepsis and could provide a basis for preventative treatments in neonates at severe risk of infection and sepsis. To confirm the applicability of these findings further work needs to be conducted exploring if similar results are seen in response to other stimuli and other types of NETosis associated with pathogen encounter.

Chapter 6

Discussion

6 Discussion

This thesis describes the relatively understudied metabolic phenotype of neonatal immune cells, especially naïve T cells and neutrophils, and explores how differential metabolic activity might explain the distinct functional characteristics of neonatal immunity. Over the past two decades a large and growing body of literature has sprung up to describe the metabolic phenotype of immune cells which has delivered a keen appreciation of how metabolic function is an underwriting force, defining cell fate and function in health and disease (O'Neill et al., 2016; Palsson-McDermott and O'Neill, 2020; Shyer et al., 2020; Bittner et al., 2023). Very early experiments demonstrated a strong demand for glucose in activated macrophages and T cells as well as demonstrating a role for metabolites in immune cell function (Wang et al., 1976; Hamilton et al., 1986; Newsholme et al., 1986). More recent work has revealed how, in addition to ATP generation, metabolic reprogramming provides the molecular building blocks needed for proliferation, which is largely sourced from glutamine and glucose (Hosios et al., 2016; Ma et al., 2017). Other experiments began to demonstrate that metabolism not only fuels the energetic and anabolic demand required for immune responses but also has a role in governing the functional phenotype and differentiation path of immune cells (Pearce et al., 2009; Chang et al., 2013; Gubser et al., 2013; Wang et al., 2018). Metabolic enzymes regulate the transcription and translation of cytokines (Chang et al., 2013; Peng et al., 2016). Additionally, cell signalling, and transcription factors are modulated through metabolites, enzymes, and their products (Sinclair et al., 2013; De Rosa et al., 2015; Ho et al., 2015). More recently still, innovative work has begun to unravel the links between metabolism and epigenetic regulation of phenotype and newly developed advanced machine learning algorithms are capable of predicting phenotype and function from metabolic data (Matias et al., 2021; Puleston et al., 2021; Mocholi et al., 2023). As there is a wealth of evidence demonstrating the central role of metabolism in defining cell function, it is a candidate ripe for understanding the numerous differences reported between adult and neonatal immune cells, where metabolic function is highly understudied (Holm et al., 2021).

Other initial considerations leading to the hypothesis that metabolic function might differ in neonates came from the understanding that mounting an immune response is an extremely metabolically demanding undertaking. This protective trade-off is potentially more manageable in adults that no longer need to fuel rapid and energetically costly growth however, balancing the energetic needs of defence and growth might be more complicated in the early stages of life (Scrimshaw, 1977; Bresnahan and Tanumihardjo, 2014). To fill the gap in the first stages of life, passive immunity from maternal antibodies, passed across the placenta and via breast milk, provides lower energy cost as pathogen clearance which can be achieved more quickly by antibody neutralisation, classical complement activation and other antibody mediated mechanisms of innate immunity (Niewiesk, 2015; Cinicola et al., 2021; Demers-Mathieu, 2023). Additionally, differences in reported blood plasma metabolites in neonates, such as glucose and pyruvate, might contribute to the distinct immune phenotype observed in neonates (Trindade et al., 2011). For this thesis, umbilical cord blood, from term elective caesarean sections, was used as a ready and accessible source of immune cells, representative of the neonate, especially at the time of birth, in order to study their immunometabolic features. Vaginal delivery can have significant impacts on neonatal immune cell function and umbilical cord blood is only representative of the immune function at the time of birth whilst the neonatal period 28 day timespan in which considerable developments in neonatal immunity occurs (Thornton et al., 2003; Lawrence et al., 2017; Olin et al., 2018).

Chapters 3 and 4 of this thesis were centred around CD4+ T cells and provided the first detailed examination of their metabolic characteristics in comparison with adults, ex vivo and over the first days of activation. This work showed that ex vivo umbilical cord blood naïve CD4+ T cells were more energetically active than their adult counterparts and demonstrate a greater metabolic switch immediately on activation which was accompanied by increased amino acid stabilised mTOR signalling. These chapters also show that the metabolic state of umbilical cord blood

CD4+ T cells post activation, is not static in comparison with adults. By 16 hours after first activation, with anti CD3/28, oxidative metabolism became roughly comparable with adults with glycolytic function relatively decreased by 48 hours, umbilical cord blood T cells were more glycolytic but less oxidative than adults. No difference was seen in the surface expression of T cell receptor (TCR) associated stimulatory CD3 or co-stimulatory CD28. Whether the same increased glycolytic reprogramming is seen with more natural TCR ligand induced activation still needs to be determined. However, TCR binding strength is modulated by the micro-RNA-118 which is highly expressed in neonatal T cells and work by Jones et al. has shown that glycolytic reprogramming is dependent on TCR binding strength, together suggesting that stronger glycolytic reprogramming may be seen in neonates by TCR induced activation (Li et al., 2007; Yu et al., 2016; Jones et al., 2017). Increased aerobic glycolysis on activation of cord blood naïve CD4+ T cells, observed in chapter 1, might also explain increased store operated calcium entry (SOCE), reported elsewhere, as calcium flux is dependent on the glycolytic metabolite phosphoenolpyruvate (Palin et al., 2013; Ho et al., 2015; Schmiedeberg et al., 2016). Further evidence also suggests that SOCE might represent an early metabolic cell cycle checkpoint controlling the exit of quiescence through effects on glycolytic and oxidative metabolism, making it an essential pathway for T cell activation and ripe for further investigation in neonates which provide a natural model of enhanced SOCE (Klein-Hessling et al., 2017; Vaeth et al., 2017). A better understanding of how increased SOCE can be induced could have wider applications, such as in cell mediated cancer treatments where both insufficient and prolonged SOCE are associated with poor T cell function and tumour clearance (Shao et al., 2022). However, despite initial increased SOCE, neonates show reduced nuclear translocation and subsequent transcription by nuclear factor of activated T cells (NFAT) (Schmiedeberg et al., 2016) likely explaining the reduced expression of IL-2 seen at 16 hours post activation in chapter 3. The additional mechanisms involved in, preventing NFAT translocation and transcription, are not yet clear and further research is required to understand this mechanism as it likely plays a central role in defining early neonatal T cell responses. One possible explanation for this dichotomy, between early and late activation strength, is the need to control a promiscuous TCR that has strong affinity for MHC presenting self-peptide (Dong et al.,

2017). Other controlling mechanisms such as up regulation of CTLA-4, a competitive inhibitor of co-stimulatory CD28, is not seen in neonates which may lead to increased T cell proliferation (Dietz et al., 2023). Neonatal T cells have been observed to express relatively high levels on FOXP3 on activation leading to the suggestion that induction of regulatory T cells may be a programmed feature in early life to limit over exuberant T cell responses (Thornton et al., 2004; Wang et al., 2010). Production of Tregs, in the first days of life, is also required for early seeding of the periphery with these peripheral Tregs responding to gut derived microbial antigens providing systemic control of related immune responses during early microbial colonisation (Li et al., 2020). Similarly to findings reported here on CD4+ T cells, greater glycolysis is thought to drive rapid expansion and terminal differentiation of murine neonatal CD8+ T cells (Tabilas et al., 2019). However, neonatal CD8+ T cells are less cytotoxic and show reduced expression of genes associated with CD8+ effector related transcription factors, rather displaying an innate like phenotype with many similarities to neutrophils (Galindo-Albarran et al., 2016; Tabilas et al., 2019). Detailed time course proteomic studies, such as those conducted in adult mice, should be conducted to provide a broader understanding of the differences in early activation of neonatal T cells. Such data could provide detailed natural models of how T cell activation can be modulated which could prove useful in diseases settings such as auto immunity (Tan et al., 2017; Howden et al., 2019). Whilst most metabolic studies (including this thesis) focus on pathways such as glycolysis, glutaminolysis and oxidative phosphorylation (including this thesis) large scale proteomic analysis has highlighted the need to broaden the scope of metabolic analysis by demonstrating that other metabolic pathways such as one carbon metabolism are among the most upregulated in early activation (Ron-Harel et al., 2016).

One carbon metabolism is associated with mitochondrial function which in turn is an important factor for memory T cell differentiation (Raud et al., 2018; Corrado and Pearce, 2022). Specifically, fatty acid oxidation by the mitochondria appears to be essential for memory formation and mitochondrial diseases and mutations in carnitine palmitoyl transferase 1A are associated with recurrent infection and poor

vaccine protection (Edmonds et al., 2002; Pearce et al., 2009; Gessner et al., 2013; Kapniciz et al., 2018). Generation of lasting memory T cells is impaired in early life, which has important implications for designing vaccination strategies for neonates and infants (Rudd et al., 2013; Pieren et al., 2022). This thesis shows greater reliance of umbilical cord blood CD4+ T cells on glycolysis, matched in the literature for CD8+ T cells, which is suggested to impair memory formation and thus might provide a target for therapeutic intervention to increase vaccine efficacy which is reliant on formation of long-term memory cells (Tabilas et al., 2019). To date, the exact mechanisms leading to the differentiation of memory T cells is not well understood with competing ideas of how this is achieved. Some have proposed asymmetric division as the underlying mechanism whilst others have highlighted the role of mitochondrial succinate dehydrogenase and orotate in memory formation (Arsenio et al., 2015; Scherer et al., 2023). Additionally, a role for epigenetic remodelling has been demonstrated in memory T cell formation. High acetate production from glucose metabolism in the effector stages of activation encourages acetylation of histones increasing accessibility and translation whilst glutamine metabolism to αKG reduces the activity of DNA methyltransferase both of which support memory differentiation and function (Araki et al., 2008; Youngblood et al., 2017). Given the time of life specific impaired memory formation in neonates, umbilical cord blood T cells might provide a very useful natural model for further elucidating the mechanisms that govern long lasting immune memory in humans.

Alongside impaired memory formation studies have suggested that neonatal naïve CD4+ T cells are poor IFN-γ producers instead favouring the formation of type 2 cytokines such as IL-4 and IL-13 and some have gone as far as describing them as defective or immature T cells (Webster et al., 2007; Hebel et al., 2014; Fike et al., 2019; Razzaghian et al., 2021). However, as more evidence has emerged demonstrating T cell responses in human neonates have time of life specific adaptations, there have been recent calls to reconsider this paradigm (Rudd, 2020; Semmes et al., 2021). Data from this thesis, does not provide strong evidence in favour of previously reported Th2 skewing, rather adult comparable production of

IFNγ were found in some RPMI ex vivo cultures whilst the use of physiologically relevant media, with comparatively higher concentrations of calcium, saw greater IFN-γ production by umbilical cord blood CD4+ T cells. Furthermore, little evidence of Th2 skewing could be seen in the circulating memory T cell population or in the production of type 2 cytokines apart from IL-13. However, assessing whether neonatal T cells showed any defects in the ability to differentiate into classically defined T helper subsets or a detailed analysis of their function was beyond the scope of this thesis which focused on the first 48 hours of activation which is considerably before the time T cells are thought to reach peak effector function (Williams and Bevan, 2007). A more prominent cytokine feature at these earlier stages of activation and division is marked by decreased IL-2 and increased IL-10 seen in culture supernatant at 16, 24 and 48 hours. These two cytokines have opposing roles during activation with IL-2 pressing on the accelerator and IL-10 applying the break. Decreased IL-2 might be explained by reduced nuclear translocation of NFAT but the mechanisms behind increased IL-10 present more of a mystery although there is some evidence that mitochondrial complex II has some important roles in IL-10 production (Nastasi et al., 2021). The purpose of increased IL-10 production might be yet another mechanism for controlling neonatal T cell function (Jankovic et al., 2010; Tao et al., 2011; Ng et al., 2013).

It is also worth considering the wider effects that the altered cytokine profile of neonates may have. As part of its role as general regulator of inflammation, IL-10 inhibits glycolysis in M1 macrophages thereby preferentially selecting M2 macrophages which have a central role in tissue remodelling and homeostasis (Duffield et al., 2005; Brancato and Albina, 2011; Dowling et al., 2021; Miki et al., 2021). Increased CXCL8 secretion, reported here and elsewhere, likely results in the recruitment of more neutrophils (Gibbons et al., 2014) which are broadly defective in pathogen clearing functions raising the obvious question of what function does this serve. In chapter 5, this thesis reports an intermediate mature like phenotype with lower CD16 and CD10 expression not found in adults. Whether this population is attracted by CXCL8 secreted from T cells or has some non-immunological role to play,

such as tissue regeneration and inflammation resolution, is yet to be determined but provides an inviting target for future research (Jones et al., 2016). Intriguingly, neonatal CD4+ T cells also have some role to play in tissue regeneration not matched by adults, as demonstrated by their role in regeneration of the neonatal heart (Bae et al., 2019; Li et al., 2019a; Dolejsi et al., 2022). Allogenic transfer of umbilical cord blood T cells could also prove useful in cancer therapies. Umbilical cord blood transplantation for treatment of lymphopenia induced by chemotherapy, more rapidly reconstitutes the T cells compartment in comparison to bone marrow transplants and provide more effective anti-tumour protection without the need for stringent tissue matching (Lee et al., 2011; Hiwarkar et al., 2015; Hiwarkar et al., 2017). Furthermore, umbilical cord blood or cord blood plasma transfusions are gaining attention as a possible new regenerative therapy as there is some evidence that they have the potential to reduce or reverse the characteristics of ageing and reverse tissue damage (Yang et al., 2010; Cao et al., 2017; Lee et al., 2019). This thesis began to explore the other potential roles of T cells in the neonate through the use of an angiogenesis cytokine panel, but few conclusive results were obtained and further, more detailed studies are required to assess the potential non-classical roles of umbilical cord blood CD4+ T cells.

This thesis also investigates the role of metabolite availability in culture, demonstrating how in vitro culture using physiologically relevant media changes the activation phenotype of naïve CD4+ T cells compared to culture in conventional RPMI media. Chapter 4 demonstrates that use of physiologically relevant media results in significant changes in the expression of cell surface receptors, cytokine production, cell proliferation and cellular metabolism, for both adult and umbilical cord blood naïve CD4+ T cells. This work raises important questions about in vitro models of T cell activation which are heavily relied on in the human context but mostly carried out in non-physiologically relevant media.

Strong evidence in the literature demonstrates that environmental metabolites possess immunomodulatory effects (Park et al., 2022; Soriano-Baguet and Brenner,

2023). For example, glucose is a well-known requirement for T cell activation, supporting growth and effector functions (Jacobs et al., 2008; Ma et al., 2017). Other metabolites, including amino acids and carbohydrate metabolites (besides glucose), not present in conventional culture media, also have immunomodulatory effects. T cell exhaustion can be induced by kynurenine metabolism whilst a-ketoglutarate metabolism is linked with impaired Treg function (Pour et al., 2019; Matias et al., 2021). Data from this thesis, and the wider literature, advocate for considering how the culture media conditions used should be adjusted to better model the system under investigation. Chapter 4 showcases that neonatal CD4+ T cells are capable INF-γ producers under more relevant media conditions whilst others have demonstrated how T cell metabolic plasticity enable utilisation of extracellular lactate in the tumour microenvironment to overcome glucose restriction (Qiu et al., 2019; Wenes et al., 2022). Adding to this, other researchers have elucidated roles for L-arginine and succinate in T cell mediated clearance or persistence of tumours, respectively (Geiger et al., 2016; Gudgeon et al., 2022). The recent move of T cell culture into the clinical setting, as the number of T cell based therapies continues to grow, raises some important questions about what culture media is best and how media can be tailored to achieve desired outcomes (MacPherson et al., 2022). Culture media, can affect the production and expression of cytokines, cell surface receptors, exhaustion markers and proliferation, all of which could be specifically optimised to meet the demands of the product (Leney-Greene et al., 2020; MacPherson et al., 2022). For example, differentiating T memory stem cells has been a long term goal for CAR T cell therapy and recent findings suggest this could be achieved through metabolic manipulation of one carbon metabolism (Rafiq et al., 2020; Lopez-Cantillo et al., 2022; Cheng et al., 2023). Overall, data presented here, and in the literature, demonstrate the need for careful thought about the effects of metabolites in T cell culture media.

Lastly, chapter 5 moved away from T cells and adaptive immunity to explore the innate immune response through studying umbilical cord blood neutrophils. Here, umbilical cord blood neutrophils were characterised by high frequencies of intermediate mature cells with lower CD10 and CD16 expression. Umbilical cord

blood neutrophils failed to produce neutrophil extracellular traps (NET)s in response to phorbol 12-myristate 13-acetate (PMA) stimulation, because of reduced ability to regenerate NAD+ and rapidly produce ATP via aerobic glycolysis. More broadly in the literature, the functional ability of umbilical cord blood neutrophils are reported to be deficient compared to adults, potentially leaving the neonates more vulnerable to infection. However, in a perplexing dichotomy of physiology and function neutrophil numbers rapidly rise in the weeks leading up to birth suggesting that they are required in the early days of life despite their diminished function (Erdman et al., 1982; Carr et al., 2010; Peterson et al., 2021).

One possible explanation is that this is a precise and carefully evolved time of life specific impairment of activation. The birthing process is a highly traumatic procedure both physically and physiologically resulting in inflammation in the tissues of the neonate (Kiilerich et al., 2021; Kyathanahalli et al., 2022). Excessive inflammation can be seriously harmful, and neutrophils act as rapid responders to inflammation, secreting reactive oxygen species, proteolytic enzymes, NETs and cytokines all of which act as positive reinforcers of inflammation (de Oliveira et al., 2016; Herrero-Cervera et al., 2022). As such, selective impairment of these abundant rapid responders at the time of birth may be a protective mechanism to limit tissue damage in response to labour induced inflammation. Furthermore, birth represents a transition from an antigen poor to an antigen rich environment. As seen here and elsewhere neonatal T cells display a strong immune suppressive phenotype with increased expression of IL-10 and FOXP3, suggesting that controlling inflammation is an important function in the early days of life (Thornton et al., 2004). Furthermore, organs of the body are only colonised by regulatory T cells in the days after birth in response to microbial colonisation of the gut (Li et al., 2020). Thus, in the first days of life, before Treg colonisation occurs, neonates may be highly vulnerable to systemic inflammation in response to commensal bacteria. Together, these factors make a strong evolutionary case for limited neutrophil function in the early neonatal period. Indeed, many of the impaired neutrophil functions of neonates are restored in the days and weeks following birth (Lawrence et al., 2017). Although neonatal neutrophil

dysfunction is perhaps a necessary adaptation at the time of birth, insights gained from neutrophil dysfunction in this setting can be usefully extrapolated to improve our understanding of neutrophil function in pathology. Neutrophils are critical mediators in the pathology of rheumatoid arthritis and sepsis both of which represent a social and monetary cost to society (Birnbaum et al., 2010; Wright et al., 2014; Shen et al., 2017). This thesis demonstrates that metabolic pathways can be targeted to modulate neutrophil function providing molecular targets for drug development to combat neutrophil related diseases.

In summary, this thesis sought to answer two questions. Firstly, are there significant immunometabolic differences between adults and neonates and secondly, if there are immunometabolic differences can they explain the functional differences between cells of the adult and neonatal immune systems. To this end, naïve CD4+ T cells, of the adaptive immune system and neutrophils of the innate immune system were isolated from adult peripheral blood and umbilical cord blood and interrogated experimentally ex vivo and in vitro using a range of methods and assays. The results show distinctly different phenotypes and metabolic requirements for immune function in neonates that differ temporally and by cell type. Broadly, naïve CD4+ T cells were more glycolytic but produced more immunoregulatory cytokines whilst neutrophils were less glycolytic and failed to produce NETs as a result. For the first time, these results characterise the metabolic phenotype of neonatal human naïve CD4+ T cells throughout the first days of activation providing a basis for further study in the field and showcase how and why metabolic function should be considered in future studies of neonatal T cell immunity. This work also provided a mechanism by which control of NETosis and loss of this function could be understood in the neonatal setting. Although a useful model, providing valuable insight into neonatal immune function with wider implications throughout immunology, these experiments can only approximate organism level biology and immune function and might not be representative of later neonatal developmental stages. Future research should take advantage of increasingly powerful flow cytometry tools and single cell sequencing techniques to study neonatal immunity in vivo and throughout a broader timespan of

neonatal development. Furthermore, central carbon metabolism of glucose was the primary metabolic pathway studied in this thesis but increasingly, other less well studied pathways are proving just as important to immune cell function thus warrant further investigation in the neonatal setting.

Adkins, B., and Du, R.Q. (1998). Newborn mice develop balanced Th1/Th2 primary effector responses in vivo but are biased to Th2 secondary responses. *Journal of Immunology* 160(9)**,** 4217-4224.

Ahl, P.J., Hopkins, R.A., Xiang, W.W., Au, B.J., Kaliaperumal, N., Fairhurst, A.M., et al. (2020). Met-Flow, a strategy for single-cell metabolic analysis highlights dynamic changes in immune subpopulations. *Communications Biology* 3(1). doi: 10.1038/s42003-020-1027-9.

Al-Hertani, W., Yan, S.R., Byers, D.M., and Bortolussi, R. (2007). Human newborn polymorphonuclear neutrophils exhibit decreased levels of MyD88 and attenuated p38 phosphorylation in response to lipopolysaccharide. *Clinical and Investigative Medicine* 30(2)**,** E44-E53.

Al-Khami, A.A., Zheng, L.Q., Del Valle, L., Hossain, F., Wyczechowska, D., Zabaleta, J., et al. (2017). Exogenous lipid uptake induces metabolic and functional reprogramming of tumor-associated myeloid-derived suppressor cells. *Oncoimmunology* 6(10). doi: 10.1080/2162402x.2017.1344804.

Amini, P., Stojkov, D., Felser, A., Jackson, C.B., Courage, C., Schaller, A., et al. (2018). Neutrophil extracellular trap formation requires OPA1-dependent glycolytic ATP production. *Nature Communications* 9. doi: 10.1038/s41467-018-05387-y.

Angelidou, A., Diray-Arce, J., Conti, M.G., Netea, M.G., Blok, B.A., Liu, M., et al. (2021). Human Newborn Monocytes Demonstrate Distinct BCG-Induced Primary and Trained Innate Cytokine Production and Metabolic Activation In Vitro. *Frontiers in Immunology* 12. doi: 10.3389/fimmu.2021.674334.

Angiari, S., Runtsch, M.C., Sutton, C.E., Palsson-McDermott, E.M., Kelly, B., Rana, N., et al. (2020). Pharmacological Activation of Pyruvate Kinase M2 Inhibits CD4(+) T Cell Pathogenicity and Suppresses Autoimmunity. *Cell Metabolism* 31(2)**,** 391-+. doi: 10.1016/j.cmet.2019.10.015.

Annunziato, F., Cosmi, L., Liotta, F., Maggi, E., and Romagnani, S. (2012). Defining the human T helper 17 cell phenotype. *Trends in Immunology* 33(10)**,** 505-512. doi: 10.1016/j.it.2012.05.004.

Aquilano, G., Capretti, M.G., Nanni, F., Corvaglia, L., Aceti, A., Gabrielli, L., et al. (2016). Altered Intracellular ATP Production by Activated CD4+T-Cells in Very Preterm Infants. *Journal of Immunology Research*. doi: 10.1155/2016/8374328.

Araki, Y., Fann, M., Wersto, R., and Weng, N.P. (2008). Histone acetylation facilitates rapid and robust memory CD8 T cell response through differential expression of effector molecules (eomesodermin and its targets: perforin and granzyme B). *Journal of Immunology* 180(12)**,** 8102-8108. doi: 10.4049/jimmunol.180.12.8102.

Arraes, S.M.A., Freitas, M.S., da Silva, S.V., Neto, H.A.D., Alves, J.C., Martins, M.A., et al. (2006). Impaired neutrophil chemotaxis in sepsis associates with GRK expression and inhibition of actin assembly and tyrosine phosphorylation. *Blood* 108(9)**,** 2906-2913. doi: 10.1182/blood-2006-05-024638.

Arsenio, J., Metz, P.J., and Chang, J.T. (2015). Asymmetric Cell Division in T Lymphocyte Fate Diversification. *Trends in Immunology* 36(11)**,** 670-683. doi: 10.1016/j.it.2015.09.004.

Awasthi, D., Nagarkoti, S., Sadaf, S., Chandra, T., Kumar, S., and Dikshit, M. (2019). Glycolysis dependent lactate formation in neutrophils: A metabolic link between NOX-dependent and independent NETosis. *Biochimica Et Biophysica Acta-Molecular Basis of Disease* 1865(12). doi: 10.1016/j.bbadis.2019.165542.

Azevedo, E.P., Rochael, N.C., Guimaraes-Costa, A.B., de Souza-Vieira, T.S., Ganilho, J., Saraiva, E.M., et al. (2015). A Metabolic Shift toward Pentose Phosphate Pathway Is Necessary for Amyloid Fibril-and Phorbol 12-Myristate 13-Acetate-induced Neutrophil Extracellular Trap (NET) Formation. *Journal of Biological Chemistry* 290(36)**,** 22174-22183. doi: 10.1074/jbc.M115.640094.

Bae, S.H., Jo, A., Park, J.H., Lim, C.W., Choi, Y., Oh, J., et al. (2019). Bioassay for monitoring the anti-aging effect of cord blood treatment. *Theranostics* 9(1)**,** 1-10. doi: 10.7150/thno.30422.

Bailis, W., Shyer, J.A., Zhao, J., Canaveras, J.C.G., Al Khazal, F.J., Qu, R.H., et al. (2019). Distinct modes of mitochondrial metabolism uncouple T cell differentiation and function. *Nature* 571(7765)**,** 403-+. doi: 10.1038/s41586-019-1311-3.

Bajwa, G., DeBerardinis, R.J., Shao, B., Hall, B., Farrar, J.D., and Gill, M.A. (2016). Cutting Edge: Critical Role of Glycolysis in Human Plasmacytoid Dendritic Cell Antiviral Responses. *Journal of Immunology* 196(5)**,** 2004-2009. doi: 10.4049/jimmunol.1501557.

Bao, Y., Ledderose, C., Graf, A.F., Brix, B., Birsak, T., Lee, A., et al. (2015). mTOR and differential activation of mitochondria orchestrate neutrophil chemotaxis. *Journal of Cell Biology* 210(7)**,** 1153-1164. doi: 10.1083/jcb.201503066.

Baruah, S., Murthy, S., Keck, K., Galvan, I., Prichard, A., Allen, L.A.H., et al. (2019). TREM-1 regulates neutrophil chemotaxis by promoting NOX-dependent superoxide production. *Journal of Leukocyte Biology* 105(6)**,** 1195-1207. doi: 10.1002/jlb.3vma0918-375r.

Basha, S., Surendran, N., and Pichichero, M. (2014). Immune responses in neonates. *Expert Review of Clinical Immunology* 10(9)**,** 1171-1184. doi: 10.1586/1744666x.2014.942288.

Basit, F., Mathan, T., Sancho, D., and de Vries, I.J.M. (2018). Human Dendritic Cell Subsets Undergo Distinct Metabolic Reprogramming for Immune Response. *Frontiers in Immunology* 9. doi: 10.3389/fimmu.2018.02489.

Bauer, M., Gerlach, H., Vogelmann, T., Preissing, F., Stiefel, J., and Adam, D. (2020). Mortality in sepsis and septic shock in Europe, North America and Australia between 2009 and 2019-results from a systematic review and meta-analysis. *Critical Care* 24(1). doi: 10.1186/s13054-020-02950-2.

Baumann, T., Dunkel, A., Schmid, C., Schmitt, S., Hiltensperger, M., Lohr, K., et al. (2020). Regulatory myeloid cells paralyze T cells through cell-cell transfer of the metabolite methylglyoxal. *Nature Immunology* 21(5)**,** 555-+. doi: 10.1038/s41590-020-0666-9.

Beier, U.H., Angelin, A., Akimova, T., Wang, L.Q., Liu, Y.J., Xiao, H.Y., et al. (2015). Essential role of mitochondrial energy metabolism in Foxp3(+) T-regulatory

cell function and allograft survival. *Faseb Journal* 29(6), 2315-2326. doi: 10.1096/fj.14-268409.

Bennstein, S.B., Scherenschlich, N., Weinhold, S., Manser, A.R., Noll, A., Raba, K., et al. Transcriptional and functional characterization of neonatal circulating ILCs. *Stem Cells Translational Medicine*. doi: 10.1002/sctm.20-0300.

Bensinger, S.J., Bradley, M.N., Joseph, S.B., Zelcer, N., Janssen, E.M., Hausner, M.A., et al. (2008). LXR signaling couples sterol metabolism to proliferation in the acquired immune response. *Cell* 134(1), 97-111. doi: 10.1016/j.cell.2008.04.052.

Berger, C., Jensen, M.C., Lansdorp, P.M., Gough, M., Elliott, C., and Riddell, S.R. (2008). Adoptive transfer of effector CD8(+) T cells derived from central memory cells establishes persistent T cell memory in primates. *Journal of Clinical Investigation* 118(1), 294-305. doi: 10.1172/jci32103.

Bermick, J.R., Issuree, P., denDekker, A., Gallagher, K.A., Santillan, D., Kunkel, S., et al. (2022). Differences in H3K4me3 and chromatin accessibility contribute to altered T-cell receptor signaling in neonatal naive CD4 T cells. *Immunology and Cell Biology* 100(7), 562-579. doi: 10.1111/imcb.12561.

Bermick, J.R., Lambrecht, N.J., denDekker, A.D., Kunkel, S.L., Lukacs, N.W., Hogaboam, C.M., et al. (2016). Neonatal monocytes exhibit a unique histone modification landscape. *Clinical Epigenetics* 8. doi: 10.1186/s13148-016-0265-7.

Birnbaum, H., Pike, C., Kaufman, R., Marynchenko, M., Kidolezi, Y., and Cifaldi, M. (2010). Societal cost of rheumatoid arthritis patients in the US. *Current Medical Research and Opinion* 26(1), 77-90. doi: 10.1185/03007990903422307.

Bittner, S., Pape, K., Klotz, L., and Zipp, F. (2023). Implications of immunometabolism for smouldering MS pathology and therapy. *Nature Reviews Neurology* 19(8), 477-488. doi: 10.1038/s41582-023-00839-6.

Blair, P.A., Norena, L.Y., Flores-Borja, F., Rawlings, D.J., Isenberg, D.A., Ehrenstein, M.R., et al. (2010). CD19(+)CD24(hi)CD38(hi) B Cells Exhibit Regulatory Capacity in Healthy Individuals but Are Functionally Impaired in Systemic Lupus Erythematosus Patients. *Immunity* 32(1), 129-140. doi: 10.1016/j.immuni.2009.11.009.

Borras, F.E., Matthews, N.C., Lowdell, M.W., and Navarrete, C.V. (2001). Identification of both myeloid CD11c(+) and lymphoid CD11c(-) dendritic cell subsets in cord blood. *British Journal of Haematology* 113(4), 925-931. doi: 10.1046/j.1365-2141.2001.02840.x.

Borregaard, N. (2010). Neutrophils, from Marrow to Microbes. *Immunity* 33(5), 657-670. doi: 10.1016/j.immuni.2010.11.011.

Borregaard, N., and Herlin, T. (1982). ENERGY-METABOLISM OF HUMAN-NEUTROPHILS DURING PHAGOCYTOSIS. *Journal of Clinical Investigation* 70(3), 550-557. doi: 10.1172/jci110647.

Borsellino, G., Kleinewietfeld, M., Di Mitri, D., Sternjak, A., Diamantini, A., Giometto, R., et al. (2007). Expression of ectonucleotidase CD39 by Foxp3(+) Treg cells: hydrolysis of extracellular ATP and immune suppression. *Blood* 110(4), 1225-1232. doi: 10.1182/blood-2006-12-064527.

Bradford, S.D., Witt, M.R., Povroznik, J.M., and Robinson, C.M. (2023). Interleukin-27 impairs BCG antigen clearance and T cell stimulatory potential by neonatal

dendritic cells. *Current Research in Microbial Sciences* 4. doi: 10.1016/j.crmicr.2022.100176.

Brancato, S.K., and Albina, J.E. (2011). Wound Macrophages as Key Regulators of Repair Origin, Phenotype, and Function. *American Journal of Pathology* 178(1)**,** 19-25. doi: 10.1016/j.ajpath.2010.08.003.

Bresnahan, K.A., and Tanumihardjo, S.A. (2014). Undernutrition, the Acute Phase Response to Infection, and Its Effects on Micronutrient Status Indicators. *Advances in Nutrition* 5(6)**,** 702-711. doi: 10.3945/an.114.006361.

Brinkmann, V., Reichard, U., Goosmann, C., Fauler, B., Uhlemann, Y., Weiss, D.S., et al. (2004). Neutrophil extracellular traps kill bacteria. *Science* 303(5663)**,** 1532-1535. doi: 10.1126/science.1092385.

Britt, E.C., Lika, J., Giese, M.A., Schoen, T.J., Seim, G.L., Huang, Z.P., et al. (2022). Switching to the cyclic pentose phosphate pathway powers the oxidative burst in activated neutrophils. *Nature Metabolism* 4(3)**,** 389-+. doi: 10.1038/s42255-022-00550-8.

Brook, B., Harbeson, D., Ben-Othman, R., Viemann, D., and Kollmann, T.R. (2017). Newborn susceptibility to infection vs. disease depends on complex in vivo interactions of host and pathogen. *Seminars in Immunopathology* 39(6)**,** 615-625. doi: 10.1007/s00281-017-0651-z.

Brustle, A., Heink, S., Huber, M., Rosenplanter, C., Stadelmann, C., Yu, P., et al. (2007). The development of inflammatory T-H-17 cells requires interferon-regulatory factor 4. *Nature Immunology* 8(9)**,** 958-966. doi: 10.1038/ni1500.

Buchmann, K. (2014). Evolution of innate immunity: clues from invertebrates via fish to mammals. *Frontiers in Immunology* 5. doi: 10.3389/fimmu.2014.00459.

Buck, M.D., O'Sullivan, D., Geltink, R.I.K., Curtis, J.D., Chang, C.H., Sanin, D.E., et al. (2016). Mitochondrial Dynamics Controls T Cell Fate through Metabolic Programming. *Cell* 166(1)**,** 63-76. doi: 10.1016/j.cell.2016.05.035.

Butte, N.F. (2005). Energy requirements of infants. *Public Health Nutrition* 8(7A)**,** 953-967. doi: 10.1079/phn2005790.

Campbell, D.E., Boyle, R.J., Thornton, C.A., and Prescott, S.L. (2015). Mechanisms of allergic disease - environmental and genetic determinants for the development of allergy. *Clinical and Experimental Allergy* 45(5)**,** 844-858. doi: 10.1111/cea.12531.

Cano-Gamez, E., Soskic, B., Roumeliotis, T.I., So, E., Smyth, D.J., Baldrighi, M., et al. (2020). Single-cell transcriptomics identifies an effectorness gradient shaping the response of CD4(+) T cells to cytokines. *Nature Communications* 11(1). doi: 10.1038/s41467-020-15543-y.

Cante-Barrett, K., Mendes, R.D., Li, Y.L., Vroegindeweij, E., Pike-Overzet, K., Wabeke, T., et al. (2017). Loss of CD44(dim) Expression from Early Progenitor Cells Marks T-Cell Lineage Commitment in the Human Thymus. *Frontiers in Immunology* 8. doi: 10.3389/fimmu.2017.00032.

Canto, E., Rodriguez-Sanchez, J.L., and Vidal, S. (2005). Naive CD4+ cells from cord blood can generate competent Th effector cells. *Transplantation* 80(6)**,** 850-858. doi: 10.1097/01.tp.0000174135.32068.65.

Cantor, J.R. (2019). The Rise of Physiologic Media. *Trends in Cell Biology* 29(11)**,** 854-861. doi: 10.1016/j.tcb.2019.08.009.

Cantor, J.R., Abu-Remaileh, M., Kanarek, N., Freinkman, E., Gao, X., Louissaint, A., Jr., et al. (2017). Physiologic Medium Rewires Cellular Metabolism and Reveals Uric Acid as an Endogenous Inhibitor of UMP Synthase. *Cell* 169(2)**,** 258-272. doi: 10.1016/j.cell.2017.03.023.

Cao, N., Liao, T.L., Liu, J.J., Fan, Z., Zeng, Q., Zhou, J.N., et al. (2017). Clinical-grade human umbilical cord-derived mesenchymal stem cells reverse cognitive aging via improving synaptic plasticity and endogenous neurogenesis. *Cell Death & Disease* 8. doi: 10.1038/cddis.2017.316.

Carr, E.L., Kelman, A., Wu, G.S., Gopaul, R., Senkevitch, E., Aghvanyan, A., et al. (2010). Glutamine Uptake and Metabolism Are Coordinately Regulated by ERK/MAPK during T Lymphocyte Activation. *Journal of Immunology* 185(2)**,** 1037-1044. doi: 10.4049/jimmunol.0903586.

Carr, R., Huizinga, T.W.J., Kleijer, M., and Davies, J.M. (1992). CHANGES IN PLASMA FCRIII DEMONSTRATE INCREASING RECEPTOR PRODUCTION DURING LATE PREGNANCY AND AFTER PRETERM BIRTH. *Pediatric Research* 32(5)**,** 505-508. doi: 10.1203/00006450-199211000-00001.

Carroll, B., Maetzel, D., Maddocks, O.D.K., Otten, G., Ratcliff, M., Smith, G.R., et al. (2016). Control of TSC2-Rheb signaling axis by arginine regulates mTORC1 activity. *Elife* 5. doi: 10.7554/eLife.11058.

Cerny, V., Hrdy, J., Novotna, O., Petrakova, P., Borakova, K., Kolarova, L., et al. (2018). Distinct characteristics of Tregs of newborns of healthy and allergic mothers. *Plos One* 13(11). doi: 10.1371/journal.pone.0207998.

Chang, C.H., Curtis, J.D., Maggi, L.B., Faubert, B., Villarino, A.V., O'Sullivan, D., et al. (2013). Posttranscriptional Control of T Cell Effector Function by Aerobic Glycolysis. *Cell* 153(6)**,** 1239-1251. doi: 10.1016/j.cell.2013.05.016.

Chen, F.M., Tse, J.K.Y., Jin, L.G., Chook, C.Y.B., Leung, F.P., Tse, G., et al. (2022). Type 2 innate immunity drives distinct neonatal immune profile conducive for heart regeneration. *Theranostics* 12(1)**,** 1161-1172. doi: 10.7150/thno.67515.

Chen, L., Cohen, A.C., and Lewis, D.B. (2006). Impaired allogeneic activation and T-helper differentiation of human cord blood naive CD4 T cells. *Biology of Blood and Marrow Transplantation* 12(2)**,** 160-171. doi: 10.1016/j.bbmt.2005.10.027.

Chen, N.X., and Field, E.H. (1995). ENHANCED TYPE-2 AND DIMINISHED TYPE-1 CYTOKINES IN NEONATAL TOLERANCE. *Transplantation* 59(7)**,** 933-941. doi: 10.1097/00007890-199504150-00002.

Cheng, H.C., Qiu, Y.J., Xu, Y., Chen, L., Ma, K.L., Tao, M.Y., et al. (2023). Extracellular acidosis restricts one-carbon metabolism and preserves T cell stemness. *Nature Metabolism* 5(2)**,** 314-+. doi: 10.1038/s42255-022-00730-6.

Cheon, I.S., Son, Y.M., Jiang, L., Goplen, N.P., Kaplan, M.H., Limper, A.H., et al. (2018). Neonatal hyperoxia promotes asthma-like features through IL-33-dependent ILC2 responses. *Journal of Allergy and Clinical Immunology* 142(4)**,** 1100-1112. doi: 10.1016/j.jaci.2017.11.025.

Chi, H. (2012). Regulation and function of mTOR signalling in T cell fate decisions. *Nature Reviews Immunology* 12(5)**,** 325-338. doi: 10.1038/nri3198.

Choi, B.K., Lee, D.Y., Lee, D.G., Kim, Y.H., Kim, S.H., Oh, H.S., et al. (2017). 4-1BB signaling activates glucose and fatty acid metabolism to enhance CD8(+) T cell

proliferation. *Cellular & Molecular Immunology* 14(9), 748-757. doi: 10.1038/cmi.2016.02.

Cinicola, B., Conti, M.G., Terrin, G., Sgrulletti, M., Elfeky, R., Carsetti, R., et al. (2021). The Protective Role of Maternal Immunization in Early Life. *Frontiers in Pediatrics* 9. doi: 10.3389/fped.2021.638871.

Cooper, M.D., and Alder, M.N. (2006). The evolution of adaptive immune systems. *Cell* 124(4), 815-822. doi: 10.1016/j.cell.2006.02.001.

Cordes, T., Wallace, M., Michelucci, A., Divakaruni, A.S., Sapcariu, S.C., Sousa, C., et al. (2016). Immunoresponsive Gene 1 and Itaconate Inhibit Succinate Dehydrogenase to Modulate Intracellular Succinate Levels. *Journal of Biological Chemistry* 291(27), 14274-14284. doi: 10.1074/jbc.M115.685792.

Corrado, M., and Pearce, E.L. (2022). Targeting memory T cell metabolism to improve immunity. *Journal of Clinical Investigation* 132(1). doi: 10.1172/jci148546.

Corripio-Miyar, Y., Hayward, A., Lemon, H., Sweeny, A.R., Bal, X., Kenyon, F., et al. (2022). Functionally distinct T-helper cell phenotypes predict resistance to different types of parasites in a wild mammal. *Scientific Reports* 12(1). doi: 10.1038/s41598-022-07149-9.

Cossarizza, A., Ortolani, C., Paganelli, R., Barbieri, D., Monti, D., Sansoni, P., et al. (1996). CD45 isoforms expression on CD4(+) and CD8(+) T cells throughout life, from newborns to centenarians: Implications for T cell memory. *Mechanisms of Ageing and Development* 86(3), 173-195. doi: 10.1016/0047-6374(95)01691-0.

Covarrubias, A.J., Aksoylar, H.I., and Horng, T. (2015). Control of macrophage metabolism and activation by mTOR and Akt signaling. *Seminars in Immunology* 27(4), 286-296. doi: 10.1016/j.smim.2015.08.001.

Daix, T., Jeannet, R., Padilla, A.C.H., Vignon, P., Feuillard, J., and Francois, B. (2021). Immature granulocytes can help the diagnosis of pulmonary bacterial infections in patients with severe COVID-19 pneumonia. *Journal of Intensive Care* 9(1). doi: 10.1186/s40560-021-00575-3.

Datta, S.R., Dudek, H., Tao, X., Masters, S., Fu, H.A., Gotoh, Y., et al. (1997). Akt phosphorylation of BAD couples survival signals to the cell-intrinsic death machinery. *Cell* 91(2), 231-241. doi: 10.1016/s0092-8674(00)80405-5.

Davies, N.P., Buggins, A.G.S., Snijders, R.J.M., Jenkins, E., Layton, D.M., and Nicolaides, K.H. (1992). BLOOD LEUKOCYTE COUNT IN THE HUMAN FETUS. *Archives of Disease in Childhood-Fetal and Neonatal Edition* 67(4), 399-403. doi: 10.1136/adc.67.4_Spec_No.399.

de Leve, S., Wirsdoerfer, F., and Jendrossek, V. (2019). Targeting the Immunomodulatory CD73/Adenosine System to Improve the Therapeutic Gain of Radiotherapy. *Frontiers in Immunology* 10. doi: 10.3389/fimmu.2019.00698.

de Oliveira, S., Rosowski, E.E., and Huttenlocher, A. (2016). Neutrophil migration in infection and wound repair: going forward in reverse. *Nature Reviews Immunology* 16(6), 378-391. doi: 10.1038/nri.2016.49.

De Rosa, V., Galgani, M., Porcellini, A., Colamatteo, A., Santopaolo, M., Zuchegna, C., et al. (2015). Glycolysis controls the induction of human regulatory T cells by modulating the expression of FOXP3 exon 2 splicing variants. *Nature Immunology* 16(11), 1174-1184. doi: 10.1038/ni.3269.

De Simone, R., Ajmone-Cat, M.A., Pandolfi, M., Bernardo, A., De Nuccio, C., Minghetti, L., et al. (2015). The mitochondrial uncoupling protein-20 is a master regulator of both M1 and M2 microglial responses. *Journal of Neurochemistry* 135(1), 147-156. doi: 10.1111/jnc.13244.

de Souza, A.P.D., de Freitas, D., Fernandes, K.E.A., da Cunha, M.D., Fernandes, J.L.A., Gassen, R.B., et al. (2016). Respiratory syncytial virus induces phosphorylation of mTOR at ser2448 in CD8 T cells from nasal washes of infected infants. *Clinical and Experimental Immunology* 183(2), 248-257. doi: 10.1111/cei.12720.

De Wit, D., Tonon, S., Olislagers, V., Goriely, S., Boutriaux, M., Goldman, M., et al. (2003). Impaired responses to toll-like receptor 4 and toll-like receptor 3 ligands in human cord blood. *Journal of Autoimmunity* 21(3), 277-281. doi: 10.1016/j.jaut.2003.08.003.

Debock, I., and Flamand, V. (2014). Unbalanced neonatal CD4(+) T-cell immunity. *Frontiers in Immunology* 5. doi: 10.3389/fimmu.2014.00393.

Delgoffe, G.M., Kole, T.P., Zheng, Y., Zarek, P.E., Matthews, K.L., Xiao, B., et al. (2009). The mTOR Kinase Differentially Regulates Effector and Regulatory T Cell Lineage Commitment. *Immunity* 30(6), 832-844. doi: 10.1016/j.immuni.2009.04.014.

Delgoffe, G.M., Pollizzi, K.N., Waickman, A.T., Heikamp, E., Meyers, D.J., Horton, M.R., et al. (2011). The kinase mTOR regulates the differentiation of helper T cells through the selective activation of signaling by mTORC1 and mTORC2. *Nature Immunology* 12(4), 295-U117. doi: 10.1038/ni.2005.

Demers-Mathieu, V. (2023). Editorial: Breast milk and passive immunity during the COVID-19 pandemic. *Frontiers in Nutrition* 10. doi: 10.3389/fnut.2023.1155901.

Dennis, P.B., Jaeschke, A., Saitoh, M., Fowler, B., Kozma, S.C., and Thomas, G. (2001). Mammalian TOR: A homeostatic ATP sensor. *Science* 294(5544), 1102-1105. doi: 10.1126/science.1063518.

Denorme, F., Rustad, J.L., Portier, I., Crandell, J.L., de Araujo, C.V., Cody, M.J., et al. (2023). Neutrophil extracellular trap inhibition improves survival in neonatal mouse infectious peritonitis. *Pediatric Research* 93(4), 862-869. doi: 10.1038/s41390-022-02219-0.

Desousa, B.R., Kim, K.K.O., Jones, A.E., Ball, A.B., Hsieh, W.Y., Swain, P., et al. (2023). Calculation of ATP production rates using the Seahorse XF Analyzer. *Embo Reports*. doi: 10.15252/embr.202256380.

Dieterlen, M.T., Bittner, H.B., Klein, S., von Salisch, S., Mittag, A., Tarnok, A., et al. (2012). Assay validation of phosphorylated S6 ribosomal protein for a pharmacodynamic monitoring of mTOR-inhibitors in peripheral human blood. *Cytometry Part B-Clinical Cytometry* 82B(3), 151-157. doi: 10.1002/cyto.b.21005.

Dietz, S., Molnar, K., Riedel, H., Haag, L., Spring, B., Orlikowsky, T.W., et al. (2023). Expression of immune checkpoint molecules on adult and neonatal T-cells. *Immunologic Research* 71(2), 185-196. doi: 10.1007/s12026-022-09340-6.

Dimeloe, S., Gubser, P., Loeliger, J., Frick, C., Develioglu, L., Fischer, M., et al. (2019). Tumor-derived TGF-beta inhibits mitochondrial respiration to suppress IFN-

gamma production by human CD4(+) T cells. *Science Signaling* 12(599). doi: 10.1126/scisignal.aav3334.

Dolejsi, T., Delgobo, M., Schuetz, T., Tortola, L., Heinze, K.G., Hofmann, U., et al. (2022). Adult T-cells impair neonatal cardiac regeneration. *European Heart Journal* 43(28)**,** 2698-+. doi: 10.1093/eurheartj/ehac153.

Dong, M.Q., Artusa, P., Kelly, S.A., Fournier, M., Baldwin, T.A., Mandl, J.N., et al. (2017). Alterations in the Thymic Selection Threshold Skew the Self-Reactivity of the TCR Repertoire in Neonates. *Journal of Immunology* 199(3)**,** 965-973. doi: 10.4049/jimmunol.1602137.

Donnelly, R.P., Loftus, R.M., Keating, S.E., Liou, K.T., Biron, C.A., Gardiner, C.M., et al. (2014). mTORC1-Dependent Metabolic Reprogramming Is a Prerequisite for NK Cell Effector Function. *Journal of Immunology* 193(9)**,** 4477-4484. doi: 10.4049/jimmunol.1401558.

Dowling, J.K., Afzal, R., Gearing, L.J., Cervantes-Silva, M.P., Annett, S., Davis, G.M., et al. (2021). Mitochondrial arginase-2 is essential for IL-10 metabolic reprogramming of inflammatory macrophages. *Nature Communications* 12(1). doi: 10.1038/s41467-021-21617-2.

Dresch, C., Troccoli, G., and Mary, J.Y. (1986). GROWTH FRACTION OF MYELOCYTES IN NORMAL HUMAN GRANULOPOIESIS. *Cell and Tissue Kinetics* 19(1)**,** 11-22. doi: 10.1111/j.1365-2184.1986.tb00711.x.

Dreschers, S., Ohl, K., Lehrke, M., Mollmann, J., Denecke, B., Costa, I., et al. (2019). Impaired cellular energy metabolism in cord blood macrophages contributes to abortive response toward inflammatory threats. *Nature Communications* 10. doi: 10.1038/s41467-019-09359-8.

Dreschers, S., Ohl, K., Schulte, N., Tenbrock, K., and Orlikowsky, T.W. (2020). Impaired functional capacity of polarised neonatal macrophages. *Scientific Reports* 10(1). doi: 10.1038/s41598-019-56928-4.

Duffield, J.S., Forbes, S.J., Constandinou, C.M., Clay, S., Partolina, M., Vuthoori, S., et al. (2005). Selective depletion of macrophages reveals distinct, opposing roles during liver injury and repair. *Journal of Clinical Investigation* 115(1)**,** 56-65. doi: 10.1172/jci200522675.

Duhen, T., Duhen, R., Lanzavecchia, A., Sallusto, F., and Campbell, D.J. (2012). Functionally distinct subsets of human FOXP3(+) Treg cells that phenotypically mirror effector Th cells. *Blood* 119(19)**,** 4430-4440. doi: 10.1182/blood-2011-11-392324.

Dumitru, C.A., Moses, K., Trellakis, S., Lang, S., and Brandau, S. (2012). Neutrophils and granulocytic myeloid-derived suppressor cells: immunophenotyping, cell biology and clinical relevance in human oncology. *Cancer Immunology Immunotherapy* 61(8)**,** 1155-1167. doi: 10.1007/s00262-012-1294-5.

Dupont, A., Heinbockel, L., Brandenburg, K., and Hornef, M.W. (2014). Antimicrobial peptides and the enteric mucus layer act in concert to protect the intestinal mucosa. *Gut Microbes* 5(6)**,** 761-765. doi: 10.4161/19490976.2014.972238.

Duran, R.V., Oppliger, W., Robitaille, A.M., Heiserich, L., Skendaj, R., Gottlieb, E., et al. (2012). Glutaminolysis Activates Rag-mTORC1 Signaling. *Molecular Cell* 47(3)**,** 349-358. doi: 10.1016/j.molcel.2012.05.043.

Eagle, H. (1955a). Nutrition needs of mammalian cells in tissue culture. *Science (New York, N.Y.)* 122(3168)**,** 501-514. doi: 10.1126/science.122.3168.501.

Eagle, H. (1955b). The minimum vitamin requirements of the L and HeLa cells in tissue culture, the production of specific vitamin deficiencies, and their cure. *The Journal of experimental medicine* 102(5)**,** 595-600. doi: 10.1084/jem.102.5.595.

Eagle, H. (1955c). The specific amino acid requirements of a human carcinoma cell (Stain HeLa) in tissue culture. *The Journal of experimental medicine* 102(1)**,** 37-48. doi: 10.1084/jem.102.1.37.

Eagle, H. (1955d). The specific amino acid requirements of a mammalian cell (strain L) in tissue culture. *The Journal of biological chemistry* 214(2)**,** 839-852.

Eagle, H. (1959). Amino acid metabolism in mammalian cell cultures. *Science (New York, N.Y.)* 130(3373)**,** 432-437. doi: 10.1126/science.130.3373.432.

Eberl, G., Colonna, M., Di Santo, J.P., and McKenzie, A.N.J. (2015). Innate lymphoid cells: A new paradigm in immunology. *Science* 348(6237). doi: 10.1126/science.aaa6566.

Edmonds, J.L., Kirse, D.J., Kearns, D., Deutsch, R., Spruijt, L., and Naviaux, R.K. (2002). The otolaryngological manifestations of mitochondrial disease and the risk of neurodegeneration with infection. *Archives of Otolaryngology-Head & Neck Surgery* 128(4)**,** 355-362. doi: 10.1001/archotol.128.4.355.

Erdman, S.H., Christensen, R.D., Bradley, P.P., and Rothstein, G. (1982). SUPPLY AND RELEASE OF STORAGE NEUTROPHILS - A DEVELOPMENTAL-STUDY. *Biology of the Neonate* 41(3-4)**,** 132-137.

Esteve-Sole, A., Teixido, I., Deya-Martinez, A., Yague, J., Plaza-Martin, A.M., Juan, M., et al. (2017). Characterization of the Highly Prevalent Regulatory CD24(hi)CD38(hi) B-Cell Population in Human Cord Blood. *Frontiers in Immunology* 8. doi: 10.3389/fimmu.2017.00201.

Everts, B., Amiel, E., Huang, S.C.C., Smith, A.M., Chang, C.H., Lam, W.Y., et al. (2014). TLR-driven early glycolytic reprogramming via the kinases TBK1-IKK epsilon supports the anabolic demands of dendritic cell activation. *Nature Immunology* 15(4)**,** 323-+. doi: 10.1038/ni.2833.

Evrard, M., Kwok, I.W.H., Chong, S.Z., Teng, K.W.W., Becht, E., Chen, J.M., et al. (2018). Developmental Analysis of Bone Marrow Neutrophils Reveals Populations Specialized in Expansion, Trafficking, and Effector Functions. *Immunity* 48(2)**,** 364-+. doi: 10.1016/j.immuni.2018.02.002.

Fang, X.H, Li, Z.J., Liu C.Y., Mor, G. and Liao, A.H. (2024) Macrophage memory: Types, mechansisms, and its role in health and disease.Immunology 171(1) 18-30. doi:10.1111/imm.13697.

Feng, Y.Q., Arvey, A., Chinen, T., Van der Veeken, J.D., Gasteiger, G., and Rudensky, A.Y. (2014). Control of the Inheritance of Regulatory T Cell Identity by a cis Element in the Foxp3 Locus. *Cell* 158(4)**,** 749-763. doi: 10.1016/j.cell.2014.07.031.

Field, C.S., Baixauli, F., Kyle, R.L., Puleston, D.J., Cameron, A.M., Sanin, D.E., et al. (2020). Mitochondrial Integrity Regulated by Lipid Metabolism Is a Cell-Intrinsic Checkpoint for Treg Suppressive Function. *Cell Metabolism* 31(2)**,** 422-+. doi: 10.1016/j.cmet.2019.11.021.

Fike, A.J., Kumova, O.K., and Carey, A.J. (2019). Dissecting the defects in the neonatal CD8(+) T-cell response. *Journal of Leukocyte Biology* 106(5)**,** 1051-1061. doi: 10.1002/jlb.5ru0319-105r.

Finlay, D.K., Rosenzweig, E., Sinclair, L.V., Feijoo-Carnero, C., Hukelmann, J.L., Rolf, J., et al. (2012). PDK1 regulation of mTOR and hypoxia-inducible factor 1 integrate metabolism and migration of CD8(+) T cells. *Journal of Experimental Medicine* 209(13)**,** 2441-2453. doi: 10.1084/jem.20112607.

Flajnik, M.F., and Kasahara, M. (2010). Origin and evolution of the adaptive immune system: genetic events and selective pressures. *Nature Reviews Genetics* 11(1)**,** 47-59. doi: 10.1038/nrg2703.

Fleischmann, C., Reichert, F., Cassini, A., Horner, R., Harder, T., Markwart, R., et al. (2021). Global incidence and mortality of neonatal sepsis: a systematic review and meta-analysis. *Archives of Disease in Childhood* 106(8)**,** 745-752. doi: 10.1136/archdischild-2020-320217.

Flores-Borja, F., Bosma, A., Ng, D., Reddy, V., Ehrenstein, M.R., Isenberg, D.A., et al. (2013). CD19(+)CD24(hi)CD38(hi) B Cells Maintain Regulatory T Cells While Limiting T(H)1 and T(H)17 Differentiation. *Science Translational Medicine* 5(173). doi: 10.1126/scitranslmed.3005407.

Forsthuber, T., Yip, H.C., and Lehmann, P.V. (1996). Induction of T(H)1 and T(H)2 immunity in neonatal mice. *Science* 271(5256)**,** 1728-1730. doi: 10.1126/science.271.5256.1728.

Frost, B.L., Jilling, T., Lapin, B., Maheshwari, A., and Caplan, M.S. (2014). Maternal breast milk transforming growth factor-beta and feeding intolerance in preterm infants. *Pediatric Research* 76(4)**,** 386-393. doi: 10.1038/pr.2014.96.

Fuchs, T.A., Abed, U., Goosmann, C., Hurwitz, R., Schulze, I., Wahn, V., et al. (2007). Novel cell death program leads to neutrophil extracellular traps. *Journal of Cell Biology* 176(2)**,** 231-241. doi: 10.1083/jcb.200606027.

Galindo-Albarran, A.O., Lopez-Portales, O.H., Gutierrez-Reyna, D.Y., Rodriguez-Jorge, O., Sanchez-Villanueva, J.A., Ramirez-Pliego, O., et al. (2016). CD8(+) T Cells from Human Neonates Are Biased toward an Innate Immune Response. *Cell Reports* 17(8)**,** 2151-2160. doi: 10.1016/j.celrep.2016.10.056.

Garaude, J., Acin-Perez, R., Martinez-Cano, S., Enamorado, M., Ugolini, M., Nistal-Villan, E., et al. (2016). Mitochondrial respiratory-chain adaptations in macrophages contribute to antibacterial host defense. *Nature Immunology* 17(9)**,** 1037-1045. doi: 10.1038/ni.3509.

Gattinoni, L., Lugli, E., Ji, Y., Pos, Z., Paulos, C.M., Quigley, M.F., et al. (2011). A human memory T cell subset with stem cell-like properties. *Nature Medicine* 17(10)**,** 1290-U1325. doi: 10.1038/nm.2446.

Geiger, R., Rieckmann, J.C., Wolf, T., Basso, C., Feng, Y.H., Fuhrer, T., et al. (2016). L-Arginine Modulates T Cell Metabolism and Enhances Survival and Anti-tumor Activity. *Cell* 167(3)**,** 829-+. doi: 10.1016/j.cell.2016.09.031.

Geltink, R.I.K., Kyle, R.L., and Pearce, E.L. (2018). Unraveling the Complex Interplay Between T Cell Metabolism and Function. *Annual Review of Immunology, Vol 36* 36**,** 461-488. doi: 10.1146/annurev-immunol-042617-053019.

Gervassi, A., Lejarcegui, N., Dross, S., Jacobson, A., Itaya, G., Kidzeru, E., et al. (2014). Myeloid Derived Suppressor Cells Are Present at High Frequency in Neonates and Suppress In Vitro T Cell Responses. *Plos One* 9(9). doi: 10.1371/journal.pone.0107816.

Gessner, B.D., Gillingham, M.B., Wood, T., and Koeller, D.M. (2013). Association of a Genetic Variant of Carnitine Palmitoyltransferase 1A with Infections in Alaska

Native Children. *Journal of Pediatrics* 163(6)**,** 1716-1721. doi: 10.1016/j.jpeds.2013.07.010.

Gibbons, D., Fleming, P., Virasami, A., Michel, M.L., Sebire, N.J., Costeloe, K., et al. (2014). Interleukin-8 (CXCL8) production is a signatory T cell effector function of human newborn infants. *Nature Medicine* 20(10)**,** 1206-1210. doi: 10.1038/nm.3670.

Gibbons, D.L., Haque, S.F.Y., Silberzahn, T., Hamilton, K., Langford, C., Ellis, P., et al. (2009). Neonates harbour highly active gamma delta T cells with selective impairments in preterm infants. *European Journal of Immunology* 39(7)**,** 1794-1806. doi: 10.1002/eji.200939222.

Glaesener, S., Jaenke, C., Habener, A., Geffers, R., Hagendorff, P., Witzlau, K., et al. (2018). Decreased production of class-switched antibodies in neonatal B cells is associated with increased expression of miR-181b. *Plos One* 13(2). doi: 10.1371/journal.pone.0192230.

Glass, D.R., Tsai, A.G., Oliveria, J.P., Hartmann, F.J., Kimmey, S.C., Calderon, A.A., et al. (2020). An Integrated Multi-omic Single-Cell Atlas of Human B Cell Identity. *Immunity* 53(1)**,** 217-+. doi: 10.1016/j.immuni.2020.06.013.

Greer, O., Shah, N.M., Sriskandan, S., and Johnson, M.R. (2019). Sepsis: Precision-Based Medicine for Pregnancy and the Puerperium. *International Journal of Molecular Sciences* 20(21). doi: 10.3390/ijms20215388.

Grieger, J.A., Clifton, V.L., Tuck, A.R., Wooldridge, A.L., Robertson, S.A., and Gatford, K.L. (2016). In utero programming of allergic susceptibility. *International archives of allergy and immunology* 169(2)**,** 80-92. doi: 10.1159/000443961.

Grudzinska, F.S., Jasper, A., Sapey E., Thickett. D.R., Mauro C., Scott A., Barlow J. (2023). Real-time assessment of neutrophil metabolism and oxidative burst using extracellular flux analysis. Front Immunol.14:1083072. doi:

Gubser, P.M., Bantug, G.R., Razik, L., Fischer, M., Dimeloe, S., Hoenger, G., et al. (2013). Rapid effector function of memory CD8(+) T cells requires an immediate-early glycolytic switch. *Nature Immunology* 14(10)**,** 1064-+. doi: 10.1038/ni.2687.

Gudgeon, N., Munford, H., Bishop, E.L., Hill, J., Fulton-Ward, T., Bending, D., et al. (2022). Succinate uptake by T cells suppresses their effector function via inhibition of mitochondrial glucose oxidation. *Cell Reports* 40(7). doi: 10.1016/j.celrep.2022.111193.

Halim, L., Romano, M., McGregor, R., Correa, I., Pavlidis, P., Grageda, N., et al. (2017). An Atlas of Human Regulatory T Helper-like Cells Reveals Features of Th2-like Tregs that Support a Tumorigenic Environment. *Cell Reports* 20(3)**,** 757-770. doi: 10.1016/j.celrep.2017.06.079.

Halonen, M., Lohman, I.C., Stern, D.A., Spangenberg, A., Anderson, D., Mobley, S., et al. (2009). Th1/Th2 Patterns and Balance in Cytokine Production in the Parents and Infants of a Large Birth Cohort. *Journal of Immunology* 182(5)**,** 3285-3293. doi: 10.4049/jimmunol.0711996.

Ham, R.G. (1965). CLONAL GROWTH OF MAMMALIAN CELLS IN A CHEMICALLY DEFINED, SYNTHETIC MEDIUM. *Proceedings of the National Academy of Sciences of the United States of America* 53**,** 288-293. doi: 10.1073/pnas.53.2.288.

Hamilton, J.A., Vairo, G., and Lingelbach, S.R. (1986). CSF-1 STIMULATES GLUCOSE-UPTAKE IN MURINE BONE MARROW-DERIVED MACROPHAGES. *Biochemical*

and Biophysical Research Communications 138(1), 445-454. doi: 10.1016/0006-291x(86)90301-3.

Han, P., McDonald, T., and Hodge, G. (2004). Potential immaturity of the T-cell and antigen-presenting cell interaction in cord blood with particular emphasis on the CD40-CD40 ligand costimulatory pathway. *Immunology* 113(1), 26-34. doi: 10.1111/j.1365-2567.2004.01933.x.

Harb, H., Irvine, J., Amarasekera, M., Hii, C.S., Kesper, D.A., Ma, Y.F., et al. (2017). The role of PKC zeta in cord blood T-cell maturation towards Th1 cytokine profile and its epigenetic regulation by fish oil. *Bioscience Reports* 37. doi: 10.1042/bsr20160485.

Harbeson, D., Ben-Othman, R., Amenyogbe, N., and Kollmann, T.R. (2018a). Outgrowing the Immaturity Myth: The Cost of Defending From Neonatal Infectious Disease. *Frontiers in Immunology* 9. doi: 10.3389/fimmu.2018.01077.

Harbeson, D., Francis, F., Bao, W., Amenyogbe, N.A., and Kollmann, T.R. (2018b). Energy Demands of Early Life Drive a Disease Tolerant Phenotype and Dictate Outcome in Neonatal Bacterial Sepsis. *Frontiers in Immunology* 9. doi: 10.3389/fimmu.2018.01918.

Hassan, J., and Reen, D.J. (1998). IL-7 promotes the survival and maturation but not differentiation of human post-thymic CD4(+) T cells. *European Journal of Immunology* 28(10), 3057-3065. doi: 10.1002/(sici)1521-4141(199810)28:10<3057::aid-immu3057>3.3.co;2-q.

Hassan, J., and Reen, D.J. (2001). Human recent thymic emigrants-identification, expansion, and survival characteristics. *Journal of Immunology* 167(4), 1970-1976. doi: 10.4049/jimmunol.167.4.1970.

He, Y.M., Li, X., Perego, M., Nefedova, Y., Kossenkov, A.V., Jensen, E.A., et al. (2018). Transitory presence of myeloid-derived suppressor cells in neonates is critical for control of inflammation. *Nature Medicine* 24(2), 224-+. doi: 10.1038/nm.4467.

Hebel, K., Weinert, S., Kuropka, B., Knolle, J., Kosak, B., Jorch, G., et al. (2014). CD4(+) T Cells from Human Neonates and Infants Are Poised Spontaneously To Run a Nonclassical IL-4 Program. *Journal of Immunology* 192(11), 5160-5170. doi: 10.4049/jimmunol.1302539.

Hegge, I., Niepel, F., Lange, A., Vogelgesang, A., Heckmann, M., and Ruhnau, J. (2019). Functional analysis of granulocyte and monocyte subpopulations in neonates. *Molecular and cellular pediatrics* 6(1), 5-5. doi: 10.1186/s40348-019-0092-y.

Heiden, M.G.V., Cantley, L.C., and Thompson, C.B. (2009). Understanding the Warburg Effect: The Metabolic Requirements of Cell Proliferation. *Science* 324(5930), 1029-1033. doi: 10.1126/science.1160809.

Helou, D.G., Shafiei-Jahani, P., Lo, R., Howard, E., Hurrell, B.P., Galle-Treger, L., et al. (2020). PD-1 pathway regulates ILC2 metabolism and PD-1 agonist treatment ameliorates airway hyperreactivity. *Nature Communications* 11(1). doi: 10.1038/s41467-020-17813-1.

Herberth, G., Hinz, D., Bauer, M., Roeder, S., Olek, S., Huehn, J., et al. (2012). Environmental exposure during pregnancy modulates fetal Treg development with consequences for the allergy risk of the child. *Journal of Reproductive Immunology* 94(1), 54-54. doi: 10.1016/j.jri.2012.03.336.

Herrero-Cervera, A., Soehnlein, O., and Kenne, E. (2022). Neutrophils in chronic inflammatory diseases. *Cellular & Molecular Immunology* 19(2)**,** 177-191. doi: 10.1038/s41423-021-00832-3.

Hidalgo, A., Chilvers, E.R., Summers, C., and Koenderman, L. (2019). The Neutrophil Life Cycle. *Trends in Immunology* 40(7)**,** 584-597. doi: 10.1016/j.it.2019.04.013.

Hikita, N., Cho, Y., Tachibana, D., Hamazaki, T., Koyama, M., and Tokuhara, D. (2019). Cell surface antigens of neonatal monocytes are selectively impaired in basal expression, but hyperresponsive to lipopolysaccharide and zymosan. *Journal of Reproductive Immunology* 136. doi: 10.1016/j.jri.2019.102614.

Hiwarkar, P., Hubank, M., Qasim, W., Chiesa, R., Gilmour, K.C., Saudemont, A., et al. (2017). Cord blood transplantation recapitulates fetal ontogeny with a distinct molecular signature that supports CD4(+) T-cell reconstitution. *Blood Advances* 1(24)**,** 2206-2216. doi: 10.1182/bloodadvances.2017010827.

Hiwarkar, P., Qasim, W., Ricciardelli, I., Gilmour, K., Quezada, S., Saudemont, A., et al. (2015). Cord blood T cells mediate enhanced antitumor effects compared with adult peripheral blood T cells. *Blood* 126(26)**,** 2882-2891. doi: 10.1182/blood-2015-06-654780.

Ho, P.C., Bihuniak, J.D., Macintyre, A.N., Staron, M., Liu, X.J., Amezquita, R., et al. (2015). Phosphoenolpyruvate Is a Metabolic Checkpoint of Anti-tumor T Cell Responses. *Cell* 162(6)**,** 1217-1228. doi: 10.1016/j.cell.2015.08.012.

Hodge, S.H., Krauss, M.Z., Kaymak, I., King, J.I., Howden, A.J.M., Panic, G., et al. (2022). Amino acid availability acts as a metabolic rheostat to determine the magnitude of ILC2 responses. *Journal of Experimental Medicine* 220(3). doi: 10.1084/jem.20221073.

Holm, S.R., Jenkins, B., Cronin, J.G., Jones, N., and Thornton, C.A. (2021). A role for metabolism in determining neonatal immune function. *Pediatric Allergy and Immunology* 32(8)**,** 1616-1628. doi: 10.1111/pai.13583.

Hornik, C.P., Benjamin, D.K., Becker, K.C., Li, J., Clark, R.H., Cohen-Wolkowiez, M., et al. (2012). Use of the Complete Blood Cell Count in Early-onset Neonatal Sepsis. *Pediatric Infectious Disease Journal* 31(8)**,** 799-802. doi: 10.1097/INF.0b013e318256905c.

Hosios, A.M., Hecht, V.C., Danai, L.V., Johnson, M.O., Rathmell, J.C., Steinhauser, M.L., et al. (2016). Amino Acids Rather than Glucose Account for the Majority of Cell Mass in Proliferating Mammalian Cells. *Developmental Cell* 36(5)**,** 540-549. doi: 10.1016/j.devcel.2016.02.012.

Hossain, F., Al-Khami, A.A., Wyczechowska, D., Hernandez, C., Zheng, L.Q., Reiss, K., et al. (2015). Inhibition of Fatty Acid Oxidation Modulates Immunosuppressive Functions of Myeloid-Derived Suppressor Cells and Enhances Cancer Therapies. *Cancer Immunology Research* 3(11)**,** 1236-1247. doi: 10.1158/2326-6066.cir-15-0036.

Howden, A.J.M., Hukelmann, J.L., Brenes, A., Spinelli, L., Sinclair, L.V., Lamond, A.I., et al. (2019). Quantitative analysis of T cell proteomes and environmental sensors during T cell differentiation. *Nature Immunology* 20(11)**,** 1542-+. doi: 10.1038/s41590-019-0495-x.

Huang, H.L., Long, L.Y., Zhou, P.P., Chapman, N.M., and Chi, H.B. (2020). mTOR signaling at the crossroads of environmental signals and T-cell fate decisions. *Immunological Reviews* 295(1)**,** 15-38. doi: 10.1111/imr.12845.

Imanishi, T., Unno, M., Kobayashi, W., Yoneda, N., Akira, S., and Saito, T. (2020). mTORC1 Signaling Controls TLR2-Mediated T-Cell Activation by Inducing TIRAP Expression. *Cell Reports* 32(3). doi: 10.1016/j.celrep.2020.107911.

Infantino, V., Iacobazzi, V., Palmieri, F., and Menga, A. (2013). ATP-citrate lyase is essential for macrophage inflammatory response. *Biochemical and Biophysical Research Communications* 440(1)**,** 105-111. doi: 10.1016/j.bbrc.2013.09.037.

Iwenofu, O.H., Lackman, R.D., Staddon, A.P., Goodwin, D.G., Haupt, H.M., and Brooks, J.S.J. (2008). Phospho-S6 ribosomal protein: a potential new predictive sarcoma marker for targeted mTOR therapy. *Modern Pathology* 21(3)**,** 231-237. doi: 10.1038/modpathol.3800995.

Jacinto, E., Facchinetti, V., Liu, D., Soto, N., Wei, S.N., Jung, S.Y., et al. (2006). SIN1/MIP1 maintains rictor-mTOR complex integrity and regulates Akt phosphorylation and substrate specificity. *Cell* 127(1)**,** 125-137. doi: 10.1016/j.cell.2006.08.033.

Jacks, R.D., Keller, T.J., Nelson, A., Nishimura, M.I., White, P., and Iwashima, M. (2018). Cell intrinsic characteristics of human cord blood naive CD4 T cells. *Immunology Letters* 193**,** 51-57. doi: 10.1016/j.imlet.2017.11.011.

Jacobs, S.R., Herman, C.E., MacIver, N.J., Wofford, J.A., Wieman, H.L., Hammen, J.J., et al. (2008). Glucose uptake is limiting in T cell activation and requires CD28-mediated akt-dependent and independent pathways. *Journal of Immunology* 180(7)**,** 4476-4486. doi: 10.4049/jimmunol.180.7.4476.

Jankovic, D., Kugler, D.G., and Sher, A. (2010). IL-10 production by CD4(+) effector T cells: a mechanism for self-regulation. *Mucosal Immunology* 3(3)**,** 239-246. doi: 10.1038/mi.2010.8.

Jensen, H., Potempa, M., Gotthardt, D., and Lanier, L.L. (2017). Cutting Edge: IL-2-Induced Expression of the Amino Acid Transporters SLC1A5 and CD98 Is a Prerequisite for NKG2D-Mediated Activation of Human NK Cells. *Journal of Immunology* 199(6)**,** 1967-1972. doi: 10.4049/jimmunol.1700497.

Jiang, G.M., Tan, Y., Wang, H., Peng, L., Chen, H.T., Meng, X.J., et al. (2019). The relationship between autophagy and the immune system and its applications for tumor immunotherapy. *Molecular Cancer* 18. doi: 10.1186/s12943-019-0944-z.

Jiang, Q., Yang, G.C., Xiao, F., Xie, J., Wang, S.J., Lu, L.W., et al. (2021). Role of Th22 Cells in the Pathogenesis of Autoimmune Diseases. *Frontiers in Immunology* 12. doi: 10.3389/fimmu.2021.688066.

Jiang, Q.K., Qiu, Y.P., Kurland, I.J., Drlica, K., Subbian, S., Tyagi, S., et al. (2022). Glutamine Is Required for M1-like Polarization of Macrophages in Response to Mycobacterium tuberculosis Infection. *Mbio* 13(4). doi: 10.1128/mbio.01274-22.

Jones, D.M., Read, K.A., and Oestreich, K.J. (2020a). Dynamic Roles for IL-2-STAT5 Signaling in Effector and Regulatory CD4(+)d T Cell Populations. *Journal of Immunology* 205(7)**,** 1721-1730. doi: 10.4049/jimmunol.2000612.

Jones, H.R., Robb, C.T., Perretti, M., and Rossi, A.G. (2016). The role of neutrophils in inflammation resolution. *Seminars in Immunology* 28(2), 137-145. doi: 10.1016/j.smim.2016.03.007.

Jones, N., Blagih, J., Zani, F., Rees, A., Hill, D.G., Jenkins, B.J., et al. (2021). Fructose reprogrammes glutamine-dependent oxidative metabolism to support LPS-induced inflammation. *Nature Communications* 12(1). doi: 10.1038/s41467-021-21461-4.

Jones, N., Cronin, J.G., Dolton, G., Panetti, S., Schauenburg, A.J., Galloway, S.A.E., et al. (2017). Metabolic Adaptation of Human CD4(+) and CD8(+) T-cells to T-cell Receptor-Mediated Stimulation. *Frontiers in Immunology* 8. doi: 10.3389/fimmu.2017.01516.

Jones, N., Vincent, E.E., Cronin, J.G., Panetti, S., Chambers, M., Holm, S.R., et al. (2019). Akt and STAT5 mediate naive human CD4+T-cell early metabolic response to TCR stimulation. *Nature Communications* 10. doi: 10.1038/s41467-019-10023-4.

Jones, N., Vincent, E.E., Felix, L.C., Cronin, J.G., Scott, L.M., Hole, P.S., et al. (2020b). Interleukin-5 drives glycolysis and reactive oxygen species-dependent citric acid cycling by eosinophils. *Allergy* 75(6), 1361-1370. doi: 10.1111/all.14158.

Jorgensen, N., Persson, G., and Hviid, T.V.F. (2019). The Tolerogenic Function of Regulatory T Cells in Pregnancy and Cancer. *Frontiers in Immunology* 10. doi: 10.3389/fimmu.2019.00911.

Juul, S.E., Haynes, J.W., and McPherson, R.J. (2005). Evaluation of eosinophilia in hospitalized preterm infants. *Journal of perinatology : official journal of the California Perinatal Association* 25(3), 182-188. doi: 10.1038/sj.jp.7211226.

Kaminski, H., Couzi, L., and Eberl, M. (2021). Unconventional T cells and kidney disease. *Nature Reviews Nephrology* 17(12), 795-813. doi: 10.1038/s41581-021-00466-8.

Kan, B., Michalski, C., Fu, H., Au, H.H.T., Lee, K., Marchant, E.A., et al. (2018). Cellular metabolism constrains innate immune responses in early human ontogeny. *Nature Communications* 9. doi: 10.1038/s41467-018-07215-9.

Kapniciz, S.M., Pacheco, S.E., and McGuire, P.J. (2018). The emerging role of immune dysfunction in mitochondrial diseases as a paradigm for understanding immunometabolism. *Metabolism-Clinical and Experimental* 81, 97-112. doi: 10.1016/j.metabol.2017.11.010.

Keating, S.E., Zaiatz-Bittencourt, V., Loftus, R.M., Keane, C., Brennan, K., Finlay, D.K., et al. (2016). Metabolic Reprogramming Supports IFN-gamma Production by CD56(bright) NK Cells. *Journal of Immunology* 196(6), 2552-2560. doi: 10.4049/jimmunol.1501783.

Kedia-Mehta, N., Pisarska, M.M., Rollings, C., O'Neill, C., De Barra, C., Foley, C., et al. (2023). The proliferation of human mucosal-associated invariant T cells requires a MYC-SLC7A5-glycolysis metabolic axis. *Science Signaling* 16(781). doi: 10.1126/scisignal.abo2709.

Keppel, M.P., Saucier, N., Mah, A.Y., Vogel, T.P., and Cooper, M.A. (2015). Activation-Specific Metabolic Requirements for NK Cell IFN-gamma Production. *Journal of Immunology* 194(4), 1954-1962. doi: 10.4049/jimmunol.1402099.

Kerdiles, Y.M., Beisner, D.R., Tinoco, R., Dejean, A.S., Castrillon, D.H., DePinho, R.A., et al. (2009). Foxo1 links homing and survival of naive T cells by regulating L-

selectin, CCR7 and interleukin 7 receptor. *Nature Immunology* 10(2)**,** 176-184. doi: 10.1038/ni.1689.

Kerdiles, Y.M., Stone, E.L., Beisner, D.L., McGargill, M.A., Ch'en, I.L., Stockmann, C., et al. (2010). Foxo Transcription Factors Control Regulatory T Cell Development and Function. *Immunity* 33(6)**,** 890-904. doi: 10.1016/j.immuni.2010.12.002.

Kiani, A., Garcia-Cozar, F.J., Habermann, I., Laforsch, S., Aebischer, T., Ehninger, G., et al. (2001). Regulation of interferon-gamma gene expression by nuclear factor of activated T cells. *Blood* 98(5)**,** 1480-1488. doi: 10.1182/blood.V98.5.1480.

Kidani, Y., Elsaesser, H., Hock, M.B., Vergnes, L., Williams, K.J., Argus, J.P., et al. (2013). Sterol regulatory element-binding proteins are essential for the metabolic programming of effector T cells and adaptive immunity. *Nature Immunology* 14(5)**,** 489-+. doi: 10.1038/ni.2570.

Kiilerich, P., Cortes, R., Lausten-Thomsen, U., Borbye-Lorenzen, N., Holmgaard, S., and Skogstrand, K. (2021). Delivery Modality Affect Neonatal Levels of Inflammation, Stress, and Growth Factors. *Frontiers in Pediatrics* 9. doi: 10.3389/fped.2021.709765.

Kim, C.H., Rott, L., Kunkel, E.J., Genovese, M.C., Andrew, D.P., Wu, L.J., et al. (2001). Rules of chemokine receptor association with T cell polarization in vivo. *Journal of Clinical Investigation* 108(9)**,** 1331-1339. doi: 10.1172/jci200113543.

Kim, S.K., Keeney, S.E., Alpard, S.K., and Schmalstieg, F.C. (2003). Comparison of L-selectin and CD11b on neutrophils of adults and neonates during the first month of life. *Pediatric Research* 53(1)**,** 132-136. doi: 10.1203/01.pdr.0000041515.78650.11.

Kim, Y.J., Park, E.J., Lee, S.H., Silwal, P., Kim, J.K., Yang, J.S., et al. (2023). Dimethyl itaconate is effective in host-directed antimicrobial responses against mycobacterial infections through multifaceted innate immune pathways. *Cell and Bioscience* 13(1). doi: 10.1186/s13578-023-00992-x.

Kishore, M., Cheung, K.C.P., Fu, H.M., Bonacina, F., Wang, G.S., Coe, D., et al. (2017). Regulatory T Cell Migration Is Dependent on Glucokinase-Mediated Glycolysis. *Immunity* 47(5)**,** 875-+. doi: 10.1016/j.immuni.2017.10.017.

Klein-Hessling, S., Muhammad, K., Klein, M., Pusch, T., Rudolf, R., Floter, J., et al. (2017). NFATc1 controls the cytotoxicity of CD8(+) T cells. *Nature Communications* 8. doi: 10.1038/s41467-017-00612-6.

Klysz, D., Tai, X.G., Robert, P.A., Craveiro, M., Cretenet, G., Oburoglu, L., et al. (2015). Glutamine-dependent alpha-ketoglutarate production regulates the balance between T helper 1 cell and regulatory T cell generation. *Science Signaling* 8(396). doi: 10.1126/scisignal.aab2610.

Kochanek, M., Schalk, E., von Bergwelt-Baildon, M., Beutel, G., Buchheidt, D., Hentrich, M., et al. (2019). Management of sepsis in neutropenic cancer patients: 2018 guidelines from the Infectious Diseases Working Party (AGIHO) and Intensive Care Working Party (iCHOP) of the German Society of Hematology and Medical Oncology (DGHO). *Annals of Hematology* 98(5)**,** 1051-1069. doi: 10.1007/s00277-019-03622-0.

Koenderman, L., Tesselaar, K., and Vrisekoop, N. (2022). Human neutrophil kinetics: a call to revisit old evidence. *Trends in Immunology* 43(11)**,** 868-876. doi: 10.1016/j.it.2022.09.008.

Koning, H., Baert, M.R.M., Oranje, A.P., Savelkoul, H.F.J., and Neijens, H.J. (1996). Development of immune functions related to allergic mechanisms in young children. *Pediatric Research* 40(3)**,** 363-375. doi: 10.1203/00006450-199609000-00001.

Kostlin, N., Kugel, H., Spring, B., Leiber, A., Marme, A., Henes, M., et al. (2014). Granulocytic myeloid derived suppressor cells expand in human pregnancy and modulate T-cell responses. *European Journal of Immunology* 44(9)**,** 2582-2591. doi: 10.1002/eji.201344200.

Kouidhi, S., Noman, M.Z., Kieda, C., Elgaaied, A.B., and Chouaib, S. (2016). Intrinsic and Tumor Microenvironment-Induced Metabolism Adaptations of T Cells and Impact on Their Differentiation and Function. *Frontiers in Immunology* 7. doi: 10.3389/fimmu.2016.0114.

Kumar, B.V., Connors, T.J., and Farber, D.L. (2018). Human T Cell Development, Localization, and Function throughout Life. *Immunity* 48(2)**,** 202-213. doi: 10.1016/j.immuni.2018.01.007.

Kurita, K., Ohta, H., Shirakawa, I., Tanaka, M., Kitaura, Y., Iwasaki, Y., et al. (2021). Macrophages rely on extracellular serine to suppress aberrant cytokine production. *Scientific Reports* 11(1). doi: 10.1038/s41598-021-90086-w.

Kyathanahalli, C., Snedden, M., and Hirsch, E. (2022). Is human labor at term an inflammatory condition?(dagger). *Biology of Reproduction*. doi: 10.1093/biolre/ioac182.

Lahoz-Beneytez, J., Elemans, M., Zhang, Y., Ahmed, R., Salam, A., Block, M., et al. (2016). Human neutrophil kinetics: modeling of stable isotope labeling data supports short blood neutrophil half-lives. *Blood* 127(26)**,** 3431-3438. doi: 10.1182/blood-2016-03-700336.

Lampropoulou, V., Sergushichev, A., Bambouskova, M., Nair, S., Vincent, E.E., Loginicheva, E., et al. (2016). Itaconate Links Inhibition of Succinate Dehydrogenase with Macrophage Metabolic Remodeling and Regulation of Inflammation. *Cell Metabolism* 24(1)**,** 158-166. doi: 10.1016/j.cmet.2016.06.004.

Langrish, C.L., Buddle, J.C., Thrasher, A.J., and Goldblatt, D. (2002). Neonatal dendritic cells are intrinsically biased against Th-1 immune responses. *Clinical and Experimental Immunology* 128(1)**,** 118-123. doi: 10.1046/j.1365-2249.2002.01817.x.

Lau-Kilby, A.W., Turfkruyer, M., Kehl, M., Yang, L.J., Buchholz, U.J., Hickey, K., et al. (2020). Type I IFN ineffectively activates neonatal dendritic cells limiting respiratory antiviral T-cell responses. *Mucosal Immunology* 13(2)**,** 371-380. doi: 10.1038/s41385-019-0234-5.

Laukka, T., Mariani, C.J., Ihantola, T., Cao, J.Z., Hokkanen, J., Kaelin, W.G., et al. (2016). Fumarate and Succinate Regulate Expression of Hypoxia-inducible Genes via TET Enzymes. *Journal of Biological Chemistry* 291(8)**,** 4256-4265. doi: 10.1074/jbc.M115.688762.

Lawrence, S.M., Corriden, R., and Nizet, V. (2017). Age-Appropriate Functions and Dysfunctions of the Neonatal Neutrophil. *Frontiers in Pediatrics* 5. doi: 10.3389/fped.2017.00023.

Le Campion, A., Bourgeois, C., Lambolez, F., Martin, B., Leaument, S., Dautigny, N., et al. (2002). Naive T cells proliferate strongly in neonatal mice in response to

self-peptide/self-MHC complexes. *Proceedings of the National Academy of Sciences of the United States of America* 99(7), 4538-4543. doi: 10.1073/pnas.062621699.

Lee, B.C., Kang, I., Lee, S.E., Lee, J.Y., Shin, N., Kim, J.J., et al. (2019). Human umbilical cord blood plasma alleviates age-related olfactory dysfunction by attenuating peripheral TNF-alpha expression. *Bmb Reports* 52(4), 259-264. doi: 10.5483/BMBRep.2019.52.4.124.

Lee, K., Gudapati, P., Dragovic, S., Spencer, C., Joyce, S., Killeen, N., et al. (2010). Mammalian Target of Rapamycin Protein Complex 2 Regulates Differentiation of Th1 and Th2 Cell Subsets via Distinct Signaling Pathways. *Immunity* 32(6), 743-753. doi: 10.1016/j.immuni.2010.06.002.

Lee, Y.S., Kim, T.S., and Kim, D.K. (2011). T lymphocytes derived from human cord blood provide effective antitumor immunotherapy against a human tumor. *Bmc Cancer* 11. doi: 10.1186/1471-2407-11-225.

Leney-Greene, M.A., Boddapati, A.K., Su, H.C., Cantor, J.R., and Lenardo, M.J. (2020). Human Plasma-like Medium Improves T Lymphocyte Activation. *Iscience* 23(1). doi: 10.1016/j.isci.2019.100759.

Leprivier, G., and Rotblat, B. (2020). How does mTOR sense glucose starvation? AMPK is the usual suspect. *Cell Death Discovery* 6(1). doi: 10.1038/s41420-020-0260-9.

Lesniewski, M.L., Haviernik, P., Weitzel, R.P., Kadereit, S., Kozik, M.M., Fanning, L.R., et al. (2008). Regulation of IL-2 expression by transcription factor BACH2 in umbilical cord blood CD4(+) T cells. *Leukemia* 22(12), 2201-2207. doi: 10.1038/leu.2008.234.

Levy, O., Coughlin, M., Cronstein, B.N., Roy, R.M., Desai, A., and Wessels, M.R. (2006). The adenosine system selectively inhibits TLR-mediated TNF-alpha production in the human newborn. *Journal of Immunology* 177(3), 1956-1966. doi: 10.4049/jimmunol.177.3.1956.

Levy, O., Martin, S., Eichenwald, E., Ganz, T., Valore, E., Carroll, S.F., et al. (1999). Impaired innate immunity in the newborn: Newborn neutrophils are deficient in bactericidal/permeability-increasing protein. *Pediatrics* 104(6), 1327-1333. doi: 10.1542/peds.104.6.1327.

Levy, O., Zarember, K.A., Roy, R.M., Cywes, C., Godowski, P.J., and Wessels, M.R. (2004). Selective impairment of TLR-mediated innate immunity in human newborns: Neonatal blood plasma reduces monocyte TNF-alpha induction by bacterial lipopeptides, lipopolysaccharide, and imiquimod, but preserves the response to R-848. *Journal of Immunology* 173(7), 4627-4634. doi: 10.4049/jimmunol.173.7.4627.

Lewis, D.B., Yu, C.C., Meyer, J., English, B.K., Kahn, S.J., and Wilson, C.B. (1991). CELLULAR AND MOLECULAR MECHANISMS FOR REDUCED INTERLEUKIN-4 AND INTERFERON-GAMMA PRODUCTION BY NEONATAL T-CELLS. *Journal of Clinical Investigation* 87(1), 194-202. doi: 10.1172/jci114970.

Li, C., Farooqui, M., Yada, R.C., Cai, J.B., Huttenlocher, A., and Beebe, D.J. (2023). The effect of whole blood logistics on neutrophil non-specific activation and kinetics ex vivo. *Research square*. doi: 10.21203/rs.3.rs-2837704/v1.

Li, J.T., Yang, K.Y., Tam, R.C.Y., Chan, V.W., Lan, H.Y., Hori, S., et al. (2019a). Regulatory T-cells regulate neonatal heart regeneration by potentiating cardiomyocyte

proliferation in a paracrine manner. *Theranostics* 9(15), 4324-4341. doi: 10.7150/thno.32734.

Li, M.Y., Zhao, W.J., Wang, Y.F., Jin, L.X., Jin, G.W., Sun, X.Y., et al. (2020). A wave of Foxp3(+) regulatory T cell accumulation in the neonatal liver plays unique roles in maintaining self-tolerance. *Cellular & Molecular Immunology* 17(5), 507-518. doi: 10.1038/s41423-019-0246-9.

Li, N., van Unen, V., Abdelaal, T., Guo, N.N., Kasatskaya, S.A., Ladell, K., et al. (2019b). Memory CD4(+) T cells are generated in the human fetal intestine. *Nature Immunology* 20(3), 301-+. doi: 10.1038/s41590-018-0294-9.

Li, Q.J., Chau, J., Ebert, P.J.R., Sylvester, G., Min, H., Liu, G., et al. (2007). miR-181a is an intrinsic modulator of T cell sensitivity and selection. *Cell* 129(1), 147-161. doi: 10.1016/j.cell.2007.03.008.

Lieschke, G.J., Grail, D., Hodgson, G., Metcalf, D., Stanley, E., Cheers, C., et al. (1994). MICE LACKING GRANULOCYTE-COLONY-STIMULATING FACTOR HAVE CHRONIC NEUTROPENIA, GRANULOCYTE AND MACROPHAGE PROGENITOR-CELL DEFICIENCY, AND IMPAIRED NEUTROPHIL MOBILIZATION. *Blood* 84(6), 1737-1746.

Lima, J., Martins, C., Leandro, M.J., Nunes, G., Sousa, M.J., Branco, J.C., et al. (2016). Characterization of B cells in healthy pregnant women from late pregnancy to post-partum: a prospective observational study. *Bmc Pregnancy and Childbirth* 16. doi: 10.1186/s12884-016-0927-7.

Liu, P.S., Wang, H.P., Li, X.Y., Chao, T., Christen, T.T.S., Christen, S., et al. (2017). alpha-ketoglutarate orchestrates macrophage activation through metabolic and epigenetic reprogramming. *Nature Immunology* 18(9), 985-+. doi: 10.1038/ni.3796.

Liu, X., Wang, M.Y., Jiang, T., He, J.J., Fu, X.M., and Xu, Y. (2019a). IDO1 Maintains Pluripotency of Primed Human Embryonic Stem Cells by Promoting Glycolysis. *Stem Cells* 37(9), 1158-1165. doi: 10.1002/stem.3044.

Liu, Y.F., Perego, M., Xiao, Q., He, Y.M., Fu, S.Y., He, J., et al. (2019b). Lactoferrin-induced myeloid-derived suppressor cell therapy attenuates pathologic inflammatory conditions in newborn mice. *Journal of Clinical Investigation* 129(10), 4261-4275. doi: 10.1172/jci128164.

Lopez-Cantillo, G., Uruena, C., Camacho, B.A., and Ramirez-Segura, C. (2022). CAR-T Cell Performance: How to Improve Their Persistence? *Frontiers in Immunology* 13. doi: 10.3389/fimmu.2022.878209.

Lorenzini, M., and Toldi, G. (2023). The Proportion of Recent Thymic Emigrant Lymphocytes in Breastfed and Formula Fed Term Neonates. *Nutrients* 15(4). doi: 10.3390/nu15041028.

Luengo, A., Li, Z.Q., Gui, D.Y., Sullivan, L.B., Zagorulya, M., Do, B.T., et al. (2021). Increased demand for NAD(+) relative to ATP drives aerobic glycolysis. *Molecular Cell* 81(4), 691-+. doi: 10.1016/j.molcel.2020.12.012.

Luevano, M., Daryouzeh, M., Alnabhan, R., Querol, S., Khakoo, S., Madrigal, A., et al. (2012). The unique profile of cord blood natural killer cells balances incomplete maturation and effective killing function upon activation. *Human Immunology* 73(3), 248-257. doi: 10.1016/j.humimm.2011.12.015.

Lunt, S.Y., and Vander Heiden, M.G. (2011). "Aerobic Glycolysis: Meeting the Metabolic Requirements of Cell Proliferation," in *Annual Review of Cell and*

Developmental Biology, Vol 27, eds. R. Schekman, L. Goldstein & R. Lehmann. (Palo Alto: Annual Reviews), 441-464.

Ma, E.H., Bantug, G., Griss, T., Condotta, S., Johnson, R.M., Samborska, B., et al. (2017). Serine Is an Essential Metabolite for Effector T Cell Expansion. *Cell Metabolism* 25(2)**,** 345-357. doi: 10.1016/j.cmet.2016.12.011.

Ma, E.H., Verway, M.J., Johnson, R.M., Roy, D.G., Steadman, M., Hayes, S., et al. (2019). Metabolic Profiling Using Stable Isotope Tracing Reveals Distinct Patterns of Glucose Utilization by Physiologically Activated CD8(+) T Cells. *Immunity* 51(5)**,** 856-+. doi: 10.1016/j.immuni.2019.09.003.

Macintyre, A.N., Gerriets, V.A., Nichols, A.G., Michalek, R.D., Rudolph, M.C., Deoliveira, D., et al. (2014). The Glucose Transporter Glut1 Is Selectively Essential for CD4 T Cell Activation and Effector Function. *Cell Metabolism* 20(1)**,** 61-72. doi: 10.1016/j.cmet.2014.05.004.

Mackay, C.R., Kimpton, W.G., Brandon, M.R., and Cahill, R.N.P. (1988). LYMPHOCYTE SUBSETS SHOW MARKED DIFFERENCES IN THEIR DISTRIBUTION BETWEEN BLOOD AND THE AFFERENT AND EFFERENT LYMPH OF PERIPHERAL LYMPH-NODES. *Journal of Experimental Medicine* 167(6)**,** 1755-1765. doi: 10.1084/jem.167.6.1755.

MacPherson, S., Keyes, S., Kilgour, M.K., Smazynski, J., Chan, V., Sudderth, J., et al. (2022). Clinically relevant T cell expansion media activate distinct metabolic programs uncoupled from cellular function. *Molecular Therapy-Methods & Clinical Development* 24**,** 380-393. doi: 10.1016/j.omtm.2022.02.004.

Magnuson, B., Ekim, B., and Fingar, D.C. (2012). Regulation and function of ribosomal protein S6 kinase (S6K) within mTOR signalling networks. *Biochemical Journal* 441**,** 1-21. doi: 10.1042/bj20110892.

Manz, M.G., and Boettcher, S. (2014). Emergency granulopoiesis. *Nature Reviews Immunology* 14(5)**,** 302-314. doi: 10.1038/nri3660.

Marchetti, P., Fovez, Q., Germain, N., Khamari, R., and Kluza, J. (2020). Mitochondrial spare respiratory capacity: Mechanisms, regulation, and significance in non-transformed and cancer cells. *Faseb Journal* 34(10)**,** 13106-13124. doi: 10.1096/fj.202000767R.

Marini, O., Costa, S., Bevilacqua, D., Calzetti, F., Tamassia, N., Spina, C., et al. (2017). Mature CD10(+) and immature CD10(-) neutrophils present in G-CSF-treated donors display opposite effects on T cells. *Blood* 129(10)**,** 1343-1356. doi: 10.1182/blood-2016-04-713206.

Martin-Loeches, I., Guia, M.C., Vallecoccia, M.S., Suarez, D., Ibarz, M., Irazabal, M., et al. (2019). Risk factors for mortality in elderly and very elderly critically ill patients with sepsis: a prospective, observational, multicenter cohort study. *Annals of Intensive Care* 9. doi: 10.1186/s13613-019-0495-x.

Martinez-Reyes, I., and Chandel, N.S. (2020). Mitochondrial TCA cycle metabolites control physiology and disease. *Nature Communications* 11(1). doi: 10.1038/s41467-019-13668-3.

Martino, D., Neeland, M., Dang, T., Cobb, J., Ellis, J., Barnett, A., et al. (2018). Epigenetic dysregulation of naive CD4+T-cell activation genes in childhood food allergy. *Nature Communications* 9. doi: 10.1038/s41467-018-05608-4.

Marzec, M., Liu, X.B., Kasprzycka, M., Witkiewicz, A., Raghunath, P.N., El-Salem, M., et al. (2008). IL-2- and IL-15-induced activation of the rapamycin-sensitive

mTORC1 pathway in malignant CD4(+) T lymphocytes. *Blood* 111(4)**,** 2181-2189. doi: 10.1182/blood-2007-06-095182.

Matias, M.I., Yong, C.S., Foroushani, A., Goldsmith, C., Mongellaz, C., Sezgin, E., et al. (2021). Regulatory T cell differentiation is controlled by alpha KG-induced alterations in mitochondrial metabolism and lipid homeostasis. *Cell Reports* 37(5). doi: 10.1016/j.celrep.2021.109911.

McKenna, E., Mhaonaigh, A.U., Wubben, R., Dwivedi, A., Hurley, T., Kelly, L.A., et al. (2021). Neutrophils: Need for Standardized Nomenclature. *Frontiers in Immunology* 12. doi: 10.3389/fimmu.2021.602963.

Melvan, J.N., Bagby, G.J., Welsh, D.A., Nelson, S., and Zhang, P. (2010). Neonatal Sepsis and Neutrophil Insufficiencies. *International Reviews of Immunology* 29(3)**,** 315-348. doi: 10.3109/08830181003792803.

Menk, A.V., Scharping, N.E., Moreci, R.S., Zeng, X., Guy, C., Salvatore, S., et al. (2018). Early TCR Signaling Induces Rapid Aerobic Glycolysis Enabling Distinct Acute T Cell Effector Functions. *Cell Reports* 22(6)**,** 1509-1521. doi: 10.1016/j.celrep.2018.01.040.

Meszaros, G., Orban, C., Kaposi, A., Toldi, G., Gyarmati, B., Tulassay, T., et al. (2015). Altered mitochondrial response to activation of T-cells in neonate. *Acta Physiologica Hungarica* 102(2)**,** 216-227. doi: 10.1556/036.102.2015.2.12.

Michael, W.Y.H., Shun, P.T., and Shan, N.G.W. (2023). Incidence and predictive risk factors of neutropenic sepsis in post-chemotherapy febrile patients in emergency department: A single-center retrospective longitudinal study. *Hong Kong Journal of Emergency Medicine* 30(5)**,** 283-290. doi: 10.1177/10249079211016225.

Michalek, R.D., Gerriets, V.A., Jacobs, S.R., Macintyre, A.N., MacIver, N.J., Mason, E.F., et al. (2011). Cutting Edge: Distinct Glycolytic and Lipid Oxidative Metabolic Programs Are Essential for Effector and Regulatory CD4(+) T Cell Subsets. *Journal of Immunology* 186(6)**,** 3299-3303. doi: 10.4049/jimmunol.1003613.

Miki, S., Suzuki, J.I., Takashima, M., Ishida, M., Kokubo, H., and Yoshizumi, M. (2021). S-1-Propenylcysteine promotes IL-10-induced M2c macrophage polarization through prolonged activation of IL-10R/STAT3 signaling. *Scientific Reports* 11(1). doi: 10.1038/s41598-021-01866-3.

Miltenyi Biotech. (2024). https://static.miltenyibiotec.com/asset/150655405641/document_smosus3i9h7jf8mkpdpb52bn0u?content-disposition=inline. [Accessed May 14 2024.

Miyara, M., Yoshioka, Y., Kitoh, A., Shima, T., Wing, K., Niwa, A., et al. (2009). Functional Delineation and Differentiation Dynamics of Human CD4(+) T Cells Expressing the FoxP3 Transcription Factor. *Immunity* 30(6)**,** 899-911. doi: 10.1016/j.immuni.2009.03.019.

Mocholi, E., Russo, L., Gopal, K., Ramstead, A.G., Hochrein, S.M., Vos, H.R., et al. (2023). Pyruvate metabolism controls chromatin remodeling during CD4+T cell activation. *Cell Reports* 42(6). doi: 10.1016/j.celrep.2023.112583.

Mold, J.E., Michaelsson, J., Burt, T.D., Muench, M.O., Beckerman, K.P., Busch, M.P., et al. (2008). Maternal Alloantigens Promote the Development of Tolerogenic Fetal Regulatory T Cells in Utero. *Science* 322(5907)**,** 1562-1565. doi: 10.1126/science.1164511.

Monticelli, L.A., Buck, M.D., Flamar, A.L., Saenz, S.A., Wojno, E.D.T., Yudanin, N.A., et al. (2016). Arginase 1 is an innate lymphoid-cell-intrinsic metabolic checkpoint controlling type 2 inflammation. *Nature Immunology* 17(6)**,** 656-+. doi: 10.1038/ni.3421.

Moore, G.E., Gerner, R.E., and Franklin, H.A. (1967). Culture of normal human leukocytes. *Jama* 199(8)**,** 519-524. doi: 10.1001/jama.199.8.519.

Morath, A., and Schamel, W.W. (2020). alpha beta and gamma delta T cell receptors: Similar but different. *Journal of Leukocyte Biology* 107(6)**,** 1045-1055. doi: 10.1002/jlb.2mr1219-233r.

Morbach, H., Eichhorn, E.M., Liese, J.G., and Girschick, H.J. (2010). Reference values for B cell subpopulations from infancy to adulthood. *Clinical and Experimental Immunology* 162(2)**,** 271-279. doi: 10.1111/j.1365-2249.2010.04206.x.

Murphy, M.P., Bayir, H., Belousov, V., Chang, C.J., Davies, K.J.A. (2022). Guidelines for measuring reactive oxygen species and oxidative damage in cells and in vivo. Nat Metab 4, 651–662. https://doi.org/10.1038/s42255-022-00591-z

Nastasi, C., Willerlev-Olsen, A., Dalhoff, K., Ford, S.L., Gadsboll, A.S.O., Buus, T.B., et al. (2021). Inhibition of succinate dehydrogenase activity impairs human T cell activation and function. *Scientific Reports* 11(1). doi: 10.1038/s41598-020-80933-7.

Newman, T.B., Puopolo, K.M., Wi, S., Draper, D., and Escobar, G.J. (2010). Interpreting Complete Blood Counts Soon After Birth in Newborns at Risk for Sepsis. *Pediatrics* 126(5)**,** 903-909. doi: 10.1542/peds.2010-0935.

Newsholme, P., Curi, R., Gordon, S., and Newsholme, E.A. (1986). METABOLISM OF GLUCOSE, GLUTAMINE, LONG-CHAIN FATTY-ACIDS AND KETONE-BODIES BY MURINE MACROPHAGES. *Biochemical Journal* 239(1)**,** 121-125. doi: 10.1042/bj2390121.

Newton, R., Priyadharshini, B., and Turka, L.A. (2016). Immunometabolism of regulatory T cells. *Nature Immunology* 17(6)**,** 618-625. doi: 10.1038/ni.3466.

Ng, T.H.S., Britton, G.J., Hill, E.V., Verhagen, J., Burton, B.R., and Wraith, D.C. (2013). Regulation of adaptive immunity; the role of interleukin-10. *Frontiers in Immunology* 4. doi: 10.3389/fimmu.2013.00129.

Nicklin, P., Bergman, P., Zhang, B.L., Triantafellow, E., Wang, H., Nyfeler, B., et al. (2009). Bidirectional Transport of Amino Acids Regulates mTOR and Autophagy. *Cell* 136(3)**,** 521-534. doi: 10.1016/j.cell.2008.11.044.

Niewiesk, S. (2015). Maternal antibodies: clinical significance, mechanism of interference with immune responses, and possible vaccination strategies. *Frontiers in Immunology* 5. doi: 10.3389/fimmu.2014.00446.

Nussbaum, C., Gloning, A., Pruenster, M., Frommhold, D., Bierschenk, S., Genzel-Boroviczeny, O., et al. (2013). Neutrophil and endothelial adhesive function during human fetal ontogeny. *Journal of Leukocyte Biology* 93(2)**,** 175-184. doi: 10.1189/jlb.0912468.

O'Neill, L.A.J., Kishton, R.J., and Rathmell, J. (2016). A guide to immunometabolism for immunologists. *Nature Reviews Immunology* 16(9)**,** 553-565. doi: 10.1038/nri.2016.70.

Olin, A., Henckel, E., Chen, Y., Lakshmikanth, T., Pou, C., Mikes, J., et al. (2018). Stereotypic Immune System Development in Newborn Children. *Cell* 174(5)**,** 1277-+. doi: 10.1016/j.cell.2018.06.045.

Opiela, S.J., Koru-Sengul, T., and Adkins, B. (2009). Murine neonatal recent thymic emigrants are phenotypically and functionally distinct from adult recent thymic emigrants. *Blood* 113(22)**,** 5635-5643. doi: 10.1182/blood-2008-08-173658.

Owen, D.L., Mahmud, S.A., Sjaastad, L.E., Williams, J.B., Spanier, J.A., Simeonov, D.R., et al. (2019). Thymic regulatory T cells arise via two distinct developmental programs. *Nature Immunology* 20(2)**,** 195-+. doi: 10.1038/s41590-018-0289-6.

Pacella, I., Procaccini, C., Focaccetti, C., Miacci, S., Timperi, E., Faicchia, D., et al. (2018). Fatty acid metabolism complements glycolysis in the selective regulatory T cell expansion during tumor growth. *Proceedings of the National Academy of Sciences of the United States of America* 115(28)**,** E6546-E6555. doi: 10.1073/pnas.1720113115.

Pai, S.Y., Truitt, M.L., and Ho, I.C. (2004). GATA-3 deficiency abrogates the development and maintenance of T helper type 2 cells. *Proceedings of the National Academy of Sciences of the United States of America* 101(7)**,** 1993-1998. doi: 10.1073/pnas.0308697100.

Palin, A.C., Ramachandran, V., Acharya, S., and Lewis, D.B. (2013). Human Neonatal Naive CD4(+) T Cells Have Enhanced Activation-Dependent Signaling Regulated by the MicroRNA miR-181a. *Journal of Immunology* 190(6)**,** 2682-2691. doi: 10.4049/jimmunol.1202534.

Palmer, A.C. (2011). Nutritionally Mediated Programming of the Developing Immune System. *Advances in Nutrition* 2(5)**,** 377-395. doi: 10.3945/an.111.000570.

Palmer, C.S., Ostrowski, M., Balderson, B., Christian, N., and Crowe, S.M. (2015). Glucose metabolism regulatesT cell activation, differentiation, and functions. *Frontiers in Immunology* 6. doi: 10.3389/fimmu.2015.00001.

Palsson-McDermott, E.M., Curtis, A.M., Goel, G., Lauterbach, M.A.R., Sheedy, F.J., Gleeson, L.E., et al. (2015). Pyruvate Kinase M2 Regulates Hif-1 alpha Activity and IL-1 beta Induction and Is a Critical Determinant of the Warburg Effect in LPS-Activated Macrophages (vol 21, pg 65, 2015). *Cell Metabolism* 21(2)**,** 347-347. doi: 10.1016/j.cmet.2015.01.017.

Palsson-McDermott, E.M., and O'Neill, L.A.J. (2020). Targeting immunometabolism as an anti-inflammatory strategy. *Cell Research* 30(4)**,** 300-314. doi: 10.1038/s41422-020-0291-z.

Panda, S.K., Kim, D.H., Desai, P., Rodrigues, P.F., Sudan, R., Gilfillan, S., et al. (2022). SLC7A8 is a key amino acids supplier for the metabolic programs that sustain homeostasis and activation of type 2 innate lymphoid cells. *Proceedings of the National Academy of Sciences of the United States of America* 119(46). doi: 10.1073/pnas.2215528119.

Papayannopoulos, V., Metzler, K.D., Hakkim, A., and Zychlinsky, A. (2010). Neutrophil elastase and myeloperoxidase regulate the formation of neutrophil extracellular traps. *Journal of Cell Biology* 191(3)**,** 677-691. doi: 10.1083/jcb.201006052.

Park, D., Lim, G., Yoon, S.J., Yi, H.S., and Choi, D.W. (2022). The role of immunomodulatory metabolites in shaping the inflammatory response of macrophages. *Bmb Reports* 55(11)**,** 519-527. doi: 10.5483/BMBRep.2022.55.11.128.

Pearce, E.L., and Pearce, E.J. (2013). Metabolic Pathways in Immune Cell Activation and Quiescence. *Immunity* 38(4)**,** 633-643. doi: 10.1016/j.immuni.2013.04.005.

Pearce, E.L., Walsh, M.C., Cejas, P.J., Harms, G.M., Shen, H., Wang, L.S., et al. (2009). Enhancing CD8 T-cell memory by modulating fatty acid metabolism. *Nature* 460(7251)**,** 103-U118. doi: 10.1038/nature08097.

Peng, M., Yin, N., Chhangawala, S., Xu, K., Leslie, C.S., and Li, M.O. (2016). Aerobic glycolysis promotes T helper 1 cell differentiation through an epigenetic mechanism. *Science* 354(6311)**,** 481-484. doi: 10.1126/science.aaf6284.

Peterson, L.S., Hedou, J., Ganio, E.A., Stelzer, I.A., Feyaerts, D., Harbert, E., et al. (2021). Single-Cell Analysis of the Neonatal Immune System Across the Gestational Age Continuum. *Frontiers in Immunology* 12. doi: 10.3389/fimmu.2021.714090.

Pettengill, M.A., and Levy, O. (2016). Circulating Human Neonatal Naive B Cells are Deficient in CD73 Impairing Purine Salvage. *Frontiers in Immunology* 7. doi: 10.3389/fimmu.2016.00121.

Pieren, D.K.J., Boer, M.C., and de Wit, J. (2022). The adaptive immune system in early life: The shift makes it count. *Frontiers in Immunology* 13. doi: 10.3389/fimmu.2022.1031924.

Pilsczek, F.H., Salina, D., Poon, K.K.H., Fahey, C., Yipp, B.G., Sibley, C.D., et al. (2010). A Novel Mechanism of Rapid Nuclear Neutrophil Extracellular Trap Formation in Response to Staphylococcus aureus. *Journal of Immunology* 185(12)**,** 7413-7425. doi: 10.4049/jimmunol.1000675.

Pollizzi, K.N., Patel, C.H., Sun, I.H., Oh, M.H., Waickman, A.T., Wen, J.Y., et al. (2015). mTORC1 and mTORC2 selectively regulate CD8(+) T cell differentiation. *Journal of Clinical Investigation* 125(5)**,** 2090-2108. doi: 10.1172/jci77746.

Porter, L., Toepfner, N., Bashant, K.R., Guck, J., Ashcroft, M., Farahi, N., et al. (2018). Metabolic Profiling of Human Eosinophils. *Frontiers in Immunology* 9. doi: 10.3389/fimmu.2018.01404.

Pour, S.R., Morikawa, H., Kiani, N., Yang, M.Y., Azimi, A., Shafi, G., et al. (2019). Exhaustion of CD4+T-cells mediated by the Kynurenine Pathway in Melanoma. *Scientific Reports* 9. doi: 10.1038/s41598-019-48635-x.

Power, L.L., Popplewell, E.J., Holloway, J.A., Diaper, N.D., Warner, J.O., and Jones, C.A. (2002). Immunoregulatory molecules during pregnancy and at birth. *Journal of Reproductive Immunology* 56(1-2)**,** 19-28. doi: 10.1016/s0165-0378(01)00146-2.

Prabhu, S.B., Rathore, D.K., Nair, D., Chaudhary, A., Raza, S., Kanodia, P., et al. (2016). Comparison of Human Neonatal and Adult Blood Leukocyte Subset Composition Phenotypes. *Plos One* 11(9). doi: 10.1371/journal.pone.0162242.

Prescott, S.L., Noakes, P., Chow, B.W.Y., Breckler, L., Thornton, C.A., Hollams, E.M., et al. (2008). Presymptomatic differences in toll-like receptor function in infants who have allergy. *Journal of Allergy and Clinical Immunology* 122(2)**,** 391-399. doi: 10.1016/j.jaci.2008.04.042.

Prescott, S.L., Taylor, A., King, B., Dunstan, J., Upham, J.W., Thornton, C.A., et al. (2003). Neonatal interleukin-12 capacity is associated with variations in allergen-specific immune responses in the neonatal and postnatal periods.

Clinical and Experimental Allergy 33(5)**,** 566-572. doi: 10.1046/j.1365-2222.2003.01659.x.

Proytcheva, M.A. (2009). Issues in Neonatal Cellular Analysis. *American Journal of Clinical Pathology* 131(4)**,** 560-573. doi: 10.1309/ajcpthbj4i4ygzqc.

Puleston, D.J., Baixauli, F., Sanin, D.E., Edwards-Hicks, J., Villa, M., Kabat, A.M., et al. (2021). Polyamine metabolism is a central determinant of helper T cell lineage fidelity. *Cell* 184(16)**,** 4186-+. doi: 10.1016/j.cell.2021.06.007.

Puleston, D.J., Buck, M.D., Geltink, R.I.K., Kyle, R.L., Caputa, G., Osullivan, D., et al. (2019). Polyamines and eIF5A Hypusination Modulate Mitochondrial Respiration and Macrophage Activation. *Cell Metabolism* 30(2)**,** 352-+. doi: 10.1016/j.cmet.2019.05.003.

Qiu, J., Villa, M., Sanin, D.E., Buck, M.D., O'Sullivan, D., Ching, R., et al. (2019). Acetate Promotes T Cell Effector Function during Glucose Restriction. *Cell Reports* 27(7)**,** 2063-+. doi: 10.1016/j.celrep.2019.04.022.

Quinn, W.J., Jiao, J., TeSlaa, T., Stadanlick, J., Wang, Z.L., Wang, L.Q., et al. (2020). Lactate Limits T Cell Proliferation via the NAD(H) Redox State. *Cell Reports* 33(11). doi: 10.1016/j.celrep.2020.108500.

Radwan, J., Babik, W., Kaufman, J., Lenz, T.L., and Winternitz, J. (2020). Advances in the Evolutionary Understanding of MHC Polymorphism. *Trends in Genetics* 36(4)**,** 298-311. doi: 10.1016/j.tig.2020.01.008.

Rafiq, S., Hackett, C.S., and Brentjens, R.J. (2020). Engineering strategies to overcome the current roadblocks in CAR T cell therapy. *Nature Reviews Clinical Oncology* 17(3)**,** 147-167. doi: 10.1038/s41571-019-0297-y.

Rath, M., Muller, I., Kropf, P., Closs, E.I., and Munder, M. (2014). Metabolism via arginase or nitric oxide synthase: two competing arginine pathways in macrophages. *Frontiers in Immunology* 5. doi: 10.3389/fimmu.2014.00532.

Raud, B., McGuire, P.J., Jones, R.G., Sparwasser, T., and Berod, L. (2018). Fatty acid metabolism in CD8(+) T cell memory: Challenging current concepts. *Immunological Reviews* 283(1)**,** 213-231. doi: 10.1111/imr.12655.

Ray, J.P., Staron, M.M., Shyer, J.A., Ho, P.C., Marshall, H.D., Gray, S.M., et al. (2015). The Interleukin-2-mTORc1 Kinase Axis Defines the Signaling, Differentiation, and Metabolism of T Helper 1 and Follicular B Helper T Cells. *Immunity* 43(4)**,** 690-702. doi: 10.1016/j.immuni.2015.08.017.

Raymond, S.L., Hawkins, R.B., Murphy, T.J., Rincon, J.C., Stortz, J.A., Lopez, M.C., et al. (2018). Impact of toll-like receptor 4 stimulation on human neonatal neutrophil spontaneous migration, transcriptomics, and cytokine production. *Journal of Molecular Medicine-Jmm* 96(7)**,** 673-684. doi: 10.1007/s00109-018-1646-5.

Razzaghian, H.R., Sharafian, Z., Sharma, A.A., Boyce, G.K., Lee, K., Da Silva, R., et al. (2021). Neonatal T Helper 17 Responses Are Skewed Towards an Immunoregulatory Interleukin-22 Phenotype. *Frontiers in Immunology* 12. doi: 10.3389/fimmu.2021.655027.

Redeker, A., Welten, S.P.M., Baert, M.R.M., Vloemans, S.A., Tiemessen, M.M., Staal, F.J.T., et al. (2015). The Quantity of Autocrine IL-2 Governs the Expansion Potential of CD8(+) T Cells. *Journal of Immunology* 195(10)**,** 4792-4801. doi: 10.4049/jimmunol.1501083.

Reynaldi, A., Smith, N.L., Schlub, T.E., Venturi, V., Rudd, B.D., and Davenport, M.P. (2016). Modeling the dynamics of neonatal CD8(+) T-cell responses. *Immunology and Cell Biology* 94(9)**,** 838-848. doi: 10.1038/icb.2016.47.

Rice, C.M., Davies, L.C., Subleski, J.J., Maio, N., Gonzalez-Cotto, M., Andrews, C., et al. (2018). Tumour-elicited neutrophils engage mitochondrial metabolism to circumvent nutrient limitations and maintain immune suppression. *Nature Communications* 9. doi: 10.1038/s41467-018-07505-2.

Riffelmacher, T., Clarke, A., Richter, F.C., Stranks, A., Pandey, S., Danielli, S., et al. (2017). Autophagy-Dependent Generation of Free Fatty Acids Is Critical for Normal Neutrophil Differentiation. *Immunity* 47(3)**,** 466-+. doi: 10.1016/j.immuni.2017.08.005.

Roberts, D.J., and Miyamoto, S. (2015). Hexokinase II integrates energy metabolism and cellular protection: Akting on mitochondria and TORCing to autophagy. *Cell Death and Differentiation* 22(2)**,** 248-257. doi: 10.1038/cdd.2014.173.

Rodriguez, P.C., and Ochoa, A.C. (2008). Arginine regulation by myeloid derived suppressor cells and tolerance in cancer: mechanisms and therapeutic perspectives. *Immunological Reviews* 222**,** 180-191. doi: 10.1111/j.1600-065X.2008.00608.x.

Rodriguez-Espinosa, O., Rojas-Espinosa, O., Moreno-Altamirano, M.M.B., Lopez-Villegas, E.O., and Sanchez-Garcia, F.J. (2015). Metabolic requirements for neutrophil extracellular traps formation. *Immunology* 145(2)**,** 213-224. doi: 10.1111/imm.12437.

Ron-Harel, N., Santos, D., Ghergurovich, J.M., Sage, P.T., Reddy, A., Lovitch, S.B., et al. (2016). Mitochondrial Biogenesis and Proteome Remodeling Promote One-Carbon Metabolism for T Cell Activation. *Cell Metabolism* 24(1)**,** 104-117. doi: 10.1016/j.cmet.2016.06.007.

Rosales, C. (2018). Neutrophil: A Cell with Many Roles in Inflammation or Several Cell Types? *Frontiers in Physiology* 9. doi: 10.3389/fphys.2018.00113.

Rose, S., Lichtenheld, M., Foote, M.R., and Adkins, B. (2007). Murine neonatal CD4(+) cells are poised for rapid Th2 effector-like function. *Journal of Immunology* 178(5)**,** 2667-2678. doi: 10.4049/jimmunol.178.5.2667.

Rudd, B.D. (2020). Neonatal T Cells: A Reinterpretation. *Annual Review of Immunology, Vol 38* 38**,** 229-247. doi: 10.1146/annurev-immunol-091319-083608.

Rudd, B.D., Venturi, V., Smith, N.L., Nzingha, K., Goldberg, E.L., Li, G., et al. (2013). Acute Neonatal Infections 'Lock-In' a Suboptimal CD8+T Cell Repertoire with Impaired Recall Responses. *Plos Pathogens* 9(9). doi: 10.1371/journal.ppat.1003572.

Saboohi, E., Saeed, F., Khan, R.N., and Khan, M.A. (2019). Immature to total neutrophil ratio as an early indicator of early neonatal sepsis. *Pakistan Journal of Medical Sciences* 35(1)**,** 241-246. doi: 10.12669/pjms.35.1.99.

Sada, Y., Dohi, Y., Uga, S., Higashi, A., Kinoshita, H., and Kihara, Y. (2016). Non-suppressive regulatory T cell subset expansion in pulmonary arterial hypertension. *Heart and Vessels* 31(8)**,** 1319-1326. doi: 10.1007/s00380-015-0727-4.

Sadiku, P., Willson, J.A., Ryan, E.M., Sammut, D., Coelho, P., Watts, E.R., et al. (2021). Neutrophils Fuel Effective Immune Responses through Gluconeogenesis and Glycogenesis. *Cell Metabolism* 33(2). doi: 10.1016/j.cmet.2020.11.016.

Saito, S. (2000). Cytokine network at the feto-maternal interface. *Journal of Reproductive Immunology* 47(2)**,** 87-103. doi: 10.1016/s0165-0378(00)00060-7.

Sallusto, F., Lenig, D., Forster, R., Lipp, M., and Lanzavecchia, A. (1999). Two subsets of memory T lymphocytes with distinct homing potentials and effector functions. *Nature* 401(6754)**,** 708-712. doi: 10.1038/44385.

Sarvaria, A., Basar, R., Mehta, R.S., Shaim, H., Muftuoglu, M., Khoder, A., et al. (2016). IL-10(+) regulatory B cells are enriched in cord blood and may protect against cGVHD after cord blood transplantation. *Blood* 128(10)**,** 1346-1361. doi: 10.1182/blood-2016-01-695122.

Sattler, S. (2017). The Role of the Immune System Beyond the Fight Against Infection. *Immunology of Cardiovascular Homeostasis and Pathology* 1003**,** 3-14. doi: 10.1007/978-3-319-57613-8_1.

Sattler, S., and Rosenthal, N. (2016). The neonate versus adult mammalian immune system in cardiac repair and regeneration. *Biochimica Et Biophysica Acta-Molecular Cell Research* 1863(7)**,** 1813-1821. doi: 10.1016/j.bbamcr.2016.01.011.

Sauer, S., Bruno, L., Hertweck, A., Finlay, D., Leleu, M., Spivakov, M., et al. (2008). T cell receptor signaling controls Foxp3 expression via PI3K, Akt, and mTOR. *Proceedings of the National Academy of Sciences of the United States of America* 105(22)**,** 7797-7802. doi: 10.1073/pnas.0800928105.

Scherer, S., Oberle, S.G., Kanev, K., Gerullis, A.K., Wu, M., de Almeida, G.P., et al. (2023). Pyrimidine de novo synthesis inhibition selectively blocks effector but not memory T cell development. *Nature Immunology* 24(3)**,** 501-+. doi: 10.1038/s41590-023-01436-x.

Schijf, M.A., Kruijsen, D., Bastiaans, J., Coenjaerts, F.E.J., Garssen, J., van Bleek, G.M., et al. (2012). Specific Dietary Oligosaccharides Increase Th1 Responses in a Mouse Respiratory Syncytial Virus Infection Model. *Journal of Virology* 86(21)**,** 11472-11482. doi: 10.1128/jvi.06708-11.

Schmiedeberg, K., Krause, H., Rohl, F.W., Hartig, R., Jorch, G., and Brunner-Weinzierl, M.C. (2016). T Cells of Infants Are Mature, but Hyporeactive Due to Limited Ca2+ Influx. *Plos One* 11(11). doi: 10.1371/journal.pone.0166633.

Schmutz, N., Henry, E., Jopling, J., and Christensen, R.D. (2008). Expected ranges for blood neutrophil concentrations of neonates: the Manroe and Mouzinho charts revisited. *Journal of Perinatology* 28(4)**,** 275-281. doi: 10.1038/sj.jp.7211916.

Scholz, G., Jandus, C., Zhang, L., Grandclement, C., Lopez-Mejia, I.C., Soneson, C., et al. (2016). Modulation of mTOR Signalling Triggers the Formation of Stem Cell-like Memory T Cells. *Ebiomedicine* 4**,** 50-61. doi: 10.1016/j.ebiom.2016.01.019.

Schonland, S.O., Zimmer, J.K., Lopez-Benitez, C.M., Widmann, T., Ramin, K.D., Goronzy, J.J., et al. (2003). Homeostatic control of T-cell generation in neonates. *Blood* 102(4)**,** 1428-1434. doi: 10.1182/blood-2002-11-3591.

Schuler, T., Hammerling, G.J., and Arnold, B. (2004). Cutting edge: IL-7-dependent homeostatic proliferation of CD8(+) T cells in neonatal mice allows the generation of long-lived natural memory T cells. *Journal of Immunology* 172(1)**,** 15-19. doi: 10.4049/jimmunol.172.1.15.

Scrimshaw, N.S. (1977). EFFECT OF INFECTION ON NUTRIENT-REQUIREMENTS. *American Journal of Clinical Nutrition* 30(9)**,** 1536-1544. doi: 10.1093/ajcn/30.9.1536.

Semmes, E.C., Chen, J.L., Goswami, R., Burt, T.D., Permar, S.R., and Fouda, G.G. (2021). Understanding Early-Life Adaptive Immunity to Guide Interventions for Pediatric Health. *Frontiers in Immunology* 11. doi: 10.3389/fimmu.2020.595297.

Sena, L.A., Li, S., Jairaman, A., Prakriya, M., Ezponda, T., Hildeman, D.A., et al. (2013). Mitochondria Are Required for Antigen-Specific T Cell Activation through Reactive Oxygen Species Signaling. *Immunity* 38(2)**,** 225-236. doi: 10.1016/j.immuni.2012.10.020.

Shao, M., Teng, X.Y., Guo, X., Zhang, H., Huang, Y., Cui, J.Z., et al. (2022). Inhibition of Calcium Signaling Prevents Exhaustion and Enhances Anti-Leukemia Efficacy of CAR-T Cells via SOCE-Calcineurin-NFAT and Glycolysis Pathways. *Advanced Science* 9(9). doi: 10.1002/advs.202103508.

Sharma, R., Smolkin, R.M., Chowdhury, P., Fernandez, K.C., Kim, Y., Cols, M., et al. (2023). Distinct metabolic requirements regulate B cell activation and germinal center responses. *Nature Immunology*. doi: 10.1038/s41590-023-01540-y.

Shen, X.F., Cao, K., Jiang, J.P., Guan, W.X., and Du, J.F. (2017). Neutrophil dysregulation during sepsis: an overview and update. *Journal of Cellular and Molecular Medicine* 21(9)**,** 1687-1697. doi: 10.1111/jcmm.13112.

Shereck, E., Day, N.S., Awasthi, A., Ayello, J., Chu, Y.Y., McGuinn, C., et al. (2019). Immunophenotypic, cytotoxic, proteomic and genomic characterization of human cord blood vs. peripheral blood CD56(Dim) NK cells. *Innate Immunity* 25(5)**,** 294-304. doi: 10.1177/1753425919846584.

Shew, S.B., and Jaksic, T. (1999). The metabolic needs of critically ill children and neonates. *Seminars in pediatric surgery* 8(3)**,** 131-139.

Shyer, J.A., Flavell, R.A., and Bailis, W. (2020). Metabolic signaling in T cells. *Cell Research* 30(8)**,** 649-659. doi: 10.1038/s41422-020-0379-5.

Sica, A., and Strauss, L. (2017). Energy metabolism drives myeloid-derived suppressor cell differentiation and functions in pathology. *Journal of Leukocyte Biology* 102(2)**,** 325-334. doi: 10.1189/jlb.4MR1116-476R.

Silva-Sanchez, A., Meza-Perez, S., Liu, M.Y., Stone, S.L., Flores-Romo, L., Ubil, E., et al. (2023). Activation of regulatory dendritic cells by Mertk coincides with a temporal wave of apoptosis in neonatal lungs. *Science Immunology* 8(84). doi: 10.1126/sciimmunol.adc9081.

Sinclair, L.V., Neyens, D., Ramsay, G., Taylor, P.M., and Cantrell, D.A. (2018). Single cell analysis of kynurenine and System L amino acid transport in T cells. *Nature Communications* 9. doi: 10.1038/s41467-018-04366-7.

Sinclair, L.V., Rolf, J., Emslie, E., Shi, Y.B., Taylor, P.M., and Cantrell, D.A. (2013). Control of amino-acid transport by antigen receptors coordinates the metabolic

reprogramming essential for T cell differentiation. *Nature Immunology* 14(5), 500-+. doi: 10.1038/ni.2556.

Singh, M., Orazulike, N.C., Ashmore, J., and Konje, J.C. (2013). Changes in Maternal Serum Transforming Growth Factor Beta-1 during Pregnancy: A Cross-Sectional Study. *Biomed Research International*. doi: 10.1155/2013/318464.

Siska, P.J., Jiao, J., Matos, C., Singer, K., Berger, R.S., Dettmer, K., et al. (2021). Kynurenine induces T cell fat catabolism and has limited suppressive effects in vivo. *Ebiomedicine* 74. doi: 10.1016/j.ebiom.2021.103734.

Slayton, W.B., Li, Y., Calhoun, D.A., Juul, S.E., Iturraspe, J., Braylan, R.C., et al. (1998). The first-appearance of neutrophils in the human fetal bone marrow cavity. *Early Human Development* 53(2), 129-144. doi: 10.1016/s0378-3782(98)00049-8.

Smith, C.L., Dickinson, P., Forster, T., Craigon, M., Ross, A., Khondoker, M.R., et al. (2014a). Identification of a human neonatal immune-metabolic network associated with bacterial infection. *Nature Communications* 5. doi: 10.1038/ncomms5649.

Smith, M., Tourigny, M.R., Noakes, P., Catherine, A., Tulic, M.K., and Prescott, S.L. (2008). Children with egg allergy have evidence of reduced neonatal CD4(+)CD25(+)CD127(lo/-) regulatory T cell function. *Journal of Allergy and Clinical Immunology* 121(6), 1460-1466. doi: 10.1016/j.jaci.2008.03.025.

Smith, N.L., Wissink, E., Wang, J., Pinello, J.F., Davenport, M.P., Grimson, A., et al. (2014b). Rapid Proliferation and Differentiation Impairs the Development of Memory CD8(+) T Cells in Early Life. *Journal of Immunology* 193(1), 177-184. doi: 10.4049/jimmunol.1400553.

Soares, M.V.D., Borthwick, N.J., Maini, M.K., Janossy, G., Salmon, M., and Akbar, A.N. (1998). IL-7-dependent extrathymic expansion of CD45RA(+) T cells enables preservation of a naive repertoire. *Journal of Immunology* 161(11), 5909-5917.

Sojka, D.K., Bruniquel, D., Schwartz, R.H., and Singh, N.J. (2004). IL-2 secretion by CD4(+) T cells in vivo is rapid, transient, and influenced by TCR-specific competition. *Journal of Immunology* 172(10), 6136-6143. doi: 10.4049/jimmunol.172.10.6136.

Sonego, F., Castanheira, F., Ferreira, R.G., Kanashiro, A., Leite, C., Nascimento, D.C., et al. (2016). Paradoxical Roles of the neutrophil in Sepsis: Protective and Deleterious. *Frontiers in Immunology* 7. doi: 10.3389/fimmu.2016.00155.

Soriano-Baguet, L., and Brenner, D. (2023). Metabolism and epigenetics at the heart of T cell function. *Trends in Immunology* 44(3), 231-244. doi: 10.1016/j.it.2023.01.002.

Soskic, B., Cano-Gamez, E., Smyth, D.J., Ambridge, K., Ke, Z.Y., Matte, J.C., et al. (2022). Immune disease risk variants regulate gene expression dynamics during CD4(+) T cell activation. *Nature Genetics* 54(6), 817-+. doi: 10.1038/s41588-022-01066-3.

Spits, H. (2002). Development of alpha beta T cells in the human thymus. *Nature Reviews Immunology* 2(10), 760-772. doi: 10.1038/nri913.

Steer, C.A., Martinez-Gonzalez, I., Ghaedi, M., Allinger, P., Matha, L., and Takei, F. (2017). Group 2 innate lymphoid cell activation in the neonatal lung drives

type 2 immunity and allergen sensitization. *Journal of Allergy and Clinical Immunology* 140(2)**,** 593-+. doi: 10.1016/j.jaci.2016.12.984.

Steer, C.A., Matha, L., Shim, H., and Takei, F. (2020). Lung group 2 innate lymphoid cells are trained by endogenous IL-33 in the neonatal period. *Jci Insight* 5(14). doi: 10.1172/jci.insight.135961.

Stiel, C.U., Ebenebe, C.U., Trochimiuk, M., Raluy, L.P., Vincent, D., Singer, D., et al. (2020). Markers of NETosis Do Not Predict Neonatal Early Onset Sepsis: A Pilot Study. *Frontiers in Pediatrics* 7. doi: 10.3389/fped.2019.00555.

Strauss-Albee, D.M., Liang, E.C., Ranganath, T., Aziz, N., and Blish, C.A. (2017). The newborn human NK cell repertoire is phenotypically formed but functionally reduced. *Cytometry Part B-Clinical Cytometry* 92(1)**,** 33-41. doi: 10.1002/cyto.b.21485.

Summer, R., Shaghaghi, H., Schriner, D., Roque, W., Sales, D., Cuevas-Mora, K., et al. (2019). Activation of the mTORC1/PGC-1 axis promotes mitochondrial biogenesis and induces cellular senescence in the lung epithelium. *American Journal of Physiology-Lung Cellular and Molecular Physiology* 316(6)**,** L1049-L1060. doi: 10.1152/ajplung.00244.2018.

Summers, C., Rankin, S.M., Condliffe, A.M., Singh, N., Peters, A.M., and Chilvers, E.R. (2010). Neutrophil kinetics in health and disease. *Trends in Immunology* 31(8)**,** 318-324. doi: 10.1016/j.it.2010.05.006.

Sundstrom, Y., Nilsson, C., Lilja, G., Karre, K., Troye-Blomberg, M., and Berg, L. (2007). The expression of human natural killer cell receptors in early life. *Scandinavian Journal of Immunology* 66(2-3)**,** 335-344. doi: 10.1111/j.1365-3083.2007.01980.x.

Szabo, S.J., Kim, S.T., Costa, G.L., Zhang, X.K., Fathman, C.G., and Glimcher, L.H. (2000). A novel transcription factor, T-bet, directs Th1 lineage commitment. *Cell* 100(6)**,** 655-669. doi: 10.1016/s0092-8674(00)80702-3.

Tabilas, C., Wang, J., Liu, X.J., Locasale, J.W., Smith, N.L., and Rudd, B.D. (2019). Cutting Edge: Elevated Glycolytic Metabolism Limits the Formation of Memory CD8(+) T Cells in Early Life. *Journal of Immunology* 203(10)**,** 2571-2576. doi: 10.4049/jimmunol.1900426.

Tan, H.Y., Yang, K., Li, Y.X., Shaw, T.I., Wang, Y.Y., Blanco, D.B., et al. (2017). Integrative Proteomics and Phosphoproteomics Profiling Reveals Dynamic Signaling Networks and Bioenergetics Pathways Underlying T Cell Activation. *Immunity* 46(3)**,** 488-503. doi: 10.1016/j.immuni.2017.02.010.

Tang, M.L.K., Kemp, A.S., Thorburn, J., and Hill, D.J. (1994). REDUCED INTERFERON-GAMMA SECRETION IN NEONATES AND SUBSEQUENT ATOPY. *Lancet* 344(8928)**,** 983-985. doi: 10.1016/s0140-6736(94)91641-1.

Tannahill, G.M., Curtis, A.M., Adamik, J., Palsson-McDermott, E.M., McGettrick, A.F., Goel, G., et al. (2013). Succinate is an inflammatory signal that induces IL-1 beta through HIF-1 alpha. *Nature* 496(7444)**,** 238-+. doi: 10.1038/nature11986.

Tao, J., Kamanaka, M., Hao, J.L., Hao, Z.F., Jiang, X., Craft, J.E., et al. (2011). IL-10 signaling in CD4(+) T cells is critical for the pathogenesis of collagen-induced arthritis. *Arthritis Research & Therapy* 13(6). doi: 10.1186/ar3545.

Taub, D.D., Hesdorffer, C.S., Ferrucci, L., Madara, K., Schwartz, J.B., and Goetzl, E.J. (2013). Distinct energy requirements for human memory CD4 T-cell

homeostatic functions. *Faseb Journal* 27(1), 342-349. doi: 10.1096/fj.12-217620.

Thornton, C.A., Capristo, C.C., Power, L.L., Holloway, J.A., Popplewell, E.J., Diaper, N.D., et al. (2003). The effect of labor on neonatal T-Cell phenotype and function. *Pediatric Research* 54(1), 120-124. doi: 10.1203/01.pdr.0000069704.25043.ba.

Thornton, C.A., Upham, J.W., Wikstrom, M.E., Holt, B.J., White, G.P., Sharp, M.J., et al. (2004). Functional maturation of CD4(+)CD25(+)CTLA4(+)CD45RA(+) T regulatory cells in human neonatal T cell responses to environmental antigens/allergens. *Journal of Immunology* 173(5), 3084-3092. doi: 10.4049/jimmunol.173.5.3084.

Tibbitt, C.A., Stark, J.M., Martens, L., Ma, J.J., Mold, J.E., Deswarte, K., et al. (2019). Single-Cell RNA Sequencing of the T Helper Cell Response to House Dust Mites Defines a Distinct Gene Expression Signature in Airway Th2 Cells. *Immunity* 51(1), 169-184. doi: 10.1016/j.immuni.2019.05.014.

Timperi, E., Folgori, L., Amodio, D., De Luca, M., Chiurchiu, S., Piconese, S., et al. (2016). Expansion of activated regulatory T cells inversely correlates with clinical severity in septic neonates. *Journal of Allergy and Clinical Immunology* 137(5), 1617-+. doi: 10.1016/j.jaci.2015.10.048.

Toumi, R., Yuzefpolskiy, Y., Vegaraju, A., Xiao, H., Smith, K.A., Sarkar, S., et al. (2022). Autocrine and paracrine IL-2 signals collaborate to regulate distinct phases of CD8 T cell memory. *Cell Reports* 39(2). doi: 10.1016/j.celrep.2022.110632.

Trifari, S., Kaplan, C.D., Tran, E.H., Crellin, N.K., and Spits, H. (2009). Identification of a human helper T cell population that has abundant production of interleukin 22 and is distinct from T-H-17, T(H)1 and T(H)2 cells. *Nature Immunology* 10(8), 864-U873. doi: 10.1038/ni.1770.

Trindade, C.E.P., Barreiros, R.C., Kurokawa, C., and Bossolan, G. (2011). Fructose in fetal cord blood and its relationship with maternal and 48-hour-newborn blood concentrations. *Early Human Development* 87(3), 193-197. doi: 10.1016/j.earlhumdev.2010.12.005.

Trotta, R., Dal Col, J., Yu, J.H., Ciarlariello, D., Thomas, B., Zhang, X.L., et al. (2008). TGF-beta utilizes SMAD3 to inhibit CD16-mediated IFN-gamma production and antibody-dependent cellular cytotoxicity in human NK cells. *Journal of Immunology* 181(6), 3784-3792. doi: 10.4049/jimmunol.181.6.3784.

Tulic, M.K., Hodder, M., Forsberg, A., McCarthy, S., Richman, T., D'Vaz, N., et al. (2011). Differences in innate immune function between allergic and nonallergic children: New insights into immune ontogeny. *Journal of Allergy and Clinical Immunology* 127(2), 470-U1817. doi: 10.1016/j.jaci.2010.09.020.

Vaeth, M., Maus, M., Klein-Hessling, S., Freinkman, E., Yang, J., Eckstein, M., et al. (2017). Store-Operated Ca2+ Entry Controls Clonal Expansion of T Cells through Metabolic Reprogramming. *Immunity* 47(4), 664-+. doi: 10.1016/j.immuni.2017.09.003.

van der Windt, G.J.W., O'Sullivan, D., Everts, B., Huang, S.C.C., Buck, M.D., Curtis, J.D., et al. (2013). CD8 memory T cells have a bioenergetic advantage that underlies their rapid recall ability. *Proceedings of the National Academy of Sciences of the United States of America* 110(35), 14336-14341. doi: 10.1073/pnas.1221740110.

Velasquez, S.Y., Himmelhan, B.S., Kassner, N., Coulibaly, A., Schulte, J., Brohm, K., et al. (2020). Innate Cytokine Induced Early Release of IFN gamma and CC Chemokines from Hypoxic Human NK Cells Is Independent of Glucose. *Cells* 9(3). doi: 10.3390/cells9030734.

Viel, S., Marcais, A., Guimaraes, F.S.F., Loftus, R., Rabilloud, J., Grau, M., et al. (2016). TGF-beta inhibits the activation and functions of NK cells by repressing the mTOR pathway. *Science Signaling* 9(415). doi: 10.1126/scisignal.aad1884.

Vivier, E., Tomasello, E., Baratin, M., Walzer, T., and Ugolini, S. (2008). Functions of natural killer cells. *Nature Immunology* 9(5)**,** 503-510. doi: 10.1038/ni1582.

vonBoehmer, H., and Fehling, H.J. (1997). Structure and function of the pre-T cell receptor. *Annual Review of Immunology* 15**,** 433-452. doi: 10.1146/annurev.immunol.15.1.433.

Voorde, J.V., Ackermann, T., Pfetzer, N., Sumpton, D., Mackay, G., Kalna, G., et al. (2019). Improving the metabolic fidelity of cancer models with a physiological cell culture medium. *Science Advances* 5(1). doi: 10.1126/sciadv.aau7314.

Wagner, A., Wang, C., Fessler, J., DeTomaso, D., Avila-Pacheco, J., Kaminski, J., et al. (2021). Metabolic modeling of single Th17 cells reveals regulators of autoimmunity. *Cell* 184(16)**,** 4168-+. doi: 10.1016/j.cell.2021.05.045.

Wang, F.L., Zhang, S., Vuckovic, I., Jeon, R., Lerman, A., Folmes, C.D., et al. (2018). Glycolytic Stimulation Is Not a Requirement for M2 Macrophage Differentiation. *Cell Metabolism* 28(3)**,** 463-+. doi: 10.1016/j.cmet.2018.08.012.

Wang, G.H., Miyahara, Y., Guo, Z.Y., Khattar, M., Stepkowski, S.M., and Chen, W.H. (2010). "Default" Generation of Neonatal Regulatory T Cells. *Journal of Immunology* 185(1)**,** 71-78. doi: 10.4049/jimmunol.0903806.

Wang, J., Wissink, E.M., Watson, N.B., Smith, N.L., Grimson, A., and Rudd, B.D. (2016). Fetal and adult progenitors give rise to unique populations of CD8(+) T cells. *Blood* 128(26)**,** 3073-3082. doi: 10.1182/blood-2016-06-725366.

Wang, R.N., Dillon, C.P., Shi, L.Z., Milasta, S., Carter, R., Finkelstein, D., et al. (2011). The Transcription Factor Myc Controls Metabolic Reprogramming upon T Lymphocyte Activation. *Immunity* 35(6)**,** 871-882. doi: 10.1016/j.immuni.2011.09.021.

Wang, T., Marquardt, C., and Foker, J. (1976). AEROBIC GLYCOLYSIS DURING LYMPHOCYTE-PROLIFERATION. *Nature* 261(5562)**,** 702-705. doi: 10.1038/261702a0.

Wang, Y.M., Li, M., Stadler, S., Correll, S., Li, P.X., Wang, D.C., et al. (2009). Histone hypercitrullination mediates chromatin decondensation and neutrophil extracellular trap formation. *Journal of Cell Biology* 184(2)**,** 205-213. doi: 10.1083/jcb.200806072.

Wang, Z.X., Guan, D., Wang, S., Chai, L.Y.A., Xu, S.L., and Lam, K.P. (2020). Glycolysis and Oxidative Phosphorylation Play Critical Roles in Natural Killer Cell Receptor-Mediated Natural Killer Cell Functions. *Frontiers in Immunology* 11. doi: 10.3389/fimmu.2020.00202.

Waters, L.R., Ahsan, F.M., Wolf, D.M., Shirihai, O., and Teitell, M.A. (2018). Initial B Cell Activation Induces Metabolic Reprogramming and Mitochondrial Remodeling. *Iscience* 5**,** 99-+. doi: 10.1016/j.isci.2018.07.005.

Wculek, S.K., Khouili, S.C., Priego, E., Heras-Murillo, I., and Sancho, D. (2019). Metabolic Control of Dendritic Cell Functions: Digesting Information. *Frontiers in Immunology* 10. doi: 10.3389/fimmu.2019.00775.

Webster, R.B., Rodriguez, Y., Klimecki, W.T., and Vercelli, D. (2007). The human IL-13 locus in neonatal CD4(+) T cells is refractory to the acquisition of a repressive chromatin architecture. *Journal of Biological Chemistry* 282(1)**,** 700-709. doi: 10.1074/jbc.M609501200.

Weinberg, S.E., Singer, B.D., Steinert, E.M., Martinez, C.A., Mehta, M.M., Martinez-Reyes, I., et al. (2019). Mitochondrial complex III is essential for suppressive function of regulatory T cells. *Nature* 565(7740)**,** 495-+. doi: 10.1038/s41586-018-0846-z.

Weinberger, B., Laskin, D.L., Mariano, T.M., Sunil, V.R., DeCoste, C.J., Heck, D.E., et al. (2001). Mechanisms underlying reduced responsiveness of neonatal neutrophils to distinct chemoattractants. *Journal of Leukocyte Biology* 70(6)**,** 969-976.

Weisel, F.J., Mullett, S.J., Elsner, R.A., Menk, A.V., Trivedi, N., Luo, W., et al. (2020). Germinal center B cells selectively oxidize fatty acids for energy while conducting minimal glycolysis. *Nature Immunology* 21(3)**,** 331-+. doi: 10.1038/s41590-020-0598-4.

Wenes, M., Jaccard, A., Wyss, T., Maldonado-Perez, N., Teoh, S.T., Lepez, A., et al. (2022). The mitochondrial pyruvate carrier regulates memory T cell differentiation and antitumor function. *Cell Metabolism* 34(5)**,** 731-+. doi: 10.1016/j.cmet.2022.03.013.

White, G.P., Watt, P.M., Holt, B.J., and Holt, P.G. (2002). Differential patterns of methylation of the IFN-gamma promoter at CpG and Non-CpG sites underlie differences in IFN-gamma gene expression between human neonatal and adult CD45RO(-) T cells. *Journal of Immunology* 168(6)**,** 2820-2827. doi: 10.4049/jimmunol.168.6.2820.

Wikby, A., Mansson, I., Johansson, B., Strindhall, J., and Nilsson, S., E. (2008) The immune risk profile is associated with age and gender: findings from three Swedish population studies of individuals 20–100 years of age. BioGerontology 9(5), 299-308. doi: 10.1007/s10522-008-9138-6

Wilhelm, C., Harrison, O.J., Schmitt, V., Pelletier, M., Spencer, S.P., Urban, J.F., et al. (2016). Critical role of fatty acid metabolism in ILC2-mediated barrier protection during malnutrition and helminth infection. *Journal of Experimental Medicine* 213(8)**,** 1409-1418. doi: 10.1084/jem.20151448.

Williams, M.A., and Bevan, M.J. (2007). Effector and memory CTL differentiation. *Annual Review of Immunology* 25**,** 171-192. doi: 10.1146/annurev.immunol.25.022106.141548.

Wilson, E.B., El-Jawhari, J.J., Neilson, A.L., Hall, G.D., Melcher, A.A., Meade, J.L., et al. (2011). Human Tumour Immune Evasion via TGF-beta Blocks NK Cell Activation but Not Survival Allowing Therapeutic Restoration of Anti-Tumour Activity. *Plos One* 6(9). doi: 10.1371/journal.pone.0022842.

Wofford, J.A., Wieman, H.L., Jacobs, S.R., Zhao, Y.X., and Rathmell, J.C. (2008). IL-7 promotes Glut1 trafficking and glucose uptake via STAT5-mediated activation of Akt to support T-cell survival. *Blood* 111(4)**,** 2101-2111. doi: 10.1182/blood-2007-06-096297.

Wolfson, R.L., Chantranupong, L., Saxton, R.A., Shen, K., Scaria, S.M., Cantor, J.R., et al. (2016). METABOLISM Sestrin2 is a leucine sensor for the mTORC1 pathway. *Science* 351(6268)**,** 43-48. doi: 10.1126/science.aab2674.

Wright, H.L., Moots, R.J., and Edwards, S.W. (2014). The multifactorial role of neutrophils in rheumatoid arthritis. *Nature Reviews Rheumatology* 10(10)**,** 593-601. doi: 10.1038/nrrheum.2014.80.

Wu, T.Z., Hu, E.Q., Xu, S.B., Chen, M.J., Guo, P.F., Dai, Z.H., et al. (2021). clusterProfiler 4.0: A universal enrichment tool for interpreting omics data. *Innovation* 2(3). doi: 10.1016/j.xinn.2021.100141.

Xu, K., Yin, N., Peng, M., Stamatiades, E.G., Chhangawala, S., Shyu, A., et al. (2021). Glycolytic ATP fuels phosphoinositide 3-kinase signaling to support effector T helper 17 cell responses. *Immunity* 54(5)**,** 976-+. doi: 10.1016/j.immuni.2021.04.008.

Xu, L.L., Kitani, A., Stuelten, C., McGrady, G., Fuss, I., and Strober, W. (2010). Positive and Negative Transcriptional Regulation of the Foxp3 Gene is Mediated by Access and Binding of the Smad3 Protein to Enhancer I. *Immunity* 33(3)**,** 313-325. doi: 10.1016/j.immuni.2010.09.001.

Yagi, Y., Kuwahara, M., Suzuki, J., Imai, Y., and Yamashita, M. (2020). Glycolysis and subsequent mevalonate biosynthesis play an important role in Th2 cell differentiation. *Biochemical and Biophysical Research Communications* 530(2)**,** 355-361. doi: 10.1016/j.bbrc.2020.08.009.

Yang, K., Shrestha, S., Zeng, H., Karmaus, P.W.F., Neale, G., Vogel, P., et al. (2013a). T Cell Exit from Quiescence and Differentiation into Th2 Cells Depend on Raptor-mTORC1-Mediated Metabolic Reprogramming. *Immunity* 39(6)**,** 1043-1056. doi: 10.1016/j.immuni.2013.09.015.

Yang, W., Bai, Y.B., Xiong, Y., Zhang, J., Chen, S.K., Zheng, X.J., et al. (2016). Potentiating the antitumour response of CD8(+) T cells by modulating cholesterol metabolism. *Nature* 531(7596)**,** 651-+. doi: 10.1038/nature17412.

Yang, W.Z., Zhang, Y., Wu, F., Min, W.P., Minev, B., Zhang, M., et al. (2010). Safety evaluation of allogeneic umbilical cord blood mononuclear cell therapy for degenerative conditions. *Journal of Translational Medicine* 8. doi: 10.1186/1479-5876-8-75.

Yang, Z., Fujii, H., Mohan, S.V., Goronzy, J.J., and Weyand, C.M. (2013b). Phosphofructokinase deficiency impairs ATP generation, autophagy, and redox balance in rheumatoid arthritis T cells. *Journal of Experimental Medicine* 210(10)**,** 2119-2134. doi: 10.1084/jem.20130252.

Yipp, B.G., and Kubes, P. (2013). NETosis: how vital is it? *Blood* 122(16)**,** 2784-2794. doi: 10.1182/blood-2013-04-457671.

Yost, C.C., Cody, M.J., Harris, E.S., Thornton, N.L., McInturff, A.M., Martinez, M.L., et al. (2009). Impaired neutrophil extracellular trap (NET) formation: a novel innate immune deficiency of human neonates. *Blood* 113(25)**,** 6419-6427. doi: 10.1182/blood-2008-07-171629.

Youngblood, B., Hale, J.S., Kissick, H.T., Ahn, E., Xu, X.J., Wieland, A., et al. (2017). Effector CD8 T cells dedifferentiate into long-lived memory cells. *Nature* 552(7685)**,** 404-+. doi: 10.1038/nature25144.

Yu, H.R., Hsu, T.Y., Huang, H.C., Kuo, H.C., Li, S.C., Yang, K.D., et al. (2016). Comparison of the Functional microRNA Expression in Immune Cell Subsets of Neonates and Adults. *Frontiers in Immunology* 7. doi: 10.3389/fimmu.2016.00615.

Yu, H.R., Hsu, T.Y., Tsai, C.C., Huang, H.C., Cheng, H.H., Lai, Y.J., et al. (2021). The Functional DNA Methylation Signatures Relevant to Altered Immune Response of Neonatal T Cells with l-Arginine Supplementation. *Nutrients* 13(8). doi: 10.3390/nu13082780.

Zaghouani, H., Hoeman, C.M., and Adkins, B. (2009). Neonatal immunity: faulty T-helpers and the shortcomings of dendritic cells. *Trends in Immunology* 30(12), 585-591. doi: 10.1016/j.it.2009.09.002.

Zaiatz-Bittencourt, V., Finlay, D.K., and Gardiner, C.M. (2018). Canonical TGF-beta Signaling Pathway Represses Human NK Cell Metabolism. *Journal of Immunology* 200(12), 3934-3941. doi: 10.4049/jimmunol.1701461.

Zeng, H., Cohen, S., Guy, C., Shrestha, S., Neale, G., Brown, S.A., et al. (2016). mTORC1 and mTORC2 Kinase Signaling and Glucose Metabolism Drive Follicular Helper T Cell Differentiation. *Immunity* 45(3), 540-554. doi: 10.1016/j.immuni.2016.08.017.

Zeng, H., Yang, K., Cloer, C., Neale, G., Vogel, P., and Chi, H.B. (2013). mTORC1 couples immune signals and metabolic programming to establish T-reg-cell function. *Nature* 499(7459), 485-+. doi: 10.1038/nature12297.

Zhang, C.S., Hawley, S.A., Zong, Y., Li, M.Q., Wang, Z.C., Gray, A., et al. (2017). Fructose-1,6-bisphosphate and aldolase mediate glucose sensing by AMPK. *Nature* 548(7665), 112-+. doi: 10.1038/nature23275.

Zhang, X., Mozeleski, B., Lemoine, S., Deriaud, E., Lim, A., Zhivaki, D., et al. (2014). CD4 T Cells with Effector Memory Phenotype and Function Develop in the Sterile Environment of the Fetus. *Science Translational Medicine* 6(238). doi: 10.1126/scitranslmed.3008748.

Zhang, Y.X., Collier, F., Naselli, G., Saffery, R., Tang, M.L.K., Allen, K.J., et al. (2016). Cord blood monocyte-derived inflammatory cytokines suppress IL-2 and induce nonclassic "T(H)2-type" immunity associated with development of food allergy. *Science Translational Medicine* 8(321). doi: 10.1126/scitranslmed.aad4322.

Zhang, Y.X., Maksimovic, J., Huang, B., De Souza, D.P., Naselli, G., Chen, H., et al. (2018). Cord Blood CD8(+) T Cells Have a Natural Propensity to Express IL-4 in a Fatty Acid Metabolism and Caspase Activation-Dependent Manner. *Frontiers in Immunology* 9. doi: 10.3389/fimmu.2018.00879.

Zhu, J., Yang, W.J., Zhou, X.D., Zophel, D., Soriano-Baguet, L., Dolgener, D., et al. (2021). High Glucose Enhances Cytotoxic T Lymphocyte-Mediated Cytotoxicity. *Frontiers in Immunology* 12. doi: 10.3389/fimmu.2021.689337.

Zhu, J.J., and Thompson, C.B. (2019). Metabolic regulation of cell growth and proliferation. *Nature Reviews Molecular Cell Biology* 20(7), 436-450. doi: 10.1038/s41580-019-0123-5.